5-24-2010

Development And Study Of Inhibitors Of Heat Shock Protein 70 Induction

Rongsheng Wang
Washington University in St. Louis

WASHINGTON UNIVERSITY IN ST. LOUIS

Department of Chemistry

Dissertation Examination Committee:
Dr. John-Stephen Taylor, Chair
Dr. Vladimir Birman
Dr. Peter Gaspar
Dr. Clayton Hunt
Dr. Kevin Moeller
Dr. Buck Rogers

DEVELOPMENT AND STUDY OF INHIBITORS OF HEAT SHOCK PROTEIN 70 INDUCTION

By

Rongsheng Wang

A dissertation presented to the
Graduate School of Arts and Sciences
of Washington University in
partial fulfillment of the requirements for the degree
of Doctor of Philosophy

December, 2010

Saint Louis, Missouri

ABSTRACT OF THE DISSERTATION

Development and study of inhibitors of heat shock protein 70 induction

By

Rongsheng Wang

Doctor of Philosophy in Chemistry

Washington University in St. Louis, 2010

Professor John-Stephen A. Taylor, Chairperson

Tumor and cancer cells that over express heat shock protein 70 (HSP70) are found to be multidrug resistant and thermo tolerant, creating a hurdle to existing therapy. Although HSP70 is recognized as an increasingly important drug target, the protein structure of this highly conserved chaperone remains challenging for direct targeting. An alternative strategy is to inhibit the transcription of HSP70. Among known small molecule inhibitors of HSP70 induction, quercetin has very low toxicity and has the advantage of being easily modified for structure-activity studies. One part of the dissertation focuses on the identification of quercetin derivatives with improved specificity and activity, and to determine the protein targets of quercetin responsible for inhibition of heat shock induction of HSP70. A library of quercetin derivatives was synthesized and screened for their ability to inhibit HSP70 induction and at the same time not enhance HSP27 phosphorylation. The derivatives that inhibit HSP70 induction were also found to be inhibitors of both Ck2 kinase and CaMKII kinase that are known to activate heat shock transcription factor 1 that leads to HSP70 induction. A biotinylated quercetin affinity

agent was also developed that was able to pull down the CK2 kinase target in vitro and several other proteins in vivo under UVA irradiation. In collaboration with mass spectrometry center, these unknown protein targets were identified by proteomic studies, and found to be previously identified chemotherapeutic targets.

Another goal of this dissertation was to develop polyamide-based gene inhibitors of heat shock induction that interfere with the binding of the heat shock transcription factor. A series of polyamides that targeted the heat shock elements were designed and synthesized and demonstrated to bind the target DNA by DNase I footprinting. These polyamides were evaluated by gel shift assay for their ability to block binding of the heat shock factor and the most effective polyamide was shown to decrease HSP70 expression in Jurkat cells by western blot assay.

Acknowledgement

I would like to express my sincere, deep and lifetime gratitude to my thesis advisor Dr. John-Stephen Taylor, who opened a door of science to me at the beginning of my doctoral training and showed later on how colorful that beautiful world is. I appreciate all his guidance in research and encouragement in mind. His serious attitude of pursuing accuracy and keep-on-asking approach to research as well as his full-of-ideas character always impressed and influenced me during my studies and hopefully in my future career.

I also want to thank my research committee Dr. Vladimir Birman, Dr. Kevin Moeller and Dr. Peter Gaspar who all taught me organic chemistry and have been very supportive and helpful during my graduate study at the department of chemistry. I am especially grateful to Dr. Clayton Hunt with whom I collaborated for most of my research projects, and Dr. Buck Rogers who very kindly agreed to be on my examination committee.

I would like to acknowledge the help and friendship from all the former and present members in Dr. Taylor's group, especially Dr. Xuan (Adele) Yue and Dr. Jianfeng Cai who helped and inspired me with their knowledge and attitudes when I initially came to the group.

I also appreciate the help from Dr. Jeff Kao and Dr. Andrew d'Avignon with NMR experiments, and from Jiawei Chen and other people in Dr. Gross's group for the help with Mass spectrometry. I want to express thanks to people in the department, especially Ed Hiss and Jessica Owens, for their help during my stay at Washington University.

Finally I would like to thank my family for their love and support behind.

Table of Contents

Chapter 1

Chapter 2

Chapter 3

Chapter 4

Chapter 1. Introduction

Background of heat shock proteins

Heat shock proteins (HSPs) are so-called stress proteins that are found in nearly all living organisms and are believed to be part of a stimuli induced mechanism that protects cells from various environmental and physiological challenges ranging from exogenous toxins to heat, oxidative stress, and ischemia/reperfusion injuries [1-5] (Figure 1.1). Most heat shock proteins function as conserved molecular chaperones to work together with co-chaperones in folding newly synthesized proteins/peptides, refolding denatured or damaged proteins/peptides, and at the same time helping the assembly of protein complexes as well as the intra/extra cellular transportation of certain proteins [6]. Heat shock proteins have been categorized according to their molecular weight class, among which heat shock protein 70s (HSP70s) and heat shock protein 90s (HSP90s) are the most highly conserved and prevalent, existing in almost all organisms from *E. coli* to humans [3, 7].

Heat shock proteins and cancer

Consistent with their diverse activities, heat shock proteins have been found to participate in oncogenesis, promote tumor survival, and induce resistance to chemotherapeutic agents [8-11]. Cancer cells are believed to be under stress due to unnatural growth properties which makes them produce high amounts of proteins. The housekeeping functions and stimuli resistance of heat shock proteins are thus needed by cancer cells to maintain high-speed reproduction and metabolism, and to inhibit apoptosis by various

therapeutic agents. Over-expression of HSP90s and HSP70s in many tumors [12] correlates with the proliferation and survival of oral [13], gastrointestinal [14], colorectal [15], histiocytic lymphoma [16], and breast cancers [17, 18]. Thus heat shock proteins have recently become of interest as targets for cancer therapy [19].

Importance of HSP70 inhibition

Our interest in HSP70 initially came from the observation that its overexpression increased cellular resistance to hyperthermia and thus radiosensitization. HSP70 knock-out mice not only showed increased sensitivity to necrosis and inflammation, but also displayed genomic instability and enhanced radiosensitivity [7]. HSP70 inhibitors would thus be promising drug candidates to be administrated in cancer therapy to improve the effect of clinical radiosensitization. Additionally, HSP70 can inhibit cell apoptosis by both caspase-dependent and independent mechanisms [20], stabilize lysosomes [21], and significantly down-regulate NF-κB activity [22] and inflammatory responses; all of which are necessary for cancer cell survival [23]. Likewise, depletion of endogenous HSP70 levels in transformed cells induces cell death [24, 25]. Therefore drugs that can inhibit HSP70 could be not only useful as adjuvants in cancer chemotherapy but also as anti-cancer agents themselves.

HSP70 protein types, structure and induction mechanism

Members of the human heat shock protein 70 family have been found to exist in all the cellular locations with different isoforms (Table 1.1) [26], five of which are constitutively expressed in cytosol and nucleus (HSP70A2, HSP70A1L, HSPA8), endoplasmic reticulum (HSPA5) and mitochondria(HSPA9). While most HSP70 proteins are present at low basal levels in normal cells and over-expressed in cancer cell lines, some HSP70s are substantially upregulated by stress stimuli, through mediation by heat shock transcription factor 1. Stress induced HSP70 transcription is a complicated process, which involves heat or stress-induced release of heat shock transcription factor 1 (HSF-1) from a complex with HSP90, followed by translocation to the nucleus where it is phosphorylated by Cam KII and CKII kinases, trimerization, and then binding to the heat shock elements (HSE) of the HSP70 gene [27]. Three types of inducible HSP70 have been found so far, among which HSPA1A and HSPA1B are the most homologous and recognize the same heat shock elements, while HSPA6 is less homologous and recognizes different heat shock elements (Table 1.2).

Both the heat shock protein 90 and heat shock protein 70 families possess N-terminal nucleotide binding domains (NBD) that bind to ATP and make use of ATP hydrolysis to carry out their functions [28]. The HSP70 family also has a C-terminal substrate-binding domain (SBD) for binding linear peptides and exposed regions of folded proteins. The two domains of HSP70 are connected by a short linker [29] (Figure 1.2). It is worth noticing that the NBD part of HSP70 (MW around 40 kDa) further consists of two sub-domains, I and II, each being divided to two regions (a, b) respectively. ATP interacts with subdomains Ia and IIa in a nucleotide binding motif related to those of hexokinase, actin and glycerol kinase, which leads to the binding of HSP70 to ATP in high affinity

with a nanomolar Kd [28, 29]. The NBD domain of HSP90 is significantly different in structure, belonging to the GHKL type, and binds ATP with a weaker micromolar Kd [28].

Development of HSP70 inhibitors

The ATPase site of HSP90 is a target for the well-known small molecule inhibitors 17-allylamino-17-demethoxy-geldanamycin (17AAG) and 17-(dimethylaminoethylamino)-17-demethoxygeldanamycin (17DMAG)[30-32] which have been successfully advanced into clinical trials (Figure 1.3). Despite the identification of HSP70 as a potential drug target due to its importance role in cancer and apoptosis [33], neurodegenerative and infectious diseases [29]; only a few inhibitors have been developed so far to directly interact with either the ATP binding domain, such as VER-155008, or the substrate binding domain of HSP70, such as phenylethynesulfonamide (Figure 1.3) [28, 34, 35]. The more hydrophilic nature of the HSP70 drug targeting sites and a high affinity ATP binding site have limited the development of HSP 70 inhibitors [28]. An alternate approach is to inhibit HSP70 expression through inhibitors of heat shock transcription factors.

To date, several methods have been reported to deactivate transcription factors by inhibiting either its activation (phosphorylation and oligomerization) [36], or blocking its contact with the DNA promoter by artificial oligomer mimics or polyamides [37-39] (Figure 1.4). In the latter case, peptide nucleic acid (PNA) have been developed to bind to the major groove of DNA, while polyamide composed of N-methyl pyrrole and N-

methyl imidazole building blocks that are linked together by amide bond, targets at the minor groove [37-39]. Both ways would limit the extent of binding of transcription factors to the major groove.

There are also some natural products that appear to interfere with heat shock transcription factor function (Figure 1.5). The most potent of these inhibitors is the diterpenoid triepoxide, triptolide, which induces pancreatic cancer cell death *in vitro* and *in vivo* via inhibition of HSP70 expression [40] by interfering with the heat shock factor transactivation process [41]. Unfortunately, triptolide has severe toxic side effects in animals and humans, and its structural complexity does not make it an attractive target for further synthetic development. Quercetin is another small molecule which belongs to the flavonoid family with multiple medicinal properties [42]. Initially extracted from red wine, quercetin was subsequently found to exist widely in leaves, fruits, and vegetables [43], and is available as a dietary supplement. Quercetin inhibits HSP70 induction at a concentration of 100 μM and inhibits the phosphorylation of heat shock transcription factor though the detailed mechanism of action and other interacting targets remain unknown. Although the bioactivities of flavonoids are notoriously non-specific, elucidation of the mechanism of action of quercetin in inhibiting HSP70 induction as well as its other targets would be very useful and fundamentally important in future drug design. Given the chemical structure of quercetin that would appear to be relatively easy to modify and its low toxicity [42], quercetin derivatives with improved efficacy and specificity for HSP70 inhibition could have potential to be chemotherapeutic drugs.

Goals of this dissertation

The goal of this dissertation is to develop inhibitors of HSP70 induction that have potential as chemotherapeutic agents and to probe the biological mechanisms behind their inhibition (Figure 1.6). Since directly inhibiting heat shock protein 70 has been problematic [28], a more feasible way would be to interfere with heat shock transcription factors. In chapter 2, I describe the structure and activity studies of quercetin derivatives that are known to inhibit heat shock protein 70 induction via interfering with heat shock transcription factor activation. This was carried out by mapping the non-active sites of quercetin and identifying derivatives with improved specificity and activity. I also investigated the effect of these derivatives on the putative kinases thought to be involved in the activation of heat shock transcription factor, and hence HSP70 induction. In chapter 3, I conjugated a biotin molecule to a non-active site of quercetin and used it to pull down possible target proteins of quercetin in vivo. In chapter 4, I describe the development of much larger, polyamide-based gene targeting agents that interfere with the binding of heat shock transcription factors to HSP A1A/HSP A1B promoters to inhibit the induction of heat shock protein 70 *in vivo*.

References:

1. Daugaard, M., M. Rohde, and M. Jaattela, *The heat shock protein 70 family: Highly homologous proteins with overlapping and distinct functions.* FEBS Lett, 2007. **581**(19): p. 3702-10.

2. Arya, R., M. Mallik, and S.C. Lakhotia, *Heat shock genes - integrating cell survival and death.* J Biosci, 2007. **32**(3): p. 595-610.

3. Mayer, M.P. and B. Bukau, *Hsp70 chaperones: cellular functions and molecular mechanism.* Cell Mol Life Sci, 2005. **62**(6): p. 670-84.

4. Schlesinger, M.J., *Heat shock proteins.* J Biol Chem, 1990. **265**(21): p. 12111-4.

5. Lindquist, S. and E.A. Craig, *The heat-shock proteins.* Annu Rev Genet, 1988. **22**: p. 631-77.

6. Hartl, F.U., *Molecular chaperones in cellular protein folding.* Nature, 1996. **381**(6583): p. 571-9.

7. Hunt, C.R., et al., *Genomic instability and enhanced radiosensitivity in Hsp70.1- and Hsp70.3-deficient mice.* Mol Cell Biol, 2004. **24**(2): p. 899-911.

8. Calderwood, S.K. and D.R. Ciocca, *Heat shock proteins: stress proteins with Janus-like properties in cancer.* Int J Hyperthermia, 2008. **24**(1): p. 31-9.

9. Calderwood, S.K., et al., *Heat shock proteins in cancer: chaperones of tumorigenesis.* Trends Biochem Sci, 2006. **31**(3): p. 164-72.

10. Garrido, C., et al., *Heat shock proteins 27 and 70: anti-apoptotic proteins with tumorigenic properties.* Cell Cycle, 2006. **5**(22): p. 2592-601.

11. Rohde, M., et al., *Members of the heat-shock protein 70 family promote cancer cell growth by distinct mechanisms.* Genes Dev, 2005. **19**(5): p. 570-82.

12. Nanbu, K., et al., *Expression of heat shock proteins HSP70 and HSP90 in endometrial carcinomas. Correlation with clinicopathology, sex steroid receptor status, and p53 protein expression.* Cancer, 1996. **77**(2): p. 330-8.

13. Kaur, J. and R. Ralhan, *Induction of apoptosis by abrogation of HSP70 expression in human oral cancer cells.* Int J Cancer, 2000. **85**(1): p. 1-5.

14. Maehara, Y., et al., *Overexpression of the heat shock protein HSP70 family and p53 protein and prognosis for patients with gastric cancer.* Oncology, 2000. **58**(2): p. 144-51.

15. Lazaris, A.C., et al., *Heat shock protein 70 and HLA-DR molecules tissue expression. Prognostic implications in colorectal cancer.* Dis Colon Rectum, 1995. **38**(7): p. 739-45.

16. Marunouchi, T. and H. Hosoya, *Regulation of hsc70 expression in the human histiocytic lymphoma cell line, U937.* Cell Struct Funct, 1993. **18**(6): p. 437-47.

17. Ciocca, D.R., et al., *Heat shock protein hsp70 in patients with axillary lymph node-negative breast cancer: prognostic implications.* J Natl Cancer Inst, 1993. **85**(7): p. 570-4.

18. Ciocca, D.R., et al., *Response of human breast cancer cells to heat shock and chemotherapeutic drugs.* Cancer Res, 1992. **52**(13): p. 3648-54.

19. Didelot, C., et al., *Anti-cancer therapeutic approaches based on intracellular and extracellular heat shock proteins.* Curr Med Chem, 2007. **14**(27): p. 2839-47.

20. Creagh, E.M., R.J. Carmody, and T.G. Cotter, *Heat shock protein 70 inhibits caspase-dependent and -independent apoptosis in Jurkat T cells.* Exp Cell Res, 2000. **257**(1): p. 58-66.

21. Gyrd-Hansen, M., J. Nylandsted, and M. Jaattela, *Heat shock protein 70 promotes cancer cell viability by safeguarding lysosomal integrity.* Cell Cycle, 2004. **3**(12): p. 1484-5.

22. Bao, X.Q. and G.T. Liu, *Induction of overexpression of the 27- and 70-kDa heat shock proteins by bicyclol attenuates concanavalin A-Induced liver injury through suppression of nuclear factor-kappaB in mice.* Mol Pharmacol, 2009. **75**(5): p. 1180-8.

23. Dudeja, V., et al., *Heat shock protein 70 inhibits apoptosis in cancer cells through simultaneous and independent mechanisms.* Gastroenterology, 2009. **136**(5): p. 1772-82.

24. Beckham, J.T., et al., *Role of HSP70 in cellular thermotolerance.* Lasers Surg Med, 2008. **40**(10): p. 704-15.

25. Mirkes, P.E., et al., *Heat shock protein 70 (Hsp70) protects postimplantation murine embryos from the embryolethal effects of hyperthermia.* Dev Dyn, 1999. **214**(2): p. 159-70.

26. Huang, L., N.F. Mivechi, and D. Moskophidis, *Insights into regulation and function of the major stress-induced hsp70 molecular chaperone in vivo: analysis of mice with targeted gene disruption of the hsp70.1 or hsp70.3 gene.* Mol Cell Biol, 2001. **21**(24): p. 8575-91.

27. Ahn, S.G., et al., *The loop domain of heat shock transcription factor 1 dictates DNA-binding specificity and responses to heat stress.* Genes Dev, 2001. **15**(16): p. 2134-45.

28. Massey, A.J., *ATPases as drug targets: insights from heat shock proteins 70 and 90.* J Med Chem. **53**(20): p. 7280-6.

29. Evans, C.G., L. Chang, and J.E. Gestwicki, *Heat shock protein 70 (hsp70) as an emerging drug target.* J Med Chem. **53**(12): p. 4585-602.

30. Neckers, L. and K. Neckers, *Heat-shock protein 90 inhibitors as novel cancer chemotherapeutic agents.* Expert Opin Emerg Drugs, 2002. **7**(2): p. 277-88.

31. Russell, J.S., et al., *Enhanced cell killing induced by the combination of radiation and the heat shock protein 90 inhibitor 17-allylamino-17-demethoxygeldanamycin: a multitarget approach to radiosensitization.* Clin Cancer Res, 2003. **9**(10 Pt 1): p. 3749-55.

32. Dote, H., et al., *ErbB3 expression predicts tumor cell radiosensitization induced by Hsp90 inhibition.* Cancer Res, 2005. **65**(15): p. 6967-75.

33. Aghdassi, A., et al., *Heat shock protein 70 increases tumorigenicity and inhibits apoptosis in pancreatic adenocarcinoma.* Cancer Res, 2007. **67**(2): p. 616-25.

34. Williamson, D.S., et al., *Novel adenosine-derived inhibitors of 70 kDa heat shock protein, discovered through structure-based design.* J Med Chem, 2009. **52**(6): p. 1510-3.

35. Leu, J.I., et al., *A small molecule inhibitor of inducible heat shock protein 70.* Mol Cell, 2009. **36**(1): p. 15-27.

36. Schust, J., et al., *Stattic: a small-molecule inhibitor of STAT3 activation and dimerization.* Chem Biol, 2006. **13**(11): p. 1235-42.

37. Armitage, B.A., *Antigene leaps forward through an open door.* Nat Chem Biol, 2005. **1**(4): p. 185-6.

38. Boffa, L.C., et al., *Invasion of the CAG triplet repeats by a complementary peptide nucleic acid inhibits transcription of the androgen receptor and TATA-binding protein genes and correlates with refolding of an active nucleosome containing a unique AR gene sequence.* J Biol Chem, 1996. **271**(22): p. 13228-33.

39. Nickols, N.G., et al., *Modulating hypoxia-inducible transcription by disrupting the HIF-1-DNA interface.* ACS Chem Biol, 2007. **2**(8): p. 561-71.

40. Phillips, P.A., et al., *Triptolide induces pancreatic cancer cell death via inhibition of heat shock protein 70.* Cancer Res, 2007. **67**(19): p. 9407-16.

41. Westerheide, S.D., et al., *Triptolide, an inhibitor of the human heat shock response that enhances stress-induced cell death.* J Biol Chem, 2006. **281**(14): p. 9616-22.

42. Formica, J.V. and W. Regelson, *Review of the biology of Quercetin and related bioflavonoids.* Food Chem Toxicol, 1995. **33**(12): p. 1061-80.

43. Prior, R.L., *Fruits and vegetables in the prevention of cellular oxidative damage.* Am J Clin Nutr, 2003. **78**(3 Suppl): p. 570S-578S.

Table 1-1. HSP70 family and properties.

Name	Altern	Homo-logy	HSP Locus	Localization	Stress Inducible
Hsp70-1a	70,72,70-1	100	A1A	Cyt, Nucl	Yes
Hsp70-1b	70, 72, 70-1	99	A1B	Cyt, Nucl	Yes
Hsp70-1t	70-hom	91	A1L	Cyt, Nucl	No
Hsp70-2	70-3,A2	84	A2	Cyt, Nucl	No
Hsp70-5	Bib, Grp78	64	A5	ER	No
Hsp70-6	70B'	85	A6	Cyto, Nucl	Yes
Hsc70	70-8,73	86	A8	Cyto, Nucl	No
mt Hsp 70	Mort,Grp75		A9	Mito	No

Table 1-2. Heat shock elements of stress-inducible human HSPA1A, A1B and A6.

(Bases of HSPA1B and HSPA6 that are different from HSPA1A are in bold size)

	Site 1	Site 2	Site 3	Site 4
HspA1A	G CGAAA	ACCCT	GGAAT	ATTCC C
HSPA1B	G CGAAA	**C**CCCT	GGAAT	ATTCC C
HSPA6	G **G**GAA**G**	**GTG**C**G**	GGAA**G**	**G**T**G**C**G** C

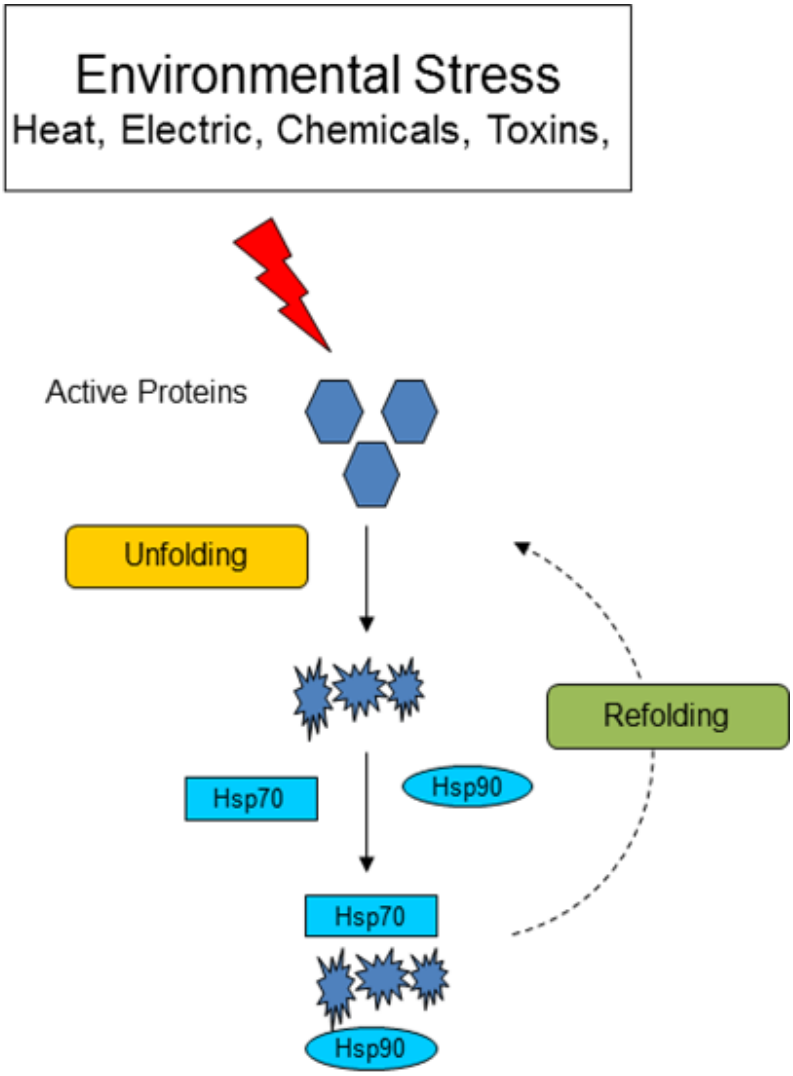

Figure 1.1 General role of heat shock proteins 70 (Hsp70) and 90 (Hsp90) as protein chaperones in the stress response.

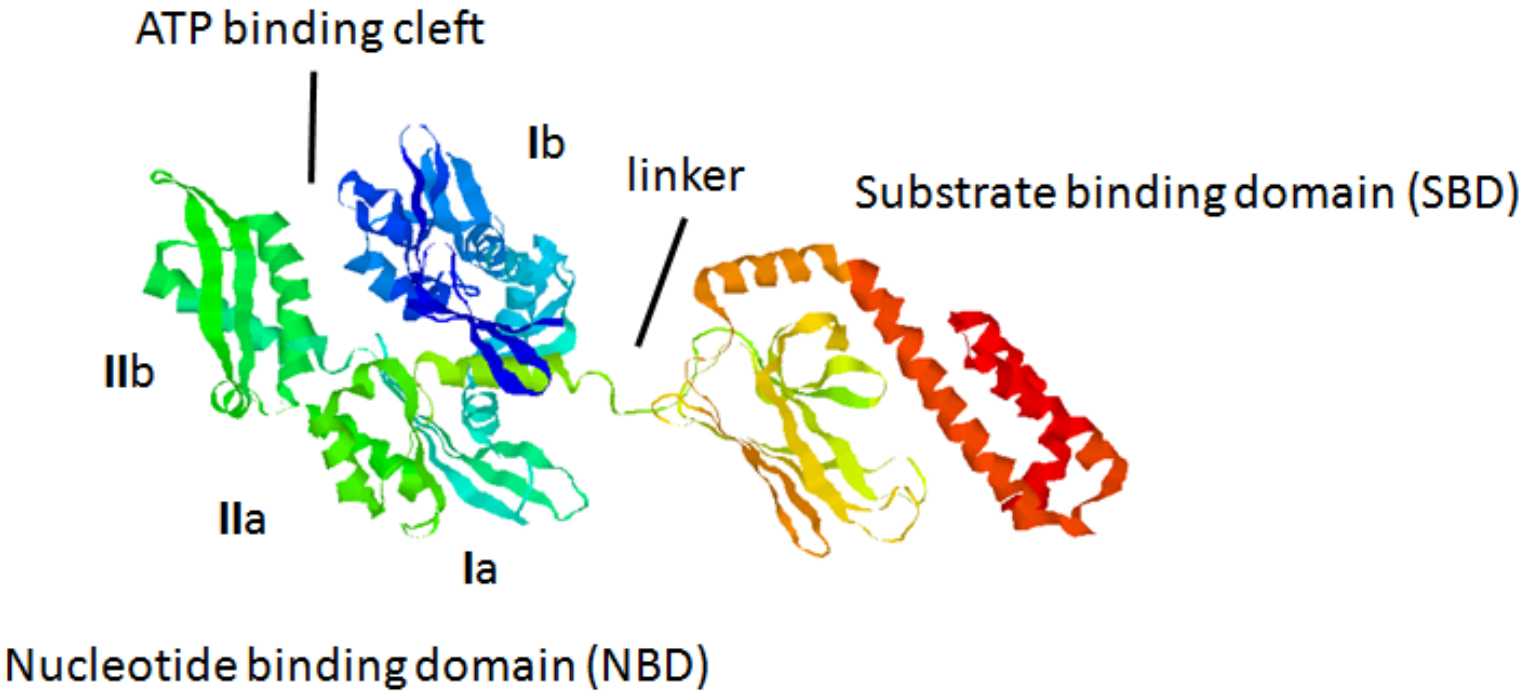

Figure 1.2 Structure of E. coli heat shock protein 70 (HSP70) (PDB code: 2KHO)[29]

A

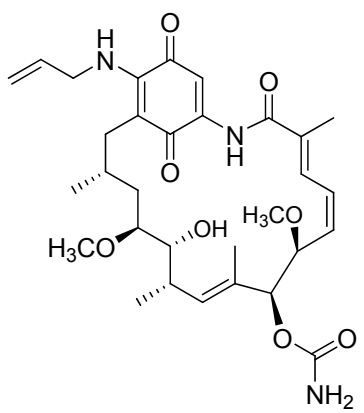

17-Allylamino-17-demethoxygeldanamycin (17-AAG)

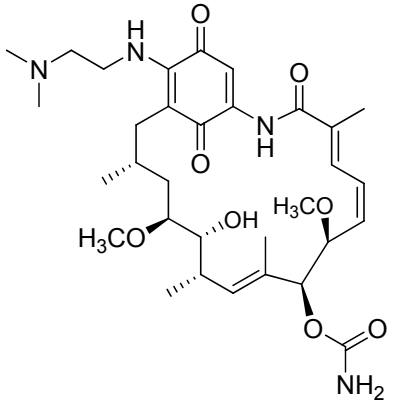

17-(Dimethylaminoethylamino)-17-demethoxygeldanamycin (17-DMAG)

B

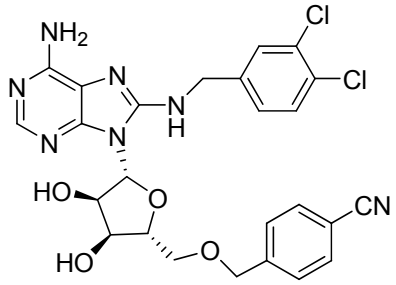

VER-155008

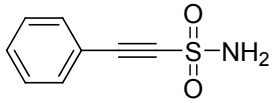

Phenylethynesulfonamide (PES)

Figure 1.3 (A) Known inhibitors that target HSP90 (B) Known inhibitors that target HSP70 [28].

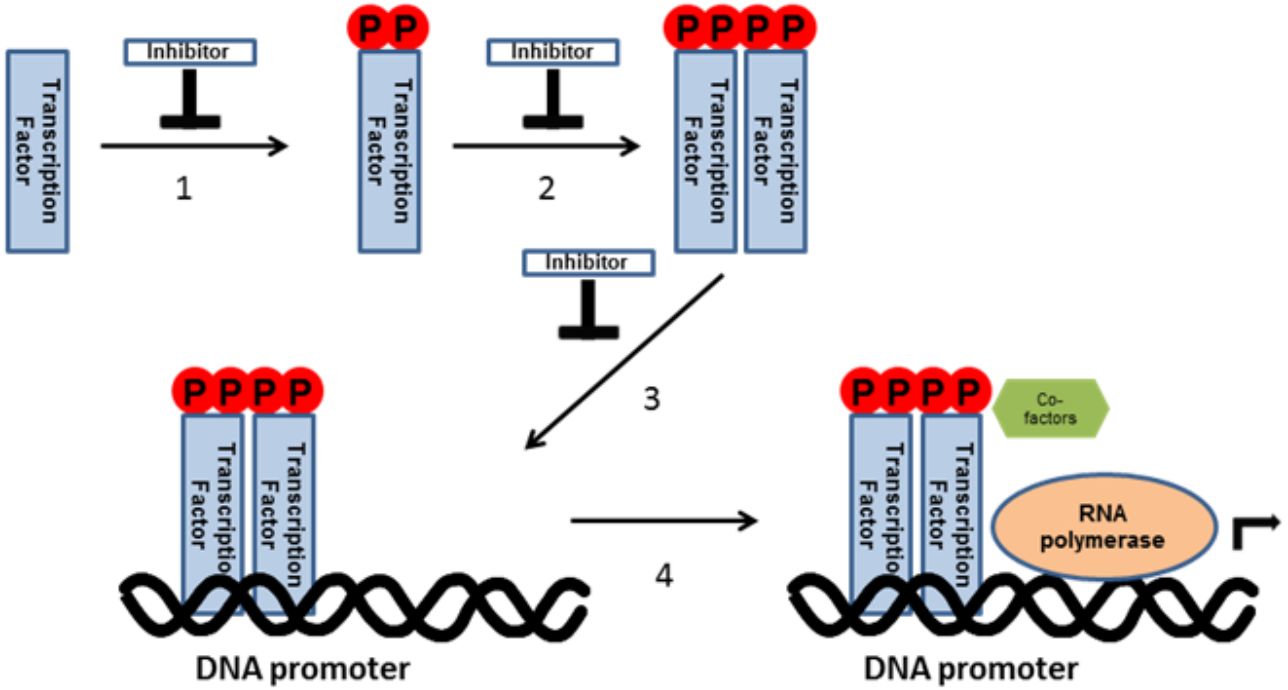

Figure 1.4 General sequences of events leading to activation of protein expression showing the various steps which inhibitors can target. Step 1. Phosphorylation; Step 2. Oligomerization; Step 3. Binding to promoter; Step 4. Initiation of transcription. (The order of step 1, step2, and step 3 are variable depending on the transcription factor and cell line)

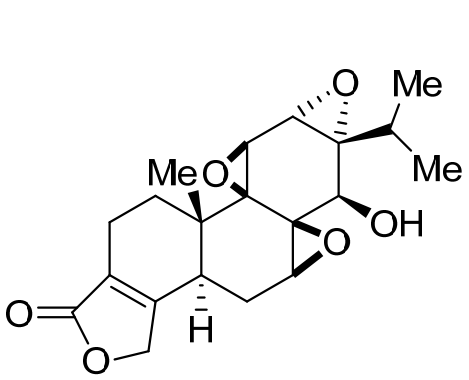

Triptolide

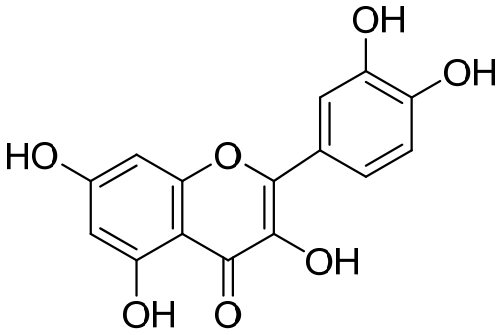

Quercetin

Figure 1.5 Natural product inhibitors of HSP70 expression.

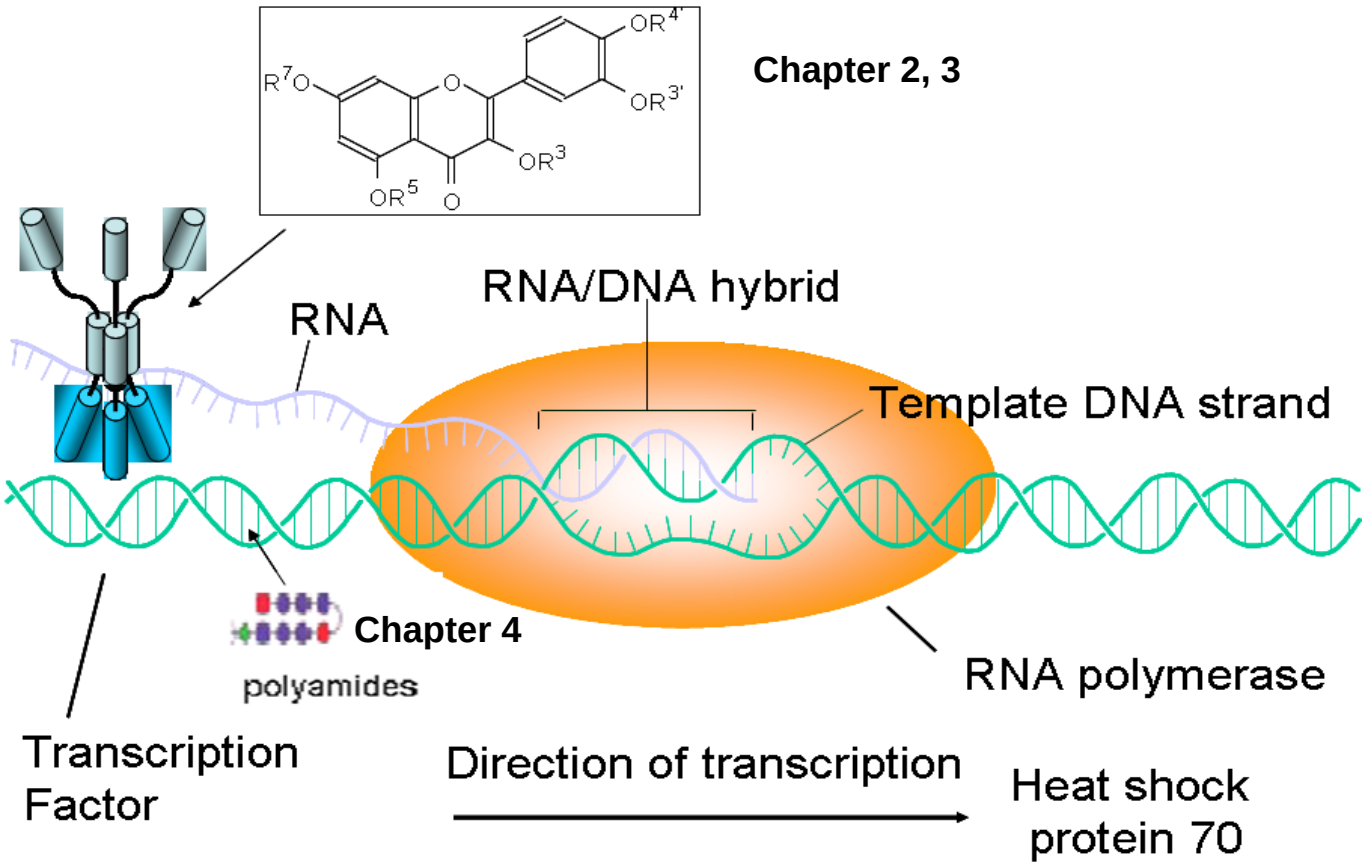

Figure 1.6 Subject areas of this dissertation

Chapter 2.

Inhibition of Heat Shock Induction of Heat Shock Protein 70 and Enhancement of Heat Shock Protein 27 Phosphorylation by Quercetin Derivatives

The text of this chapter was taken in part from a manuscript coauthored with Kao Jeffrey L-F, Hilliard Carolyn A, Pandita Raj K, Roti Roti Joseph L, Hunt Clayton R, Taylor John-Stephen (Washington University in St Louis).

(*Journal of Medicinal Chemistry*, **2009**; 52(7); 1912-1921.)

Abstract

Inhibitors of heat-induced heat shock protein 70 (HSP70) expression have the potential to enhance the therapeutic effectiveness of heat-induced radiosensitization of tumors as well as other anti-cancer treatments. Among known small molecule inhibitors, quercetin has the advantage of being easily modified for structure-activity studies. Herein, We report the ability of five monomethyl and five carbomethoxymethyl derivatives of quercetin to inhibit heat-induced HSP70 expression and enhance HSP27 phosphorylation in human cells. While quercetin and several derivatives inhibit HSP70 induction and enhance HSP27 phosphorylation at Ser78, other analogues selectively inhibit HSP70 induction without enhancing HSP27 phosphorylation that would otherwise aid in cell survival. We also show that good inhibitors of HSP70 induction are also good inhibitors of both CK2 and CamKII, kinases that are known to activate HSP70 expression by phosphorylation of heat shock transcription factor 1. Derivatives that show poor inhibition of either or both kinases are not good inhibitors of HSP70 induction, suggesting that quercetin's effectiveness is due to its ability to inhibit both kinases.

Introduction

Recently it has been shown that inhibition of HSP70 in tumor cells by either a gene knockout [1] or by antisense agents [2] enhances heat-induced radiosensitization (HIR) and tumor apoptosis. It would be therefore highly desirable to have a small molecular inhibitor of heat induced HSP70 that could be administered either prior to HIR to further enhance killing or directly as part of anti-cancer chemotherapy.

Heat induction and regulation of HSP70 is a rather complicated process, involving initial release of the heat shock transcription factor 1 (HSF1) from HSP90, followed by trimerization, translocation into the nucleus, and then binding to the heat shock element (HSE) (Figure 2.1) [3-5]. For transcription to occur the trimer must first be activated by phosphorylation at serine 230 with calcium/calmodulin kinase II (CamKII) [6] and/or threonine 142 by casein kinase 2 (CK2) [7]. In contrast, phosphorylation at other sites down regulates the transcriptional activity of HSF1. For example, phosphorylation at serine 121 by mitogen activated kinase 2 (MK2) causes unfolding of HSF1 and rebinding to HSP90 [8]. Likewise, phosphorylation of serine 307 by ERK or serine 363 by JNK inactivates HSF1 [9].

A number of small molecule inhibitors of heat-induced HSP70 expression have been reported, the most effective of which are triptolide and quercetin (Figure 2.2) [10]. Triptolide is a highly functionalized molecule that has been found to prevent heat shock HSF1 from activating transcription in the steps following trimerization, phosphorylation and DNA binding [11]. Quercetin, on the other hand, is a structurally much simpler natural product of the flavone family, that has been reported to have a wide variety of biological activities [12, 13], one of which is the inhibition of heat-induced HSP70

expression by as yet unknown mechanisms [14, 15]. Quercetin inhibits a number of kinases [16], including CK2 which has been shown to enhance HSP70 induction through phosphorylation of HSF1 threonine 142 [7]. It is therefore possible that quercetin inhibits HSP70 induction by blocking phosphorylation of HSF1 by CK2 and/or CamKII [6]. Quercetin is also metabolized *in vivo* and it is possible that some of the metabolites are the active pharmaceutical agents [17].

To guide the design and synthesis of biotinylated probes for identifying the target(s) of quercetin inhibition of heat-induced HSP70 expression, and to enhance its specificity, we synthesized all of the mono-methyl (Figure 2.3, 2.4) and selected carbomethoxymethyl (Figure 2.5, 2.6, 2.7) derivatives of quercetin. Systematic methylation ("methyl scanning") has been previously proposed and validated as a general method for mapping the interactions of biologically active molecules with receptors and for designing affinity probes [18, 19]. The quercetin derivatives were tested for their ability to inhibit heat-induced HSP70 expression and modulate HSP27 phosphorylation in human Jurkat cells and human HeLa cells, respectively, by Western blot analysis. Two classes of active agents were discovered, one that both inhibits HSP70 induction and enhances HSP27 phosphorylation, and another that inhibits HSP70 induction without enhancing HSP27 phosphorylation. Quercetin and derivatives that inhibited HSP70 induction were also found to inhibit both CK2 and CamKII kinases. On the other hand, derivatives that showed poor inhibition of either or both kinases did not inhibit HSP70 induction, indicating that quercetin's effectiveness is due to its ability to inhibit more than one enzyme.

Results

Chemistry

Synthesis of O-alkylated quercetin derivatives. To determine the importance of individual hydroxyl groups on the inhibition of heat-induced HSP70 expression and other biological activities, I synthesized the mono-methylated quercetin derivatives **D2**, **D3**, **D4**, **D6**, and **D7** according to previously reported procedures [20]. Because we ultimately intend to attach affinity tags such as biotin to quercetin to help in identifying the protein target(s) of quercetin activity, I also synthesized a number of carboxymethylated derivatives by the same synthetic route (Figure 2.5, 2.6, 2.7). Thus, quercetin was benzylated to give 20% of the tribenzyl derivative **2** and 60% of the tetrabenzyl derivative **1**. The tribenzyl derivative was selectively carbomethoxymethylated at the 3'-OH to give **4**, whereas the tetrabenzyl derivative was carbomethoxymethylated at the 5-OH to give **3**. The products were debenzylated with palladium hydroxide and hydrogen to afford the methyl esters **D8** and **D1** respectively.

To carbomethoxymethylate positions **3** and **7**, I utilized the 3', 4'-diphenylmethylene derivative of quercetin, compound **5** (Figure 2.6). This derivative reacted with methylbromoacetate under basic conditions at the 3-OH to give **6**, which then afforded the carboxymethyl derivative **D5** following removal of the diphenylmethylene group by refluxing with acetic acid, which also hydrolyzed the ester. To obtain the O7 derivative, the 3-OH of compound **5** was first benzylated to give **7** which was then carbomethoxymethylated at the 7 position. Removal of the benzyl and diphenylmethylene groups was carried out in two steps by hydrogenolysis with palladium

hydroxide followed by hydrolysis with acetic acid and water which also unexpectedly hydrolyzed the ester to the carboxymethyl product D**9**.

Many attempts to methylate **D9** to produce **D10** were unsuccessful and so other synthetic routes were investigated. The best of these involved a previously reported method for selectively methylating or benzylating the 7-OH of quercetin by treatment of quercetin pentaacetate with the alkylating agent in the presence of potassium carbonate and potassium iodide in acetone [22]. Thus treatment of quercetin pentaacetate [23] under these conditions with methyl bromoacetate yielded compound **10** which could be deacetylated in high yield under neutral conditions with N-methyl-2-dimethylaminoacetohydroxamic acid [24] to give **D10** (Figure 2.7). This deacetylation method was chosen as more basic conditions, such as sodium methoxide and methanol at 0 ^{o}C, tend to result in air oxidation of the product [25] whereas more acidic conditions lead to hydrolysis of the methyl ester on the other hand.

Structural characterization. The sites of alkylation in all the compounds were confirmed by analysis of the coupling patterns in the 1D ^{1}H NMR spectra together with correlations in the COSY, HMQC and HMBC spectra. As an illustration, the B ring hydrogens H5' and H6' of **D1** (Figure 2.8) and **D10** (Figure 2.9) were assigned by the large ortho coupling, and the strong crosspeak in the COSY spectrum (crosspeak a, panel A). These assignments led to the assignment of H2' through meta coupling with H6' that could be detected in the 1D ^{1}H NMR spectrum. The carbons directly attached to these protons could then be assigned through the HMQC spectra (Panel B). The hydrogen signal at 10 ppm in **D1** could then be assigned to the 4'-OH by the presence of a long range correlation to C5' at 116 ppm (Figure 2.8, crosspeak e) and to a quaternary carbon

signal at 146 ppm (crosspeak b) together with the absence of a correlation to C2' in the HMBC spectrum (panel C). The signal at 146 ppm could therefore be assigned to C3' which in turn showed a correlation to the α hydrogen of the carbomethoxymethylene group (crosspeak d, panel C). The position of the carbomethoxymethylene group in **D10** could be assigned to O7 via a correlation between the α-methylene protons and a quaternary carbon signal at 162 ppm (Figure 2.9, crosspeak d in panel C). The signal at 162 ppm could be assigned to C7 via multiple bond correlations to the two meta coupled protons in the A ring in the HMBC spectrum (crosspeaks b & c in panel C).

Biological Studies

Inhibition of heat induced HSP70 expression by quercetin derivatives. I collaborated with Dr Clayton Hunt to examine the ability of the quercetin and its derivatives to inhibit heat induced HSP70 expression, we chose human Jurkat cells due to their low basal level of HSP70 expression and the large induction upon heat shock. Western blot analysis of the cellular proteins in Jurkat cells following heat shock revealed that pre-heat treatment with the quercetin derivatives **D1**, **D2**, **D7** and **D10** all had a similar inhibitory effect on HSP70 induction as did quercetin, indicating that the 3' and 7 hydroxyls are important for activity (Figures 2.10A, Table 1). Compound **D1** which bears a carbomethoxymethyl group at O3' is not as good an inhibitor as **D2,** which bears a methyl group, indicating that the 3' hydroxyl group occupies a more sterically constrained site in the target protein than does the 7 hydroxyl group. Compound **D9**, which bears a carboxylic acid group at O7, does not inhibit HSP70 like **D10** which bears an ester group, presumably because it forms a salt at neutral pH that greatly reduces its membrane permeability.

Enhancement of HSP27 phosphorylation. In examining the effects of quercetin treatment on other heat shock proteins, we found that quercetin enhances HSP27 phosphorylation at Ser78 in the absence of heat shock. Phosphorylated HSP27 has anti-apoptotic activity [26] which would tend to counteract any lethal effects achieved from inhibiting HSP70 induction. Thus, it would be highly desirable to inhibit HSP70 without enhancing phosphorylation of HSP27. The HSP27 studies were carried out in HeLa cells, which unlike Jurkat cells, have a high basal level of HSP27, making it easier to detect drug-induced phosphorylation of HSP27 by Western analysis. HeLa cells, however, are not as suitable for concurrent inhibition studies of HSP70 induction since they have high basal level of HSP70. Only **D7** and **D10** showed enhancement of HSP27 phosphorylation in HeLa cells, and both of these compounds also showed good to strong inhibition of HSP70 induction in Jurkat cells (Figure 2.10 B, Table 1). On the other hand, **D1** and **D2** which were also good inhibitors of HSP70 induction did not activate HSP27 phosphorylation.

Effect of quercetin on HSF1 binding to the HSE. In order to gain insight into the mechanism by which quercetin inhibits HSP70 induction, gel mobility shift analysis was carried out to examine binding of heat shock element (HSE) DNA by heat shock transcription factor 1 (HSF1), the transcription factor responsible for heat induced HSP70 gene transcription (Figure 2.11A upper panel). No HSF1/HSE complex was detected with nuclear extracts prepared from control, non-heated Jurkat cells but the complex was readily detected with extracts prepared immediately following a 43 °C 30 min heat shock. The amount of complex increased by 1 h post-heat then declined by 4 h post-heat and returned to control levels by 8 h post-heat. In Jurkat cells treated 1 h prior to heat shock

with quercetin, however, only a very low level of complex formed in extracts from heated cells. Since an identical low level of complex was also detected in extracts from quercetin-treated but non-heated cells, this response appears to be due to drug induced cell stress not heat. In contrast to Jurkat cells, HeLa cells displayed an accelerated loss of HFS1/HSE complex during recovery from heat shock with nearly undetectable levels by 4 h post-heat (Figure 2.11A, lower panel). Moreover, quercetin treatment did not inhibit HSF1/HSE complex formation in heated HeLa cells as it did in Jurkat cells suggesting a complex interaction between the drug and possibly multiple cell specific factors.

Further information about the mechanism by which quercetin inhibits heat-induced HSP70 expression was obtained by Western blot analysis of the nuclear extracts for the presence and size of the HSF1 protein (Figure 2.11B). In non-heated Jurkat control cells, HSF1 is not detected in nuclear extracts while only a very low level can be detected in HeLa cells. Surprisingly, nuclear extracts from quercetin treated Jurkat cells contained significant levels of HSF1 while similar HeLa cell extract contained the very low levels detected in untreated extracts. In both Jurkat and Hela cells, heating increased HSF1 nuclear extract levels and induced a corresponding decrease in gel mobility that reflects the increased level of heat-induced phosphorylation required for transcriptional activity [6]. While quercetin treatment did not block the heat-induced increase in nuclear HSF1 levels in either Jurkat and HeLa cells, the drug did inhibit the decrease in HSF1 mobility, presumably by inhibiting the critical phosphorylation modifications required for transcription activation. Thus in Jurkat cells, quercetin treatment appears to affect at least two steps in heat induced HSP70 expression, HSF1 post translational modification and

DNA binding activity. Quercetin treatment of HeLa cells does not result in loss of HSF1 DNA binding activity but does appear to inhibit heat induced phosphorylation.

Kinase inhibition assays. We then determined whether or not the activity of the quercetin analogs correlated with their ability to inhibit either or both CKII and CamKII kinases that have previously been shown to phosphorylate HSF1. I used an enzyme-linked inhibition assay that utilizes luciferase to quantify the amount of ATP remaining in a kinase reaction [27]. The IC_{50} values for quercetin and D1-D10 are listed in Table 2 in comparison to their relative ability to inhibit HSP70 induction. Good inhibition of HSP70 induction appears to correlate with good inhibition of both CK2 and CamKII. Quercetin derivatives that showed poor inhibition (IC_{50} > 100 μM) of either or both kinases showed little to no ability to inhibit heat induction of HSP70. The only exception was D9 which was a very good inhibitor of both kinases, but showed no ability to inhibit HSP70 induction, which we attribute to the presence of a carboxylate which reduces membrane permeability.

Discussion

Inhibition of heat-induced HSP70 expression has been shown to enhance radiosensitization by heat [1, 2] and thus small molecule inhibitors of HSP70 induction have potential therapeutic value. Quercetin has long been known to inhibit heat-induced HSP70 expression, though the exact mechanism is unclear. The results herein suggest that quercetin treatment blocks heat-induced phosphorylation of the HSF1 transcription factor that is responsible for inducing HSP70 expression. In Jurkat, but not HeLa cells an

additional level of inhibition appears to be loss of HSF1 HSE element binding capacity, which has also been reported in quercetin/heated human COLO 320DM cells [28]. Unfortunately, quercetin is also well known to affect many additional biological processes, probably as a result of its ability to inhibit a number of different kinases [16], which diminishes its potential as a therapeutic. On the other hand it seems reasonable that the specificity for inhibiting HSP70 induction could be increased by selective modification of quercetin. Also identifying the target of quercetin responsible for inhibiting HSP70 induction could aid in the development of more selective inhibitors. To these ends we have been able to show that the C7 and C3' hydroxyls on quercetin can be derivatized with a bulky carbomethoxymethyl group without affecting its ability to inhibit heat induced HSP70, and could therefore be used to attach a biotin affinity probe.

The finding that the 3' and 7 hydroxyls of quercetin can be modified without affecting inhibition of heat-induced HSP70 expression suggested modification of these hydroxyls might also increase the selectivity by interfering with binding to other protein targets. Quercetin has been crystallized with a number of kinases, and inspection of the crystal structures reveals that the 7-OH of quercetin is buried in the Hck kinase complex [29] as well as in the F1-ATPase [30] and therefore O7 derivatives would not be expected to inhibit these enzymes. The O7 position of quercetin is not buried, however, in the phosphoinositide 3-kinase complex [31], but the O3'-position is, suggesting that quercetin derivatized at both the O7 and O3' positions would also not inhibit any of these enzymes, but would still inhibit HSP70 induction. This class of doubly derivatized quercetin remains to be synthesized and examined for its ability to inhibit HSP70 induction.

Given that quercetin is a well known kinase inhibitor, and that the pathway for heat induction of HSP70 expression involves phosphorylation of the heat shock factor 1 (HSF1) by CK2 and CamKII kinases, we investigated whether the two might be correlated. It has previously been established that quercetin is an inhibitor of CK2 kinase, but its ability to inhibit CamKII kinase has not been reported. we now show that quercetin is also a good inhibitor of CamKII and that quercetin derivatives **D1**, **D2**, **D7** and **D10**, that are good inhibitors of HSP70 induction, are also good inhibitors of both CK2 and CamKII kinases. Quercetin derivatives that were good inhibitors of only one or neither of the two kinases, however, were not good inhibitors of HSP70 induction. It would seem that full activation of HSP70 by HSF1 may only require phosphorylation by either CK2 or CamKII, both of which quercetin and derivatives **D1**, **D2**, **D7** and **D10** are able to inhibit due to their broader specificity.

The ability of quercetin to enhance phosphorylation of HSP27 has not been previously recognized. Phosphorylation of serine 78 has been shown to be carried out by MAPKAP2 kinase [32], which in turn is activated by MAPK kinase. It is not clear how quercetin activates phosphorylation of HSP27, as inhibiting any of the kinases in the pathway should abolish activation. Activation of HSP27 has been associated with poor prognosis and resistance to chemotherapy or radiation [33] and so the quercetin analogs **D1** and **D2** which retain the ability to inhibit HSP70 induction without inducing HSP27 phosphorylation may have superior therapeutic properties to **D7** and **D10**.

Conclusion

One goal of this study was to find derivatives of quercetin that could be elaborated into affinity probes to identify the targets responsible for inhibition of heat-induction of HSP70. We identified two such derivatives, which are now in the process of being converted to biotinylated probes. In the course of evaluating these derivatives, we discovered that their ability to inhibit HSP70 induction correlated with their ability to inhibit both CK2 and CamKII, kinases that are known to activate HSP70 transcription by phosphorylating HSF1. Derivatives that show poor inhibition of either or both kinases are poor inhibitors of HSP70 induction, suggesting that HSP70 expression can be activated by either kinase. This would appear to be a case in which making the drug more specific reduces its effectiveness, suggesting that future screens for HSP70 inhibitors be carried out for activity against both kinases. In collaboration with Dr Clayton Hunt, I have also discovered that quercetin enhances the phosphorylation of HSP27 required for its anti-apoptotic action, which would serve to diminish the radiosensitizing or antitumor effects of inhibiting HSP70 induction. Two derivatives of quercetin, **D1** and **D2**, were found, however, that could inhibit HSP70 induction without enhancing HSP27 phosphorylation, but the degree to which they may be able to enhance heat-induced radiosensitization remains to be determined. In addition to probing the mechanism of inhibition of HSP70 induction, this family of methylated quercetin derivatives might also be useful for mapping out interactions with other targets.

Experimental section

Abbreviations

17AAG, 17-allylamino-17-demethoxy-geldanamycin; 17DMAG, 17-(dimethylaminoethylamino)-17-demethoxygeldanamycin; CaMKII, Ca^{2+}/calmodulin-dependent protein kinase II; CK2, casein inase II; COSY, correlation spectroscopy; DCM, dichloromethane; DMEM, dulbecco's modified essential medium; DMF, dimethyl formamide; DMSO, dimethyl sulfoxide; DTT, dithiothreitol; EDTA, ethylenediaminetetraacetic acid; ERK, extracellular signal-regulated protein kinase; ESI, electrospray ionization; EtOAc, ethyl acetate; EtOH, ethanol; FAB, fast-atom bombardment; HIR, heat-induced radiosensitization; HMBC, heteronuclear multiple bond coherence spectroscopy; HMQC, heteronuclear multiple quantum coherence spectroscopy; HSE, heat shock element; HSF1, heat shock factor 1; HSP, heat shock protein; IC50, 50% inhibitory concentration; JNK, c-Jun N-terminal kinase; MeOH, methanol; MK2(MAPKAP2), mitogen-activated protein kinase activated protein kinase 2; RPMI, roswell park memorial institute; Ser 78, serine 78; THF, tetrahydrofuran; TLC, thin layer chromatography; Tris, tris(hydroxymethyl)aminomethane;

General procedures

Reagents and solvents were obtained from either Sigma Aldrich or Alfa Aesar. Anhydrous solvents were distilled and then stored over activated 5 Å molecular sieves. All other commercial materials were used without further purification unless otherwise stated. Analytical thin-layer chromatography was performed on Aldrich Silica gel 60 F_{254} plates (0.25 mm) and compounds were visualized with UVG-54 mineral light UV lamp at

254 nm. Flash column chromatography was conducted using the indicated solvent on E. Merck silica gel 60 (40-63 μm). ^{1}H NMR and ^{13}C NMR spectra were recorded with Mercury-300, Inova-500 and Inova-600 (Varian Assoc., Palo Alto, CA) spectrometers and the data were processed with VNMR software. Proton and carbon chemical shifts were measured in parts per million (ppm) downfield from an internal TMS standard. Proton spectra were obtained in [D_6] DMSO with a 8200-Hz spectral width collected into 32K data points. Carbon spectra were obtained with a 34000-Hz spectral width collected into 64k data points. The gradient COSY experiments were collected with a spectral width of 8200 Hz and 2048 complex points in F2 dimension and 512 real points in F1 dimension. The proton-detected heteronuclear multiple quantum coherence (HMQC) spectra were recorded using a 0.3 s ^{1}H-^{13}C nulling period. The 90^{o} 1H pulse width was 9.8 μs and the 90^{o} ^{13}C pulse width was 12.5 μs. Phase sensitive 2D spectra were obtained by employing the Hypercomplex method. A 2 x 256 x 2048 data matrix with 16 scans per t1 value was collected. Gaussian line broadening was used in weighting both the t2 and the t1 dimension. After two-dimensional Fourier transform, the spectra resulted in 512 x 2048 data points, which were phase and baseline, corrected in both dimensions. Analytical HPLC purity test was performed in System Gold High Pressure Liquid Chromatography with a solvent pump module 125 and model 168 diode array UV detector. A Waters XTerra MS C18 (5 μm, 6×250 mm) reverse phase column was used. Generally a linear gradient of solvent B (80% acetonitrile/water/0.1% trifluoroacetic acid) in solvent A (water/0.1% trifluoroacetic acid) was from 10% to 30% at the first 20 minutes, then from 30% to 50% in the following 10 minutes, and all the way up to 100%

in the next 10 minutes. In the final 15 minutes, percentage of solvent B dropped back from 100% to 10%.

The organic synthesis of mono-methyl quercetin derivatives were based on literature report [20] (Figure 2.3, 2.4). Compounds D6, D1, D3, D7 were additionally re-crystallized twice before further studies on bioactivities. Compound D4 was separated and purified by HPLC to afford a purity above 95%, before further biological studies.

Compound D6. ^{1}H NMR ([D_6]DMSO, 300 MHz) [Figure 2.12] δ 10.73 (s, 1H), 9.49 (s, 1H), 9.28 (s, 1H), 8.67 (s, 1H), 7.65 (d, J=2Hz, 1H), 7.50 (d, J=8Hz, 1H), 6.89 (d, J=8Hz, 1H), 6.48 (d, J=2Hz, 1H), 6.38 (d, J=2Hz, 1H), 3.85 (s, 3H)

Compound D2. ^{1}H NMR ([D_6]DMSO, 300 MHz) [Figure 2.13] δ 10.78 (s, 1H), 9.76 (s, 1H), 9.45 (s, 1H), 7.73(d, J=2Hz, 1H), 7.67 (dd, J=8Hz, 2Hz, 1H), 6.92 (d, J=8Hz, 1H), 6.46 (d, J=2Hz, 1H), 6.18 (d, J=2Hz, 1H), 3.85(s, 3H)

Compound D3. ^{1}H NMR ([D_6]DMSO, 300 MHz) [Figure 2.14] δ 12.46 (s, 1H), 10.82 (s, 1H), 9.49 (s, 1H), 9.36 (s, 1H), 7.67 (s, 1H), 7.64 (d, J=2Hz, 1H), 7.09 (s, J=8Hz, 1H), 6.43 (d, J=2Hz, 1H), 6.19 (d, J=2Hz, 1H), 3.85(s, 3H)

Compound D7. ^{1}H NMR ([D_6]DMSO, 300 MHz) [Figure 2.15] δ 9.65 (s, 1H), 9.51 (s, 1H), 9.31 (s, 1H), 7.73 (d, J=2Hz, 1H), 7.58 (d, J=8Hz, 1H), 6.90 (d, J=8Hz, 1H), 6.71 (d, J=2Hz, 1H), 6.36 (d, J=2Hz, 1H), 3.86 (s, 3H)

Compound D4. ^{1}H NMR ([D_4]CD_3OD, 300 MHz) δ 7.63 (d, J=2Hz, 1H), 7.55 (d, J=8Hz, 2Hz, 1H), 6.90 (d, J=8Hz, 1H), 6.41 (d, J=2Hz, 1H), 6.21 (d, J=2Hz, 1H), 3.79 (s, 3H).

The selective synthesis of mono-carbomethoxymethyl derivatives was conducted by similar routes with modifications (Figure 2.5, 2.6, 2.7), as illustrated below.

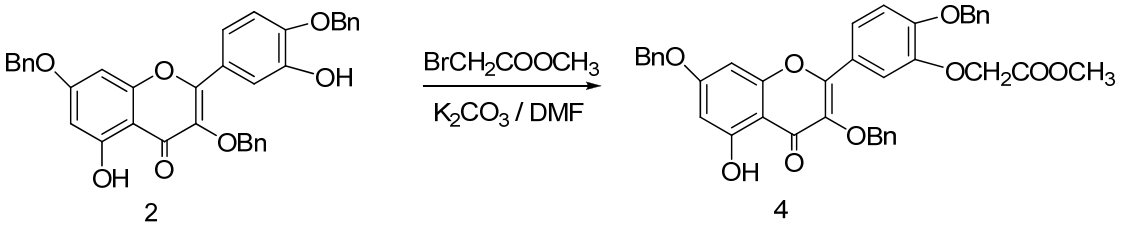

Compound 4. A solution of **2** (0.60 g, 1.1 mmol) in DMF (20 mL) was mixed with potassium carbonate (0.19 g, 1.4 mmol) under nitrogen. Methyl bromoacetate (0.160 g, 1.05 mmol) was then slowly added. The resulting solution was stirred at room temperature for 12 h, diluted with 40 mL of water and extracted with 60 mL ethyl acetate. The organic phase was washed with water, dried over anhydrous sodium sulfate and concentrated under reduced pressure. The residue was purified by flash column chromatography using DCM/Hexane (85:15) to afford 4 in 90% yield (0.58 g). ^{1}H NMR ($CDCl_3$, 300 MHz) [Figure 2.16] δ 12.67 (s, 1H, OH), 7.61 (d, J=2Hz, 1H), 7.60 (dd, J=9, 2Hz, 1H), 7.47-7.23 (m, 15H), 6.94 (d, J=9Hz, 1H), 6.45 (d, J=2Hz, 1H), 6.40 (d, J=2Hz, 1H), 5.20 (s, 2H), 5.08 (s, 2H), 5.05 (s, 2H), 4.55 (s, 2H), 3.72 (s, 3H). ^{13}C NMR ($CDCl_3$, 75 MHz) [Figure 2.17] δ 179.0 (C=O), 169.4 (COO), 164.8, 162.3, 156.9, 156.2, 151.3, 147.6, 137.8, 136.8, 136.6, 136.1, 129.0, 128.9, 128.6, 128.5, 128.4, 127.8, 127.6, 124.0, 123.6, 115.9, 114.0, 106.4, 98.9, 93.3, 74.7, 71.1, 70.7, 66.8 (OCH_2), 52.4 (OCH_3). MS (FAB) [M+Na^+] m/z 667.2, HRMS (FAB) $C_{39}H_{32}O_9Na$ [M+Na^+], calculated m/z 667.1944, found 667.1932.

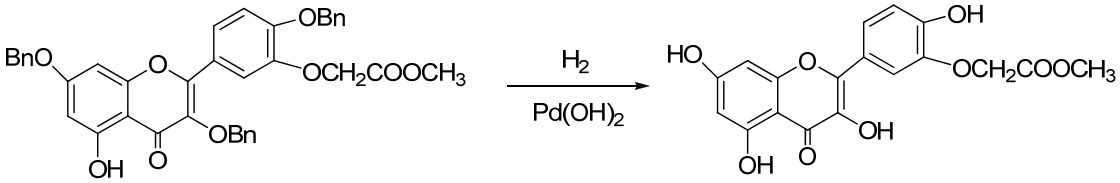

4 D1

Compound D1. A suspension of compound 4 (100 mg) was dissolved in a minimum amount of EtOH/THF (1:1) and treated with 10% palladium hydroxide (0.01 g). The suspension was stirred over night at room temperature under one atmosphere of hydrogen from a balloon. After filtration with Celite to remove the palladium, the filtrate was concentrated under reduce pressure, followed by a recrystallization with methanol and water to give D1 in 75% yield (43 mg). ^{1}H NMR ([D_6]DMSO, 300 MHz) [Figure 2.18] δ 10.79 (s, 1H, OH), 9.98 (s, 1H, OH), 9.48 (s, 1H, OH), 7.73 (dd, J=8.4, 2Hz, 1H), 7.69 (d, J= 2Hz, 1H), 6.98 (d, J=8.4Hz, 1H), 6.44 (d, J=2Hz, 1H), 6.19 (d, J=2Hz, 1H), 4.83 (s, 2H), 3.74 (s, 3H). ^{13}C NMR ([D_6]DMSO, 151 MHz) [Figure 2.19] δ 175.9 (C=O), 169.4 (COO), 163.9, 160.7, 156.1, 149.2, 146.2, 145.6, 135.9, 122.6, 121.9, 116.1, 114.2, 103.0, 98.2, 93.4, 65.9 (OCH_2), 51.8 (OCH_3). MS (ESI) [M+Na^+] m/z 397.1, HRMS (ESI) $C_{18}H_{14}O_9Na$ [M+Na^+], calculated m/z 397.0536, found 397.0543. Purity 97.7% (analyzed by HPLC under UV 280 nm)

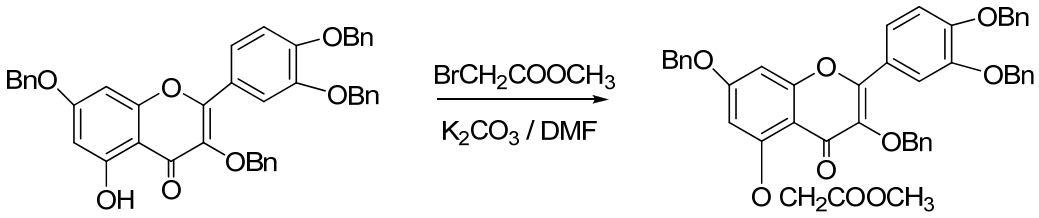

1 3

Compound 3. Two equivalents of methyl bromoacetate (0.46 g, 3.0 mmol) and anhydrous potassium carbonate (0.42 g, 3.0 mmol) were added to a solution of compound 1 (1.0 g, 1.5 mmol) in 35 mL DMF under nitrogen. After stirring for 24 h, the resulting mixture was worked up with 50 mL water and extracted with 100 mL EtOAc. The organic phase was washed with water, dried over anhydrous sodium sulfate and concentrated under reduced pressure. The red crude product was recrystallized with EtOAc to afford 3 in 92% yield (1.0 g). ^{1}H NMR ($CDCl_3$, 300 MHz) [Figure 2.20] δ 7.80 (d, J=2Hz, 1H), 7.62(dd, J=9, 2Hz, 1H), 7.55-7.29 (m, 20H), 7.02 (d, J=9Hz, 1H), 6.66 (d, J=2Hz, 1H), 6.41 (d, J=2Hz, 1H), 5.30 (s, 2H), 5.17 (s, 2H), 5.14 (s, 2H), 5.02 (s, 2H), 4.89 (s, 2H), 3.80 (s, 3H). ^{13}C NMR ($CDCl_3$, 75MHz) [Figure 2.21] δ 174.0 (C=O), 169.0 (COO), 162.8, 159.2, 158.9, 153.5, 150.8, 148.4, 140.0, 137.3, 137.2, 137.0, 135.7, 129.2, 129.0, 128.8, 128.8, 128.7, 128.4, 128.3, 128.2, 128.1, 128.0, 127.6, 127.4, 124.0, 122.4, 115.4, 114.0, 110.3, 98.9, 95.1, 74.3, 71.3, 71.1, 70.9, 66.8 (OCH_2), 52.7 (OCH_3) MS (FAB) $[M+Li]^+$ m/z 741.5. HRMS (FAB) $C_{46}H_{38}O_9Li$ $[M+Li^+]$, calculated m/z 741.2676, found 741.2677.

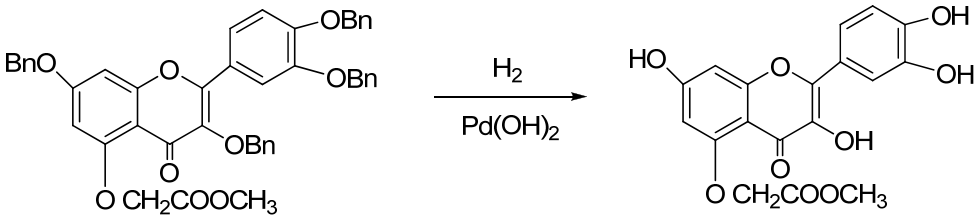

3 D8

Compound D8. Compound **3 (**255 mg, 0.35 mmol) was dissolved in a minimum amount of THF/EtOH (1:1). After addition of 10% $Pd(OH)_2$ (38 mg), the suspension was stirred for 16 h under one atmosphere of hydrogen from a balloon. The suspension was filtered through Celite, diluted with EtOH and concentrated under vacuum. The residue

was purified by recrystallization with MeOH/H_2O to afford **D8** as a green solid in 86% yield (111 mg). ^{1}H NMR ([D_6]DMSO, 300 MHz) [Figure 2.22] δ 10.76 (s, 1H, OH), 9.48 (s, 1H, OH), 9.27 (s, 1H, OH), 8.75 (s, 1H, OH), 7.64 (d, J=2Hz, 1H), 7.49 (dd, J=8.5, 2Hz, 1H), 6.87 (d, J=8.5Hz, 1H), 6.51 (d, J=2Hz, 1H), 6.25 (d, J=2Hz, 1H), 4.89 (s, 2H), 3.72 (s, 3H). ^{13}C NMR ([D_6]DMSO, 75MHz) [Figure 2.23] δ 170.8 (C=O), 168.8 (COO), 162.1, 158.6, 157.8, 147.0, 145.1, 142.1, 137.2, 122.2, 119.3, 115.7, 114.8, 105.5, 98.0, 97.6, 65.8 (OCH_2), 51.8 (OCH_3) MS (FAB) $[M+Na]^+$ m/z 397.1, HRMS (FAB) $C_{18}H_{14}O_9Na$ $[M+Na^+]$, calculated m/z 397.0536 found 397.0518. Purity 97.8% (analyzed by HPLC under UV 280 nm).

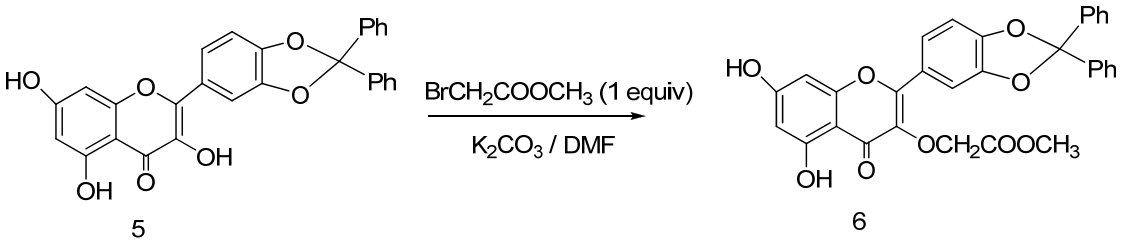

Compound 6. A suspension of **5** (0.70 g, 1.50 mmol) was dissolved in 20 mL of DMF, followed by addition of anhydrous potassium carbonate (0.311 g, 2.25 mmol) and methyl bromoacetate (0.23 g, 1.5 mmol). The mixture was stirred overnight at room temperature, under nitrogen. The solution was diluted with 50 mL water, acidified with 1.0 N HCl and extracted with 100 mL ethyl acetate. The organic layer was washed with water, brine and dried over anhydrous sodium sulfate. The residue after concentration in vacuum was purified by flash column chromatography using 5% EtOAc in DCM, to afford **6** in 37% yield (0.30 g). ^{1}H NMR ($CDCl_3$, 300 MHz) [Figure 2.24] δ7.78 (dd, J=8.5, 2Hz, 1H), 7.71 (d, J=2Hz, 1H), 7.64-7.61 (m, 4H), 7.45-7.40(m, 6H), 7.02 (d, J=8.5Hz, 1H), 6.39 (d, J=2Hz, 1H), 6.28 (d, J=2.0Hz, 1H), 4.80 (s, 2H), 3.73 (s, 3H). ^{13}C

NMR ($CDCl_3$, 151 MHz) [Figure 2.25] δ 177.9 (C=O), 169.6 (COO), 162.4, 162.0, 156.6, 155.4, 149.5, 147.4, 139.7, 136.7, 129.3, 128.3, 126.2, 124.2, 123.8, 117.9, 108.9, 108.5, 105.6, 99.2, 93.9, 68.4 (OCH_2), 52.0 (OCH_3). MS (FAB) [$M+Na^+$], m/z 561.1. HRMS(FAB) $C_{31}H_{22}O_9Na$ [$M+Na^+$], calculated m/z 561.1162, found 561.1164.

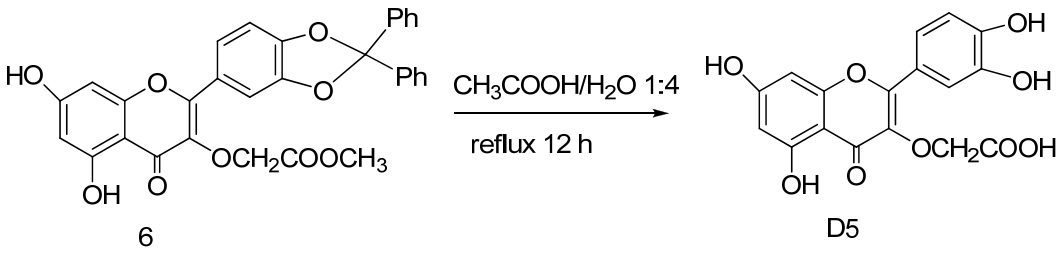

Compound D5. Compound **6** (0.30 g, 0.56 mmol) was mixed with 50 mL CH_3CO_2H/H_2O (4:1) and refluxed overnight. The solution is worked up by addition of 50 mL of water and then carefully neutralized by dropwise addition of saturated $NaHCO_3$. After the extraction with 100 mL EtOAc, the organic layer was washed with brine, dried over anhydrous sodium sulfate and vacuum concentrated. The crude residue was recrystallized with methanol to afford 0.156 g of **D5** as a red solid in 74% yield. ^1H NMR ([D_6] DMSO, 300 MHz) [Figure 2.26] δ 12.56 (s, 1H, OH), 7.60 (d, J=2Hz, 1H), 7.57 (s, 1H), 6.89 (d, J=8Hz, 1H), 6.45 (d, J=2Hz, 1H), 6.22 (d, J=2Hz, 1H), 4.68 (s, 2H). ^{13}C NMR ([D_6]DMSO, 75 MHz) [Figure 2.27] δ 177.3 (C=O), 172.0 (CO_2H), 169.8, 164.1, 161.0, 156.1, 155.1, 148.6, 145.0, 135.7, 121.0, 120.6, 115.5, 103.9, 98.5, 93.4, 67.7 (OCH_2-CO_2H). MS (ESI) [$M+H^+$], m/z 361.0. HRMS (ESI) $C_{17}H_{13}O_9$ [$M+H^+$], calculated 361.0560, found 361.0599. Purity 97.8% (analyzed by HPLC under UV 280 nm).

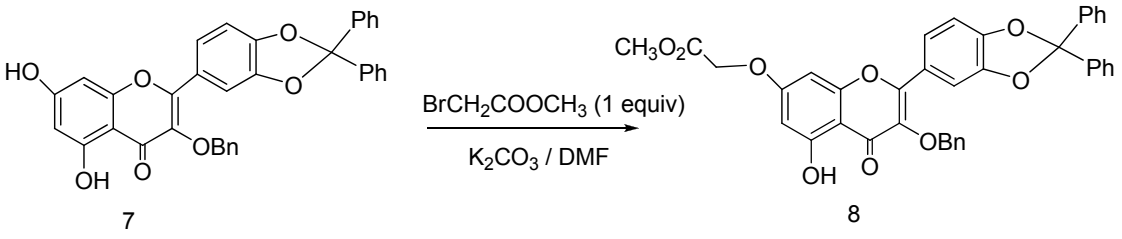

Compound 8. Compound **7** (0.50 g, 0.90 mmol) in 30 mL DMF was mixed with methyl bromoacetate (0.138 g, 0.90 mmol), followed by addition of anhydrous potassium carbonate (0.152 g, 1.10 mmol). The mixture was stirred under nitrogen for 6 h at room temperature and then neutralized with 1.0 N HCl. The solution was extracted with 100 mL EtOAc, washed with water, and dried over anhydrous sodium sulfate. The solvent was removed under vacuum and the residue was flash chromatographed using EtOAc/petroleum ether (1:1) to afford 0.360 gm of the desired product **8** in 64% yield. ^{1}H NMR ($CDCl_3$, 300 MHz) [Figure 2.28] δ 12.72 (s, 1H, OH), 7.59-7.13 (m, 17H), 6.91 (d, J=9.6Hz, 1H), 6.38 (d, J=3.9Hz, 1H), 6.34 (d, J=3.9Hz, 1H), 5.02 (s, 2H), 4.68 (s, 2H), 3.80 (s, 3H). ^{13}C NMR ($CDCl_3$, 75MHz) [Figure 2.29] δ 178.4 (C=O), 168.1(COO), 163.0, 161.8, 156.4, 156.2, 149.0, 147.0, 139.5, 137.0, 135.9, 129.1, 128.6, 128.1, 127.9, 126.0, 123.9, 123.8, 117.6, 108.7, 108.1, 106.2, 97.9, 92.4, 74.0, 64.7 (OCH_2), 52.1 (OCH_3) MS (ESI) m/z 629.2 for [M+H$^+$], m/z 651.2 for [M+Na$^+$], m/z 667.1 for [M+K$^+$], MS (FAB) [M+Na$^+$], m/z 651.1. HRMS (ESI) $C_{38}H_{29}O_9$ [M+H$^+$], calculated m/z 629.1830, found 629.1830.

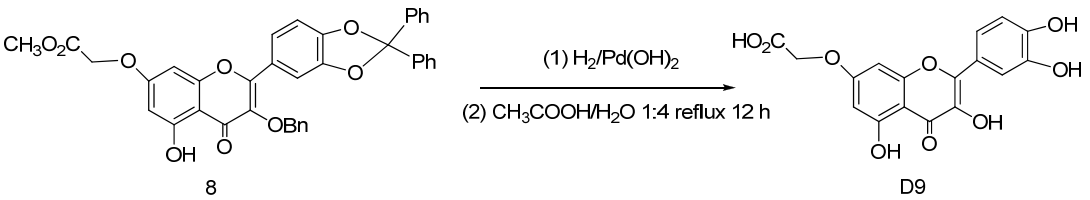

Compound D9. Compound **8** (0.482 g) in 20 mL of EtOH/THF (1:2) was mixed with 10% $Pd(OH)_2$ (10 mg) and stirred overnight under hydrogen from a balloon. The suspension was filtered through Celite and the clear green filtrate was diluted with 20 mL EtOH and concentrated under vacuum. The residue was refluxed with acetic acid as described in the preparation of **D5** to give 0.224 g of **D9** in 78% yield. ^{1}H NMR ([D_6]DMSO, 300 MHz) [Figure 2.30] δ 12.50 (s, 1H, OH), 9.67 (s, 1H, OH), 9.53 (s, 1H, OH), 9.33 (s, 1H, OH), 7.73 (d, J=2Hz, 1H), 7.58 (dd, J=8.5, 2Hz, 1H), 6.90 (d, J=8.5Hz, 1H), 6.69 (s, 1H), 6.36 (s, 1H), 4.84 (s, 2H). ^{13}C NMR ([D_6]DMSO, 75 MHz) [Figure 2.31] δ 175.8 (C=O), 169.5(CO_2H), 163.2, 160.2, 155.7, 147.8, 147.2, 145.0, 136.0, 121.7, 120,0, 115.5, 115.1, 104.2, 97.7, 92.4, 64.8 (OCH_2). MS (ESI) [M+H^+], m/z 361.1. HRMS (ESI) $C_{17}H_{13}O_9$ [M+H^+], calculated m/z 361.0560, found m/z 361.0555. Purity 97.7% (analyzed by HPLC under UV 280 nm).

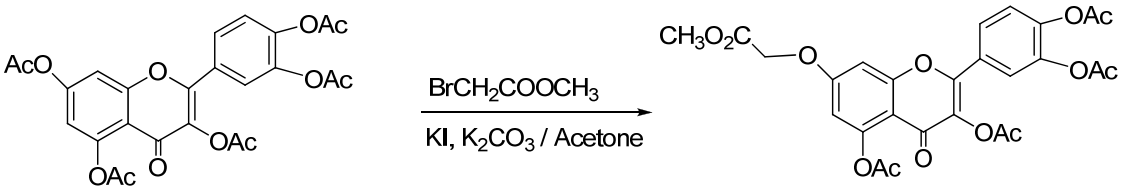

9 10

Compound 10. Quercetin pentaacetate **9** (1.0 g, 1.95 mmol) in 50 mL dry acetone was mixed with methyl bromoacetate (1.0 g, 6.55 mmol), anhydrous potassium carbonate (2.0 g, 14.5 mmol) and 0.168 g potassium iodide. The suspension was refluxed until **9** was completely consumed as judged by TLC. The suspension was filtered and the filtrate was concentrated under vacuum, and flash chromatographed using EtOAc/Hexane (4:3). The product was recrystallized with acetone/hexane to afford 0.577 g of **10** as a white solid in 54% yield. ^{1}H NMR ($CDCl_3$, 300 MHz) [Figure 2.32] δ 7.74 (dd, J=8.5,

2Hz, 1H), 7.70 (d, J=2Hz, 1H), 7.37 (d, J=8.5Hz, 1H), 6.83 (d, J=2Hz, 1H), 6.72 (d, J=2Hz, 1H), 4.66 (s, 2H), 3.76 (s, 3H), 2.36 (s, 3H), 2.26 (s, 9H). ^{13}C NMR ($CDCl_3$, 151 MHz) [Figure 2.33] δ 169.8 (C=O), 169.3 (COO), 168.0, 167.9, 167.8, 167.7 (4 $CH_3\underline{C}$=O), 161.8, 157.8, 153.3, 150.9, 144.2, 142.2, 133.9, 127.9, 126.4, 123.8, 123.7, 111.8, 109.0, 99.6, 65.4 (OCH_2), 52.6 (OCH_3), 21.0, 20.8, 20.6, 20.5 (4 $\underline{C}H_3C$=O) MS: ESI [M+Na^+] 565.1, [M+H^+] 543.0, [M-CH_2CO+H^+] 501.1, [M-2CH_2CO+H^+] 459.1, [M-3CH_2CO+H^+] 417.1 HRESI $C_{26}H_{22}O_{13}Na$ [M+Na^+], calculated 565.0958, found 565.0948.

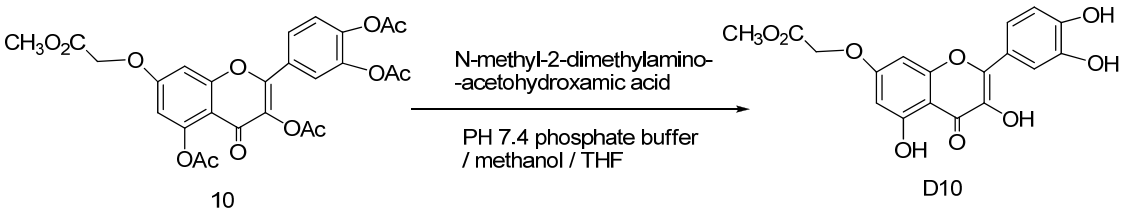

Compound D10. Twenty mg (0.036 mmol) of **10** was dissolved in 10 mL of THF/MeOH/pH 7 phosphate buffer (9:2:9), after which 5 equivalent of N-methyl-2-dimethylaminoacetohydroxamic acid (24 mg, 0.180 mmol) was added. The solution was stirred under nitrogen atmosphere at room temperature for 12 h after which the mixture was worked up with water, acidified to pH 6 by 1 M HCl and extracted with 50 mL of EtOAc. The organic phase was washed with water and dried over anhydrous sodium sulfate. The residue after concentration in vacuum was recrystallized from MeOH/H_2O to afford 11 mg of **D10** as a green solid in 83% yield. ^{1}H NMR ([D_6]DMSO, 300 MHz) [Figure 2.34] δ 9.66(s,1H), 9.53(s, 1H), 9.31(s,1H), 7.73 (d, J=2Hz, 1H), 7.57 (dd, J=8.4, 2Hz, 1H), 6.89 (d, J=8.4Hz, 1H), 6.74 (d, J=2Hz, 1H), 6.39 (d, J=2Hz, 1H), 4.97 (s, 2H), 3.73 (s, 3H). ^{13}C NMR ([D_6]DMSO, 151MHz) [Figure 2.35] δ 176.4 (C=O), 169.0

(COO), 163.5, 160.8, 156.2, 148.3, 147.9, 145.5, 136.5, 122.2, 120.4, 116.0, 115.7, 104.8, 98.2, 93.0, 65.3 (OCH_2), 52.4 (OCH_3). MS (ESI) $[M+Na]^+$ 397.1, HRESI $C_{18}H_{14}O_9Na$ $[M+Na]^+$, calculated 397.0536, found 397.0535. Purity 98.7% (analyzed by HPLC under UV 280 nm).

HSP70 Inhibition Assays. Exponentially growing Jurkat cells, grown in RPMI media with 10% fetal bovine serum, were treated with 150 uM of quercetin or its derivatives for 1 h prior to being heated at 43 °C for 30 min. The cells were allowed to recover at 37 °C for 8 h to allow for HSP70 expression and cells harvested for Western blot analysis with mouse monoclonal antibodies against inducible HSP70 (Assay Designs, SPA-810) and actin (ICN, clone C4). Secondary antibodies were goat anti-mouse conjugated horse radish peroxidase (Millipore) or alkaline phosphatase (Jackson ImmunoResearch). Protein bands were visualized by either chemiluminescence (SuperSignal West Femto Substrate, Thermo Scientific) or colorimetric (BCIP/NBT, Sigma) detection.

HSP27 Phosphorylation Assays. Phosphorylation of HSP27 was detected by Western blot analysis of total cell extracts prepared from exponentially growing HeLa cells. Cells were grown in DMEM media with 10% calf serum and treated for 1 hr with 50 μg/mL (150 μM) of quercetin or its derivatives before protein isolation. A rabbit antibody specific for human HSP27 phosphorylated on serine 78 (Assay Designs, SPA-523) coupled with goat anti-rabbit alkaline phosphatase secondary antibody (Jackson ImmunoResearch) was utilized for colorimetric detection.

HSF1 Electrophoretic Mobility Shift Assays (EMSA). Analysis of HSF1 interactions with the HSE DNA promoter element was carried out by EMSA essentially as described previously [21] except that nuclear extracts (from Jurkat or Hela cells) were utilized in place of whole cell extracts. The heat shock element probe (HSE) d(GCGAAACTGCTGGAAGATTCCT) was 5'-^{32}P end labeled followed by annealing to the complementary oligonucleotide to produce the duplex DNA. Western blot analysis of the same nuclear extracts utilized for EMSA was carried out with rabbit anti-HSF1(Cell SignalingTechnology) followed by goat anti-rabbit HRP (Millipore) and chemiluminescent detection.

Kinase inhibition assays. Phosphate kinases CAMKII and CK2, substrates, and buffers were from New England BioLabs. Inhibition assays were carried out with the PKlight HTS Protein Kinase Assay kit (Lonza) according to the manufacturer's procedure. Briefly, this assay involves determining in triplicate the extent of phosphorylation of a peptide substrate in the presence and absence of various concentrations of inhibitor by quantifying the amount of ATP consumed via a luciferase-based bioluminescence assay. A kinase concentration (EC_{50}) is used that results in 50% consumption of ATP in the absence of inhibitor under the reaction time and conditions. The data was then fit via non-linear least squares fitting to a standard sigmoidal dose-response equation. CK2 inhibition assay: Casein Kinase II (CK2) was incubated at 30 °C for 30 min with 300 μM substrate (RRRADDSDDDDD), 100 μM ATP, in a buffer containing 20 mM Tris-HCl, 50 mM KCl, 10 mM $MgCl_2$, with or without the presence of inhibitor. CamKII inhibition assay: Ca^{2+}/Calmodulin-Dependent Protein Kinase II (CaMKII) supplemented with 200 μM ATP, 1.2 μM calmodulin and 2 mM $CaCl_2$ was

incubated for 10 min at 30 °C to preactivate the enzyme and then diluted to the required concentration. The activated CaMKII was then incubated at 30°C for 30 min with or without the inhibitor, along with 300 μM autocamtide-2 (KKALRRQETVDAL), 100 μM ATP, in a buffer containing 50 mM Tris-HCl, 10 mM $MgCl_2$, 2 mM DTT, 0.1 mM Na_2EDTA at pH 7.5.

References:

1. Hunt, C.R., et al., *Genomic instability and enhanced radiosensitivity in Hsp70.1- and Hsp70.3-deficient mice.* Mol Cell Biol, 2004. **24**(2): p. 899-911.

2. Wei, Y.Q., et al., *Inhibition of proliferation and induction of apoptosis by abrogation of heat-shock protein (HSP) 70 expression in tumor cells.* Cancer Immunol Immunother, 1995. **40**(2): p. 73-8.

3. Shamovsky, I. and E. Nudler, *New insights into the mechanism of heat shock response activation.* Cell Mol Life Sci, 2008. **65**(6): p. 855-61.

4. Voellmy, R., *On mechanisms that control heat shock transcription factor activity in metazoan cells.* Cell Stress Chaperones, 2004. **9**(2): p. 122-33.

5. Morimoto, R.I., *Regulation of the heat shock transcriptional response: cross talk between a family of heat shock factors, molecular chaperones, and negative regulators.* Genes Dev, 1998. **12**(24): p. 3788-96.

6. Holmberg, C.I., et al., *Phosphorylation of serine 230 promotes inducible transcriptional activity of heat shock factor 1.* Embo J, 2001. **20**(14): p. 3800-10.

7. Soncin, F., et al., *Transcriptional activity and DNA binding of heat shock factor-1 involve phosphorylation on threonine 142 by CK2.* Biochem Biophys Res Commun, 2003. **303**(2): p. 700-6.

8. Wang, X., et al., *Phosphorylation of HSF1 by MAPK-activated protein kinase 2 on serine 121, inhibits transcriptional activity and promotes HSP90 binding.* J Biol Chem, 2006. **281**(2): p. 782-91.

9. Dai, R., et al., *c-Jun NH2-terminal kinase targeting and phosphorylation of heat shock factor-1 suppress its transcriptional activity.* J Biol Chem, 2000. **275**(24): p. 18210-8.

10. Powers, M.V. and P. Workman, *Inhibitors of the heat shock response: biology and pharmacology.* FEBS Lett, 2007. **581**(19): p. 3758-69.

11. Westerheide, S.D., et al., *Triptolide, an inhibitor of the human heat shock response that enhances stress-induced cell death.* J Biol Chem, 2006. **281**(14): p. 9616-22.

12. Pietta, P.G., *Flavonoids as antioxidants.* J Nat Prod, 2000. **63**(7): p. 1035-42.

13. Choi, J.A., et al., *Induction of cell cycle arrest and apoptosis in human breast cancer cells by quercetin.* Int J Oncol, 2001. **19**(4): p. 837-44.

14. Zanini, C., et al., *Inhibition of heat shock proteins (HSP) expression by quercetin and differential doxorubicin sensitization in neuroblastoma and Ewing's sarcoma cell lines.* J Neurochem, 2007. **103**(4): p. 1344-54.

15. Fujita, M., et al., *Synergistic cytotoxic effect of quercetin and heat treatment in a lymphoid cell line (OZ) with low HSP70 expression.* Leuk Res, 1997. **21**(2): p. 139-45.

16. Davies, S.P., et al., *Specificity and mechanism of action of some commonly used protein kinase inhibitors.* Biochem J, 2000. **351**(Pt 1): p. 95-105.

17. Jones, D.J., et al., *Characterisation of metabolites of the putative cancer chemopreventive agent quercetin and their effect on cyclo-oxygenase activity.* Br J Cancer, 2004. **91**(6): p. 1213-9.

18. Pirrung, M.C., et al., *Methyl scanning: total synthesis of demethylasterriquinone B1 and derivatives for identification of sites of interaction with and isolation of its receptor(s).* J Am Chem Soc, 2005. **127**(13): p. 4609-24.

19. Kim, H., et al., *Glyceraldehyde 3-phosphate dehydrogenase is a cellular target of the insulin mimic demethylasterriquinone B1.* J Med Chem, 2007. **50**(15): p. 3423-6.

20. Bouktaib, M., et al., *Hemisynthesis of all the O-monomethylated analogues of quercetin including the major metabolites, through selective protection of phenolic functions.* Tetrahedron, 2002. **58**(50): p. 10001-10009.

21. Goswami, P.C., et al., *Proto-oncogene mRNA levels and activities of multiple transcription factors in C3H 10T 1/2 murine embryonic fibroblasts exposed to 835.62 and 847.74 MHz cellular phone communication frequency radiation.* Radiat Res, 1999. **151**(3): p. 300-9.

22. Jurd.L., *Plant Polyphenols.V.Selective alkylation of the 7-hydroxyl group in polyhydroxyflavones.* J.Am.Chem.Soc, 1958. **80**: p. 6.

23. Picq, M., et al., *Pentasubstituted quercetin analogues as selective inhibitors of particulate 3';5'-Cyclic-AMP phosphodiesteras from rat brain.* J.Med.Chem, 1982. **25**: p. 7.

24. Ono, M. and I. Itoh, *N-Methyl-2-(dimethylamino)acetohydroxamic acid as a new reagent for the selective cleavage of active esters under neutral conditions.* Tetrahedron Letters, 1989. **30**(2): p. 207-10.

25. Li, M., X. Han, and B. Yu, *Facile synthesis of flavonoid 7-O-glycosides.* J Org Chem, 2003. **68**(17): p. 6842-5.

26. Arya, R., M. Mallik, and S.C. Lakhotia, *Heat shock genes - integrating cell survival and death.* J Biosci, 2007. **32**(3): p. 595-610.

27. Worzella, T. and A. Gallagher, *Optimizing kinase assays for ultrahigh-throughput profiling using the Kinase-Glo Plus Assay.* Jala, 2007. **12**(2): p. 99-103.

28. Hosokawa, N., et al., *Inhibition of the activation of heat shock factor in vivo and in vitro by flavonoids.* Mol Cell Biol, 1992. **12**(8): p. 3490-8.

29. Sicheri, F., I. Moarefi, and J. Kuriyan, *Crystal structure of the Src family tyrosine kinase Hck.* Nature, 1997. **385**(6617): p. 602-9.

30. Fabian, M.A., et al., *A small molecule-kinase interaction map for clinical kinase inhibitors.* Nat Biotechnol, 2005. **23**(3): p. 329-36.

31. Walker, E.H., et al., *Structural determinants of phosphoinositide 3-kinase inhibition by wortmannin, LY294002, quercetin, myricetin, and staurosporine.* Mol Cell, 2000. **6**(4): p. 909-19.

32. Stokoe, D., et al., *Identification of MAPKAP kinase 2 as a major enzyme responsible for the phosphorylation of the small mammalian heat shock proteins.* FEBS Lett, 1992. **313**(3): p. 307-13.

33. Garrido, C., et al., *HSP27 as a mediator of confluence-dependent resistance to cell death induced by anticancer drugs.* Cancer Res, 1997. **57**(13): p. 2661-7.

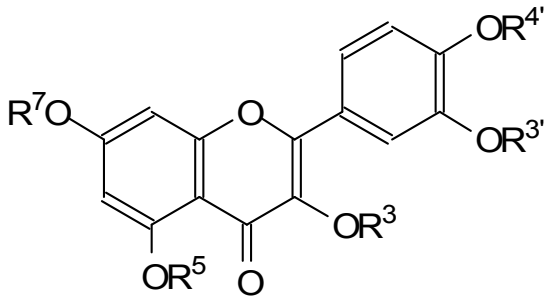

Cmpd	R3	R5	R7	R3'	R4'	HSP70 inhibition	HSP27 phosphorylation
Quercetin						+++	+++
D1				$CH_2CO_2CH_3$		++	-
D2				CH3		+++	-
D3					CH_3	+	-
D4	CH3					-	-
D5	CH_2CO_2H					-	-
D6		CH3				-	-
D7			CH3			+++	+++
D8		$CH_2CO_2CH_3$				-	-
D9			CH_2CO_2H			-	-
D10			$CH_2CO_2CH_3$			+++	+++

Table 1. Quercetin derivatives. The substituent is an H unless otherwise noted.

	Q	D1	D2	D3	D4	D5
CK2	5.6 ± 1.2	53 ± 3.7	0.50 ± 0.01	>100	0.83 ± 0.10	2.45 ± 0.25
CamKII	3.3 ± 0.6	6.3 ± 1.3	0.91 ± 0.25	16.4 ± 1.9	>100	>100
HSP70	+++	++	+++	+	-	-
		D6	**D7**	**D8**	**D9**	**D10**
CK2		>100	9.7 ± 1.4	>100	9.7 ± 3.6	0.85 ± 0.30
CamKII		4.0 ± 1.1	8.9 ± 0.3	69 ± 6.0	9.3 ± 1.8	9.1 ± 0.1
HSP70		-	+++	-	-	+++

Table 2. IC_{50} values (μM) for inhibition of CK2 and CamKII by quercetin and derivatives D1-D10.

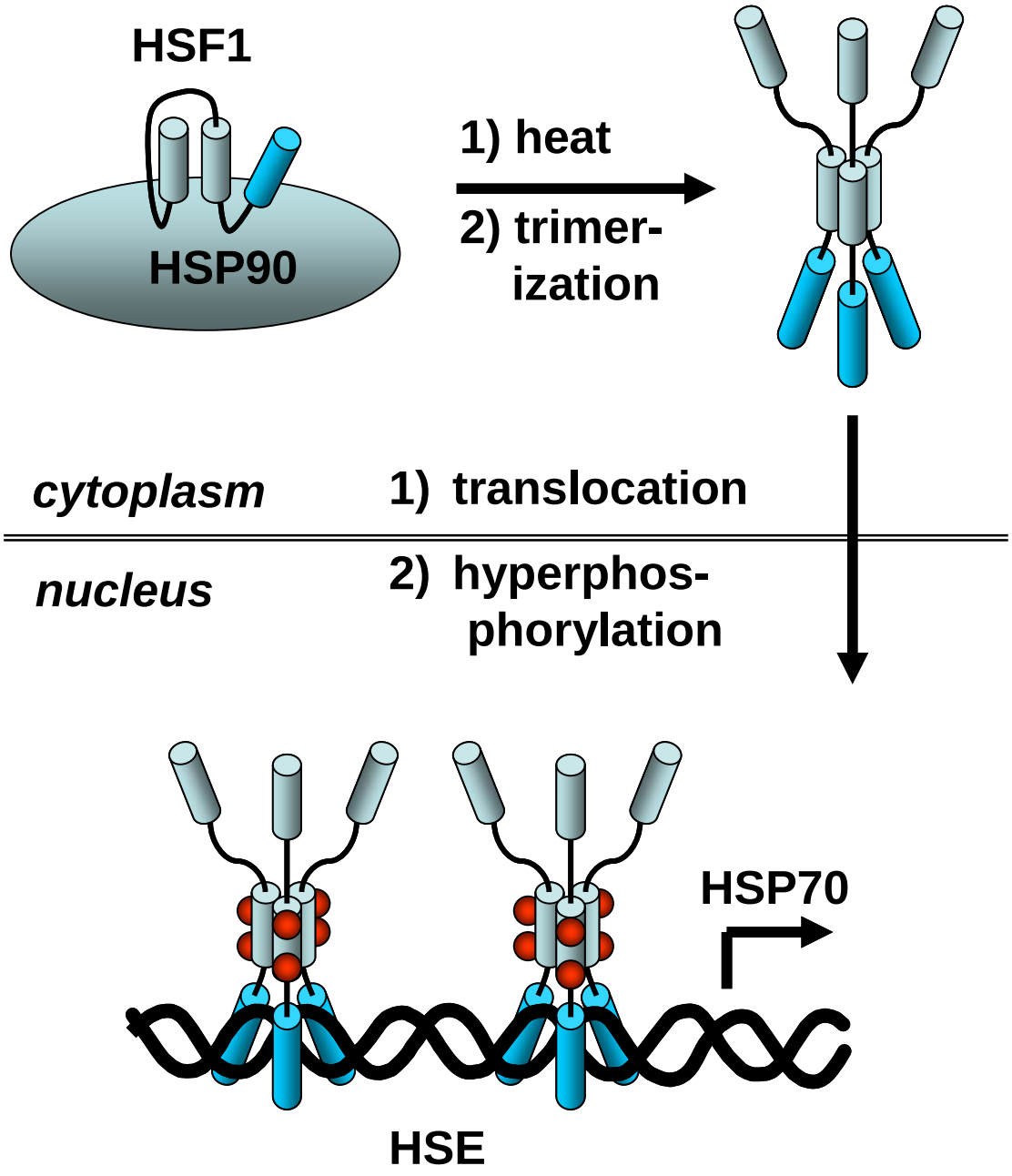

Figure 2.1 Schematic of the pathway for heat shock induction of HSP70 expression.

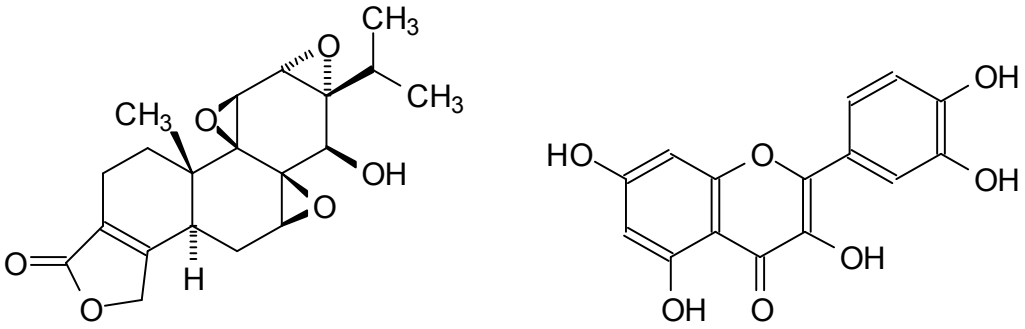

Figure 2.2 Two known inhibitors of heat induced HSP70 expression.

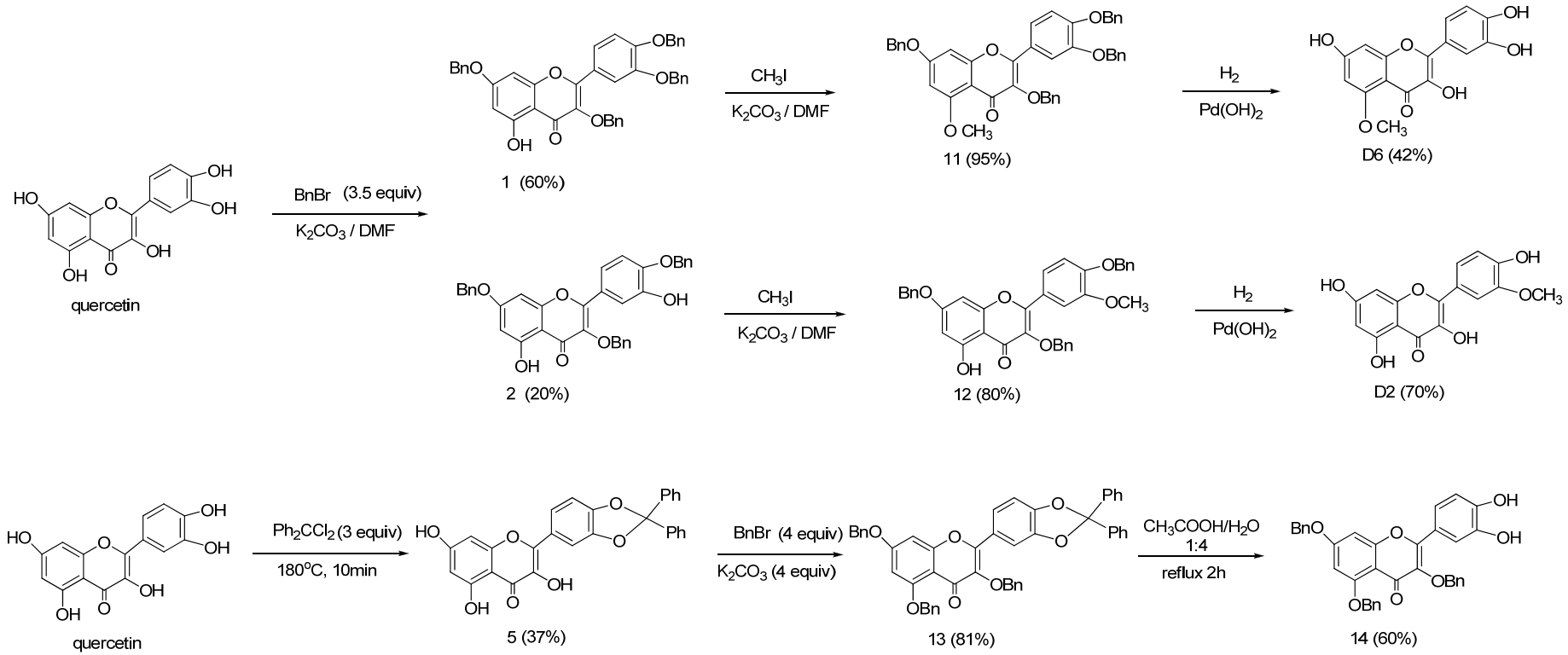

Figure 2.3 Scheme of the synthesis of quercetin mono-methyl derivatives (D6, D2) based on published procedure [20].

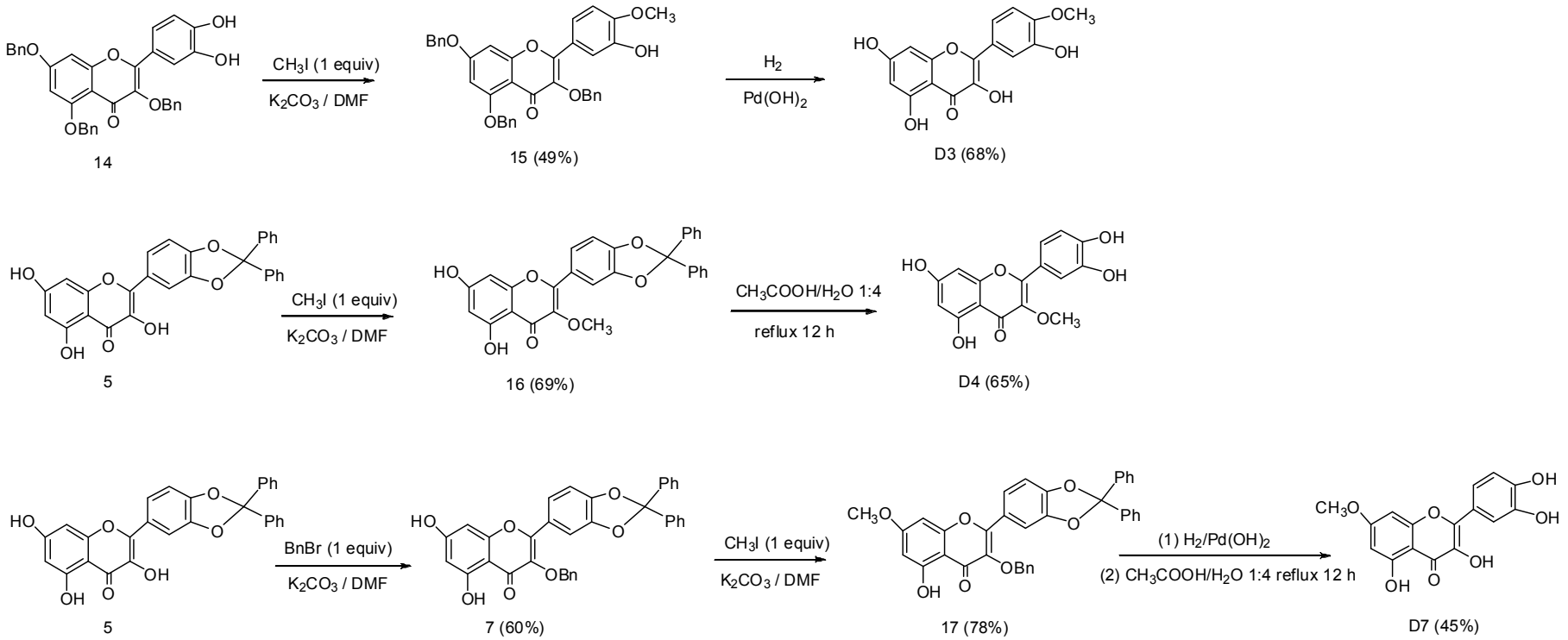

Figure 2.4 Scheme of the synthesis of quercetin mono-methyl derivatives (D3, D4, D7) based on published procedure [20].

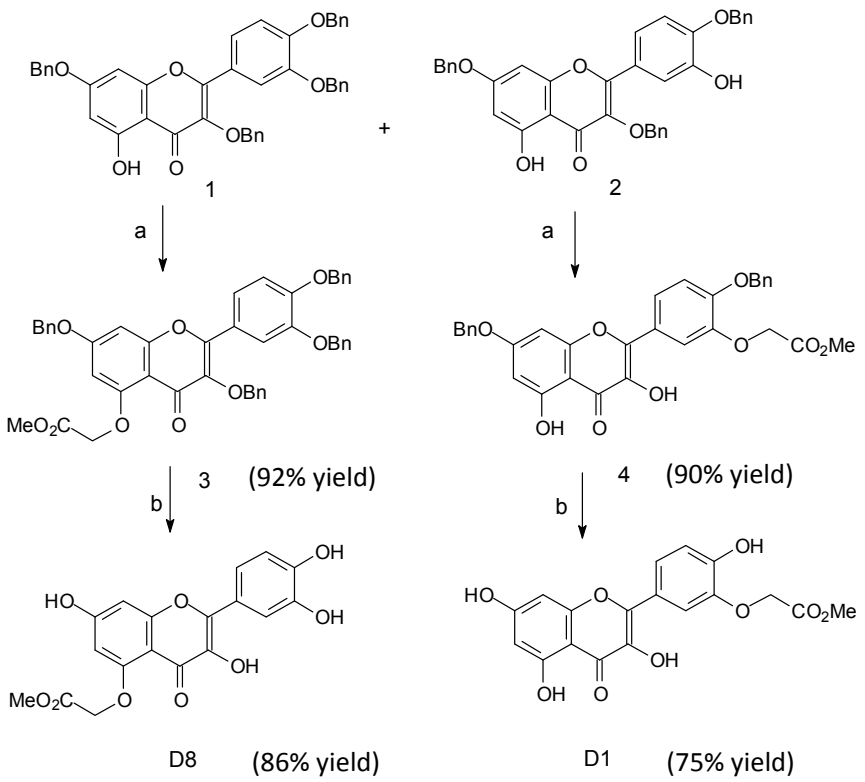

Reagents and conditions: a) $BrCH_2CO_2CH_3$, K_2CO_3/DMF; b) H_2/$Pd(OH)_2$

Figure 2.5 Scheme for the synthesis of quercetin mono-carbomethoxy methyl derivatives D1 and D8.

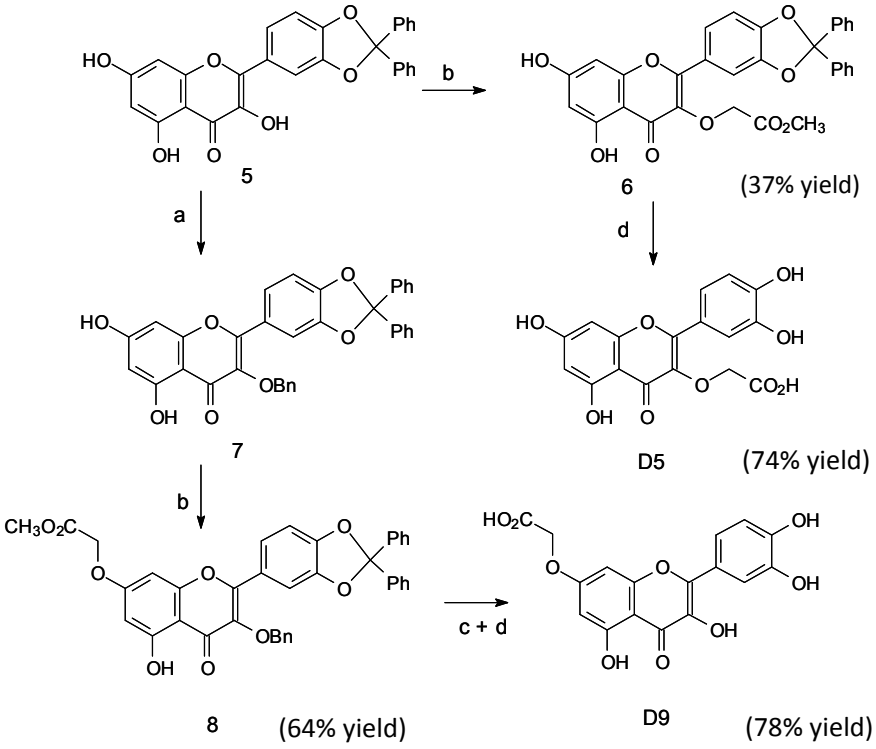

Figure 2.6 Scheme for the synthesis of quercetin mono-carbomethoxy methyl derivatives D5 and D9.

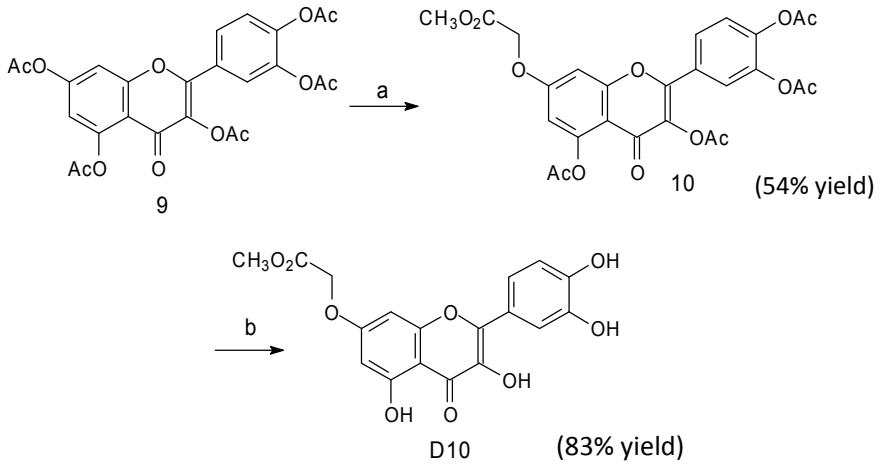

Reagents and conditions: a) $BrCH_2CO_2CH_3$, KI, K_2CO_3/acetone, b) N-methyl-2-dimethylamino-acetohydroxamic acid, THF/MeOH, phosphate buffer

Figure 2.7 Scheme for the synthesis of quercetin mono-carbomethoxy methyl derivatives D10.

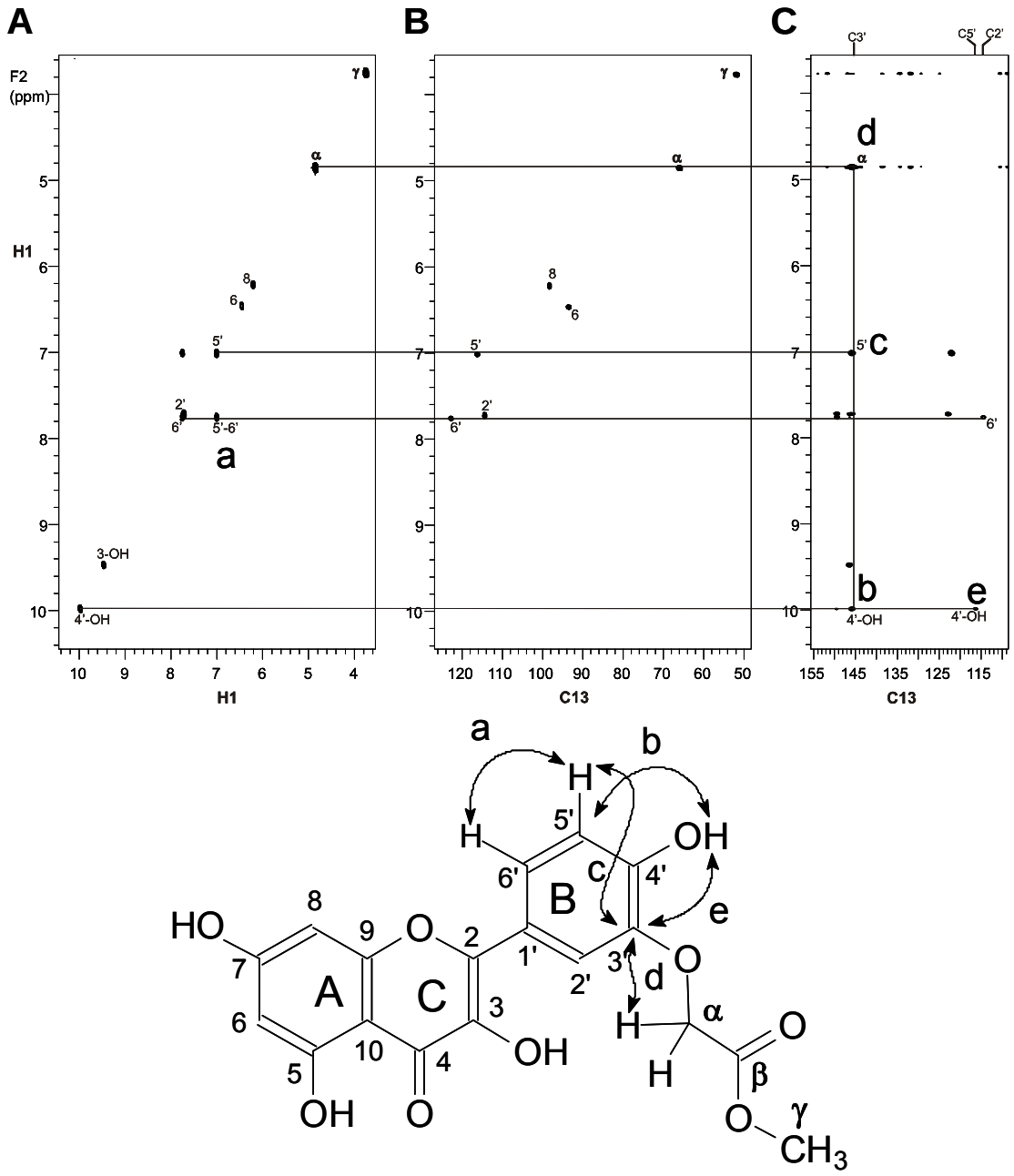

Figure 2.8 Structure assignment of **D1**. (A) COSY, (B) HMQC and (C) HMBC of **D1** in [D_6]DMSO.

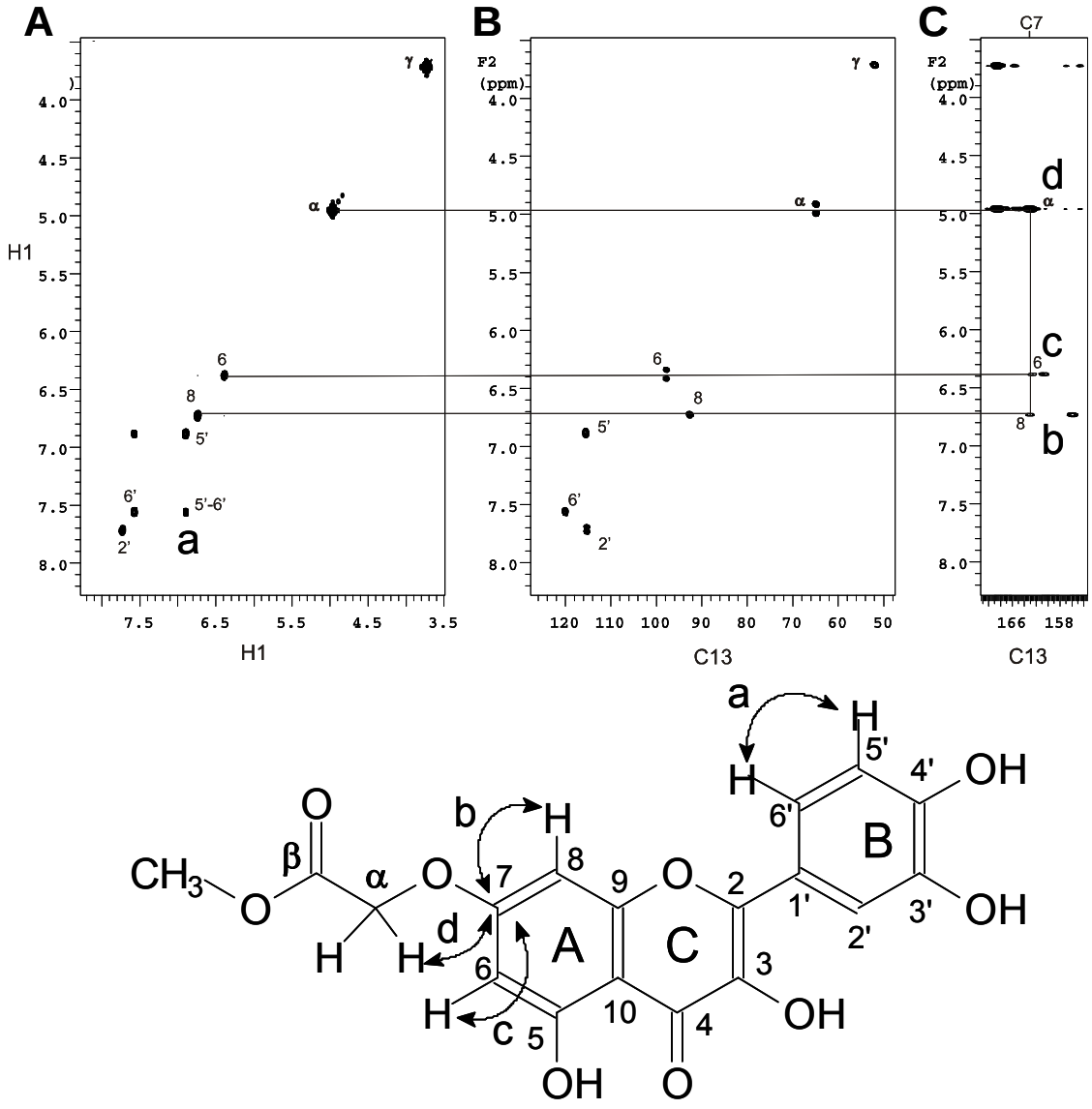

Figure 2.9 Structure assignment of **D10**. (A) COSY (B) HMQC and (C) HMBC of **D10** in [D_6]DMSO.

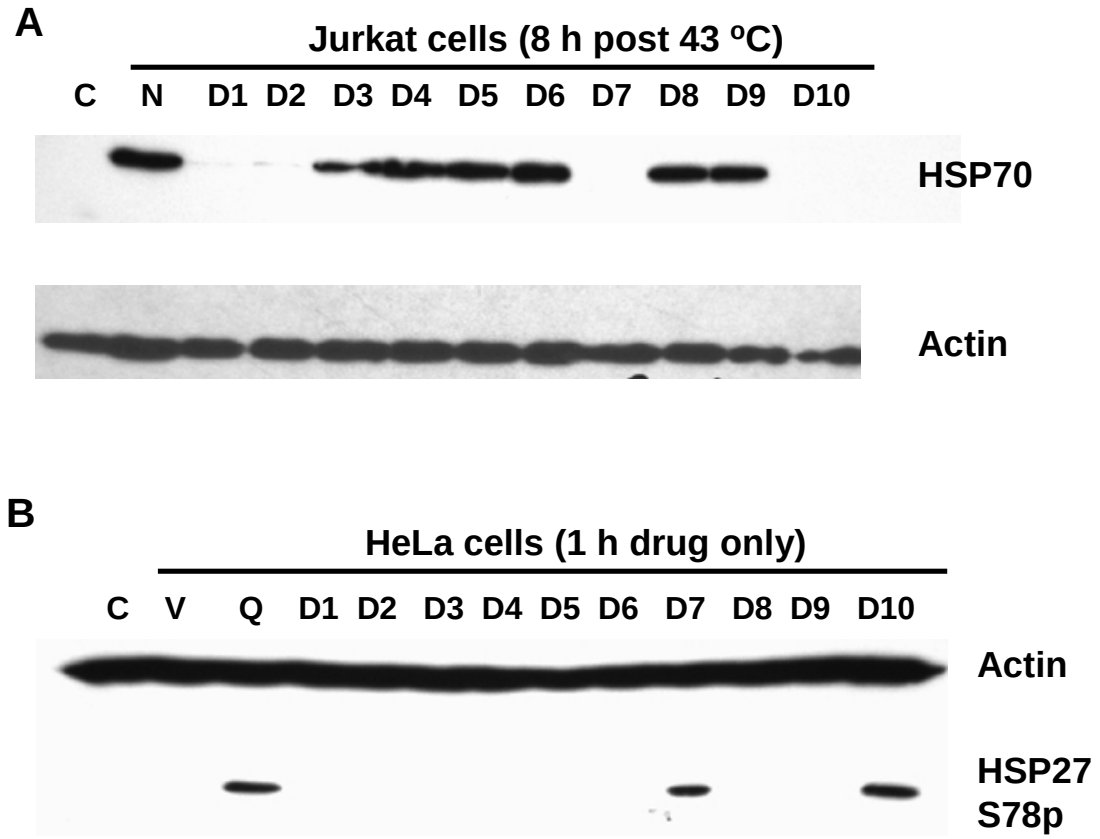

Figure 2.10 Effect of quercetin and its derivatives on heat induced HSP70 expression and phosphorylation of HSP27. **Panel A**. Inhibition of heat induced HSP70 expression. Jurkat cells pre-treated 1 h with 50 μg/mL (approx. 150 μM) of the quercetin derivatives **D1**-**D10** were heat shocked as indicated then allowed to recover at 37 °C for 8 h before protein isolation and analysis. HSP70 and actin protein levels were determined by Western blotting: Lane C: non-heated cells; N: heated no drug; **D1**-**D10**, quercetin derivatives. **Panel B**. Drug induced phosphorylation of human HSP27 Ser78. HeLa cells were treated for 1 h with drug (50 μg/mL, approx. 150 μM) before cellular proteins were isolated for Western blot analysis with actin and HSP27 Ser78P antibodies: Lane C: no drug; V: DMSO vehicle only; Q: quercetin; **D1**-**D10**: quercetin derivatives.

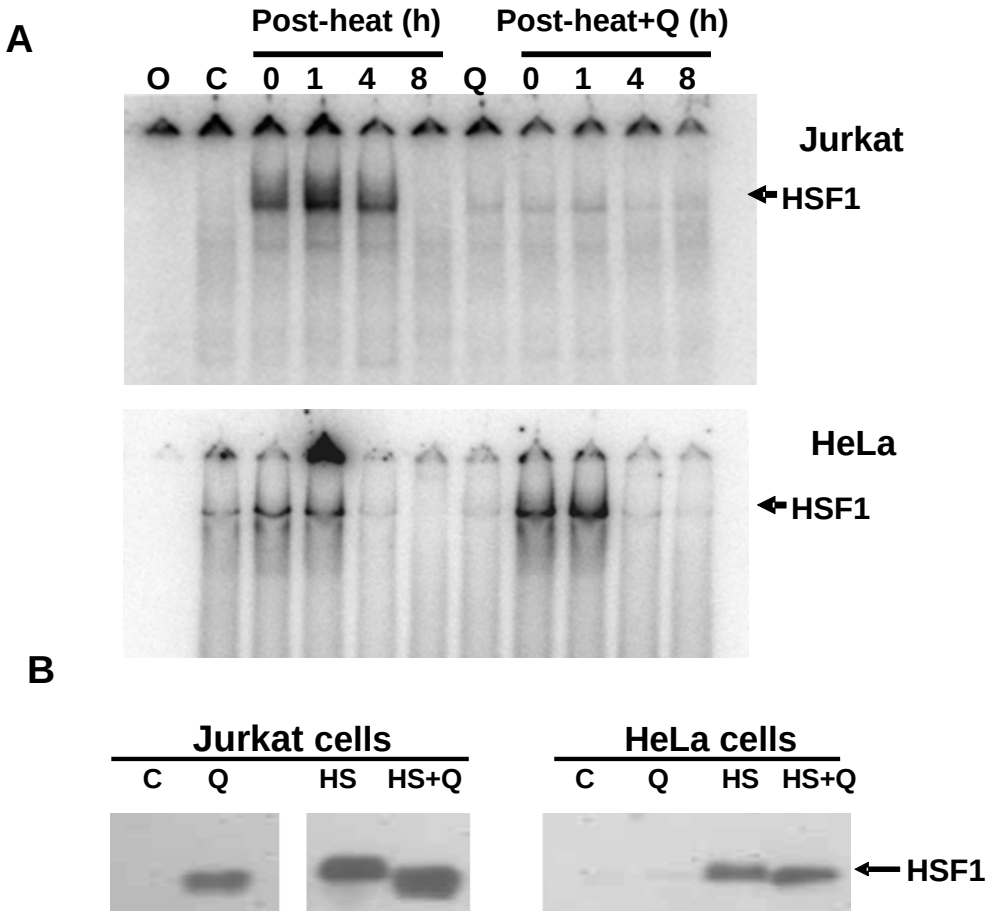

Figure 2.11 Effect of quercetin on HSF1 binding to HSE DNA. Jurkat (Panel A-upper) or HeLa cells (Panel A-lower) were heated or pre-treated with quercetin (50 μg/mL, approx. 150 μM) 1 h prior to heating and allowed to recover at 37 °C for 0-8 h at 37 °C. Cells were isolated and nuclear extracts prepared for EMSA analysis with a 5'-radiolabeled HSE oligodeoxynucleotide. Position of the HSF1-HSE complex is indicated by the arrows. Lane O: HSE oligonucleotide without extract; C: unheated extract; Q: quercetin treated, no heat. HSF1 content of EMSA nuclear extracts (Panel B). Nuclear extracts utilized in Panel A were subjected to Western blot analysis with anti-HSF1 antibody to determine the HSF1 levels and relative size. Lane C: nuclear extract from unheated cells; Q: quercetin treated for 2.5 h; HS: 1 h after a 43 °C/30 min heat shock; HS+Q: 1 h quercetin treatment, 43 °C/30 min heat shock and 1 h recovery.

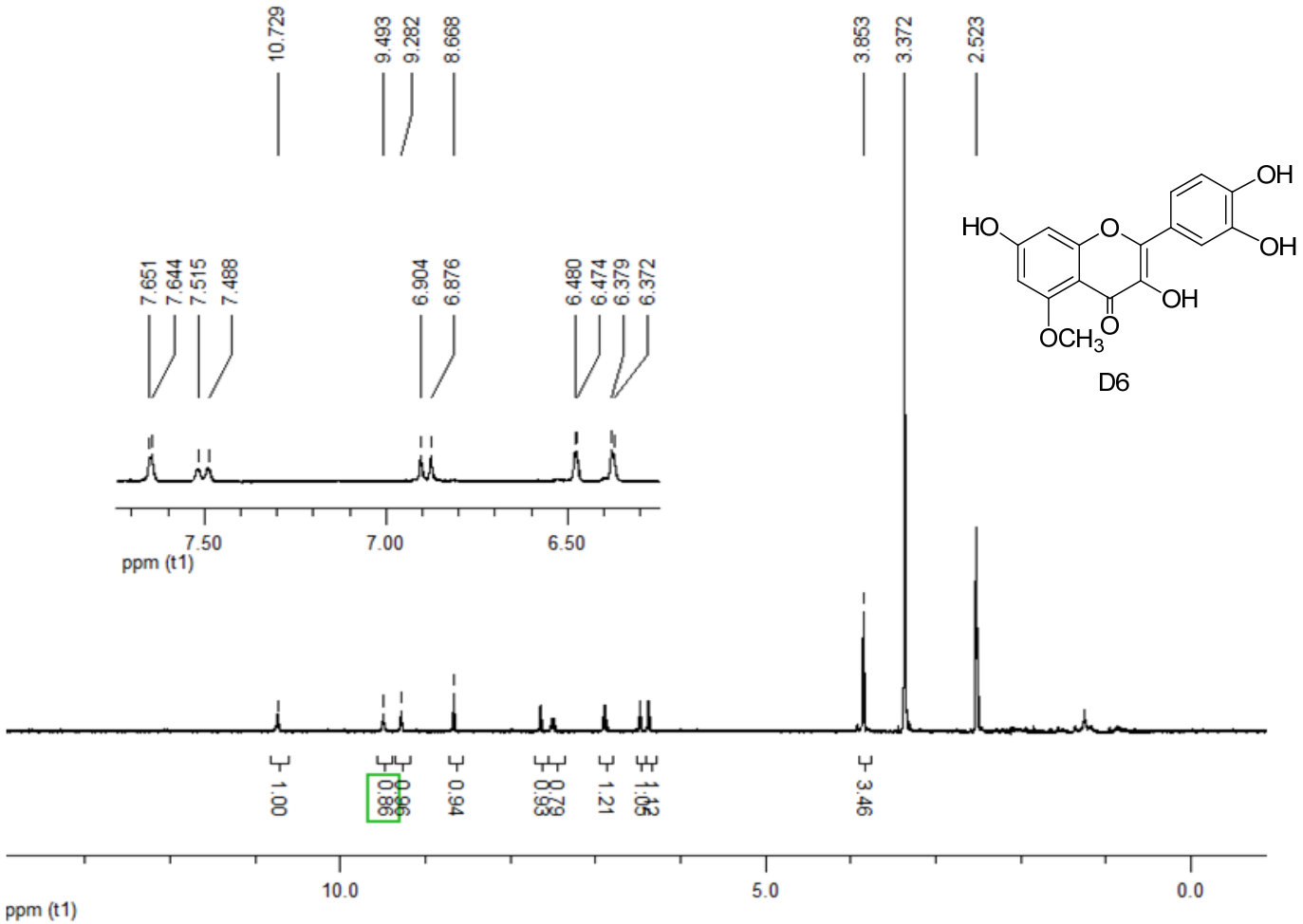

Figure 2.12 ^{1}H NMR ([D_6]DMSO, 300 MHz) spectrum of compound D6.

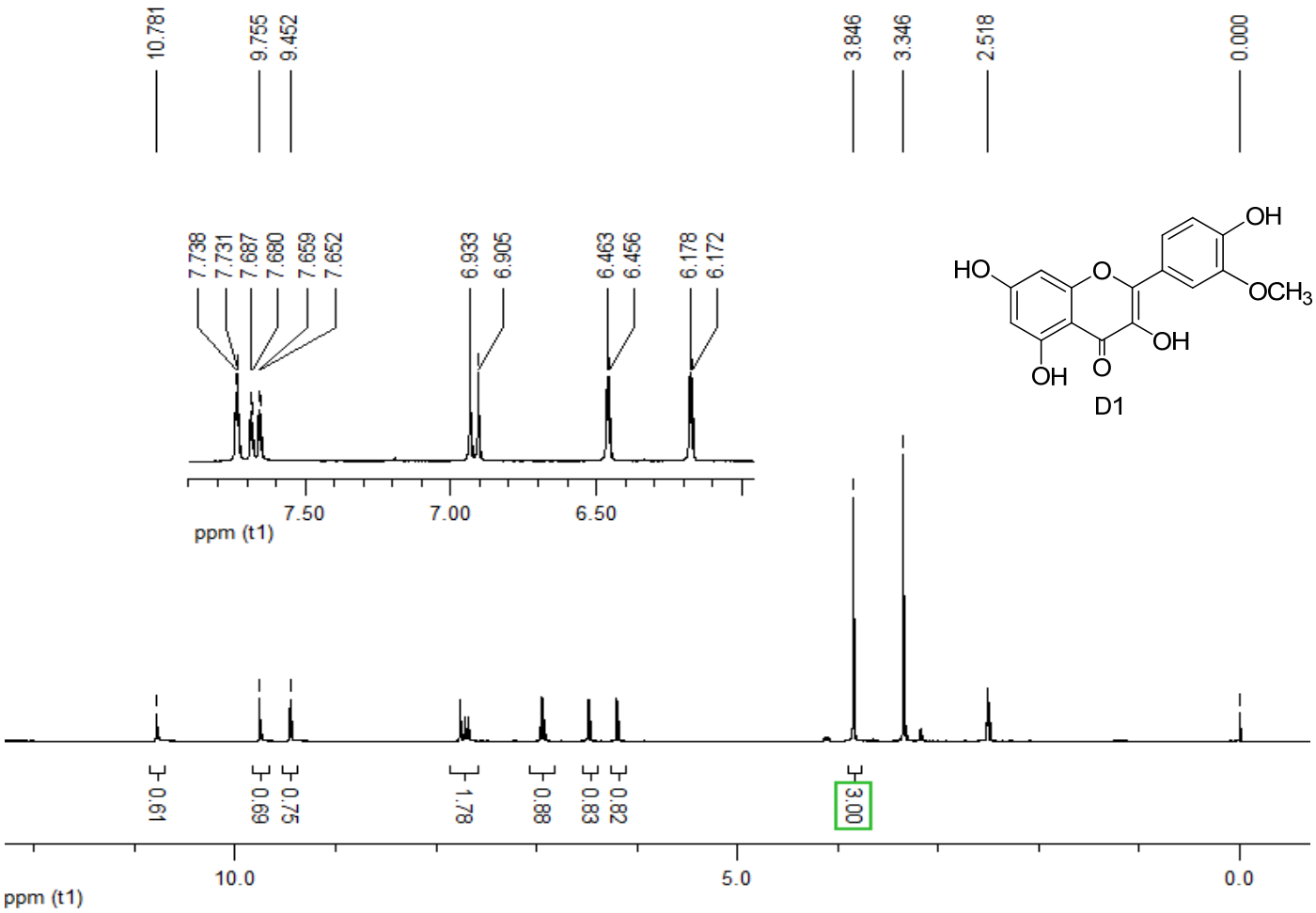

Figure 2.13 ^{1}H NMR ([D_6]DMSO, 300 MHz) spectrum of compound D1.

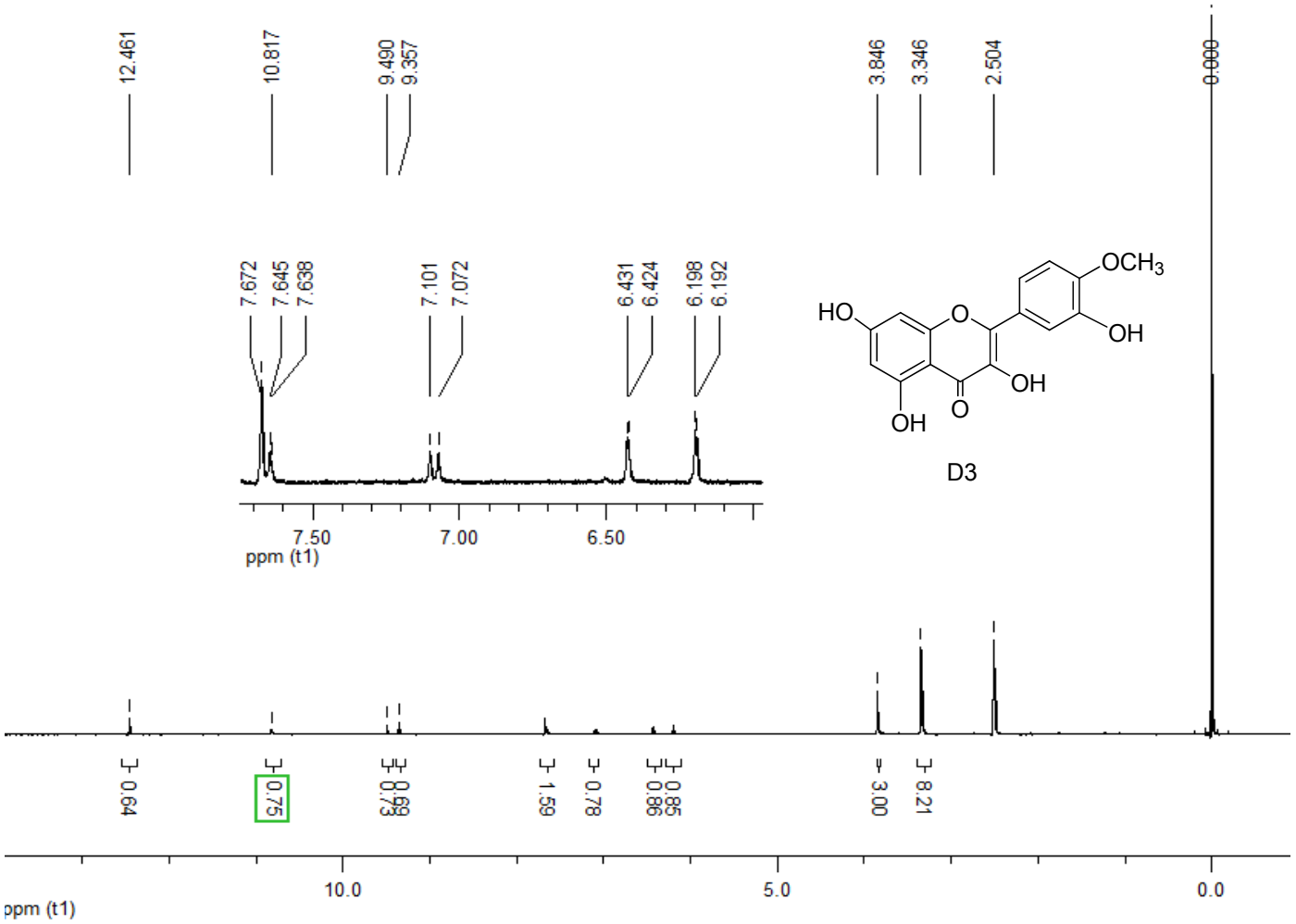

Figure 2.14 ^{1}H NMR ([D_6]DMSO, 300 MHz) spectrum of compound D3.

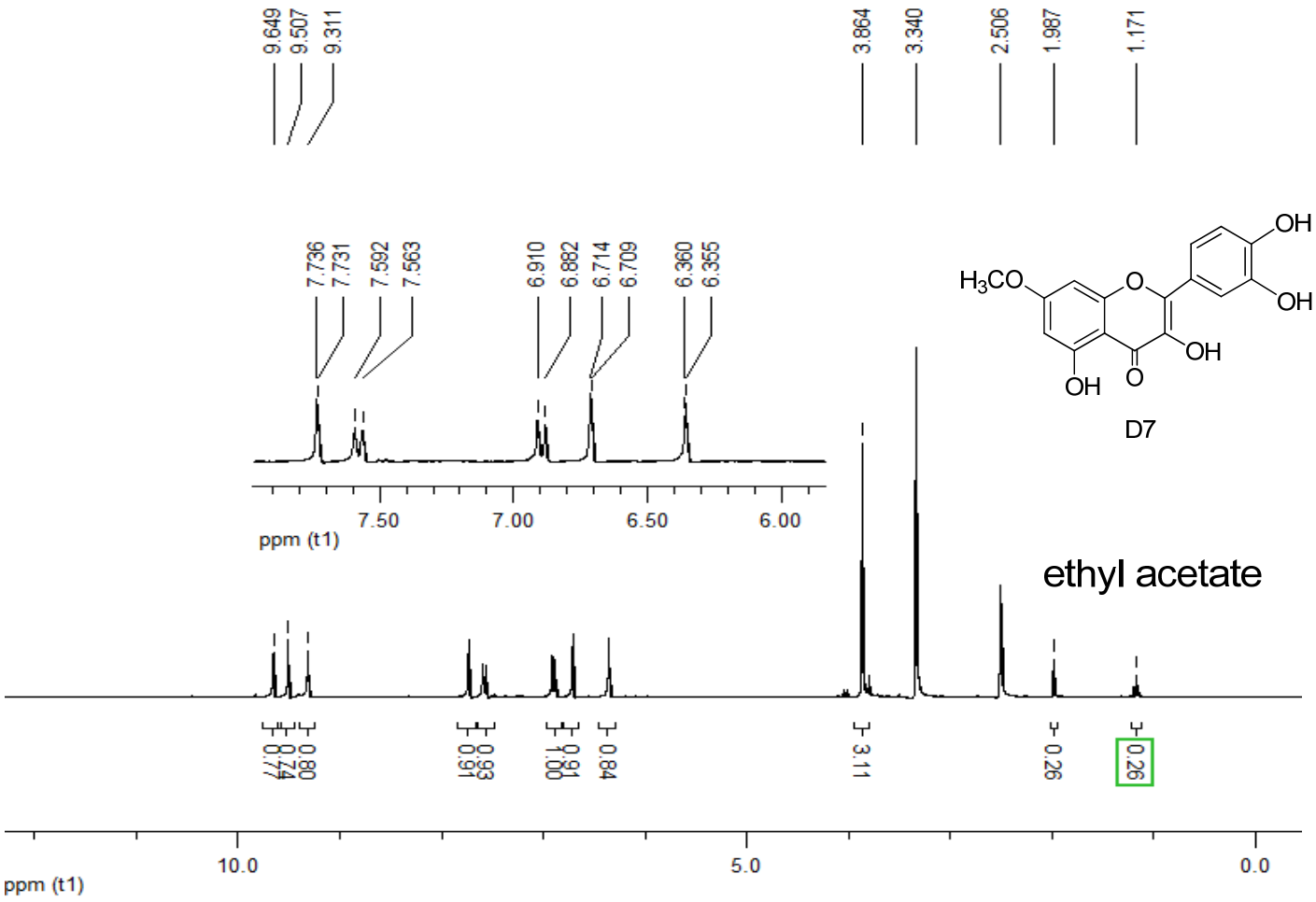

Figure 2.15 ^{1}H NMR ([D_6]DMSO, 300 MHz) spectrum of compound D7.

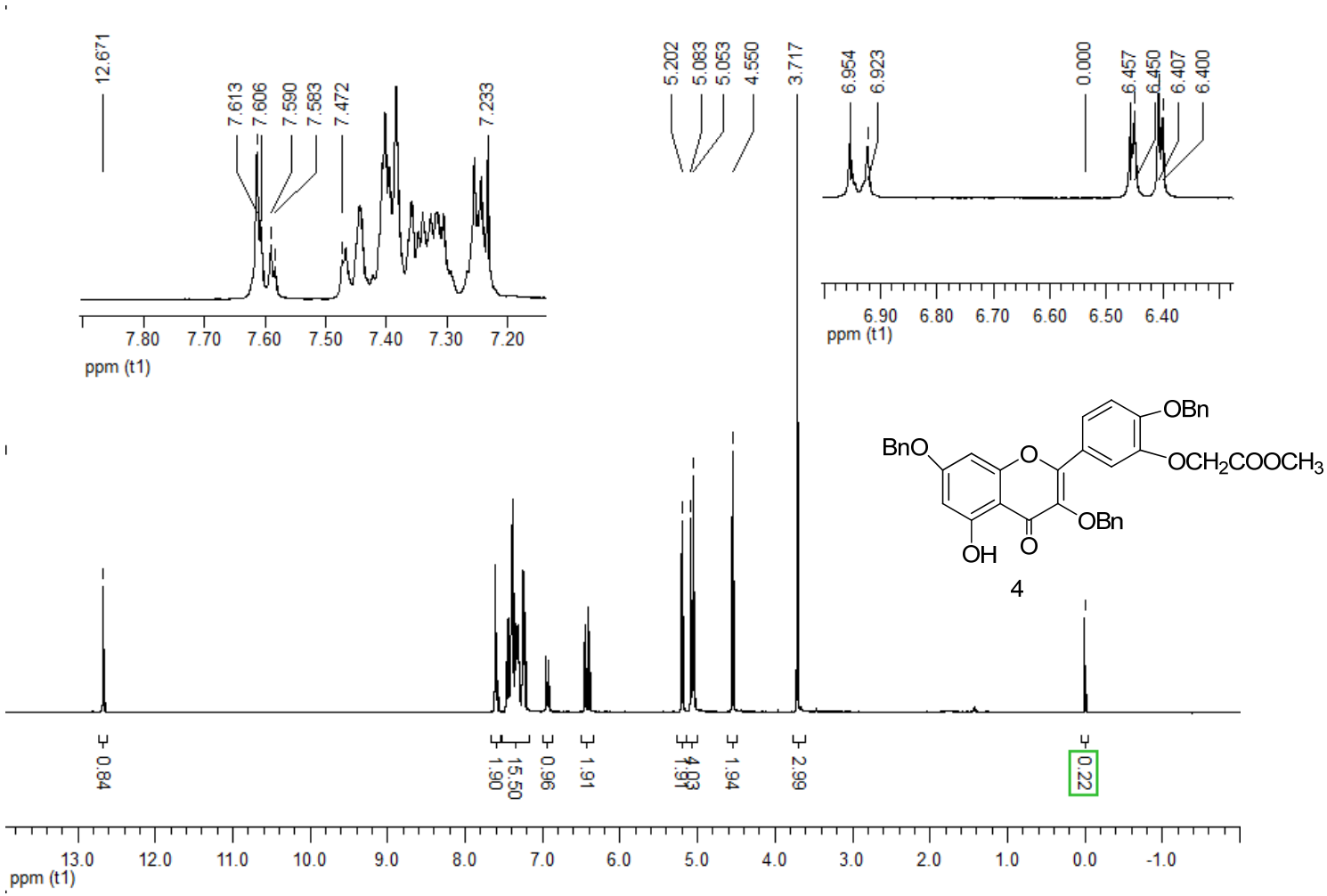

Figure 2.16 ^{1}H NMR ($CDCl_3$, 300 MHz) spectrum of compound 4.

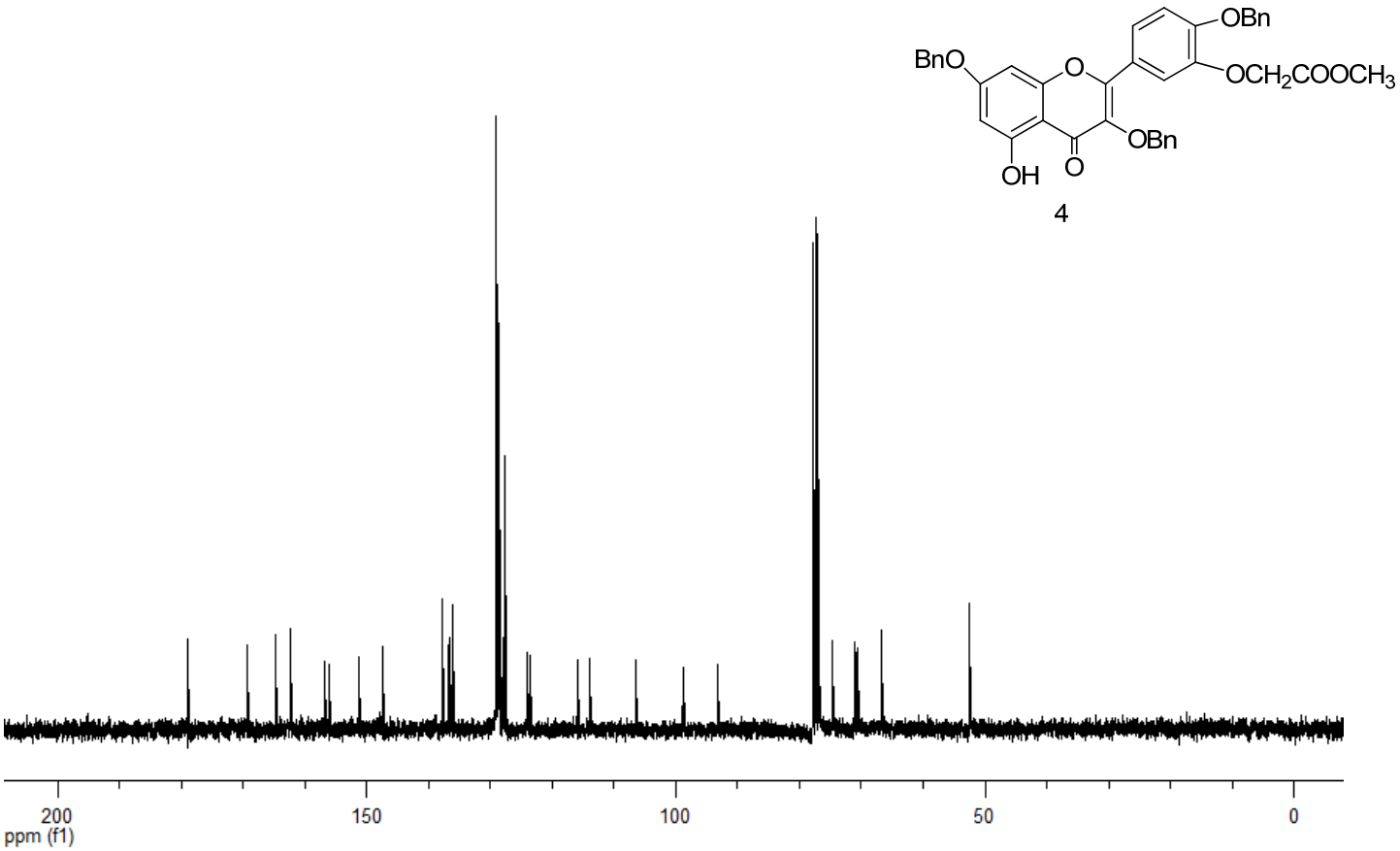

Figure 2.17 ^{13}C NMR ($CDCl_3$, 75 MHz) spectrum of compound 4.

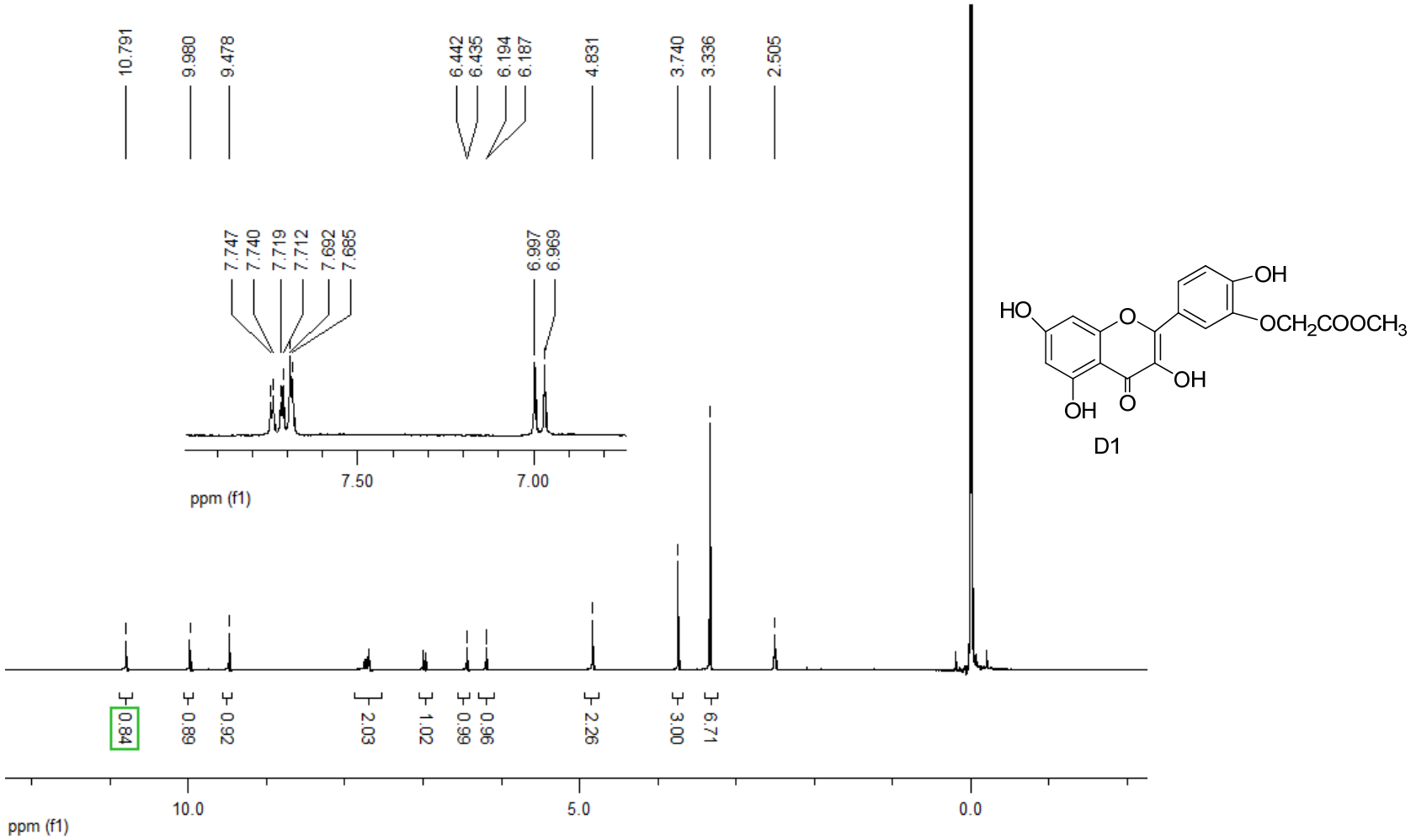

Figure 2.18 ^{1}H NMR ([D_6]DMSO, 300 MHz) spectrum of compound D1.

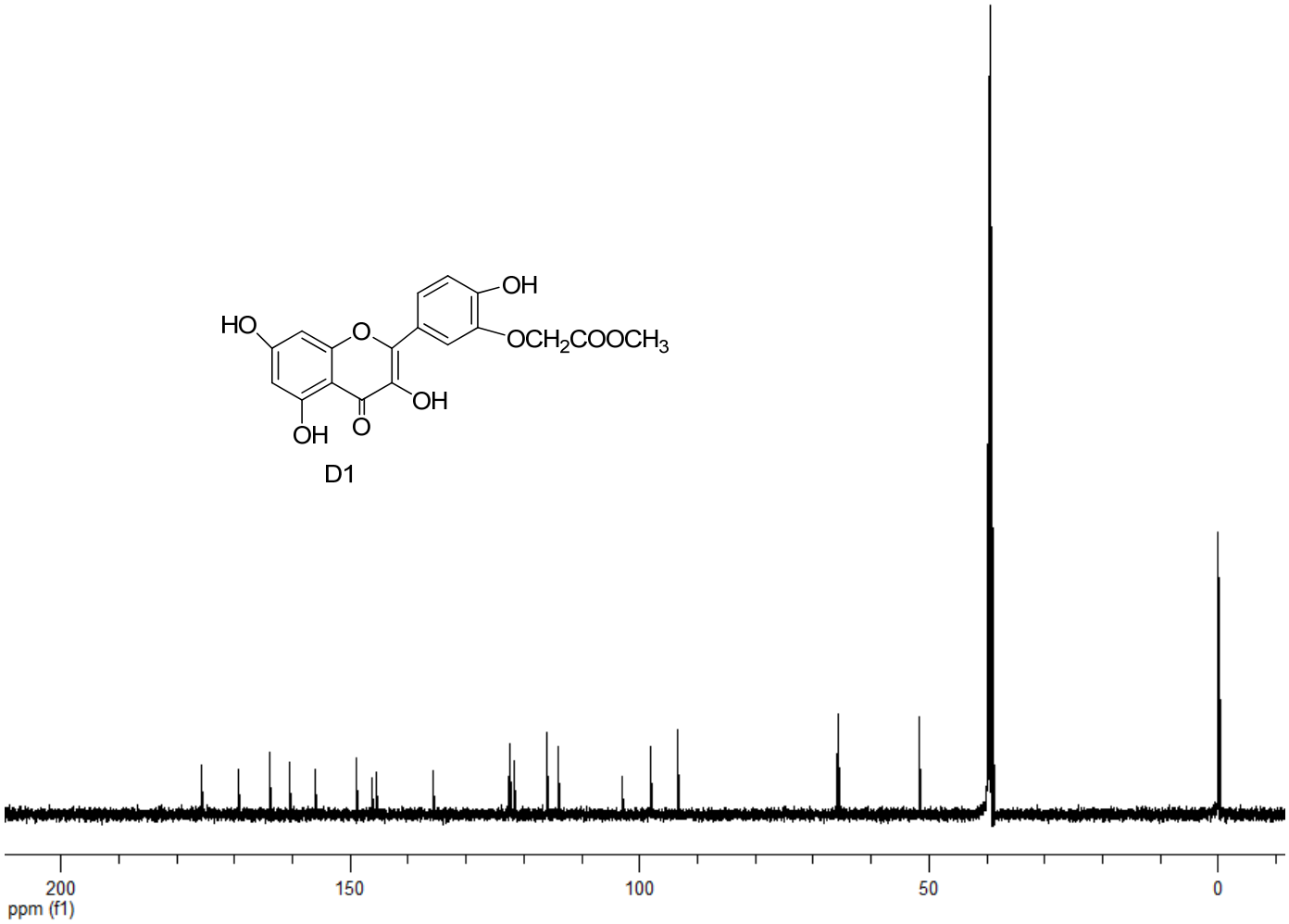

Figure 2.19 ^{13}C NMR ([D_6]DMSO, 151 MHz) spectrum of compound D1.

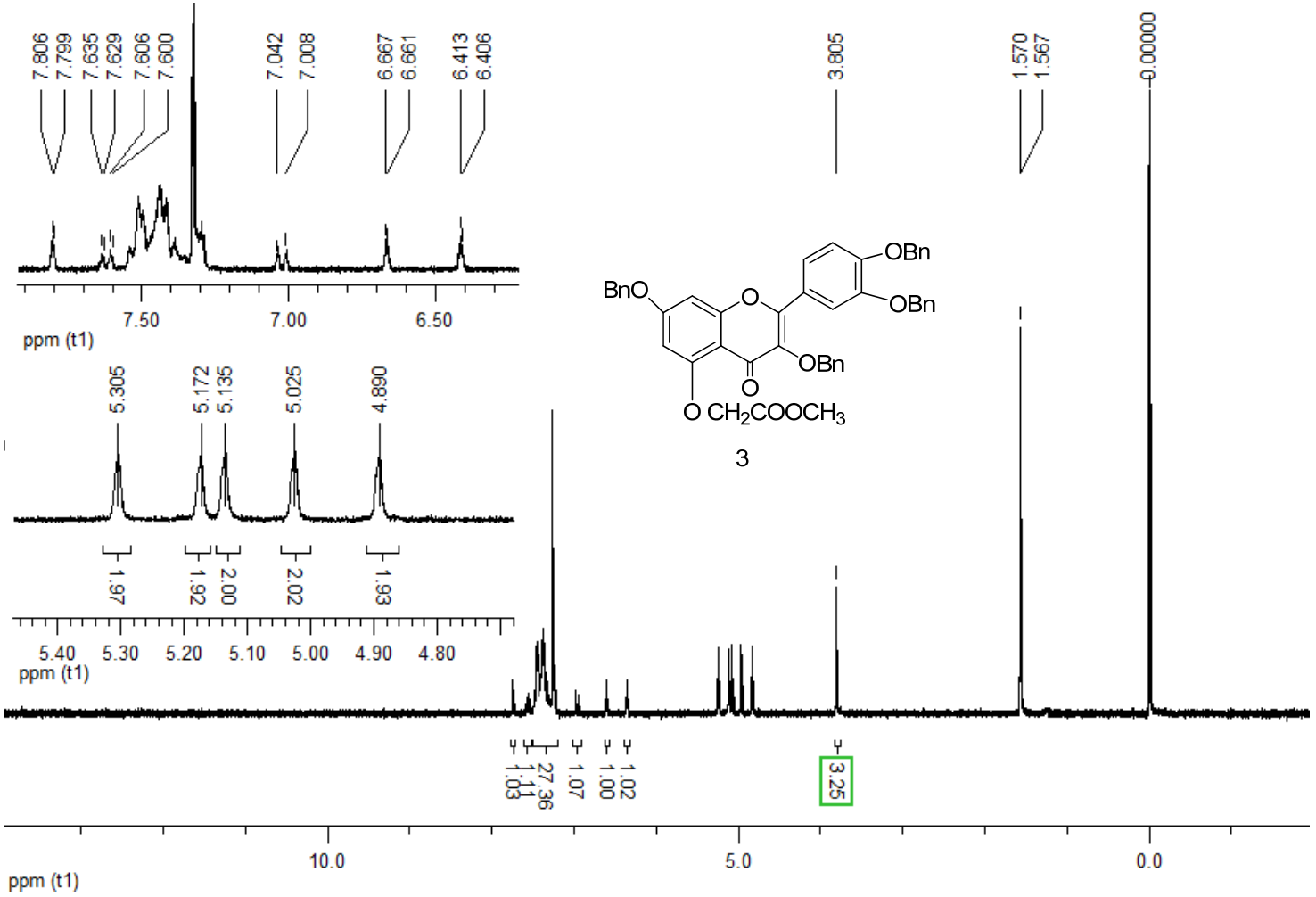

Figure 2.20 ^{1}H NMR ($CDCl_3$, 300 MHz) spectrum of compound 3.

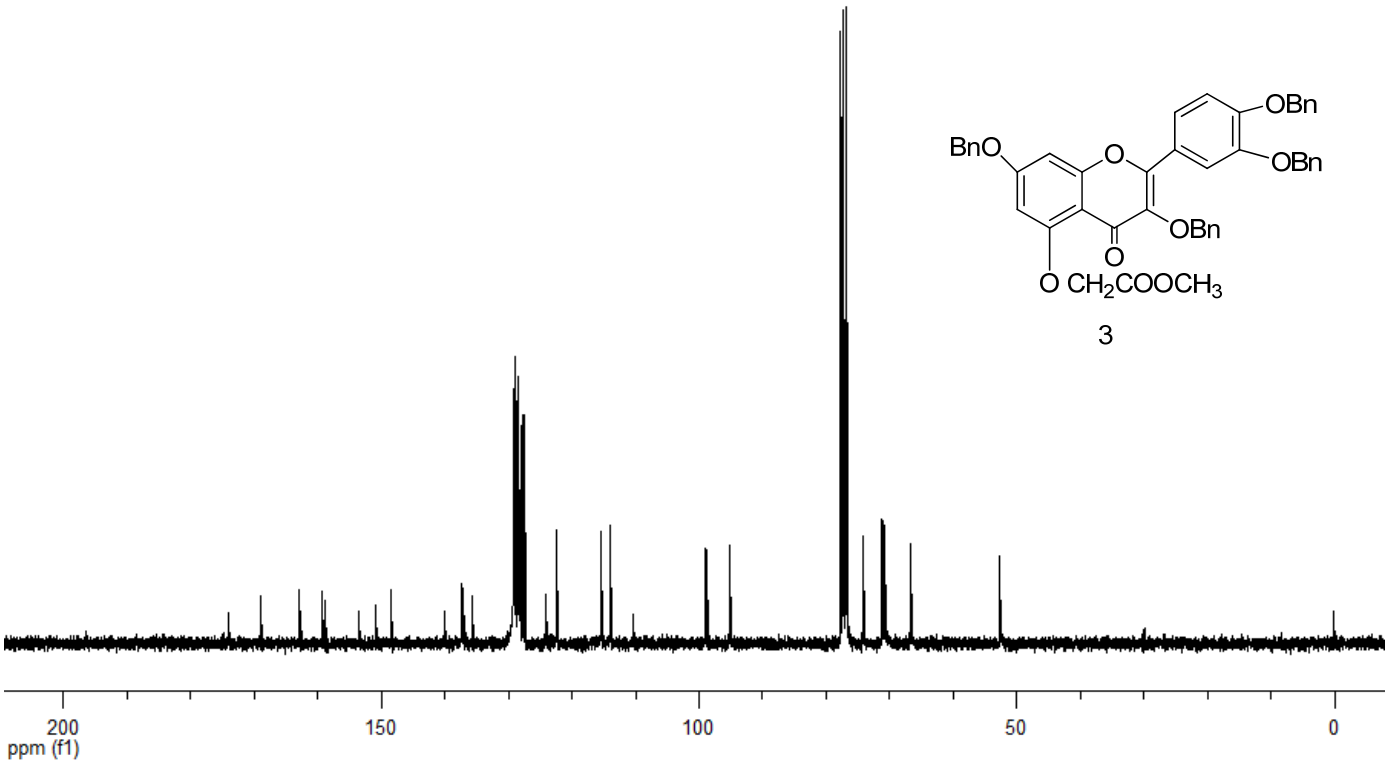

Figure 2.21 ^{13}C NMR ($CDCl_3$, 75 MHz) spectrum of compound 3.

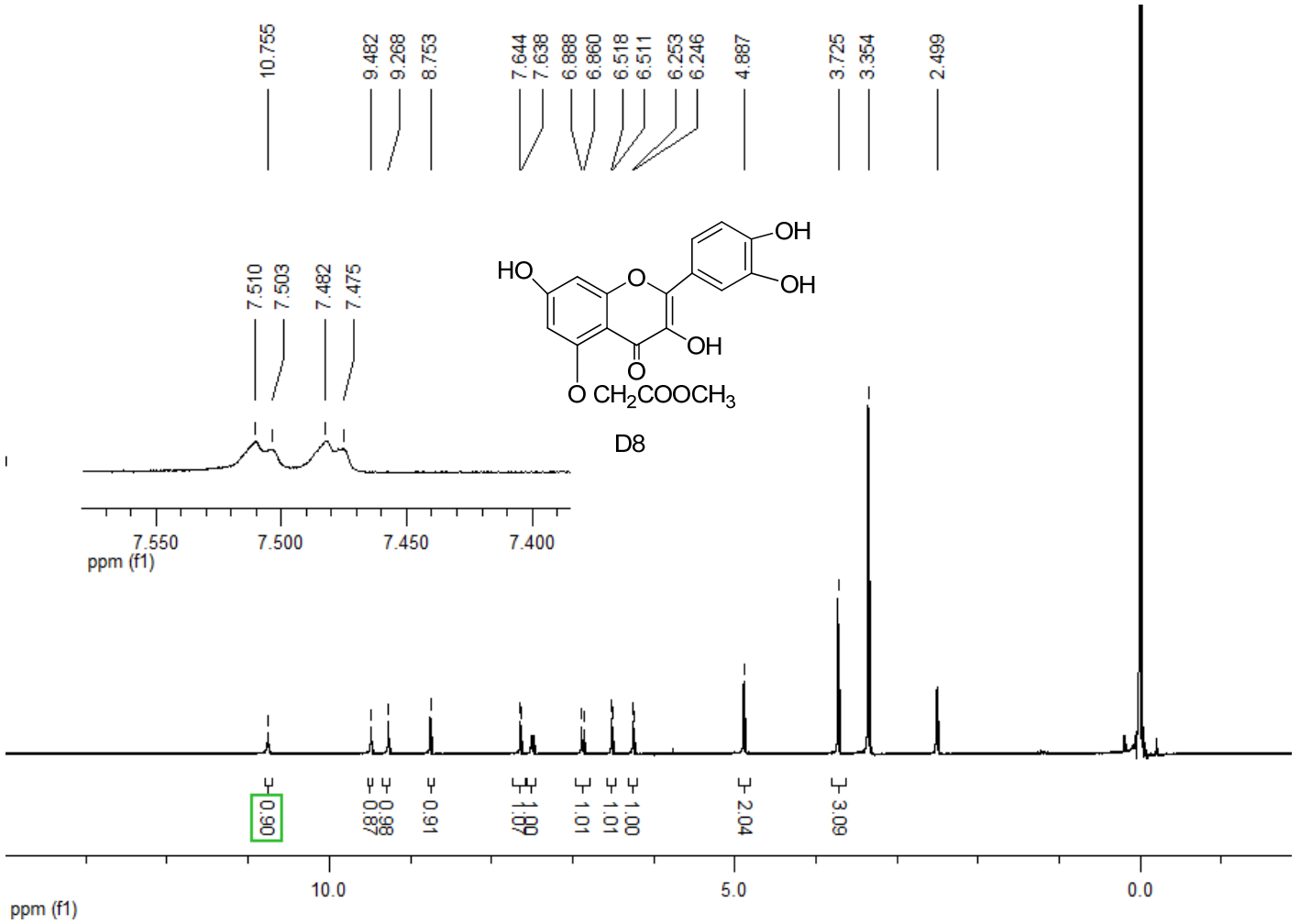

Figure 2.22 ^{1}H NMR ([D_6]DMSO, 300 MHz) spectrum of compound D8.

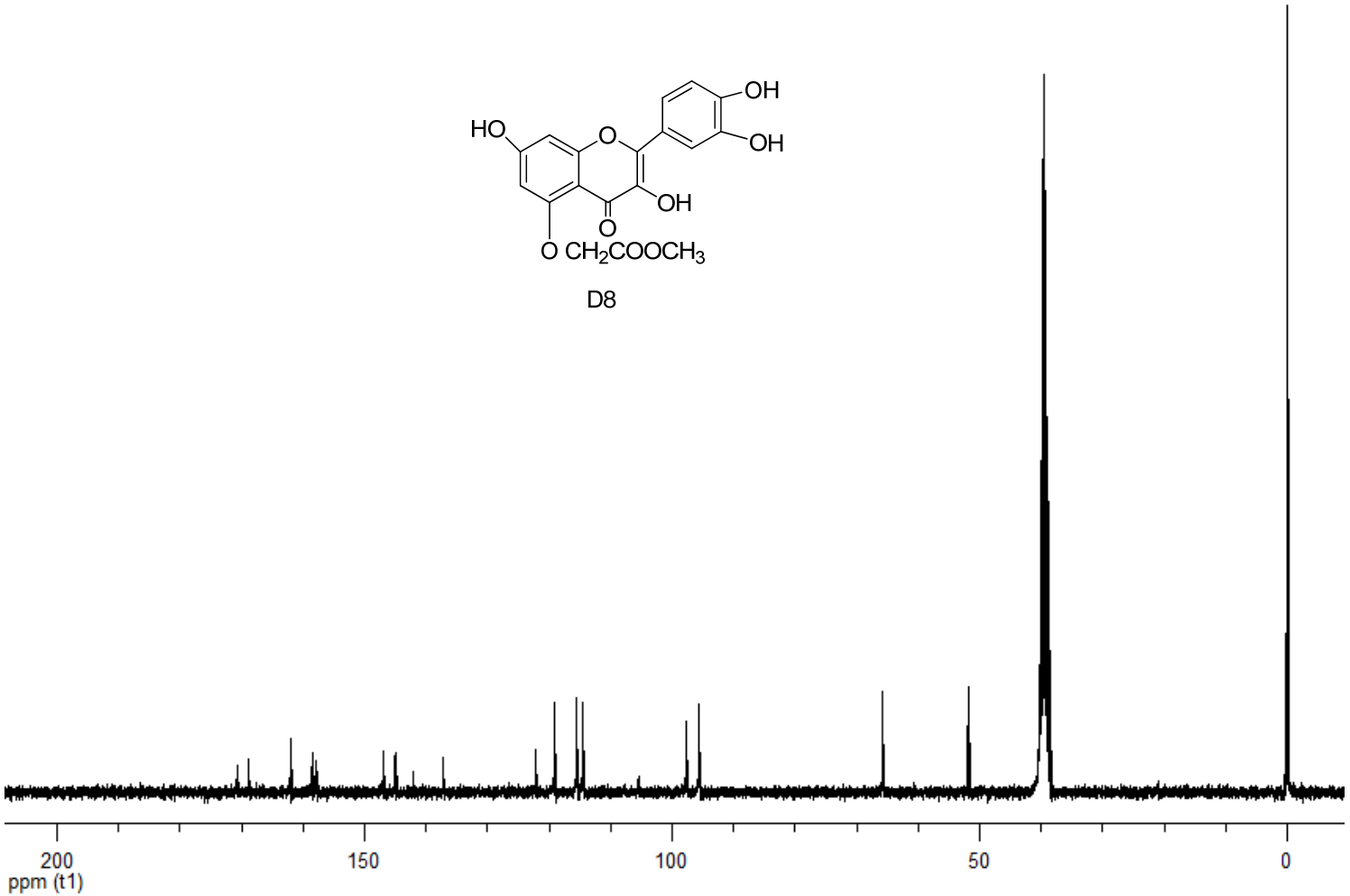

Figure 2.23 ^{13}C NMR ([D_6]DMSO, 75 MHz) spectrum of compound D8.

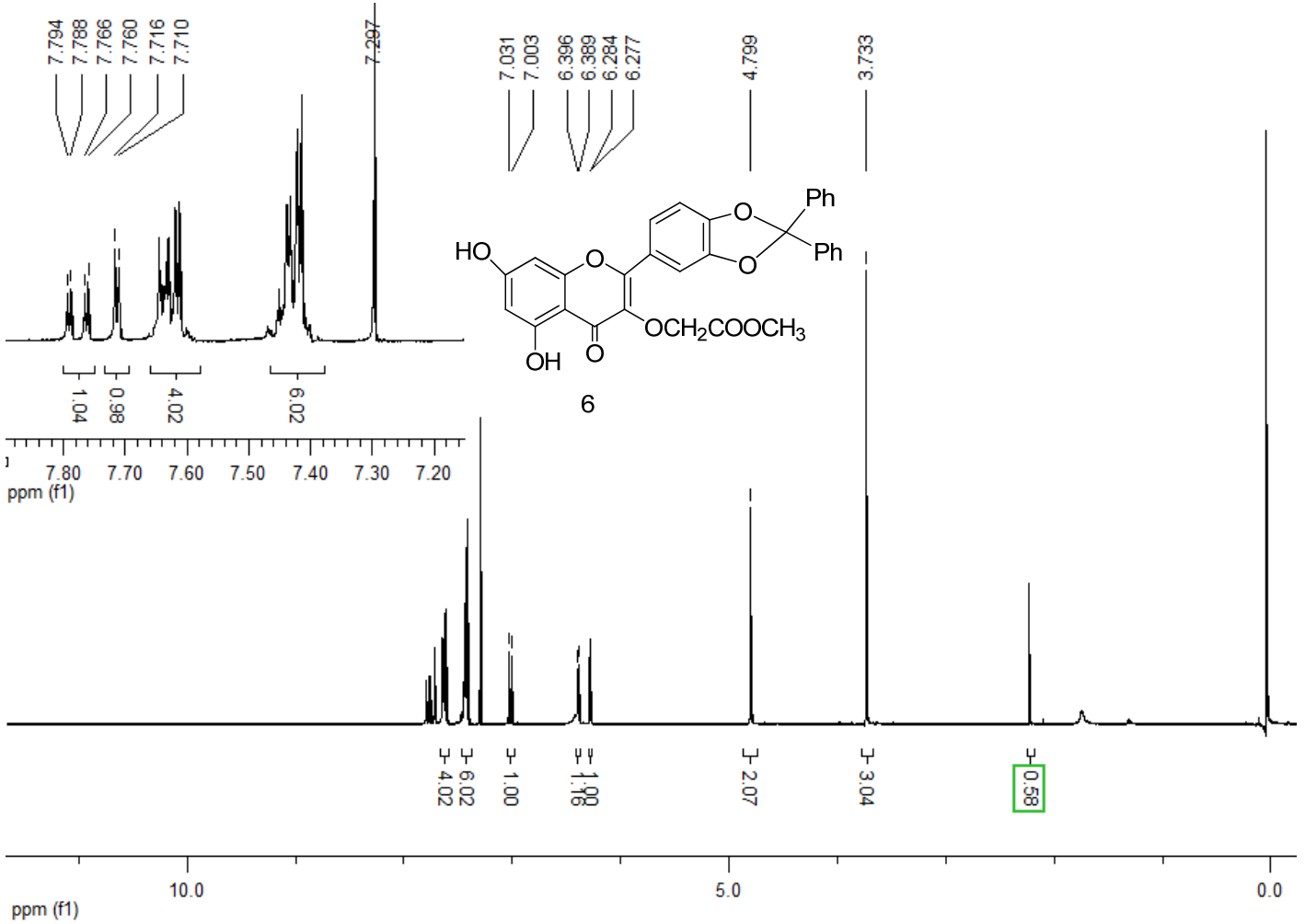

Figure 2.24 ^{1}H NMR ($CDCl_3$, 300 MHz) spectrum of compound 6.

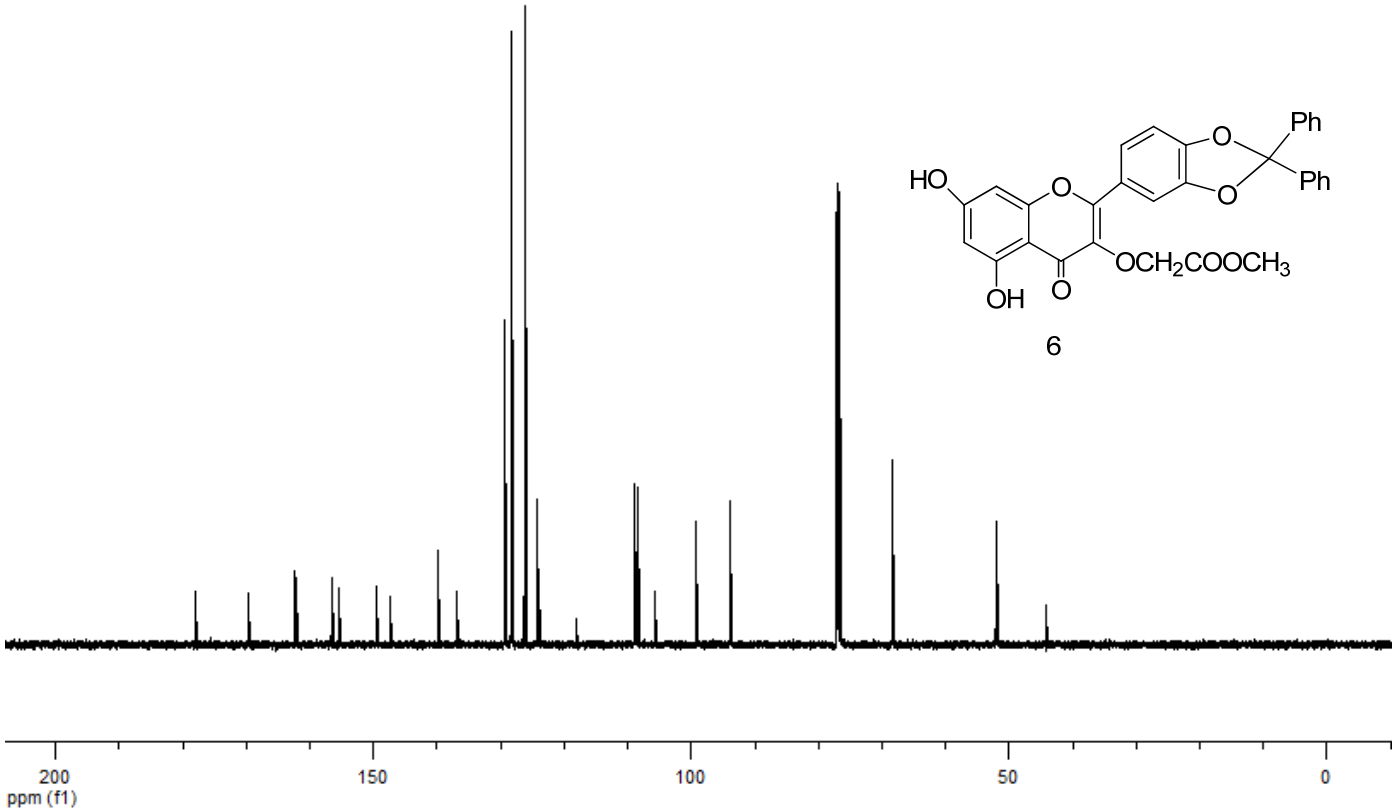

Figure 2.25 ^{13}C NMR ($CDCl_3$, 151 MHz) spectrum of compound 6.

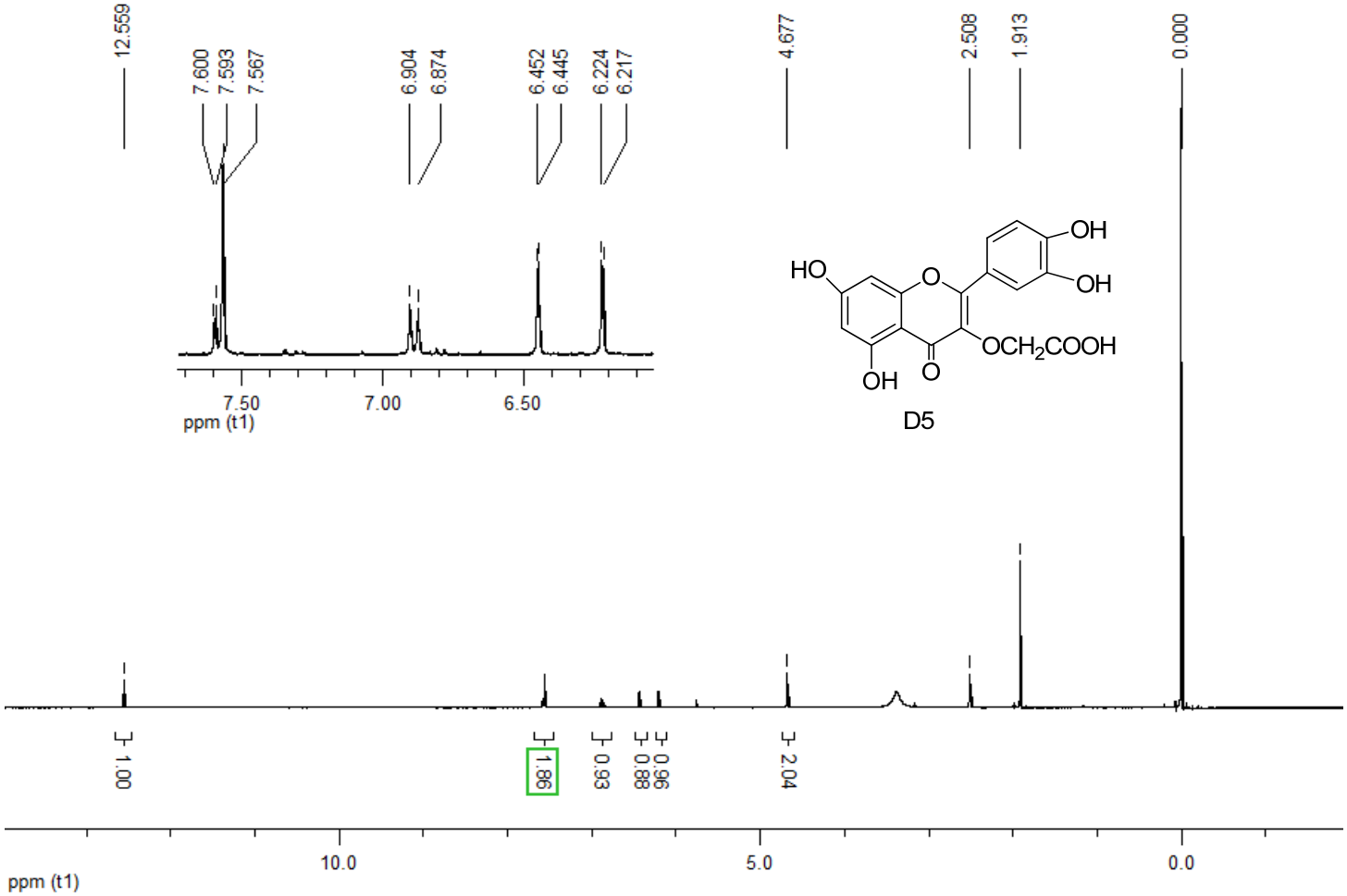

Figure 2.26 ^{1}H NMR ([D_6]DMSO, 300 MHz) spectrum of compound D5.

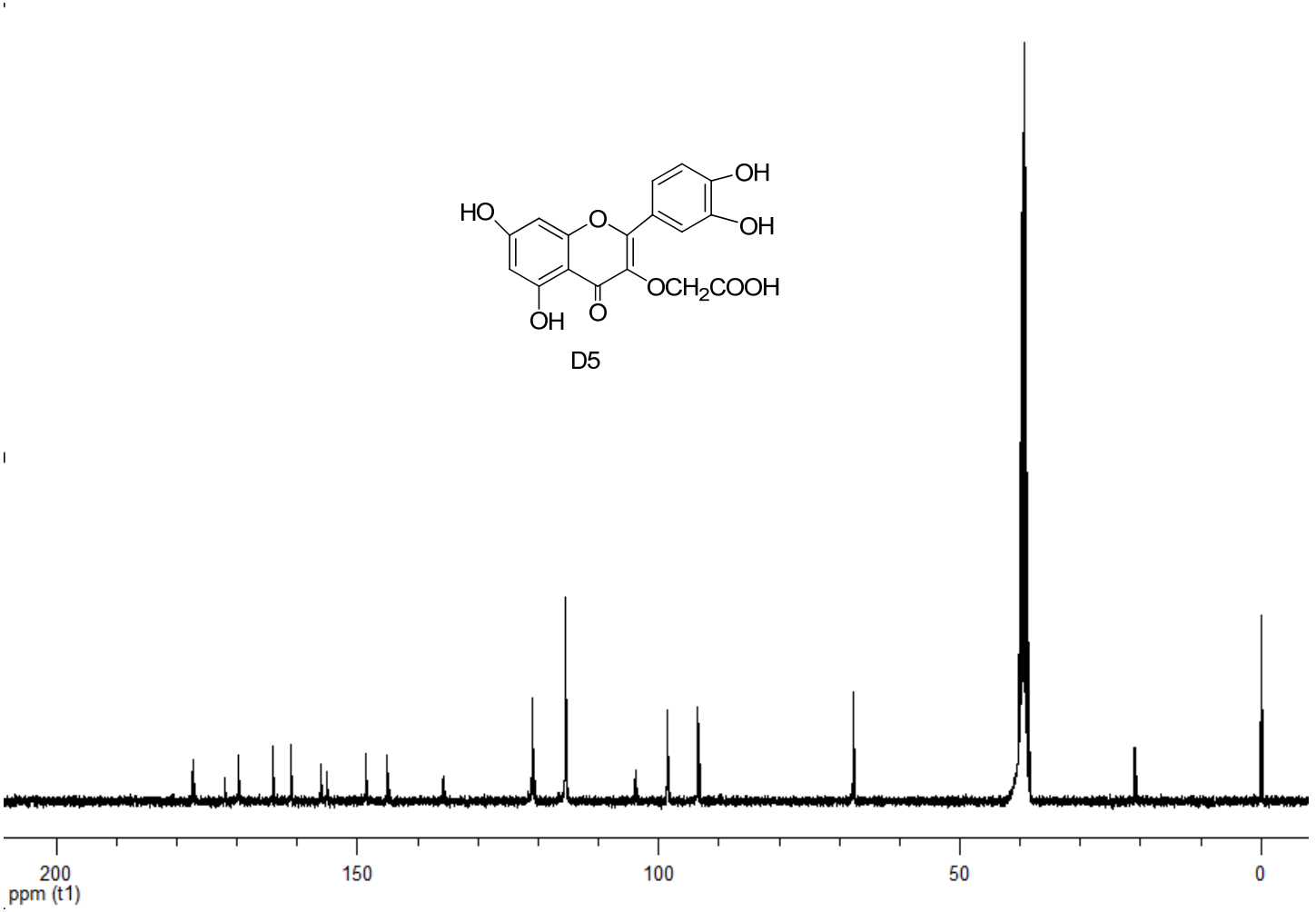

Figure 2.27 ^{13}C NMR ([D_6]DMSO, 75 MHz) spectrum of compound D5.

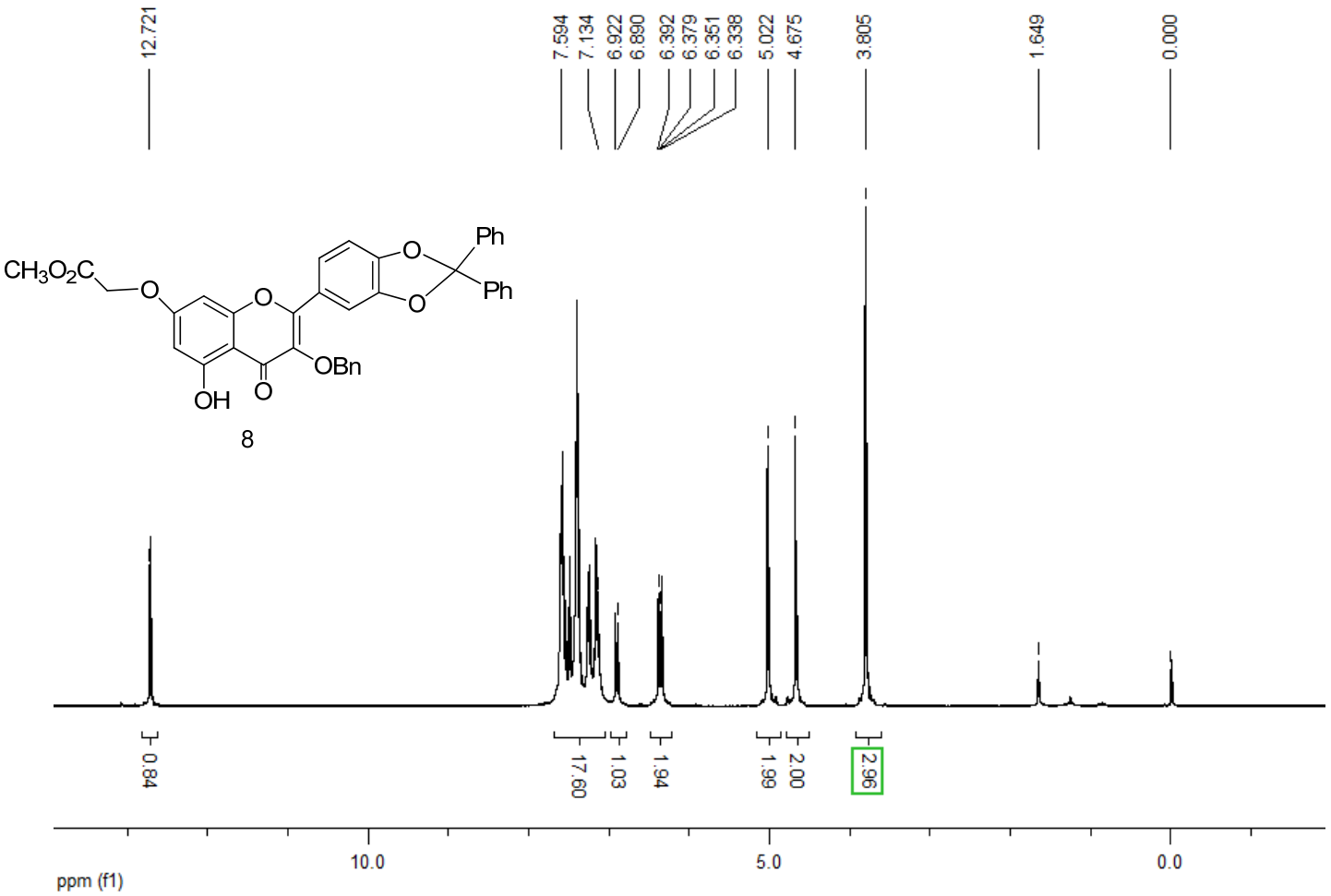

Figure 2.28 ^{1}H NMR ($CDCl_3$, 300 MHz) spectrum of compound 8.

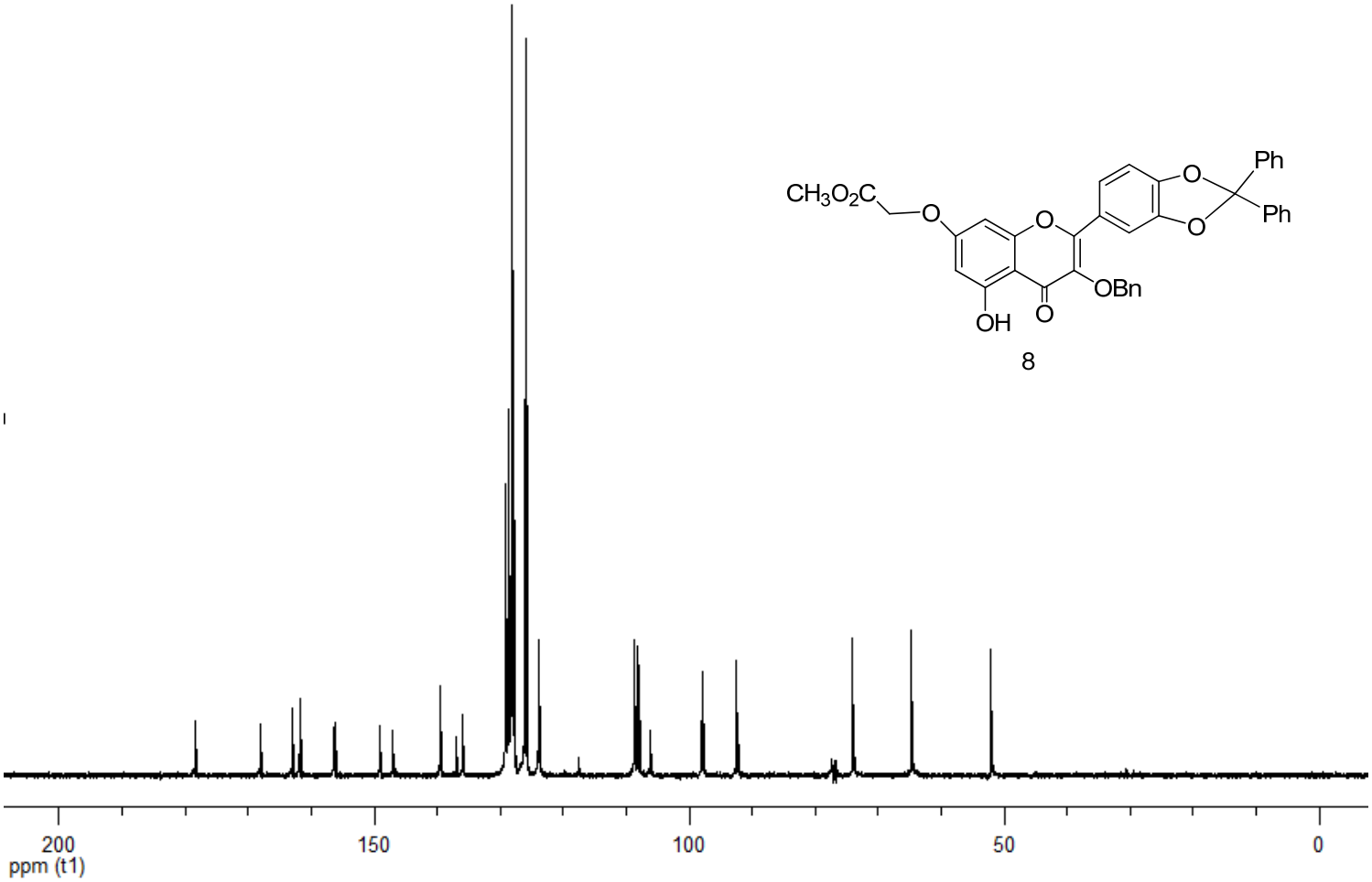

Figure 2.29 ^{13}C NMR ($CDCl_3$, 75 MHz) spectrum of compound 8.

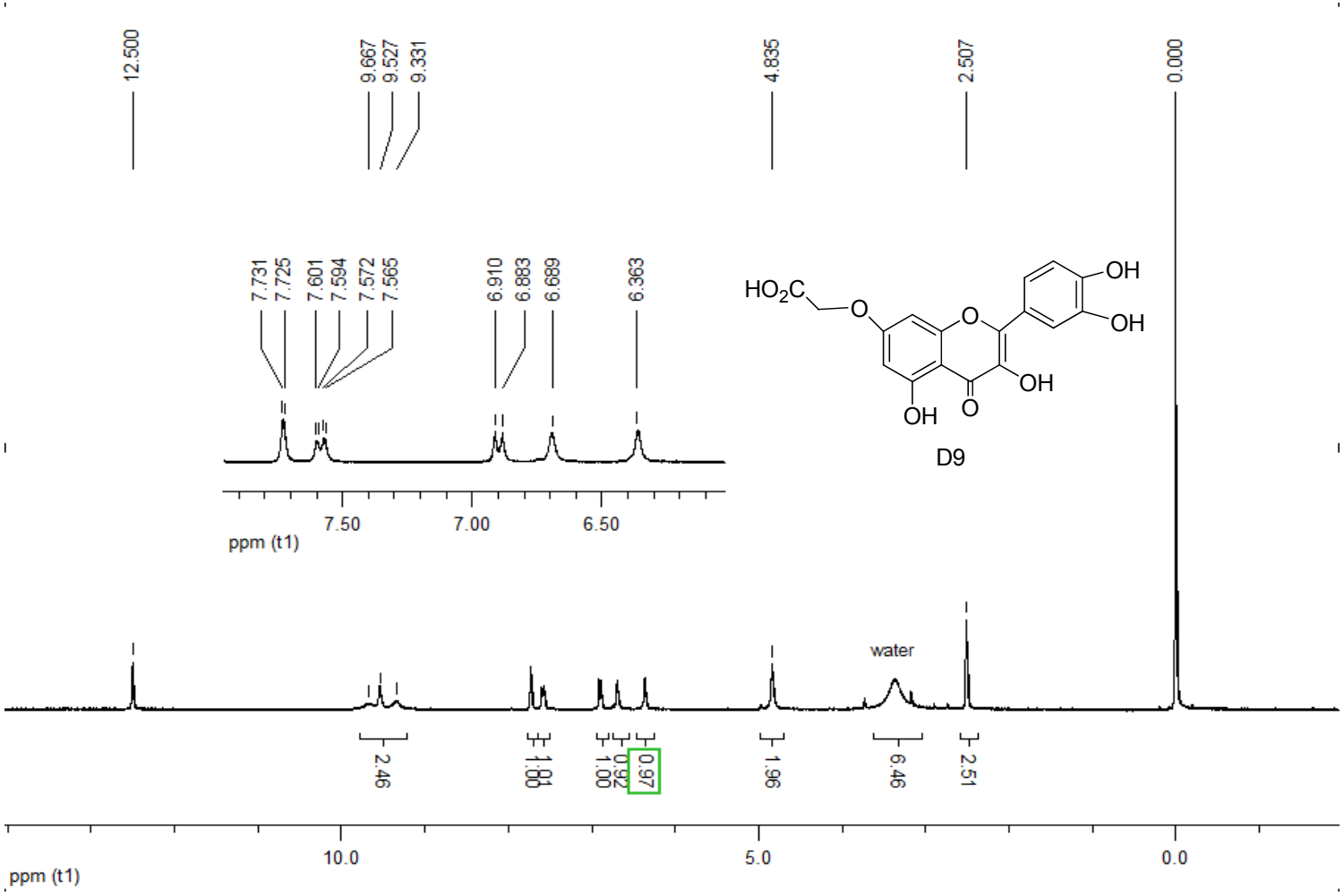

Figure 2.30 ^{1}H NMR ([D_6]DMSO, 300 MHz) spectrum of compound D9.

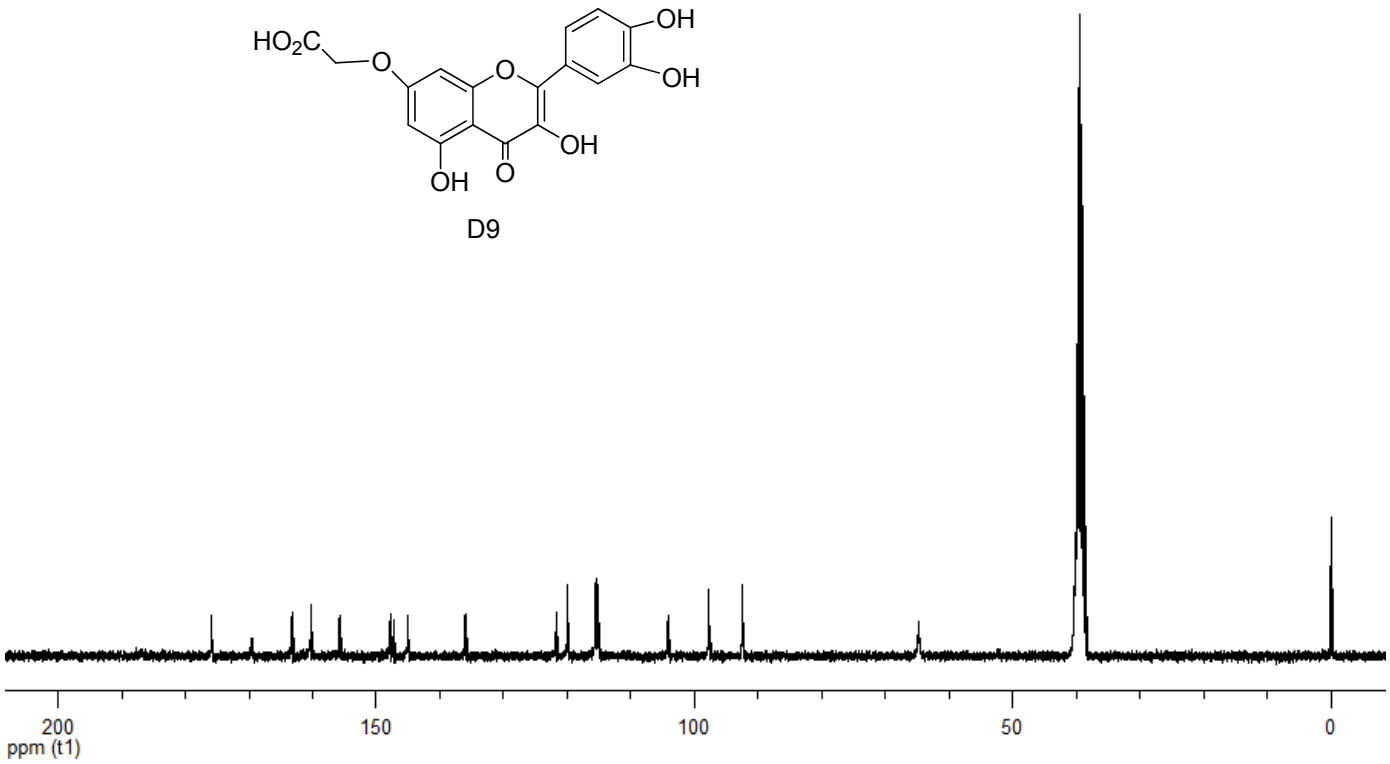

Figure 2.31 ^{13}C NMR ([D_6]DMSO, 75 MHz) spectrum of compound D9.

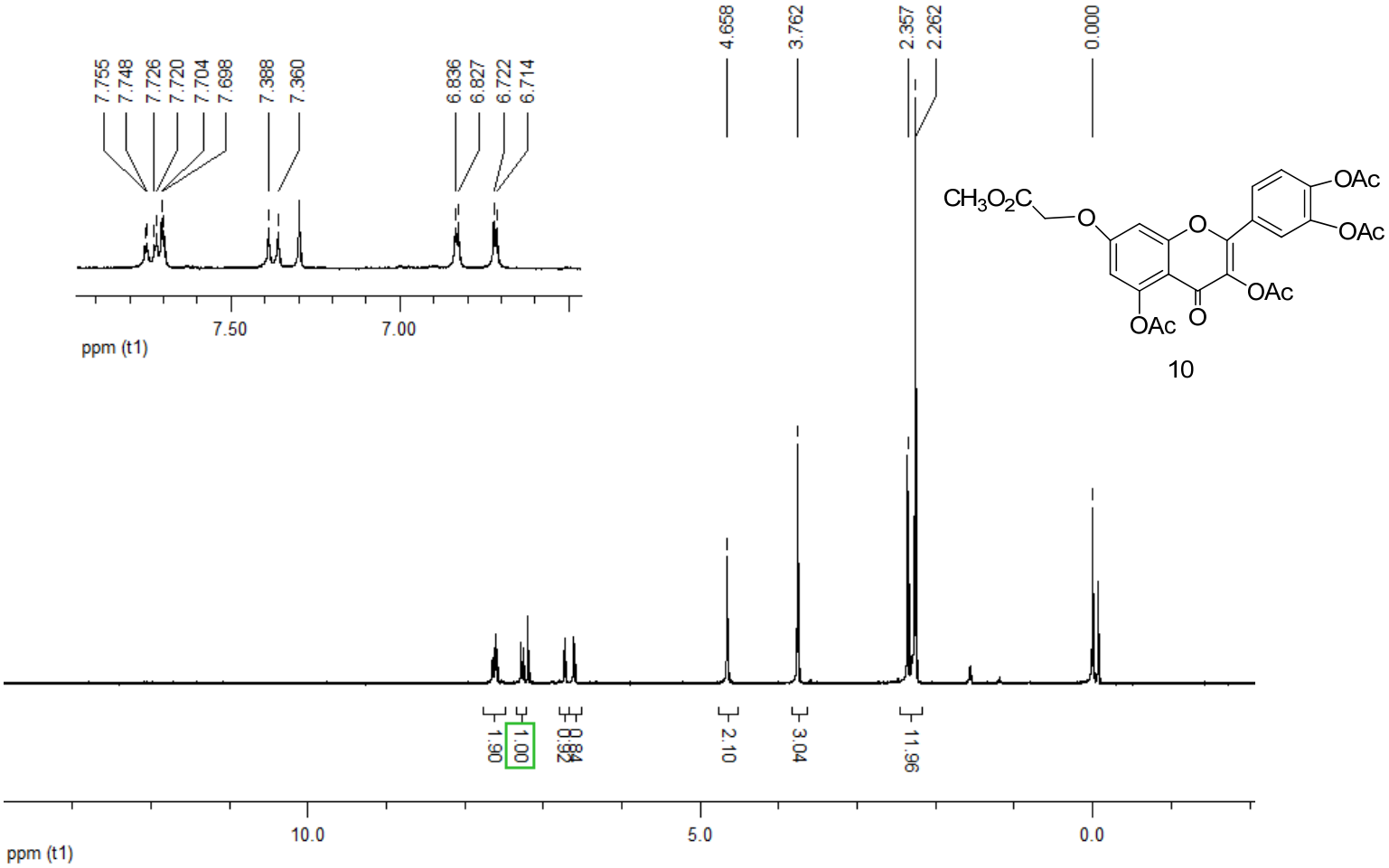

Figure 2.32 ^{1}H NMR ($CDCl_3$, 300 MHz) spectrum of compound 10.

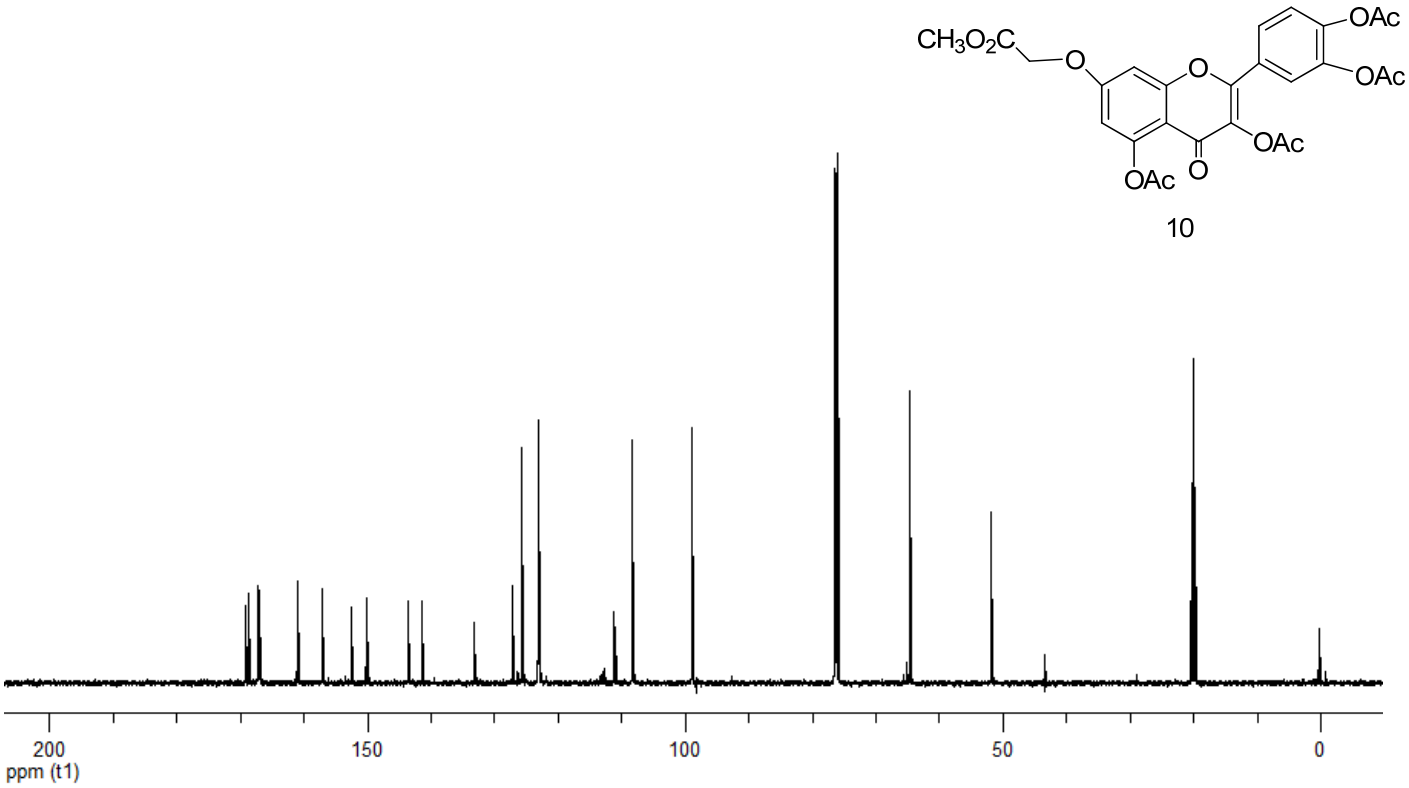

Figure 2.33 ^{13}C NMR ($CDCl_3$, 151 MHz) spectrum of compound 10.

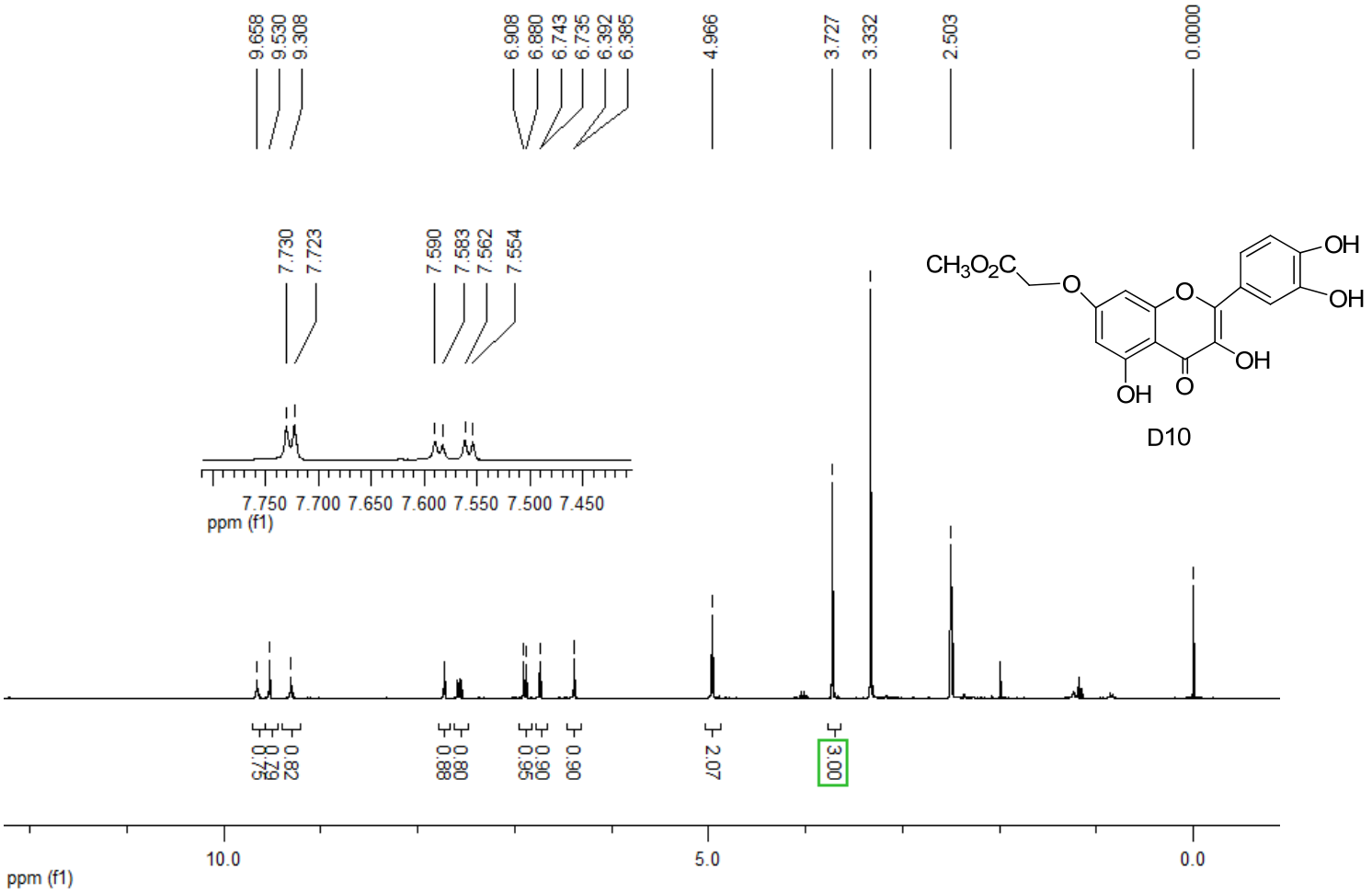

Figure 2.34 ^{1}H NMR ([D_6]DMSO, 300 MHz) spectrum of compound D10.

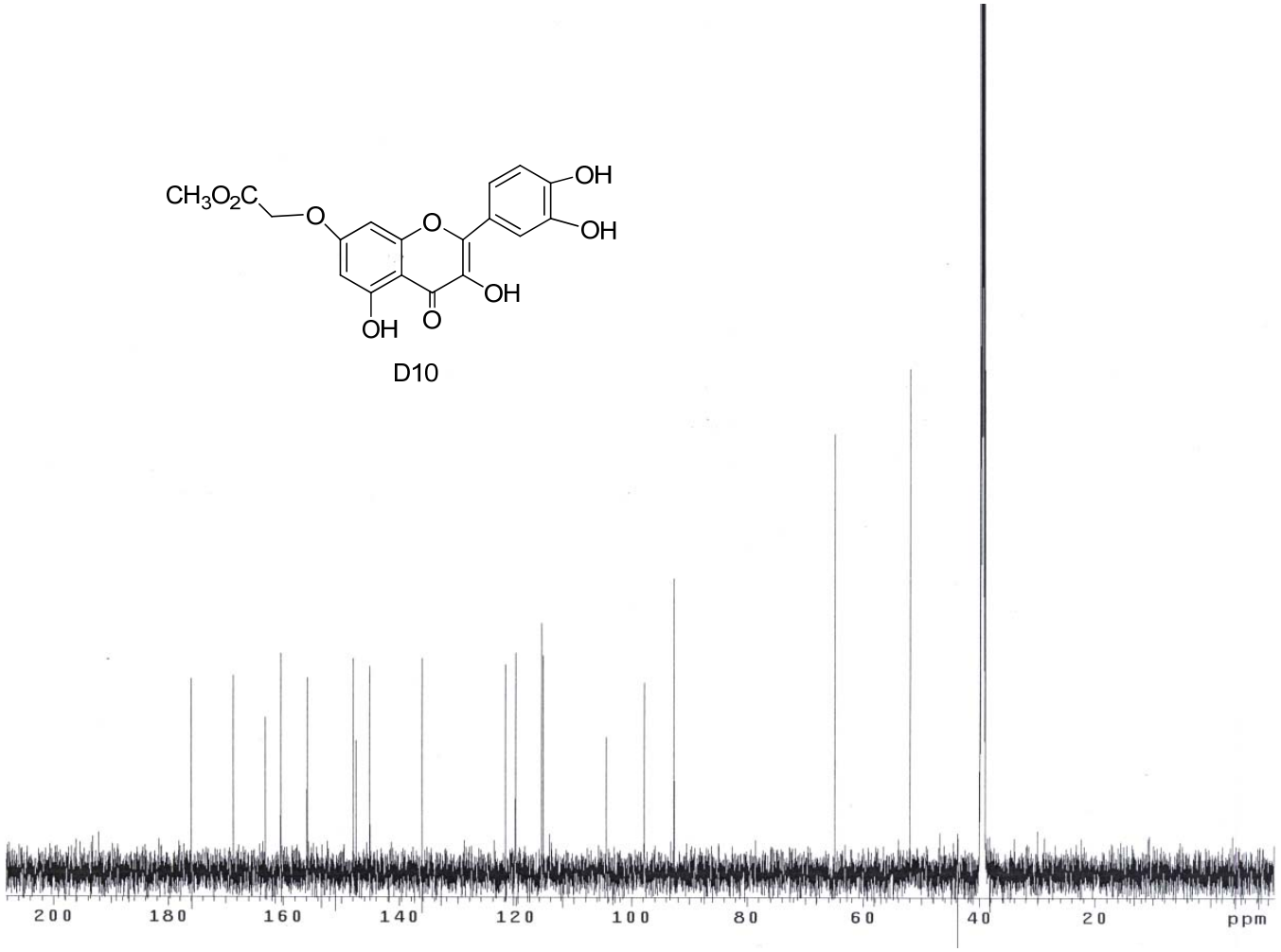

Figure 2.35 ^{13}C NMR ([D_6]DMSO, 151 MHz) spectrum of compound D10.

Chapter 3.

Identification of Quercetin Binding Proteins with a Biotinylated Quercetin Photoaffinity Reagent

The text of this chapter was taken in part from a manuscript coauthored with Clayton R. Hunt, Jiawei Chen, and John-Stephen Taylor (Washington University)

Rongsheng E.Wang, Clayton R. Hunt, Jiawei Chen, John-Stephen Taylor (Manuscript submitted, 2010)

Abstract

Quercetin is a naturally occurring flavonoid natural product that is found in many foods and has been found to have a wide range of medicinal effects. Though a number of quercetin target proteins have been identified, there has been no systematic approach to identifying all potential targets of quercetin. We are describing an O7- biotinylated derivative of quercetin (BioQ) that can act as a photoaffinity proteomics reagent for capturing quercetin target proteins, which can then be identified by LC MS/MS. BioQ was shown to inhibit heat induction of HSP70 with almost the same efficiency as quercetin, and to inhibit and photocrosslink to CK2 kinase, a known target of quercetin involved in activation of the heat shock transcription factor. When normal or heat shocked Jurkat cells were incubated with BioQ, then UV-irradiated before being lysed, a number of proteins could be recovered by subsequent incubation with streptavidin beads. Following gel electrophoresis, isolated protein bands were trypsinized and analyzed by LC MS/MS to identify heat shock proteins HSP70 and HSP90 as potential targets, along with ubiquitin-activating enzyme, a spliceosomal protein, mitochondrial and RuvB-like 2 ATPases, and eukaryotic translation initiation factor 3. Most of these proteins have been previously identified as potential therapeutic targets for cancer, suggesting that some of the anticancer properties of quercetin may be related to their inhibition.

Introduction

Quercetin has antioxidant [1, 2], anti-inflammatory[3] and anticancer [4-6] activities with almost no human toxicity [7]. At the molecular level, quercetin has been found to inhibit many ATP binding enzymes and in particular kinases [8], suggesting that some of its biological effects may be due to inhibition of signaling pathways. Thus quercetin is an interesting lead compound for further pharmaceutical development [5] and has been the subject of over 7,000 research publications. In spite of this, very little is known about all the proteins it targets and which are predominantly responsible for a particular biological effect.

As introduced in chapter 1, our interest in quercetin initially arose from its well known ability to inhibit the heat induction of heat shock protein 70 (HSP70), also known as HSP70-1a, HSP70-1 and HSP72. The HSP70 deficient mouse embryonic fibroblasts are more sensitive to radiation following heat treatment [9] suggesting that agents that suppress heat induction of HSP70 might function as radiosensitizers. Despite the classification as a heat responsive protein, HSP70 is also induced, along with other heat shock proteins, in response to wide range of chemical and physiological stresses, and is overexpressed in many cancers [10-12]. Thus small molecule inhibitors of HSP70 and its induction may have potential therapeutic value for treating cancer. Unfortunately, quercetin's multiple biological effects and the high concentration required to inhibit HSP70 induction diminish its potential as a therapeutic adjuvant.

Identifying the protein target(s) of quercetin's inhibition of HSP70 and its induction, however, could aid in the development of more selective agents. One systematic approach has involved screening chromatographic fractions of cells extracts for

quenching of protein fluorescence in the presence of quercetin, followed by SDS-PAGE of the active fractions, and MASCOT analysis of the trypsinized fragments [13]. Unfortunately, without authentic protein samples, it is difficult to establish which of the protein bands detected in the SDS-PAGE gel are quercetin binding proteins.

A more promising method for identifying protein targets of a bioactive compound is to derivatize the compound with biotin which serves as an affinity tag allowing the bound proteins to be isolated with streptavidin [14, 15]. The isolated proteins are then separated and identified by bottom up mass spectrometry. There have been several reports in which compounds with K_d's of around 1 nM can be isolated in this manner from cell lysates [16-18]. To identify more weakly binding proteins, phage display libraries have been used in place of cell lysates to afford a higher concentration of protein [19], although this approach is limited by the contents of the library. Another approach is to increase the affinity of the compound by attaching a photocrosslinking agent [14, 15, 20] or by making use of intrinsic photoaffinity properties of the compound. In all cases, biotin must be attached to the compound at a position that does not interfere with target protein binding.

In chapter 2, to guide the synthesis of biotinylated quercetin derivatives, we synthesized all of the mono-methyl and selected carbomethoxymethyl derivatives of quercetin and determined their ability to inhibit heat shock induction of HSP70s [21]. We found that the C7 and C3' hydroxyls on quercetin can be derivatized with a bulky carbomethoxymethyl group without affecting its ability to inhibit HSP70 induction, and could therefore be used to attach biotin (Figure 3.1). We also found that all quercetin derivatives capable of inhibiting heat induction of HSP70, were also able to inhibit two

protein kinases known to activate heat shock transcription factor 1 (HSF1), CAMK2 and CK2, suggesting that these may be targets of quercetin's action. The K_d's for these enzymes, and for most known enzyme targets of quercetin are in the micromolar range, indicating that a photoaffinity approach would be required to pull down the quercetin binding proteins. Luckily, quercetin has been shown to be photoactive [22], and to photocrosslink malate dehydrogenase to which it binds [23]. In this chapter, I am presenting the synthesis of the C7-biotinylated quercetin derivative, 7-BioQ, and show that it can be photocrosslinked to CK2 in vitro, and to various proteins in vivo following heat shock, among which were heat shock protein 70 and 90, two ATPases, an ubiquitin activating protein, and a translation initiation factor. Most of these proteins have been previously identified as potential therapeutic targets for cancer, suggesting that their inhibition may also be partially responsible for the anticancer effects of quercetin.

Results

Synthesis of the Biotin Quercetin Conjugate, BioQ. The selective coupling of biotin to the 7-OH of quercetin was carried out by two synthetic routes (Figure 3.2) based on a previously developed method for the selective methylation and benzylation of the 7-OH [27]. The first route was to alkylate the 7-OH with *tert*-butylchloroacetate after which the ester would be converted to an acid and coupled to an amine derivative of biotin. Thus, quercetin pentaacetate was refluxed in anhydrous acetone with excess *tert*-butyl chloroacetate in the presence of potassium carbonate and catalytic potassium iodide with TLC monitoring to minimize over-alkylation. The *tert*-butyl ester **2** was converted

to the acid **3** by treatment with 20 % trifluoroacetic acid in methylene chloride under anhydrous conditions to limit competing hydrolysis of the remaining acetate protecting groups. Coupling of the amino biotin derivative **6** [26] with the tetra-acetate acid **3** was problematic. Both reactants are very polar and only dissolved well in dimethyl formamide or water-acetonitrile mixtures. When the reaction was carried out in the presence of N, N-diisopropylethylamine (DIPEA) with HATU, DCC, or ByBOP, extensive decomposition of the quercetin tetra-acetate occurred, which may have been the result of deacetylation. Similar results were observed with DCC or EDC in dimethyl formamide in the absence of base, suggesting the possible involvement of the amino group of amino biotin **6** and hence the necessity of a buffered solution in neutral to acidic pH. Final treatment with EDC and N-hydroxysuccinamide at a slightly acidic pH of 6, in the presence of MES buffer, afforded the desired coupled product **5** in 10 % to 15 % yield. Attempts to improve the yield by further lowering the pH, however, failed to give desired product. Complete deacetylation was attempted under basic conditions, such as aqueous sodium hydroxide or sodium methoxide in methanol, but only afforded the desired biotinylated quercetin **9** in low yield. Biotinylated quercetin could be obtained, however, in 74% yield upon treatment with the hydroxamic acid **8** under near neutral conditions in pH 7.4 phosphate buffer.

Because direct coupling of the quercetin acid **3** with biotin amine **6** was so problematic we investigated whether we could directly alkylate the 7-OH of quercetin with the commercially available biotin alkylator –biotin(PEO) iodoacetamide **7**. Ideally, one could simply use the method described above in which quercetin penta-acetate is alkylated selectively at O7 by refluxing the alkylating agent with potassium carbonate in

acetone. We were, however, concerned that the iodine containing **7** might self-react under these conditions, so we decided instead to alkylate the quercetin tetraacetate **4** under milder conditions. Quercetin tetra-acetate **4** has been previously prepared by treatment of the penta-acetate **1** with lipase [28], or more recently, with imidazole and thiophenol in N-methyl-2-pyrrolidone (NMP) [29]. We found that the latter method using the more convenient solvent dichloromethane in place of NMP afforded quercetin tetra-acetate **4** in 65% yield (Figure 3.2). Treatment of **4** with the iodoacetamide **7** in anhydrous dimethyl formamide with cesium carbonate in the dark afforded the desired biotinylated quercetin tetra-acetate **5** in 85% yield. Attempts to use potassium carbonate, in place of cesium carbonate, failed to give the desired product. Deacetylation of compound **5** with N-methyl-2-dimethylamino-acetohydroxamic acid again afforded biotinylated quercetin **9**.

Structural Characterization of BioQ 9. To verify that the biotin was indeed coupled to the hydroxyl at position 7 of quercetin, and had not been coupled to another hydroxyl that might have been produced by transesterification of the acetate groups, we characterized the product by COSY, HMQC, and HMBC NMR (Figures 3.3-3.6). Aromatic protons H15 and 16 could be readily identified by their large ortho-coupling in the 1D ^{1}H NMR and a strong crosspeak B in the COSY spectrum (Figure 3.4). This allowed identification of proton 12 through a crosspeak A with H16, leaving aromatic protons H6 and H8 which showed a crosspeak C between them. The assignment of protons H6 and H8 allowed identification of C7 in the HMBC spectrum through crosspeaks J and H (Figure 3.6). C7 in turn showed a crosspeak F to the H17 protons of the acetamide group verifying the connection of the biotin derivative to O7. The

assignment of the H17 protons was confirmed by a crosspeak E with C18 via HMBC, which in turn showed a correlation K with the amide NH (d) (Figure 3.6). The biotin group could be easily identified by the crosspeak (D) between H19 and H20 (Figure 3.4). The rest of structure could be confirmed by key proton-carbon crosspeaks in the HMBC spectrum (Figure 3.6), such as crosspeaks G (H^b - C21), Q (H^a – C21), I (H6 – C5), L (H8 – C9), M (H15 – C14), N (H16 – C11), O (H12 – C11) and P (H12 – C14).

Substrate activities of BioQ. Previously, we had shown that quercetin and its 7-*O*-methyl and carbomethoxymethyl derivatives could inhibit Casein kinase II (CK2) and Ca^{2+}/calmodulin-dependent protein kinase II (CAMK2), and that this inhibition was correlated to its ability to inhibit heat induction of HSP70s [21]. To determine whether derivatization of quercetin at O7 with a much larger biotin-containing group would interfere with binding to these enzymes, the ability of BioQ to inhibit these enzymes was assayed by the same *in vitro* protein kinase inhibition assay we used previously for the simple quercetin derivatives (Table 1). The IC50s of both quercetin and BioQ for CK2 were similar and about 5 μM, while the IC50 of BioQ for CAMK2 was about 8-fold higher than for quercetin (25 μM compared to 3 μM). To determine whether BioQ could inhibit heat induction of HSP70s, Jurkat cells, which have a very low basal expression of HSP70s, were heat shocked in the presence of 145 μM quercetin and BioQ, and assayed by a western blot. BioQ showed substantial inhibition of HSP70 induction compared to the controls, though not as complete as quercetin (Figure 3.7). The lower inhibition of HSP70 induction by BioQ is consistent with a higher IC50 for CAMK2 than observed for quercetin, and my previous conclusion that effective inhibitors had to be good inhibitors of both CK2 and CAMK2 [21]. It may also be that BioQ is not as permeable as quercetin

and unable to achieve a high enough concentration in the cell to be completely effective against CAMK2, which required an IC50 of 25 μM. None-the-less, the ability of BioQ to cause substantial inhibition of heat shock induction of HSP70 validated its use as an affinity probe for proteins involved in this and possibly other biological process. In this regard, other 7-*O*-quercetin derivatives have been shown to retain antitumor activity [30].

Casein kinase 2 pull-down in vitro by BioQ probe. Our attention then focused on demonstrating that I could pull down casein kinase 2 (CK2) which we had demonstrated could be inhibited by the BioQ probe. Initial experiments indicated that the streptavidin agarose beads would also bind and pull down proteins in the absence of BioQ when using the same buffer that would be used to lyse the cells. Despite many attempts, I was unsuccessful at finding a wash buffer that would remove non-specifically bound proteins from the streptavidin beads without removing BioQ bound proteins.

Because quercetin has been reported to be photoreactive and capable of photocrosslinking to malate dehydrogenase [23], we thought that UV irradiation could be used to photocrosslink BioQ to CK2 and other target proteins *in vivo*. Photocrosslinking would thus prevent CK2 or other target proteins from dissociating during affinity purification with the streptavidin and allow more stringent washing steps. Quercetin and BioQ show two absorption maxima at about 320 and 380 nm of about equal absorptivity, the latter of which would be preferred for photocrosslinking in vivo. Irradiation of quercetin and BioQ in 10 mM pH 7.2 PBS buffer with Woods glass filtered medium pressure mercury arc lamp which passes light from 320-400 nm, and has a peak intensity at 365 nm, led to the irreversible bleaching of the longer wavelength absorption maximum for quercetin within 10 min, and both wavelength maxima for BioQ within 30

min (Figure 3.8). No bleaching was observed, however, in Tris buffer, possibly due radical quenching by the buffer [31].

In a model study an equimolar mixture of DRVYIHPFHL (angiotensin I) RPKPQFFGLM (substance P) was irradiated with 4 mM of BioQ. Analysis by LC MS/MS showed the formation of an adduct between angiotensin I and a biotin-containing fragment of BioQ (Figure 3.9), demonstrating BioQ's ability to photocrosslink to a protein target. The quercetin portion of the biotin fragment detected has been previously identified in the photolysis of quercetin [22, 23].

To verify the ability of BioQ to photocrosslink to a target protein, I incubated increasing concentrations of CK2 (from 1 μg to 4 μg) with BioQ in 400 μL 10 mM PBS buffer (pH 7.2) with and without irradiation for 30 min with Woods glass filtered medium pressure mercury arc lamp. The mixture was then incubated with streptavidin beads, followed by centrifugation and washing of the beads to remove non-specifically bound protein. CK2 is a tetramer consisting of two 45 kDa α-subunits and two 25 kDa β-subunits which can be readily detected as two discreet bands on an SDS-PAGE gel. The SDS-PAGE analysis, however, did not detect any photo-crosslinked CK2 by silver staining (Figure 3.10a). As Casein kinase II is an ATP dependent kinase that is known to autophosphorylate, it was possible that autophosphorylation was required for CK2 to bind to quercetin. We therefore incubated CK2 and BioQ in the presence of 2 μM ATP in PBS buffer for 30 min, after which some samples were additionally photoirradiated for 30 min prior to analysis by SDS-PAGE. After much experimentation, we found that a 2% SDS Tris-HCl buffer was sufficient to remove non-specifically bound proteins from the streptavidin agarose beads, without denaturing the streptavidin and causing the

release of the biotinylated CK2. Analysis of SDS-PAGE (Figure 3.10b) showed that a significant amount of both α and β subunits appeared in lane 6 once the concentration of CK2 reached 4 μg/400 μL (70 nM).

BioQ protein pull down from cells. Having verified that photoirradiated BioQ could pull down a known quercetin binding protein, we carried out pull down experiments with cells that had been incubated with BioQ. In one set of experiments the photocrosslinking step was carried out after cell lysis (Figure 3.12), and in a second set before cell lysis (Figure 3.13). As can be seen from lanes 1-4 of the 12% SDS PAGE gel shown in Figure 3.12, a large number of proteins were pulled down by the streptavidin beads in the absence of a denaturing wash whether incubated with BioQ and/or heat shock. With the exception of contaminating keratin proteins, the high protein background was reduced considerably with a denaturing wash as shown in lane 7 for cells that were incubated with BioQ and heat shocked. When cell lysates that had been incubated with BioQ with or without heat shock were also UV irradiated for 30 min prior and subjected to a denaturing wash following pull-down with the streptavidin beads, discrete new bands A-F were observed (lanes 5 & 6). Similar results were obtained when the cells were irradiated prior to lysis (Figure 3.13).

To confirm that the proteins appearing in the gel had been photomodified with BioQ, a western blot with a biotin-specific antibody was carried out (Figure 3.12, lane 8-10, Figure 3.13, 9-14). Samples for lanes 8-10 of Figure 3.12 were identically prepared, except that sample for lane 8 was not UV irradiated and the sample for lane 10 lacked BioQ, and neither showed any band with the anti-biotin antibody. Lane 9, however, clearly showed several bands that corresponded to the major bands observed in the silver

stained gel. Likewise, lane 12 of Figure 3.13 in which the heat shocked cells had been irradiated prior to lysis and followed by a standard wash showed the presence of significant amounts of biotinylated proteins.

Mass spectrometric identification of proteins pulled down *in vivo.* Proteins contained in discrete bands A to F of the gel in Figure 3.13 that were confirmed to be biotinylated (lane 12) were isolated, trypsinized and analyzed by LC-MS/MS. Corresponding sections of a control lane were similarly analyzed so that contaminating proteins such as keratins and albumins could be excluded. Mascot search [32] of the NCBI database led to the identification of candidate target proteins shown in Table 2. For each band only candidates with the highest probability are listed. In the case of band A, it appeared that two proteins were present, ubiquitin activating enzyme E1 (MW 118 kD) and spliceosomal protein SAP 130 (MW 137 kD) had similar scores, which also closely matched the apparent MW of about 110 kD. Likewise, for band D, two proteins were detected, RuvB-like 2 (MW 51 kD) and mitochondrial ATP synthase (MW 56 kD) which scored similarly, and closely matched the apparent molecular weight of 50 kD. Heat shock protein 90 (MW 98 kD), was identified as the only protein identified in band B which migrated with an apparent weight of about 100 kD. Likewise, band C was a good match for HSP 70 and band E most closely matched eukaryotic translation initiation factor 3.

Discussion

The strategy for coupling photoaffinity and affinity purification agents to a biologically active ligand to facilitate isolation of a target protein is a powerful approach

to identifying potential therapeutic targets [14, 15, 20]. The general idea appears to have been first described over 20 years ago for the isolation of ACTH receptors, [33] and successfully implemented a few years later for isolation of a melanocyte-stimulating hormone receptor [34]. In both cases, biotin had been selected as the affinity purification agent because of its high affinity for streptavidin, which in principal would enable facile separation of a protein bearing a biotinylated ligand from non-target proteins. In practice, however, it was difficult to find conditions that would reduce the non-specific binding of the proteins to the streptavidin without dissociating the biotinylated ligand protein complex. We also found this to be the case for the biotinylated quercetin affinity probe. This led to the idea of using a photoaffinity crosslinker to covalently link the biotinylated ligand to the target protein, and permit the use of more stringent wash conditions.

In our case, quercetin was known to have intrinsic photoreactivity, and reported to crosslink to malate dehydrogenase [23], thereby only necessitating the attachment of the biotin to create a pull down probe. We had already determined that the O7-position of quercetin did not interfere with the ability of quercetin to inhibit HSP70 induction in vivo, or to inhibit two of the presumed target proteins CK2 and CAMK2, and so this site was chosen for biotinylation [21]. As we had found for a simpler derivative, quercetin biotinylated at the O7 position retained its ability to penetrate cells and inhibit heat shock induction of HSP70 (Figure 3.7) and inhibit the putative kinase targets involved (Table 1). Initial attempts to demonstrate photocrosslinking of BioQ to BSA or malate dehydrogenase however failed, possibly because the derivatization of the O7 position interfered with binding to these proteins. We did confirm, however, that the BioQ was photoreactive, and could be photobleached by irradiation with a UVA light source

(Figure 3.8). In a very limited study in collaboration with Jiawei Chen, I found that irradiation of BioQ with angiotensin I resulted in an adduct of the peptide (Figure 3.9).

We therefore turned to CK2 kinase as a model target, which we showed was inhibited by BioQ, but initially did not show any photocrosslinking with BioQ. The inhibition assay was conducted in the presence of ATP and a peptide substrate, but the initial photocrosslinking experiments were carried out in the absence of ATP. When ATP was added, however, photocrosslinking took place, suggesting that CK2, which is known to autophosphorylate [35], must be in its phosphorylated state to bind quercetin. Further experiments established that ATP was consumed by CK2 in the presence of quercetin and the absence of substrate (Figure 3.11). This suggests that quercetin may be binding to a site other than the ATP binding pocket, such as the allosteric cleft between α/β surface of CK2 [36], where the interaction of α, β subunits is believed crucial to the function of CK2 kinase. In accord with this idea, BioQ pulled down both subunits, though it appeared to have a higher affinity for the β subunit (Figure 3.10).

BioQ was also able to specifically pull down target proteins from normal and heat-shocked cells as shown in Figure 3.12 using a photocrosslinking step that followed cell lysis and a stringent wash step. In the absence of the stringent wash step many non-specifically bound proteins were also eluted from the streptavidin beads (Figure 3.12, lanes 1-4). In the presence of a stringent wash step, and the absence of a photocrosslinking step, no distinct protein bands were observed other than what could be attributed to contaminating keratin proteins (Figure 3.12, lane 7). Only in the presence of the stringent wash step and photocrosslinking could discrete proteins be observed (lanes 5 & 6) that could be detected by a biotin antibody (Figure 3.12, lane 9). Similar results

were observed for the pull down experiment in which photocrosslinking was carried out prior to cell lysis.

Protein identification was only carried out on the sample of cells that were heat shocked and then irradiated prior to lysis (Figure 3.13), in order to obtain sufficient protein for analysis and to avoid artifacts that may result from irradiating the cells following lysis. Analysis of the protein bands by LC MS/MS indentified ubiquitin-activating enzyme E1 (UBA1), splicesomal protein (SAP130), heat shock proteins 90 and 70-2 (HSP90AA1, HSPA2), RuvB-like 2 (RUVBL2) helicase and mitochondrial ATP synthase (ATP5B) ATPases, and eukaryotic translation initiation factor 3 (SF3B3), as possible targets of quercetin (Table 2). Five of these proteins have known or putative ATP binding domains (UBA1, HSP90AA1, HSPA2, RUVBL2 and ATP5B), which is in accord with quercetin's known ability to inhibit ATPases and kinases. The remaining two proteins, SF3B3, EIF3F are not associated with nucleotide binding domains, and may bind through some other site. Quercetin has previously been shown to bind to mitochondrial ATP synthase between the β and γ subunits and thereby inhibit ATPase activity [37]. ATP synthetase has been found to be upregulated in breast cancer, and the ATP synthetase inhibitor aurovertin B is being investigated as a therapeutic agent [38]. RuvB-like 2, is also an ATPase as well as a putative helicase that has been found to be overexpressed in hepatocellular carcinoma and required for cell viability [39].

Both splicesomal protein (SAP130) and eukaryotic translation initiation factor 3 which we identified as targets of quercetin are important in translation or post-translation protein synthesis steps [40, 41]. As such, these proteins may play a role in the expression of inducible heat shock proteins 70-1 and 90 [42], which quercetin is known to inhibit

[43]. The spliceosome is a known target of some anticancer compounds [44], while the eukaryotic initiation factor has been found to be upregulated in breast and prostate cancer, and thus represents a new therapeutic target [40, 45]. Our observation that quercetin binds to constitutively expressed HSP70-2 and HSP90 could also explain the decreasing level of these proteins in quercetin treated cells [46, 47], which might result from the deactivation of these proteins and their subsequent degradation or aggregation in the cell. Both HSP70 and HSP90 proteins are of current interest as anticancer targets [48-51].

Another potential target of quercetin that we identified was the ubiquitin-activating enzyme E1 which initiates protein degradation through the E1-E2-E3 mediated proteosome pathway [52]. Binding to this enzyme could explain the observation that quercetin inhibits the ubiquitin-protesome pathway for degradation of unfolded proteins [53]. Currently, ubiquitin-activating enzyme E1 is being investigated as a therapeutic target for treatment of leukemia and multiple myeloma [54]. Inhibition of the proteosome pathway, together with the heat shock protein pathway for repairing unfolded proteins could induce cell apoptosis, which may be one of the mechanisms behind the anti-tumor activity of quercetin.

Conclusion

We have shown that biotin linked to the 7-hydroxyl of quercetin, BioQ, can be used as a photoaffinity agent to isolate quercetin binding/target proteins from cells which can then be identified by bottom up mass spectrometry. Many of the proteins identified as

targets of quercetin have also been found to be potential therapeutic targets for cancer, and all might play a role in the apoptotic and anti-tumor activities of quercetin. It is conceivable that the anticancer activity of quercetin is due to simultaneous but low level inhibition of multiple therapeutic targets, which might explain how a molecule with low specificity and toxicity can achieve a positive therapeutic effect.

The site for attaching biotin to quercetin was originally chosen because it did not substantially interfere with quercetin inhibition of heat induced HSP70 induction or the inhibition of CK2 and CAMK2 kinase activity, which are thought to be involved in heat shock transcription factor activation. Surprisingly, neither of these kinases was detected in the assay, possibly because they were only present at much lower levels than the other proteins. In this case, screening against a phage display library of proteins might prove to be more advantageous [19]. A phage display library could also provide the means and sufficient sensitivity to identify the preferred peptide binding sites for interaction with quercetin.

Though we have identified a number of possible quercetin targets, it is also likely, that a number of targets were not pulled down by the BioQ probe, either because the position of the biotin interfered with binding, or because of an inefficient photocrosslinking reaction. The mechanism and amino acid specificity of the photocrosslinking reaction has yet to be investigated. To screen for all the possible targets of quercetin, it might be necessary to attach biotin along with an additional photocrosslinking agent to other positions of quercetin. In any case, this approach appears to be a fruitful one for beginning to unravel the biomolecular basis for the medicinal effects of a ubiquitous natural product in our diet.

Experimental Section

Abbreviations

ATP: adenosine triphosphate; HSP70: heat shock protein 70; SDS: sodium dodecyl sulfate; PAGE: polyacrylamide gel electrophoresis; Kd: dissociation constant; CAMK2: Calcium/calmodulin dependent protein kinase II; CK2: casein kinase 2; BioQ: Biotin conjugated quercetin (conjugation at position 7); UV: ultra violet; NMR: nuclear magnetic resonance; COSY: homonuclear correlation spectroscopy; HMBC: heteronuclear multiple bond correlation; HMQC: heteronuclear multiple quantum correlation; TLC: thin layer chromatography; HCl: hydrochloric acid; MES: 2-(N-morpholino)ethanesulfonic acid; DMSO: dimethyl sulfoxide; HPLC: high pressure liquid chromatography; Tris: Tris(hydroxylmethyl)aminomethane; EDTA: ethylene diamine tetraacetic acid; BSA: bovine serum albumin; HRP: horseradish peroxidase; LTQ: linear trap quadruple; NCBI: national center for biotechnology information; HATU: 2-(1H-7-Azabenzotriazol-1-yl)--1,1,3,3-tetramethyl uronium hexafluorophosphate Methanaminium; DCC: dicyclohexyl carbodiimide; EDC: 1-ethyl-3-(3-dimethylaminopropyl) carbodiimide; PyBOP: benzotriazol-1-yl-oxytripyrrolidinophosphonium hexafluorophosphate; NMP: N-methyl-2-pyrrolidone; IC50: concentration of 50% inhibition; LC MS/MS: liquid chromatography-tandem mass spectrometry; UBA1: ubiquitin-activating enzyme E1; SAP130: splicesomal protein 130; HSP90: heat shock protein 90; HSPA2: heat shock protein 70-2; RUVBL2: RuvB-like 2; ATP5B: mitochondrial ATP synthase; EIF3F: eukaryotic translation initiation factor 3.

General procedures

Anhydrous dimethyl formamide and acetone were from EMD chemicals Inc. Anhydrous dichloromethane was freshly prepared by refluxing with calcium hydride followed by distillation. All other reagents were directly purchased from Omni Solvent or Sigma Aldrich unless otherwise specified. Analytical thin-layer chromatography was performed on Aldrich Silica gel 60 F_{254} plates (0.25 mm). Compounds were visualized by UVG-54 mineral light UV lamp at 254 nm. Flash column chromatography was conducted using the indicated solvent on E. Merck silica gel 60 (40-63 μm). ^{1}H NMR and ^{13}C NMR spectra were carried out on Varian Mercury-300 MHz, 500 MHz or 600 MHz spectrometers. UV-Vis full spectra were obtained on a Varian Cary 100 UV Bio UV-Visible spectrophotometer. High capacity streptavidin agarose resin, Silver SNAP stain kit and Avidin conjugated horseradish peroxidase was from Pierce Thermo Fisher Scientific Inc, and the Western blot kit was from Bio-Rad Laboratories. ECL staining reagents as well as mouse anti-actin antibody and horseradish peroxidase conjugated anti-mouse secondary antibody were from GE Healthcare Systems. Silver staining was carried out by a standard protocol [24] or with the Pierce Silver Stain Kit (Pierce). Protease inhibitor cocktail tablets were from Roche Pharmaceuticals. ^{1}H NMR, ^{13}C NMR were recorded with Mercury-300, Inova-500 and Inova-600 (Varian Assoc., CA) instruments while 2D NMR were recorded with Inova-600 spectrometer. All the data were processed with VNMR series software (Varian Assoc., CA) with standard functions and the chemical shifts were referenced by TMS standard. Proton spectra were collected in around 8000 Hz spectral width and 32K data points. Carbon spectra were collected in 30000 Hz spectral width and 64 K data points. The COSY experiments were obtained

with 512 real points in the F1 dimension and 2000 complex points in the F2 dimension. HMBC (Heteronuclear Multiple Bond Correlation) were collected with 10.2 seconds 90^{o} ^{1}H pulse width and 14.0 seconds 90^{o} ^{13}C pulse width. HMQC (Heteronuclear Multiple Quantum Correlation) were recorded using a 0.3 s H-^{13}C nulling period, with other parameters exactly the same as they are in HMBC.

7-*O*-carbo-*ter*-butoxymethyl-quercetin tetraacetate 2

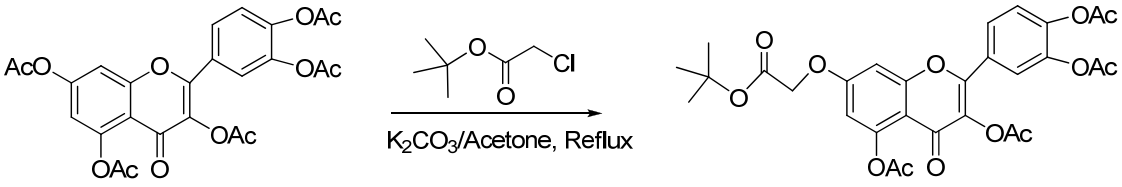

1 2

Quercetin pentaacetate **1** (1.0 g, 1.95 mmol) [25] was dissolved together with *tert*-butyl chloroacetate (3.0 g, 19.5 mmol) in 50 mL anhydrous acetone, followed by the addition of anhydrous potassium carbonate (2.0 g, 15 mmol) and potassium iodide (0.166 g, 1 mmol). The suspension was refluxed for two hours at which point TLC indicated the reaction was near completion. The reaction mixture was filtered to give a yellowish clear solution, concentrated in a rotatory evaporator and the residue purified by flash column chromatography (ethyl acetate/hexane 4:3) to give a solid that was recrystallized with acetone/hexane to give white solid 2 in 65 % yield (0.66 g, 1.27 mmol) [Figure 3.12]. ^{1}H NMR (300 MHz, $CDCl_3$) [Figure 3.16] δ 7.69 (dd, J=8.0, 2.0Hz, 1H), 7.66 (d, J=2.0Hz, 1H), 7.34 (d, J=8.0Hz, 1H), 6.80 (d, J=2.0Hz, 1H), 6.67 (d, J=2.0Hz, 1H), 4.60 (s, 2H), 2.42 (s, 3H), 2.33 (s, 9H), 1.50 (s, 9H). ^{13}C NMR (75 MHz, $CDCl_3$) [Figure

3.17] δ 170.2, 169.7, 168.3, 168.2, 168.1, 166.8 (6 C=O), 162.3, 158.2, 153.6, 151.2, 144.5, 142.4, 134.2, 128.3, 126.7, 124.2, 124.0, 112.0, 109.2, 100.1, 83.6 ($C(CH_3)_3$), 66.2 (OCH_2-COO), 28.3 (3 CH3), 21.4(CH_3CO), 21.0 ($2CH_3CO$), 20.8 (CH_3CO). MS ($C_{29}H_{28}O_{13}$), LRESI: [M+H^+] 585.2, [M+Na^+] 607.1, [M+K^+] 623.1, [M+H^+-CH_2CO] 543.1. HRESI: [M+H^+] 585.1606, Calculated 585.1603.

7-*O*-carboxymethyl quercetin tetraacetate 3

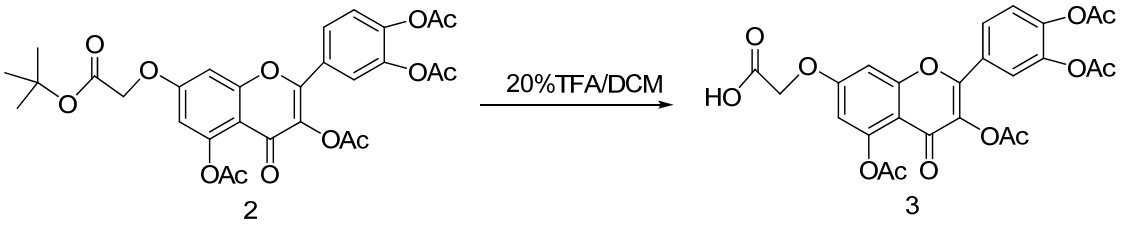

To 200 mg of **2** (0.38 mmol) in 4 mL anhydrous dichloromethane under nitrogen was slowly added 1 mL dry trifluoro acetic acid. After 3 h stirring at room temperature the solution was concentrated under rotatory evaporation under vacuum. The residue was dissolved in chloroform, washed with water and then brine until the aqueous layer becomes neutral. The organic phase was concentrated under rotavapor evaporation and purified by flash column chromatography (ethyl acetate/hexane/acetic acid 4.5:4.5:1) to afford **3** as a pale white solid in 72% yield (142 mg, 0.27 mmol). ^{1}H NMR (500 Mhz, $(CD_3)_2CO$) [Figure 3.18] δ 7.89 (dd, J=8.5, 2.0Hz, 1H), 7.85 (d, J=2.0Hz, 1H), 7.48 (d, J=8.5Hz, 1H), 7.18 (d, J=2.0Hz, 1H), 6.85 (d, J=2.0Hz, 1H), 4.94 (s, 2H), 2.32-2.29 (m, 12H). ^{13}C NMR (151 MHz, $(CD_3)_2CO$) [Figure 3.19] δ 169.9, 169.0, 168.4, 168.1, 168.0, 168.0 (6 C=O), 163.1, 158.5, 153.6, 151.4, 145.3, 143.2, 134.3, 128.5, 126.9, 124.8,

124.3, 111.7, 109.6, 100.5, 65.7 (O*C*H_2-COO), 20.7, 20.2, 20.1, 20.0 (4 *C*H_3CO). MS ($C_{25}H_{20}O_{13}$), LRESI: [M+Na^+] 551.1, HRESI: [M+Na^+] 551.0820 calculated 551.0802.

Quercetin-3, 5, 3', 4'-tetraacetate 4

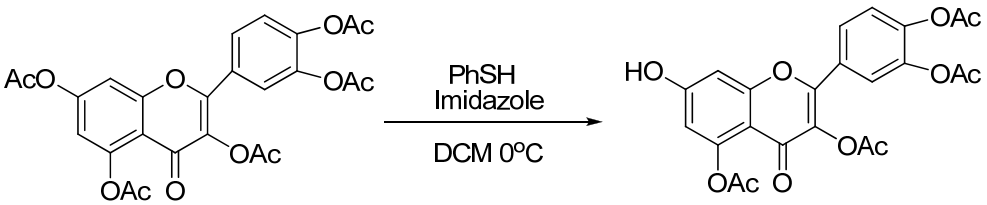

1 4

To quercetin penta-acetate (700 mg, 1.37mmol) in anhydrous dichloromethane at 0 ^oC was added imidazole (93.2 mg, 1.37 mmol) and 181 mg thiophenol (1.2 equivalents). After 1 h, at which point TLC indicated that the reaction was near completion, the reaction was diluted with dichloromethane, concentrated under vacuum in a rotatory evaporator, and the residue was dissolved in ethyl acetate. The organic phase was washed with 1N HCl and then brine and concentrated to a residue. Flash column chromatography (ethyl acetate/hexane: 4:3) afforded a yellow oil which was precipitated with methanol to give **4** as a pale white solid in 65% yield (418 mg, 0.89 mmol)

BioQ tetraacetate 5

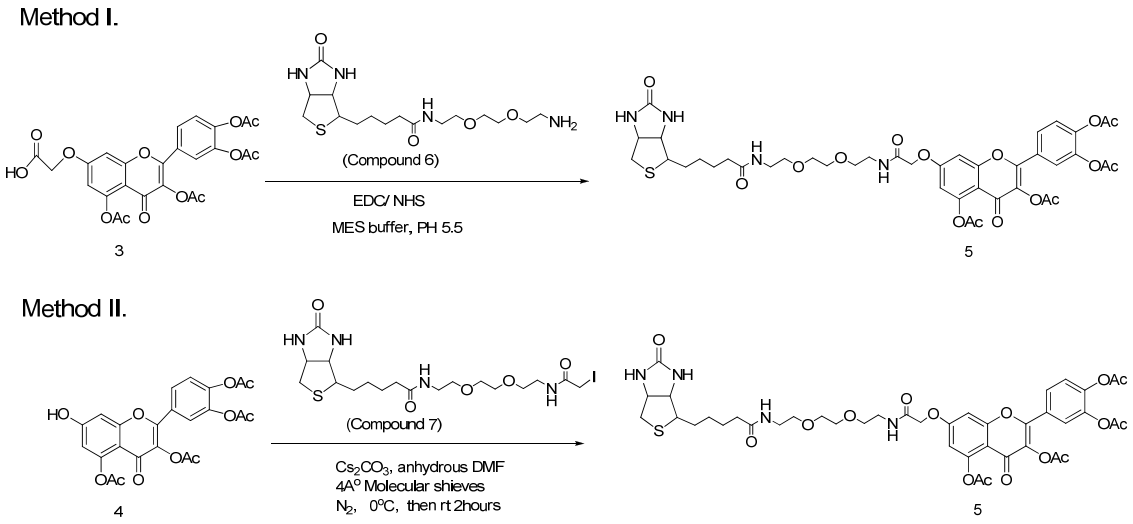

Method I. Compound **3** (20 mg, 0.038 mmol) was first incubated with 1-ethyl-3-[3-dimethylaminopropyl]carbodiimide hydrochloride (9.6 mg, 0.05 mmol) and N-hydroxysucciimide (5.7 mg, 0.05 mmol) in 50% MES buffer/acetonitrile (0.1 M, pH=5.5) for 20 minutes. After addition of **6** (20 mg, 0.053 mmol) [26], the mixture was left stirring under nitrogen atmosphere for 12 h at room temperature. The solution was then vacuum concentrated to remove acetonitrile and the residue was added to 50 mL ethyl acetate for extraction. The organic phase was washed with saturated ammonium chloride and brine for three times each and then vacuum concentrated for purification by serial column chromatography (5-8% methanol in dichloromethane) to finally afford **5** (5 mg, 0.006 mmol, 15%).

Method II. Compound **4** (20 mg, 0.042 mmol) and compound **7** (30 mg, 0.055 mmol) [26] were dissolved in 5mL anhydrous dimethyl formamide. The clear solution was kept dry with 4 A^0 molecular sieves under the protection of nitrogen atmosphere.

Cesium carbonate (17 mg, 0.05 mmol) was then added at 0 °C and the solution was left stirring at room temperature for 1.5 hours during which the flask was wrapped with aluminum foil to protect the reactants from light. Hydrochloric acid (1 M) was then added to stop the reaction by making the solution weakly acidic (around pH 6). The solvents are all vacuum concentrated and the remaining residue was purified by flash column chromatography (5% methanol in dichloromethane) to afford compound **5** (33 mg, 0.037 mmol, 87%). ^{1}H NMR ($CDCl_3$ 600 MHz) [Figure 3.20] δ 7.73 (d, J=8.4Hz, 1H), 7.70 (s, 1H), 7.36 (d, J=8.4Hz, 1H), 7.07 (s, H-N in ethylene glycol, 1H), 6.91 (s, 1H), 6.72 (s, 1H), 6.45 (NH in biotin, 1H), 6.31 (NH in biotin, 1H), 4.64 (s, CH_2, 2H), 4.51 (m, 1H), 4.32 (m, 1H), 3.60-3.37 (m, 12H), 3.15 (m, 1H), 2.88 (dd, 12.0 Hz, 4.2 Hz, 1H), 2.68 (d, 13.2 Hz, 1H), 2.43-2.34 (m, 12H, 4 CH_3CO), 2.21 (m, 2H), 2.09 (acetic acid), 1.67-1.62 (m, 4H), 1.43-1.41 (m, 2H). ^{13}C NMR (151 MHz [D_6]DMSO) [Figure 3.21] δ 174.7, 173.6, 169.9, 169.7, 168.1, 167.9, 167.8, 167.2 (8 C=O), 164.5, 161.2, 157.9, 153.5, 151.0, 144.4, 142.3, 133.9, 127.8, 126.4, 124.0, 123.8, 112.0, 109.2, 100.0, 70.2, 70.1, 69.6, 69.5, 67.7, 62.0, 60.6, 55.0, 40.3, 39.2, 39.0, 35.6, 27.7, 25.2, 21.1, 20.7, 20.7, 20.6 (4 CH_3). MS ($C_{41}H_{48}O_{16}N_4S$) LRESI: [$M+H^+$] 885.3, [$M+Na^+$] 907.3, [$M-CH_2CO+H^+$] 843.3; HRESI: [$M+H^+$] 885.2827, cal 885.2786, [$M+Na^+$] 907.2618, cal 907.2686.

BioQ 9.

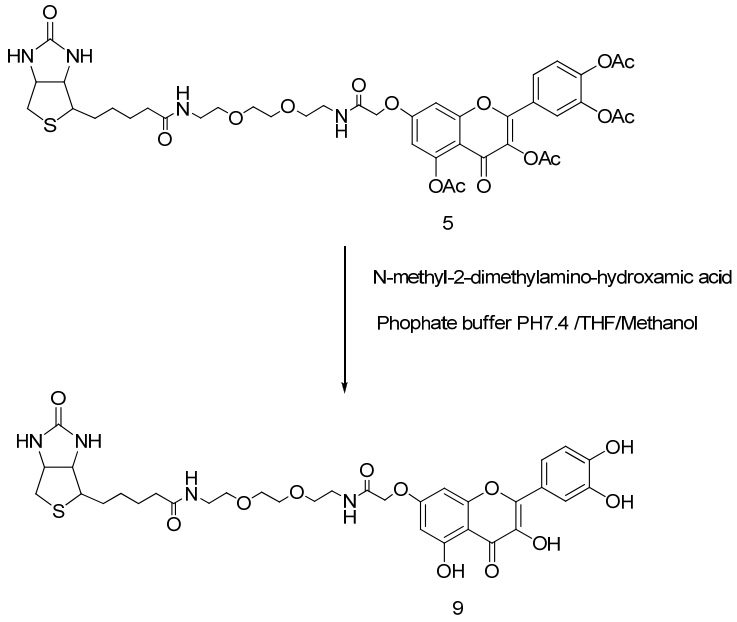

5

9

A solution of compound **5** (30 mg, 0.034 mmol) in 10 mL tetrahydrofuran/phosphate buffer/methanol (4.5:4.5:1, pH=7.4) was subjected to hydrolysis with N-methyl-2-dimehtylamino-acetohydroxamic acid (4.5 equivalent, 20mg, 0.15mmol) under a nitrogen atmosphere for 12 h. Hydrochloric acid (1 M) was added to work up the reaction by acidifying the solution to pH 5. The mixture, after vacuum concentration, was extracted with 50 mL ethyl acetate and washed with saturated ammonium chloride. The organic phase residue was purified by high performance liquid chromatography (Solvent A: water/1% acetic acid, Solvent B: acetonitrile/1% acetic acid; linear increase of solvent B to 50% over 30 minutes and then to 100% over the following 10 minutes) to afford compound **9** (18 mg, 0.025 mmol, 74%) at 32 min (retention time) (Figure 3.15). The reactant (compound 5) was also analyzed by HPLC to have a retention time of 36.3min. (Figure 3.14). Purity 98.27% (280nm). ^{1}H NMR ([D_6]DMSO, 300 MHz) [Figure 3.22] δ 8.20 (s, N-H), 7.82 (s, N-H), 7.72 (s, 1H), 7.56 (d, J=8.0Hz, 1H), 6.89 (d, J=8.0Hz, 1H),

6.70 (s, 1H), 6.41 (s, 1H), 6.40 (NH in biotin, 1H), 6.36 (NH in biotin, 1H), 4.63 (s, CH_2, 2H), 4.29 (m, 1H), 4.11 (m, 1H), 3.49-3.07 (m, 13H), 2.80 (dd, 12.0 Hz, 4.2 Hz, 1H), 2.58 (d, 13.8 Hz, 1H), 2.05 (m, 2H), 1.91 (s, acetic acid), 1.58-1.04 (m, 6H). ^{13}C NMR (151 MHz [D_6]DMSO) [Figure 3.23] δ 176.4, 172.5, 167.4, 163.5 (4 C=O), 163.1, 160.7, 156.2, 148.3, 147.8, 145.5, 136.5, 122.2, 120.4, 116.0, 115.6, 104.8, 98.4, 93.1, 69.9 (2 C overlap), 69.6, 69.2, 67.6 (2 C overlap), 61.4, 59.6, 55.8, 38.8, 38.7, 35.5, 28.6, 28.4, 25.6. MS ($C_{33}H_{40}O_{12}N_4S$) LRESI: [M+H^+] 717.2, [M+Na^+] 739.3, [M+K^+] 755.2. HRESI: [M+H^+] 717.2442, calculated 717.2363; [M+Na^+] 739.2256, calculated 739.2263; [M+K^+] 755.1984, calculated 755.3343.

Kinase inhibition and autophosphorylation assays. The kinase inhibition assay and autophosphorylation assay were carried out with the PKLight assay kit for ATP leftover by kinase (Lonza Rockland, Rockland ME), following the previously reported procedure [21]. For the kinase inhibition test, casein kinase II (CK2) was incubated with 300 μM peptide substrate (RRRADDSDDDDD), 100 μM ATP in a buffer of 20 mM Tris-HCl, 50mM KCl, 10mM $MgCl_2$ at 30^{o}C for 30 min, with inhibitors added in increasing concentrations; preactivated Ca^{2+}/ calmodulin-dependent protein kinase II (CAMK2) was mixed with increasing concentrations of inhibitor, 300 μM autocamtide-2 (KKALRRQETVDAL), 100 μM ATP in a pH 7.5 buffer of 50 mM Tris-HCl, 10 mM $MgCl_2$, 2 mM DTT, 0.1 mM Na_2EDTA at 30^{o}C for 30 min. Autophosphorylation assay for CK2 (0.035, 0.07 and 0.35 μM) was carried out in presence of 1 μM ATP, 10 μM quercetin in a buffer of 20 mM Tris-HCl, 50 mM KCl, 10 mM $MgCl_2$ at 30 ^{o}C for both 10 min and 40 min, with or without 300 μM peptide substrate (RRRADDSDDDDD).

Model peptide photocrosslinking study. 100 μM Angiotensin I peptide (NRVYIHPFHL) and 100 μM Substance P (RPKPQFFGLM) were mixed with 4 mM BioQ in 200 μL of 10 mM PBS buffer, pH 7.2, and irradiated under the photoirradiation conditions described for the protein pull down assays. After irradiation the sample was diluted 50-100 fold and subjected to LC-MS/MS analysis [Figure 3.9].

Western blotting of HSP70 and biotin labeled proteins. Western blotting to detect heat shock protein 70 generally followed a previously described procedure [21]. For the detection of biotin, proteins were transferred from the SDS polyacrylamide gels to nitro-cellulose membranes which were then immersed in 3% BSA overnight at 4 °C to block non-specific binding. After washing with PBS Tween buffer, the blots were incubated with horseradish peroxidase (HRP) conjugated anti-biotin antibody for one hour. The blots were finally stained in a 50 mL solution containing 30 mg 4-chloro-1-napthol and 0.01% hydrogen peroxide which produces a purple color at sites of horseradish peroxidase (HRP) activity.

General procedure for protein pull down experiments. The protein solution, cell lysate or cell suspension was irradiated for 30 min in a glass tube that was immersed in ice 10 cm away from a 450 W UV medium pressure mercury arc lamp in a water cooled immersion apparatus that was shielded with Wood's glass (transmits ultraviolet between 320 and 400 nm with a peak at 365 nm). The cell suspension was then lysed as described in a subsequent section, and the protein-containing solutions and cell lysates (400 μL - 1 mL) were incubated with 20 μL of streptavidin agarose beads for 1 h. The binding of BioQ to beads was monitored by a color change from white to yellow, due to the presence of quercetin. The beads were then centrifuged at 14000 rpm for 5 minutes and

the supernatant removed. The beads were then washed by treatment with lysis buffer (10 mM phosphate buffer, pH 7.2, 100 mM NaCl, 0.2% Triton X-100, and protease cocktail) or denaturing buffer (20 mM Tris•HCl, 2% SDS, pH 7.4) and shaken well for three minutes before each spin-down collection. The washing procedure was repeated at least three times. The beads were then resuspended in 20 μl of 2 × SDS-PAGE gel loading buffer (50 mM Tris•HCl, 100 mM dithiothreitol, 8 M urea, 2% SDS, 10% glycerol) and boiled for ten minutes in order to denature the streptavidin and release the biotin conjugates. Samples were loaded to SDS polyacrylamide gel and ran under 125 V for around one hour at which point the 10 kD protein would reach the bottom of the gel. The gel was then silver stained.

BioQ pull down of casein kinase II in vitro. The indicated concentrations of casein kinase II were mixed with 150 μM BioQ in 0.01M PBS buffer/protease cocktail (pH 7.2), or 0.01 M PBS buffer (pH 7.2)/protease cocktail/2 μM ATP/Mg^{2+}. Photocrosslinking was carried out with 400 μL of solution for 30 minutes and then immediately incubated with the streptavidin beads and processed as described above.

BioQ protein pull down from Jurkat cells. Jurkat cells were exponentially grown in RPMI media with 10% fetal bovine serum, until about 15×10^6 cells were obtained, after which the cells were harvested and treated with 3% aqueous DMSO as blank controls or 150 μM BioQ in 3% aqueous DMSO for two hours prior to a 43 °C heat shock, then allowed to recover at 37 °C for 1 h when the level of active heat shock factor in the cells typically reaches a maximum. The Jurkat cells were then cooled to 0 ^{o}C while being transported to the UV facility (10 min), where they were UV-irradiated as

described above at 4 °C immediately before or after cell lysis. The Jurkat cells were lysed by sonication in a cold room in 2 mL of cell lysis buffer (10 mM phosphate buffer, pH 7.2, 100 mM NaCl, 0.2% Triton X-100, and protease inhibitors) and centrifuged at 5000 rpm for 10 min. The supernatant was then incubated with the streptavidin beads and processed as described in the general procedure.

Silver staining of SDS-PAGE gel. The SDS polyacrylamide gels were incubated overnight in 100 mL solution of ethanol: glacial acetic acid: water (30:10:60) with gentle shaking to fix proteins. After washing with deionized water, the gel was silver stained either by a published procedure [24], or using the Pierce Silver Stain Kit (Pierce).

In-gel trypsin digestion. All equipment was first thoroughly washed with 70% ethanol followed by deionized water using non-latex gloves and a face mask. Silver stained bands were immediately excised with a gel cutter or scalpel blade, taking only the stained gel area. The excised bands as well as corresponding sections from a control lane were further cut into small pieces and collected in microfuge tubes, into which destaining buffers supplied with the silver SNAP stain kit were added. After destaining, gel pieces were washed at least three times with 100 mM sodium bicarbonate until the gel color turned a pale white. Acetonitrile (200 μl) was added to each tube for 5 min to dehydrate the slices, and then removed, after which the samples were dried by centrifugal evaporation in a Speedvac. Oxidized cysteines were reduced by adding 50 μL of 10 mM DTT/50 mM ammonium bicarbonate to the dried slices for 30 min at room temperature. After decanting the DTT solution from the gel slices, they were incubated with 50 mM iodoacetamide solution in 50 mM ammonium bicarbonate for 30 min at room temperature in the dark to cap the freshly reduced cysteines. The gel slices were then

washed three times with 100 mM ammonium bicarbonate and two times with 50 mM ammonium bicarbonate in 50% acetonitrile. The gel slices were dehydrated with 200 μL of acetonitrile for 5 min and then 500 μL acetonitrile for 20 min. After removal of the acetonitrile, the samples were completely dried in a centrifugal evaporator and subjected to trypsin digestion. Promega sequencing grade trypsin (10 ng) was dissolved in 1 mL ice-cold 50 mM ammonium bicarbonate and 20-50 μL was added to each sample on ice and incubated in a cold room for 1 h at which point the gel pieces had completely rehydrated and swelled. Excess trypsin solution was then removed and enough 50 mM ammonium bicarbonate was added to cover the gel pieces to keep them hydrated while digested overnight. After 12 h, the liquid was transferred to microfuge tubes on ice and the gel pieces were then extracted with 1% trifluoroacetic acid / 50% acetonitrile in water for 10 min with sonication and combined with the previous extract. The extraction was repeated again with 10% trifluoroacetic acid / 50% aqueous acetonitrile. The combined extracts were lyophilized in SpeedVac and resuspended in 0.1% TFA, followed by μC-18 zip-tip (Millipore) desalting to provide clean peptide fragments for liquid chromatography / mass spectrometric analysis.

LC MS/MS of trypsinized proteins. A 75 um i.d. fused-silica capillary column was packed with C18 reverse-phase material (Magic, 5um, 300 A, Michrom, CA) and pre-equilibrated with 100% solvent A (water, 0.1% formic acid). For each single run, 5 μL of digested sample was loaded to the column and subjected to gradient elution from 2% solvent B (3% water, 97% acetonitrile, 0.1% formic acid) to 50% solvent B over 50 min, followed by an increase to 85% solvent B in 5 min at a flow rate of 260 nanoliter /min, followed by a 5 min re-equilibration. The solution out of the column was directly

sprayed into an LTQ-Orbitrap mass spectrometer (Thermo Fisher, Waltham, MA), using a PicoView PV-500 nanospray source (New Objective,Woburn, MA). A full mass spectrum of eluting peptides was obtained with the FT mass spectrometer component at high mass resolving power (100,000 for ions of m/z 400). Ions submitted to MS/MS were placed in a dynamic exclusion list for 8 seconds. The MS/MS collections for the six most abundant eluting ions were performed with wide-band activation, in the LTQ mass spectrometer at normalized collision energy of 35%, with a 2 Da isolation width. Raw data was uploaded to Mascot licensed version (Matrix Science, MA) and submitted to identity search through NCBInr database. MS/MS results on the model peptide were manually analyzed with Xcalibur software (Thermo scientific, USA).

References:

1. Pietta, P.G., *Flavonoids as antioxidants.* J. Nat. Prod., 2000. **63**(7): p. 1035-42.

2. Boots, A.W., G.R. Haenen, and A. Bast, *Health effects of quercetin: from antioxidant to nutraceutical.* Eur J Pharmacol, 2008. **585**(2-3): p. 325-37.

3. Bischoff, S.C., *Quercetin: potentials in the prevention and therapy of disease.* Curr Opin Clin Nutr Metab Care, 2008. **11**(6): p. 733-40.

4. Murakami, A., H. Ashida, and J. Terao, *Multitargeted cancer prevention by quercetin.* Cancer Lett, 2008. **269**(2): p. 315-25.

5. Hirpara, K.V., et al., *Quercetin and its derivatives: synthesis, pharmacological uses with special emphasis on anti-tumor properties and prodrug with enhanced bio-availability.* Anticancer Agents Med Chem, 2009. **9**(2): p. 138-61.

6. Vargas, A.J. and R. Burd, *Hormesis and synergy: pathways and mechanisms of quercetin in cancer prevention and management.* Nutr Rev, 2010. **68**(7): p. 418-28.

7. Harwood, M., et al., *A critical review of the data related to the safety of quercetin and lack of evidence of in vivo toxicity, including lack of genotoxic/carcinogenic properties.* Food Chem Toxicol, 2007. **45**(11): p. 2179-205.

8. Davies, S.P., et al., *Specificity and mechanism of action of some commonly used protein kinase inhibitors.* Biochem J, 2000. **351**(Pt 1): p. 95-105.

9. Hunt, C.R., et al., *Genomic instability and enhanced radiosensitivity in Hsp70.1- and Hsp70.3-deficient mice.* Mol Cell Biol, 2004. **24**(2): p. 899-911.

10. Ciocca, D.R. and S.K. Calderwood, *Heat shock proteins in cancer: diagnostic, prognostic, predictive, and treatment implications.* Cell Stress Chaperones, 2005. **10**(2): p. 86-103.

11. Calderwood, S.K. and D.R. Ciocca, *Heat shock proteins: Stress proteins with Janus-like properties in cancer.* International Journal of Hyperthermia, 2008. **24**(1): p. 31-39.

12. Powers, M.V., P.A. Clarke, and P. Workman, *Death by chaperone: HSP90, HSP70 or both?* Cell Cycle, 2009. **8**(4): p. 518-26.

13. Bohl, M., et al., *Identification of actin as quercetin-binding protein: an approach to identify target molecules for specific ligands.* Anal Biochem, 2005. **346**(2): p. 295-9.

14. Cheng, K.W., et al., *Identification and characterization of molecular targets of natural products by mass spectrometry.* Mass Spectrom Rev, 2010. **29**(1): p. 126-55.

15. Li, X. and Y. Hu, *Identifying the Cellular Targets of Bioactive Small Molecules with Activity-Based Probes.* Curr Med Chem, 2010.

16. Low, W.K., et al., *Isolation and identification of eukaryotic initiation factor 4A as a molecular target for the marine natural product Pateamine A.* Methods Enzymol, 2007. **431**: p. 303-24.

17. Peddibhotla, S., et al., *Simultaneous arming and structure/activity studies of natural products employing O-H insertions: an expedient and versatile strategy for natural products-based chemical genetics.* J Am Chem Soc, 2007. **129**(40): p. 12222-31.

18. Glansdorp, F.G., et al., *Using chemical probes to investigate the sub-inhibitory effects of azithromycin.* Org Biomol Chem, 2008. **6**(22): p. 4120-4.

19. Kim, H., et al., *Glyceraldehyde 3-phosphate dehydrogenase is a cellular target of the insulin mimic demethylasterriquinone B1.* J Med Chem, 2007. **50**(15): p. 3423-6.

20. Tomohiro, T., M. Hashimoto, and Y. Hatanaka, *Cross-linking chemistry and biology: development of multifunctional photoaffinity probes.* Chem Rec, 2005. **5**(6): p. 385-95.

21. Wang, R.E., et al., *Inhibition of heat shock induction of heat shock protein 70 and enhancement of heat shock protein 27 phosphorylation by quercetin derivatives.* J Med Chem, 2009. **52**(7): p. 1912-21.

22. Fahlman, B.M. and E.S. Krol, *UVA and UVB radiation-induced oxidation products of quercetin.* J Photochem Photobiol B, 2009. **97**(3): p. 123-31.

23. Seddon, A.P. and K.T. Douglas, *Photo-induced covalent labelling of malate dehydrogenase by quercetin.* Biochem Biophys Res Commun, 1981. **102**(1): p. 15-21.

24. Sambrook, J., T. Maniatis, and E.F. Fritsch, *Molecular cloning : a laboratory manual*. 2nd ed. 1989, Cold Spring Harbor, N.Y.: Cold Spring Harbor Laboratory Press.

25. Picq, M., et al., *Selective inhibition of separated forms of cyclic nucleotide phosphodiesterase from rat heart by some pentasubstituted quercetin analogs.* Biochem Pharmacol, 1982. **31**(17): p. 2777-82.

26. Spura, A., et al., *Biotinylation of substituted cysteines in the nicotinic acetylcholine receptor reveals distinct binding modes for alpha-bungarotoxin and erabutoxin a.* J Biol Chem, 2000. **275**(29): p. 22452-60.

27. Jurd, L., *Plant Polyphenols. V. Selective Alkylation of the 7-Hydroxy Group in Polyhydroxyflavones.* J Am Chem Soc, 1958. **80**(20): p. 5531-5536.

28. Natoli, M., G. Nicolosi, and M. Piattelli, *Regioselective Alcoholysis of Flavonoid Acetates with Lipase in an Organic-Solvent.* Journal of Organic Chemistry, 1992. **57**(21): p. 5776-5778.

29. Li, M., X. Han, and B. Yu, *Facile synthesis of flavonoid 7-O-glycosides.* J Org Chem, 2003. **68**(17): p. 6842-5.

30. Beutler, J.A., et al., *Structure-activity requirements for flavone cytotoxicity and binding to tubulin.* J Med Chem, 1998. **41**(13): p. 2333-8.

31. Redpath, J.L., *Radioprotection of enzyme and bacterial systems by dithiothreitol.* Radiat Res, 1973. **55**(1): p. 109-17.

32. Perkins, D.N., et al., *Probability-based protein identification by searching sequence databases using mass spectrometry data.* Electrophoresis, 1999. **20**(18): p. 3551-67.

33. Finn, F.M., C.J. Stehle, and K. Hofmann, *Synthetic tools for adrenocorticotropin receptor identification.* Biochemistry, 1985. **24**(8): p. 1960-5.

34. Ahmed, A.R., et al., *Isolation and partial purification of a melanocyte-stimulating hormone receptor from B16 murine melanoma cells. A novel approach using a cleavable biotinylated photoactivated ligand and streptavidin-coated magnetic beads.* Biochem J, 1992. **286 (Pt 2)**: p. 377-82.

35. Hathaway, G.M. and J.A. Traugh, *Cyclic nucleotide-independent protein kinases from rabbit reticulocytes. Purification of casein kinases.* J Biol Chem, 1979. **254**(3): p. 762-8.

36. Raaf, J., et al., *The CK2 alpha/CK2 beta interface of human protein kinase CK2 harbors a binding pocket for small molecules.* Chem Biol, 2008. **15**(2): p. 111-7.

37. Gledhill, J.R., et al., *Mechanism of inhibition of bovine F1-ATPase by resveratrol and related polyphenols.* Proc Natl Acad Sci U S A, 2007. **104**(34): p. 13632-7.

38. Huang, T.C., et al., *Targeting therapy for breast carcinoma by ATP synthase inhibitor aurovertin B.* J Proteome Res, 2008. **7**(4): p. 1433-44.

39. Rousseau, B., et al., *Overexpression and role of the ATPase and putative DNA helicase RuvB-like 2 in human hepatocellular carcinoma.* Hepatology, 2007. **46**(4): p. 1108-18.

40. Saramaki, O., et al., *Amplification of EIF3S3 gene is associated with advanced stage in prostate cancer.* Am J Pathol, 2001. **159**(6): p. 2089-94.

41. Dong, Z., et al., *Role of eIF3a in regulating cell cycle progression.* Exp Cell Res, 2009. **315**(11): p. 1889-94.

42. Jolly, C., et al., *Intron-independent association of splicing factors with active genes.* J Cell Biol, 1999. **145**(6): p. 1133-43.

43. Hosokawa, N., et al., *Flavonoids inhibit the expression of heat shock proteins.* Cell Struct Funct, 1990. **15**(6): p. 393-401.

44. van Alphen, R.J., et al., *The spliceosome as target for anticancer treatment.* Br J Cancer, 2009. **100**(2): p. 228-32.

45. Nupponen, N.N., et al., *Amplification and overexpression of p40 subunit of eukaryotic translation initiation factor 3 in breast and prostate cancer.* Am J Pathol, 1999. **154**(6): p. 1777-83.

46. Aquino, D.A., et al., *The constitutive heat shock protein-70 is required for optimal expression of myelin basic protein during differentiation of oligodendrocytes.* Neurochem Res, 1998. **23**(3): p. 413-20.

47. Aalinkeel, R., et al., *The dietary bioflavonoid, quercetin, selectively induces apoptosis of prostate cancer cells by down-regulating the expression of heat shock protein 90.* Prostate, 2008. **68**(16): p. 1773-89.

48. Powers, M.V., et al., *Targeting HSP70: The second potentially druggable heat shock protein and molecular chaperone?* Cell Cycle, 2010. **9**(8).

49. Holzbeierlein, J.M., A. Windsperger, and G. Vielhauer, *Hsp90: a drug target?* Curr Oncol Rep, 2010. **12**(2): p. 95-101.

50. Didelot, C., et al., *Anti-cancer therapeutic approaches based on intracellular and extracellular heat shock proteins.* Curr Med Chem, 2007. **14**(27): p. 2839-47.

51. Whitesell, L. and S. Lindquist, *Inhibiting the transcription factor HSF1 as an anticancer strategy.* Expert Opin Ther Targets, 2009. **13**(4): p. 469-78.

52. Schulman, B.A. and J.W. Harper, *Ubiquitin-like protein activation by E1 enzymes: the apex for downstream signalling pathways.* Nat Rev Mol Cell Biol, 2009. **10**(5): p. 319-31.

53. Landis-Piwowar, K.R., V. Milacic, and Q.P. Dou, *Relationship between the methylation status of dietary flavonoids and their growth-inhibitory and apoptosis-inducing activities in human cancer cells.* J Cell Biochem, 2008. **105**(2): p. 514-23.

54. Xu, G.W., et al., *The ubiquitin-activating enzyme E1 as a therapeutic target for the treatment of leukemia and multiple myeloma.* Blood, 2010. **115**(11): p. 2251-9.

Table 1. IC50 values for casein kinase II (CK2) and calmodulin-dependent kinase II (CAMK2) inhibition using the PKLight protein kinase assay.

	Quercetin (μM)	BioQ (μM) (IC50)
CK2	5.6 ± 1.2	3.2 ± 0.7
CAMK2	3.0 ± 0.6	25.9 ±0.8

Table 2. LC-MS/MS identification of proteins pulled down from Jurkat cells using Mascot.[1]

Band	App. MW	Name	Gene ID	GI number	MW	Mascot score
A	110	ubiquitin-activating enzyme E1 (UBA1)	7317	23510338	118,858	205
		spliceosomal protein SAP 130 (SF3B3)	23450	6006515	136,590	252
B	100	heat shock protein HSP 90-alpha 2 (HSP90AA1)	3320	61656603	98,622	663
C	70	heat shock protein 70-2 (HSPA2)	3306	23271312	70,237	524
D	50	RuvB-like 2 helicase ATPase (RUVBL2)	10856	5730023	51,026	450
		mitochondrial ATP synthase beta subunit ATPase (ATP5B)	506	32189394	56,525	447
E	40	eukaryotic translation initiation factor 3, subunit 5 epsilon (EIF3F)	8665	4503519	37,654	179
F	37	unknown				

[1] The target proteins were identified by comparison of the proteins detected in a control and sample band so that contaminating keratins and albumins were excluded.

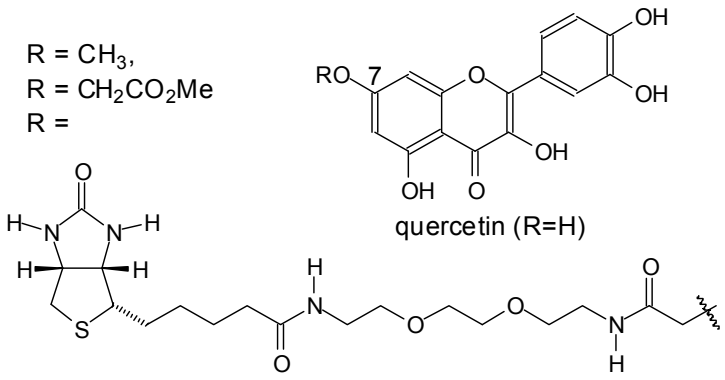

Figure 3.1 Structure of quercetin and derivatives. BioQ was designed for pulling down protein targets of quercetin.

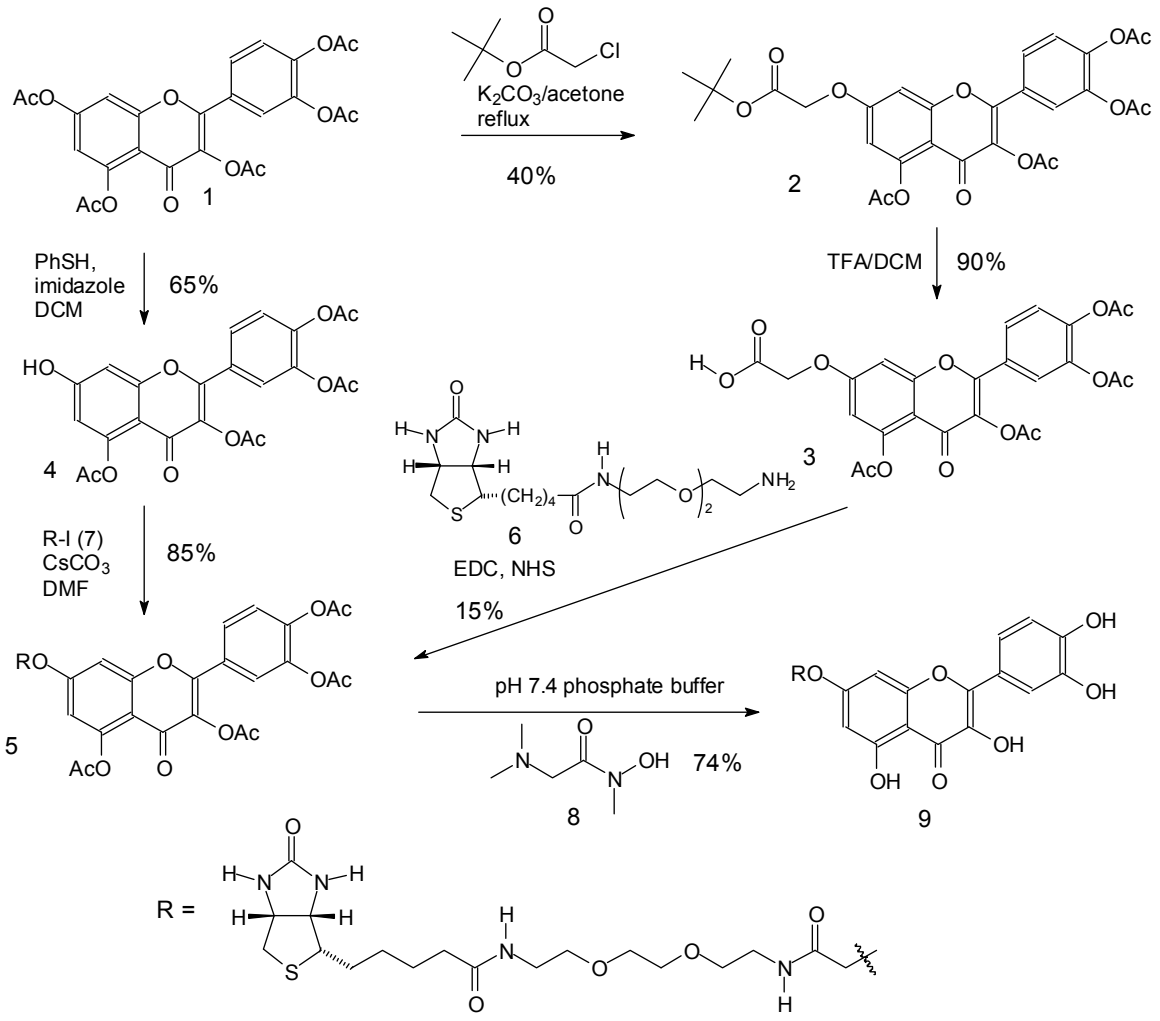

Figure 3.2 Two synthetic routes to BioQ.

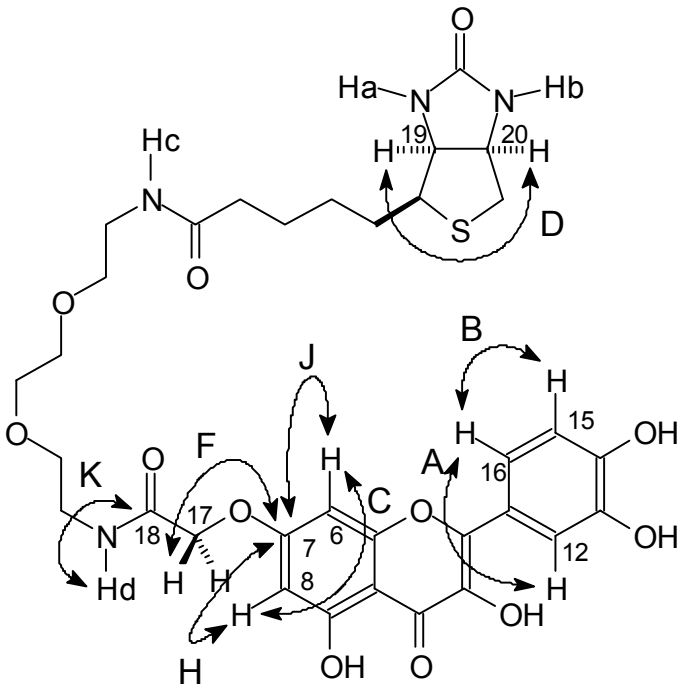

Figure 3.3 Structural characterization of BioQ by COSY, HMQC, and HMBC. Through bond correlations A, B, C, D were observed in ^{1}H-^{1}H COSY, one bond correlations between ^{13}C-^{1}H were made by HMQC, and multiple through bond correlations F, H, J, and K were by HMBC.

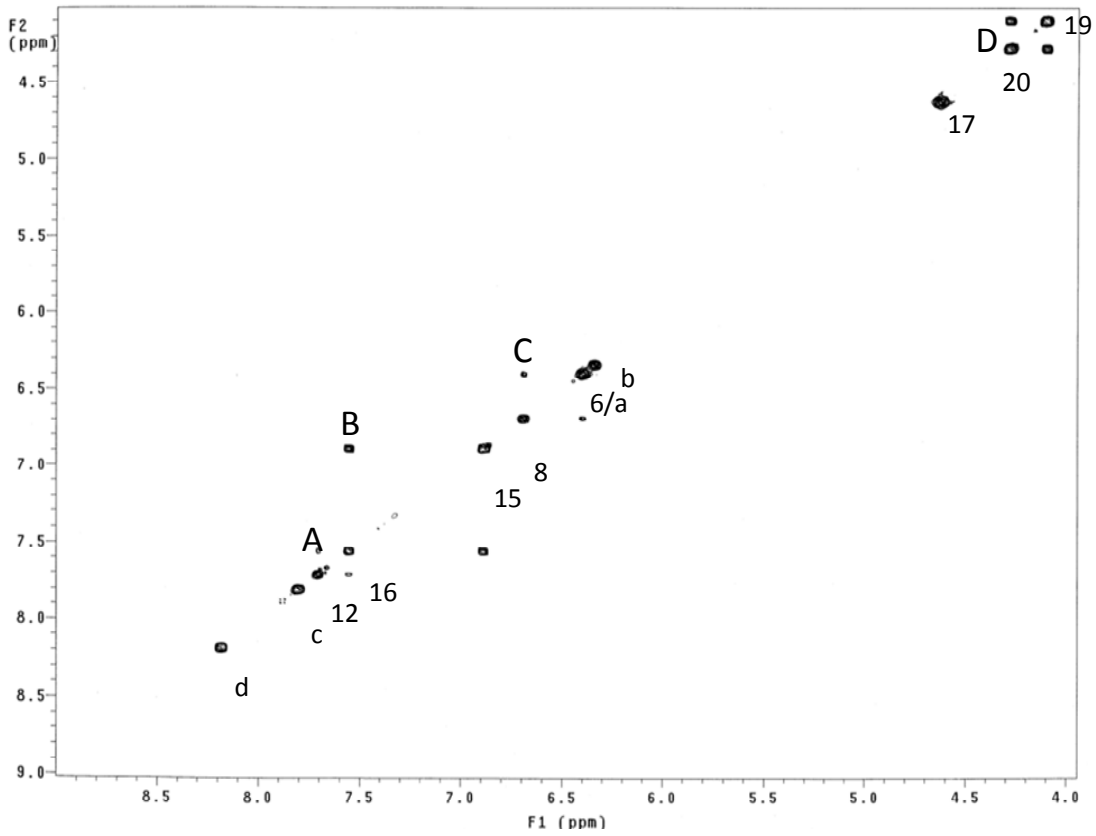

Figure 3.4 COSY spectrum of BioQ. Numbers correspond to the proton assignments, and the letters correspond to the ^{1}H-^{1}H correlations shown in Figure 3.3.

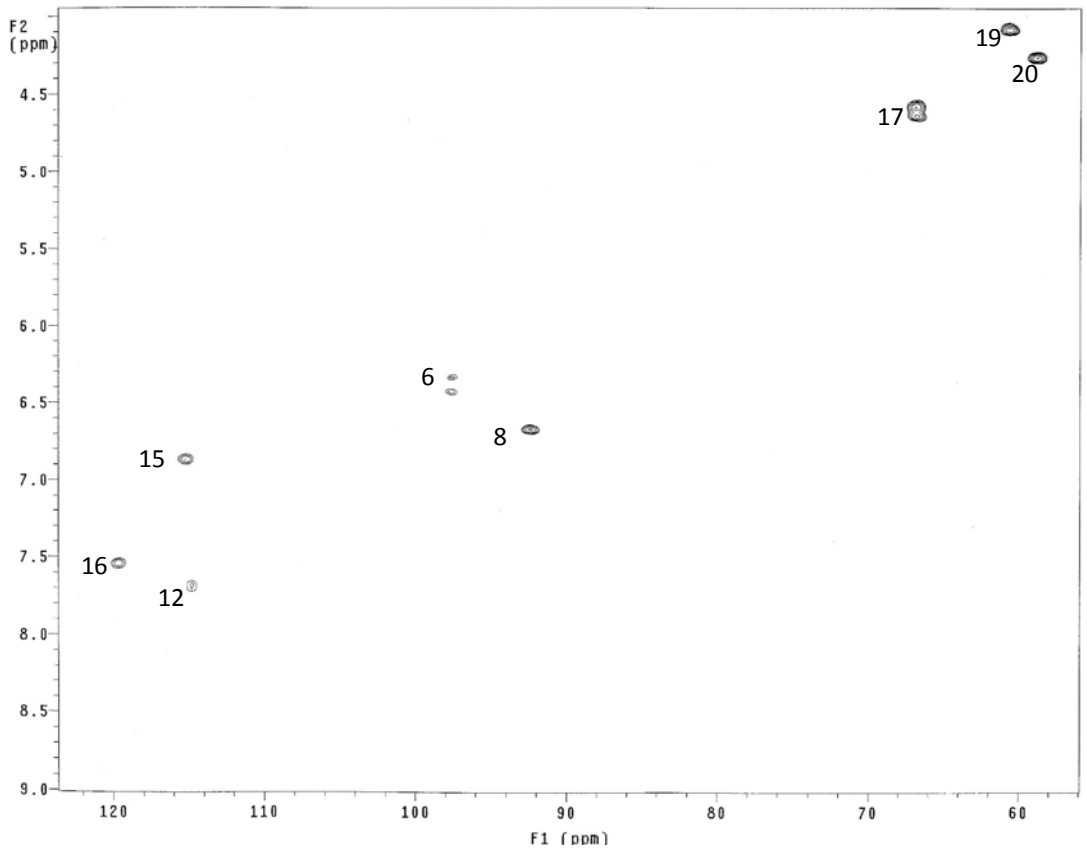

Figure 3.5 HMQC spectrum of BioQ. Numbers correspond to the carbon assignments for the one bond ^{13}C-^{1}H correlations shown in Fig. 3.3.

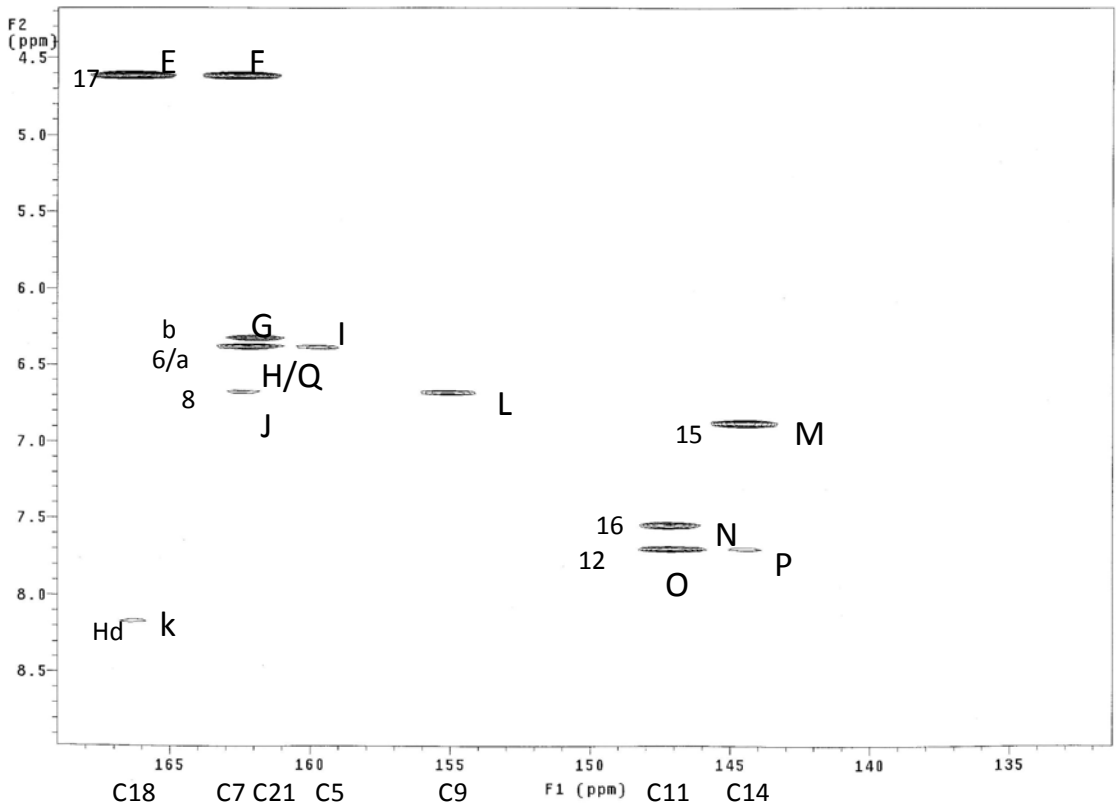

Figure 3.6 HMBC spectrum of BioQ. Numbers next to the crosspeaks correspond to the proton assignments, while numbers along the bottom axis correspond to the carbon assignments, and the letters correspond to the ^{13}C-^{1}H correlations shown in Figure 3.3.

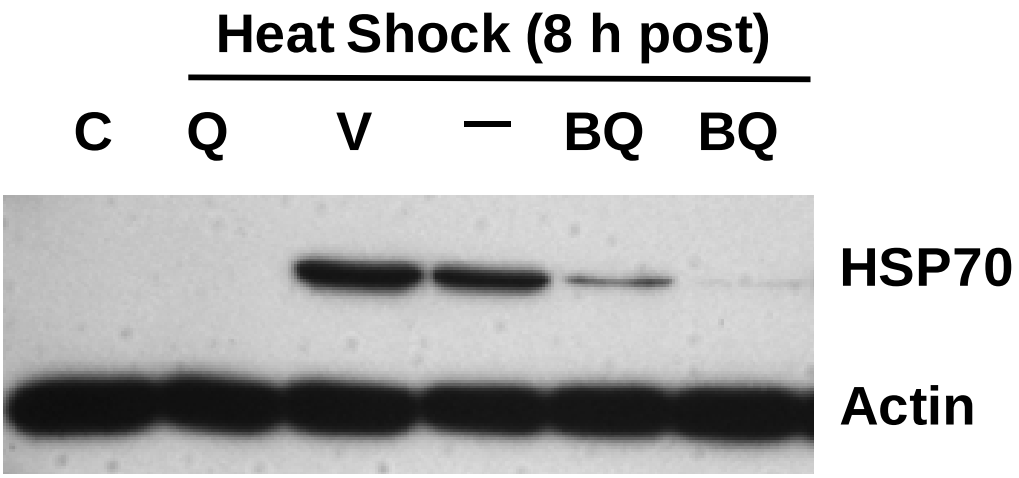

Figure 3.7 Ability of BioQ to inhibit heat shock induction of HSP70 in Jurkat cells. Jurkat cells were treated with quercetin (Q), DMSO vehicle (V) or BioQ (BQ) for 2 h prior to a 30 min 43°C heat shock (HS) then allowed to recover at 37°C for 8 h before Western blot analysis of HSP70 and actin levels. Control unheated Jurkat cells (C) and heated Jurkat cells in the absence of any additive (-). Both quercetin and biotinylated quercetin were utilized at 145 μM. The results were repeatable.

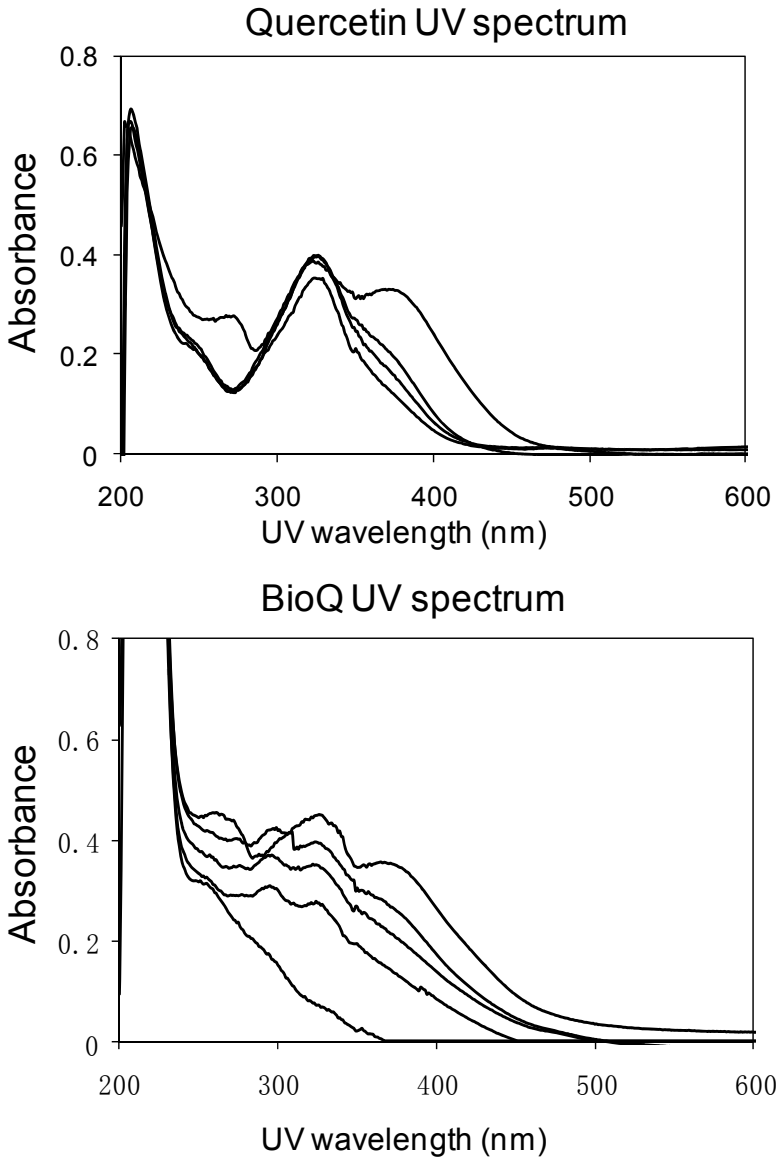

Figure 3.8 Photobleaching of Quercetin and BioQ. The ultraviolet-vis spectrum of quercetin and biotinylated quercetin in 10 mM pH 7.2 PBS buffer, before and after irradiation for 10 min intervals (top to bottom) with Woods glass filtered medium pressure mercury arc light.

A)

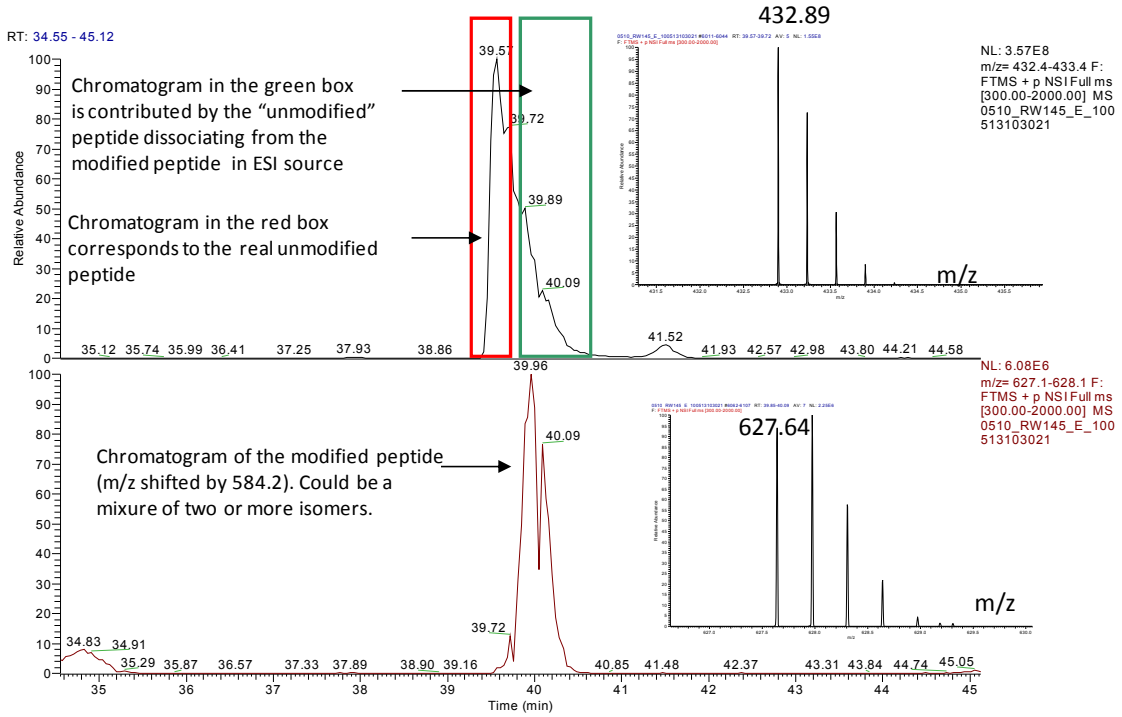

Figure 3.9 LC MS of irradiated DRVYIHPFHL and BioQ. A) top panel: LC ion trace for mass 432.89 corresponding to peptide $+3H^+$. Bottom panel: LC ion trace for mass 627.64 corresponding to peptide + BioQ fragment + $3H^+$. The tail on the peak for the 432.89 triply charged peptide ion is due to decomposition of the adducted peptide in the ESI source.

B)

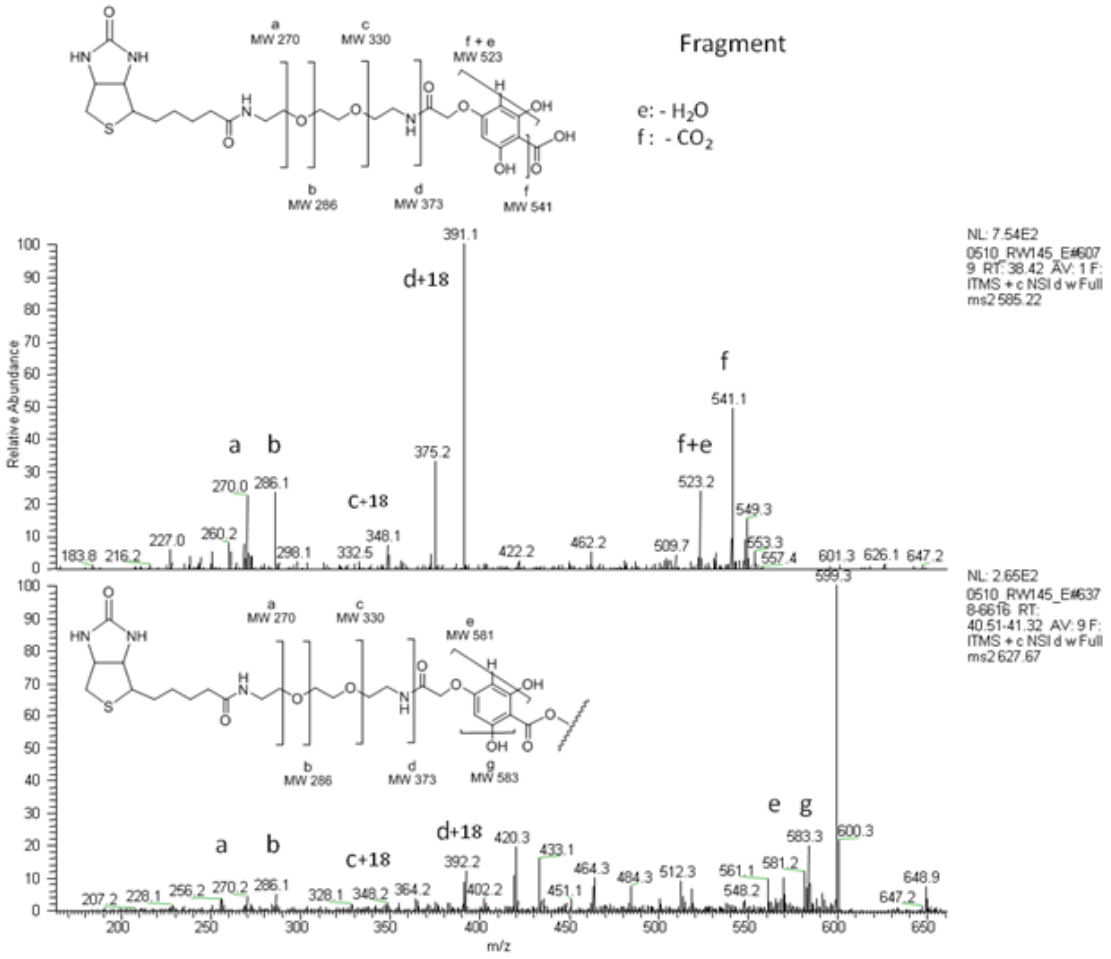

Figure 3.9 LC MS of irradiated DRVYIHPFHL and BioQ. B) Top panel: MS/MS of $[M+H]^+$ = 585.22 corresponding to the photoproduct of BioQ with key fragmentations identified. Bottom panel: MS/MS of $[M+3H]^{3+}$ = 627.67 corresponding to the peptide adduct of Figure 3.9A bottom panel, showing presence of the same BioQ fragment.

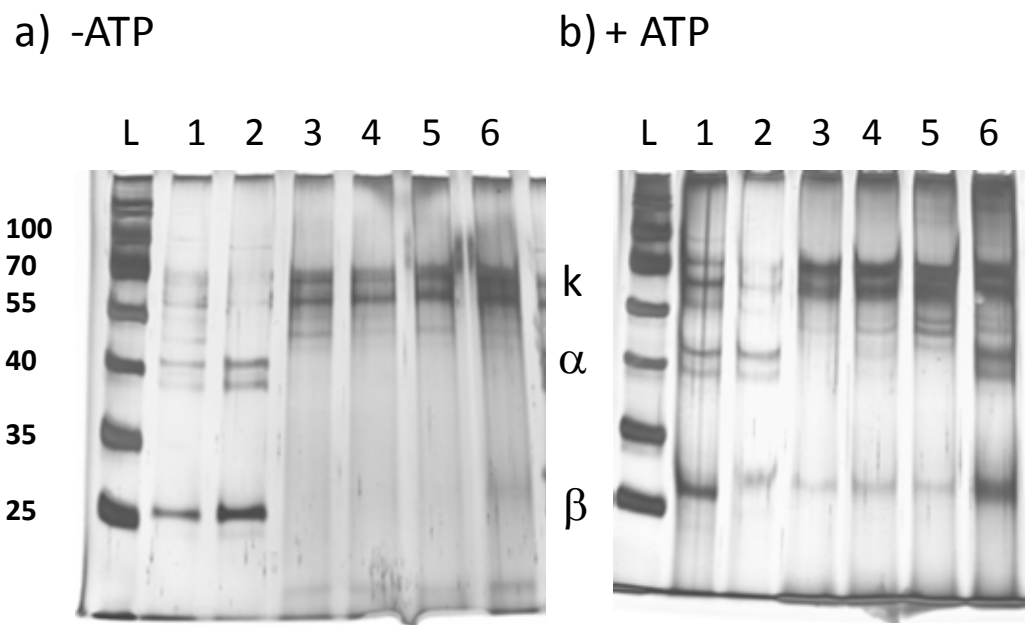

Figure 3.10 Casein Kinase II pull down by BioQ. Increasing concentrations of CK2 (lanes 3-6: 17.5, 35, 52.5, 70 nM) in 400 μL, 10 mM PBS buffer (pH 7.2), were incubated with 150 μM BioQ and then photoirradiated at 365 nM for 30 min in the (a) absence or (b) presence of 10 mM $MgCl_2$ and 2 μM ATP. The biotinylated proteins were then pulled down by streptavidin beads and subjected to a denaturing wash prior to electrophoresis. L is a Fermentas prestained protein ladder. Lanes a1 and b2 contained 0.05 μg CK2, and lanes a2 and b1 contained 0.1 μg of CK2. The positions of the α and β subunits of CK2 are identified on the gel, as well as the contaminant keratin.

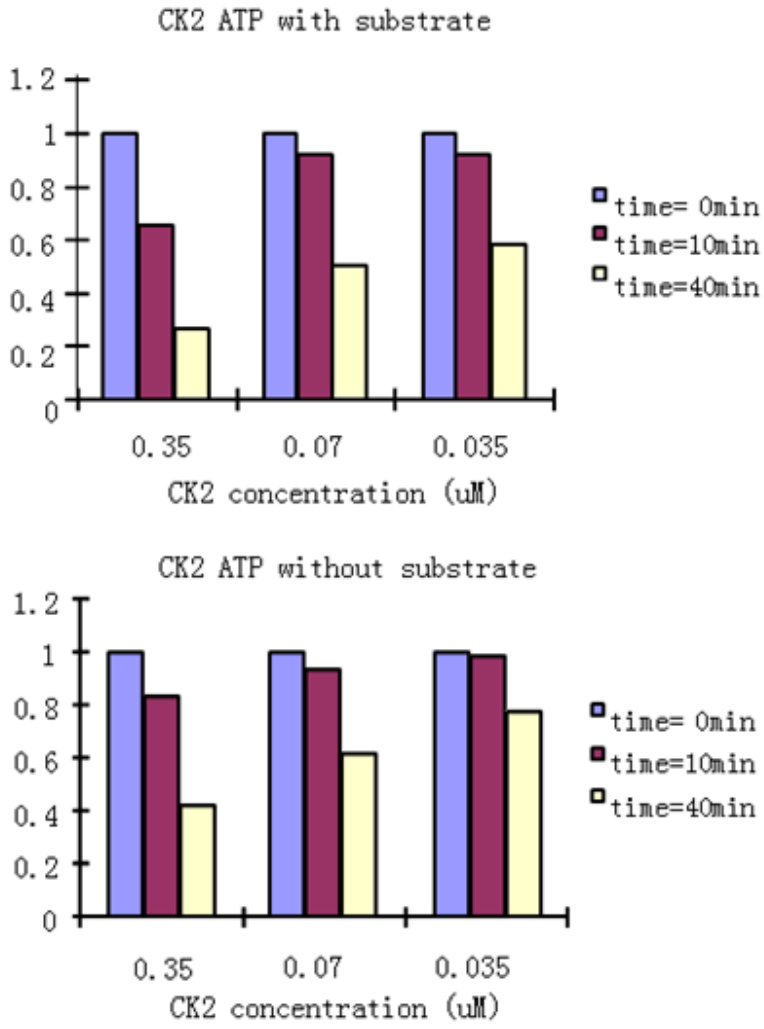

Figure 3.11 Autophosphorylation of CK2. Luciferase coupled assay for ATP consumption of CK2 incubated with quercetin in the presence and absence of the peptide substrate (RRRADDSDDDDD).

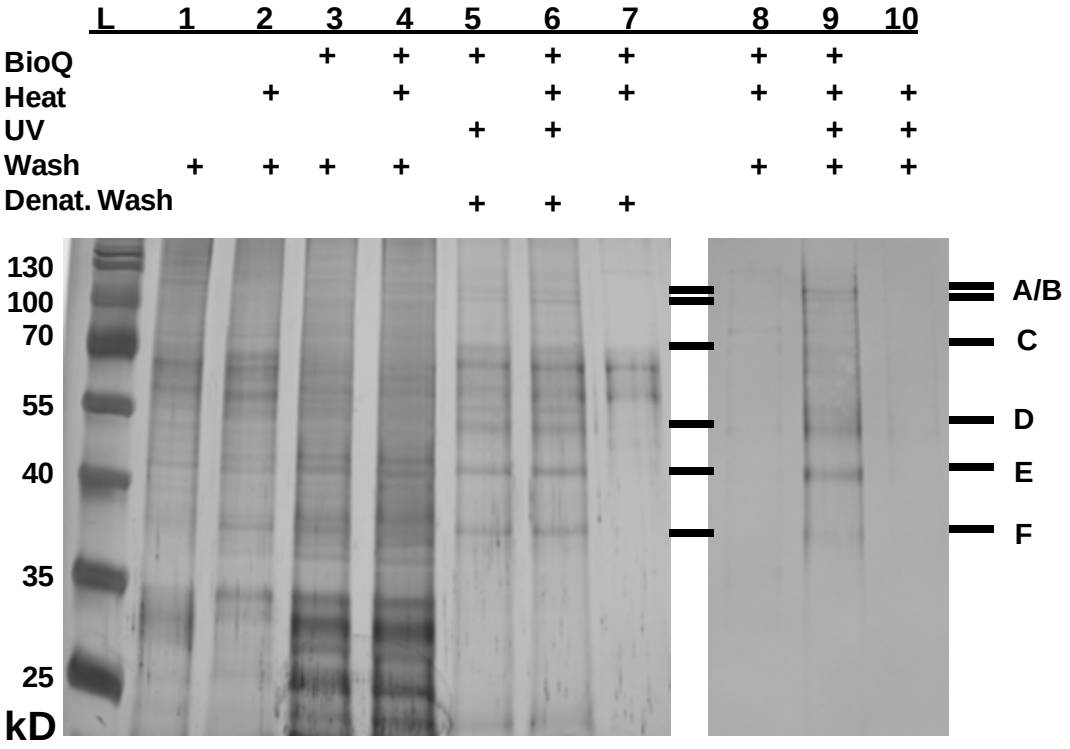

Figure 3.12 Proteins pulled down from Jurkat cells incubated with BioQ that were UV irradiated following lysis. **Left**: Silver stained 12% SDS polyacrylamide electrophoresis gel of proteins. Lanes 1 and 2: proteins pulled down from lysates of normal or heat shocked Jurkat cells in the absence of BioQ and UV irradiation. Lanes 3 and 4: proteins pulled down from lysates of normal or heat shocked cells that had been incubated with 150 μM BioQ in absence of UV irradiation. Lanes 5 and 6: proteins pulled down from lysates of normal or heat shocked cells that had been incubated with BioQ and UV irradiated following lysis, and then subjected to a denaturing wash. Lane 7: proteins pulled down under the same conditions as for lane 6, except that the lysate was not UV irradiated. **Right**: Western blot of corresponding lanes with anti-biotin antibody. Legend: heat, heat shock applied after incubation with BioQ but before lysis; wash, washing beads with cell lysis buffer; denaturing wash, washing beads with 2% SDS buffer.

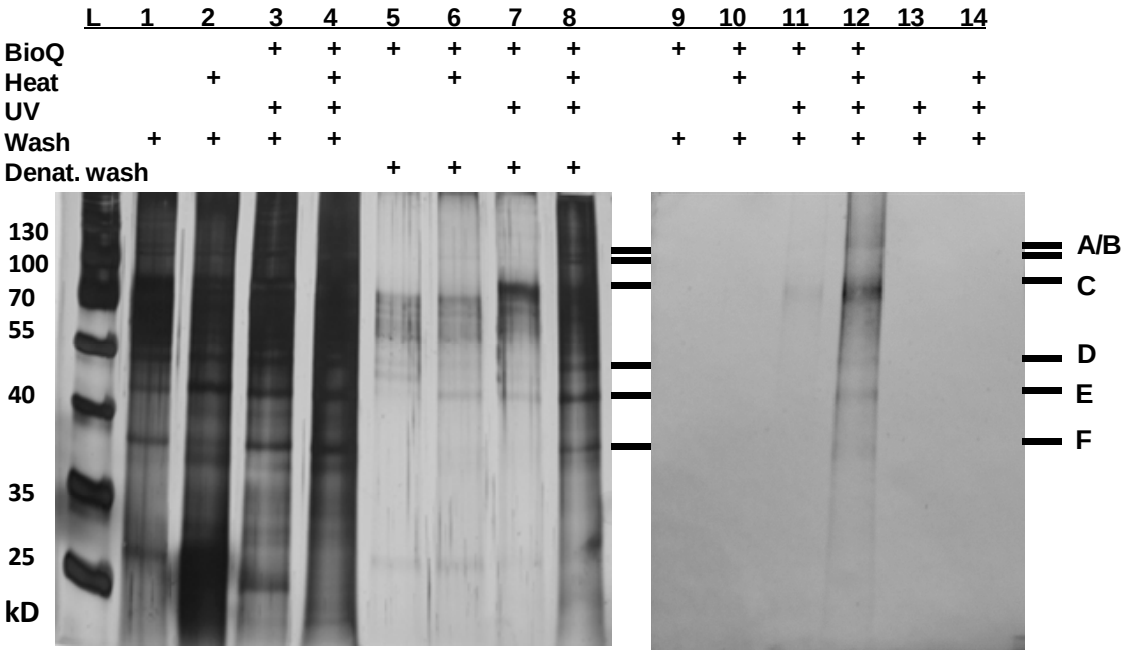

Figure 3.13 Proteins pulled down from Jurkat cells irradiated with BioQ prior to lysis. **Left**: Proteins pulled down with streptavidin beads from Jurkat cells under similar sets conditions as in the gel in Figure 3.12. **Right**: Western blot with anti-biotin antibody.

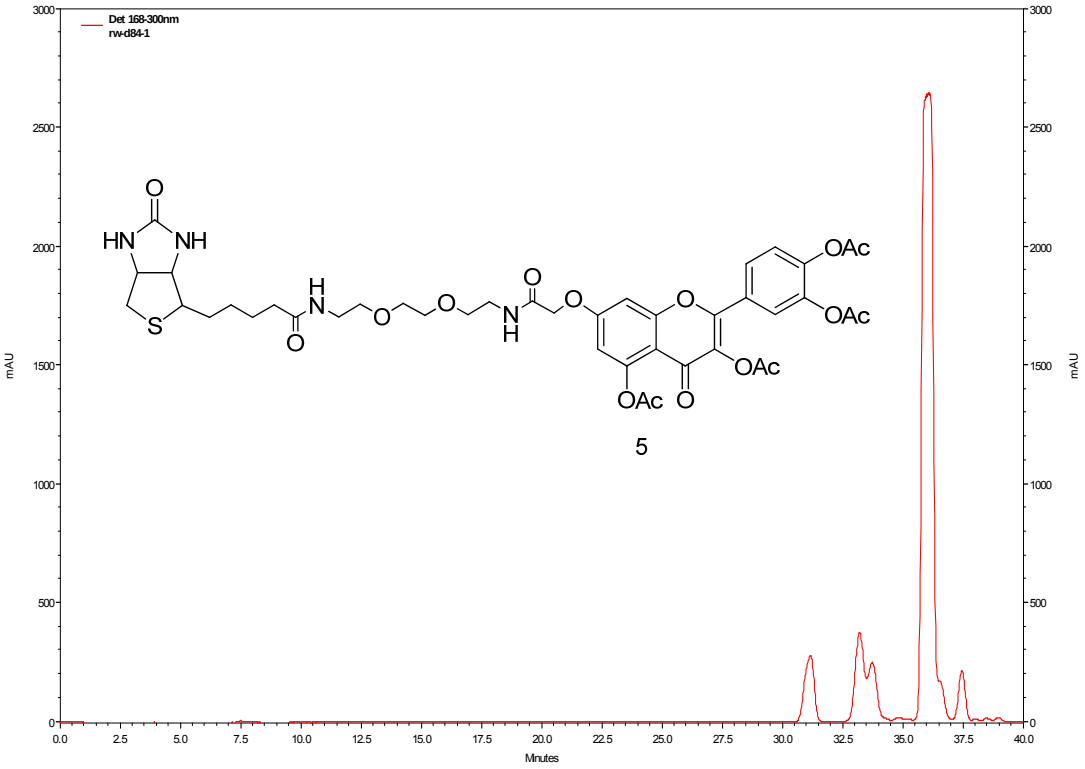

Figure 3.14 HPLC spectrum of compound **5**.

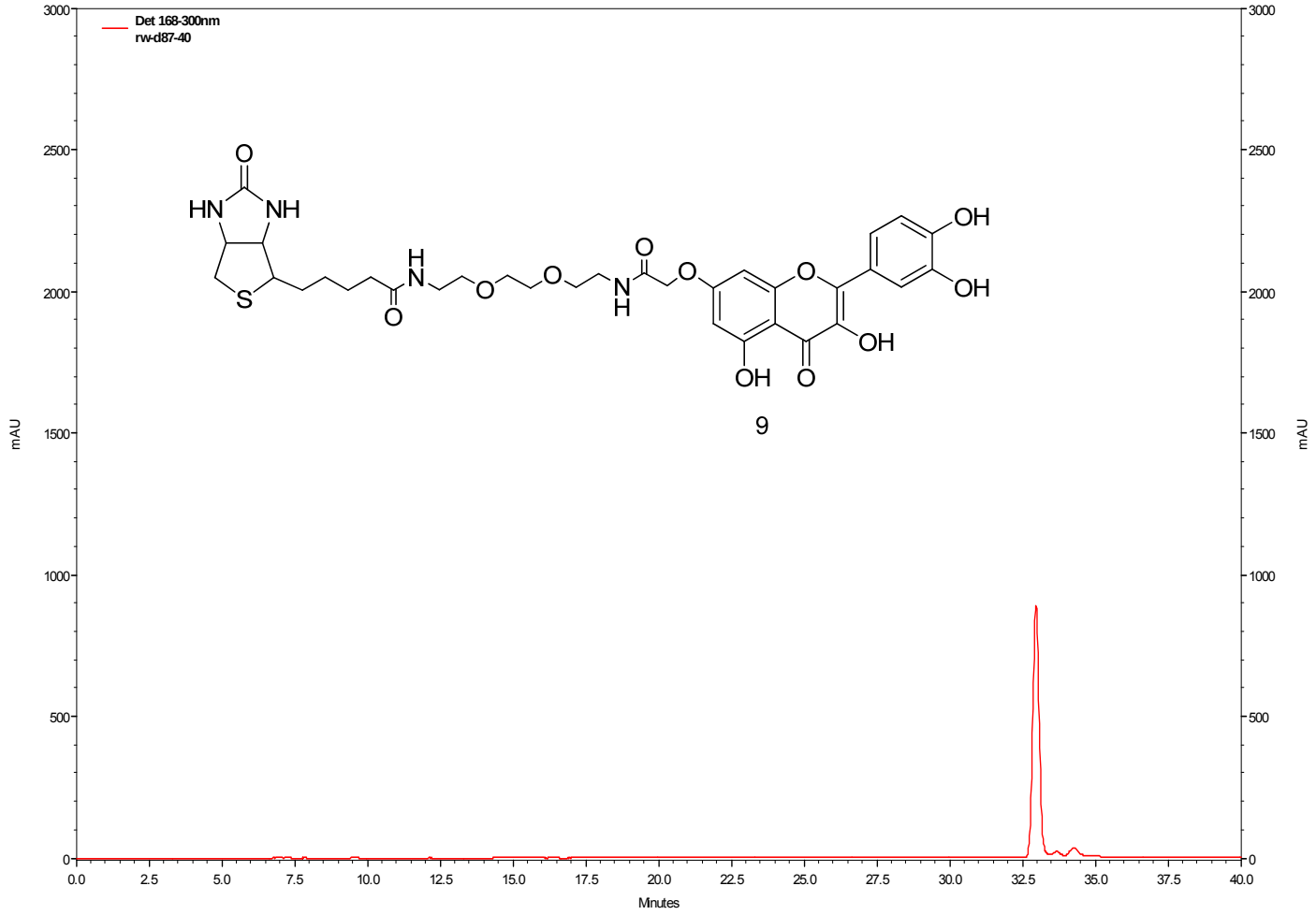

Figure 3.15 HPLC spectrum of compound **9**.

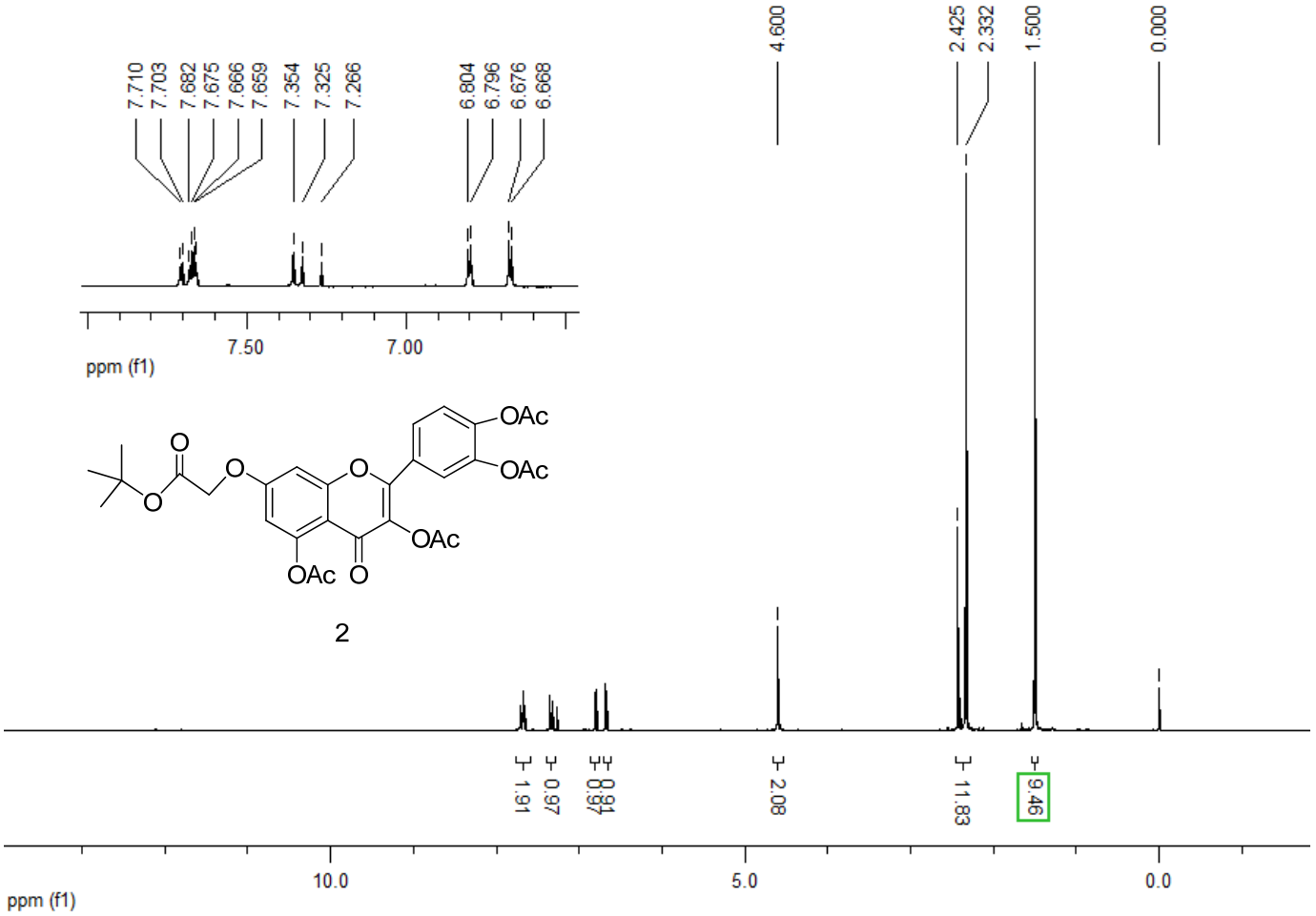

Figure 3.16 [1] HNMR (300MHz, $CDCl_3$) spectrum of compound **2.**

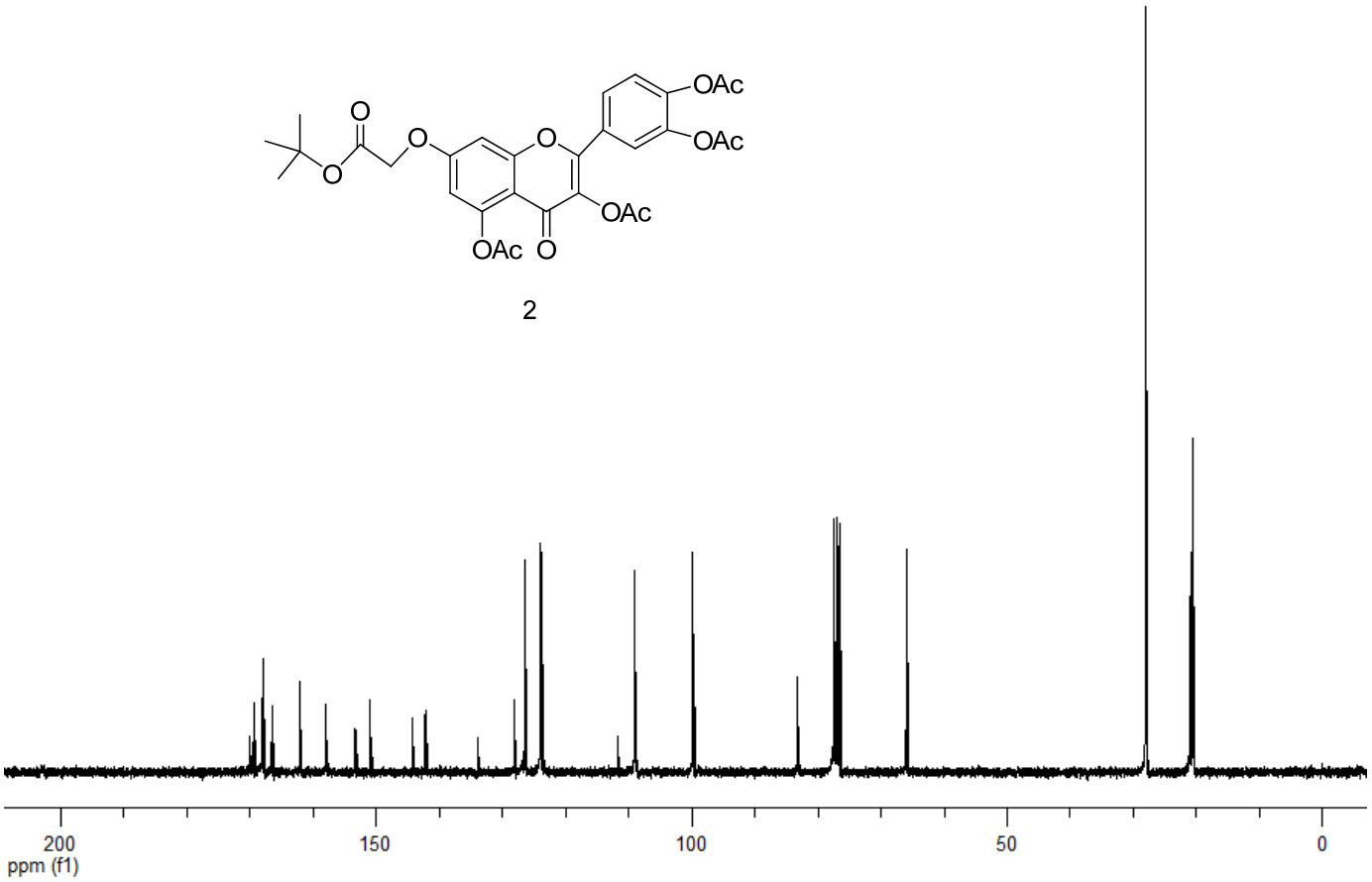

Figure 3.17 ^{13} CNMR (75MHz, $CDCl_3$) spectrum of compound **2.**

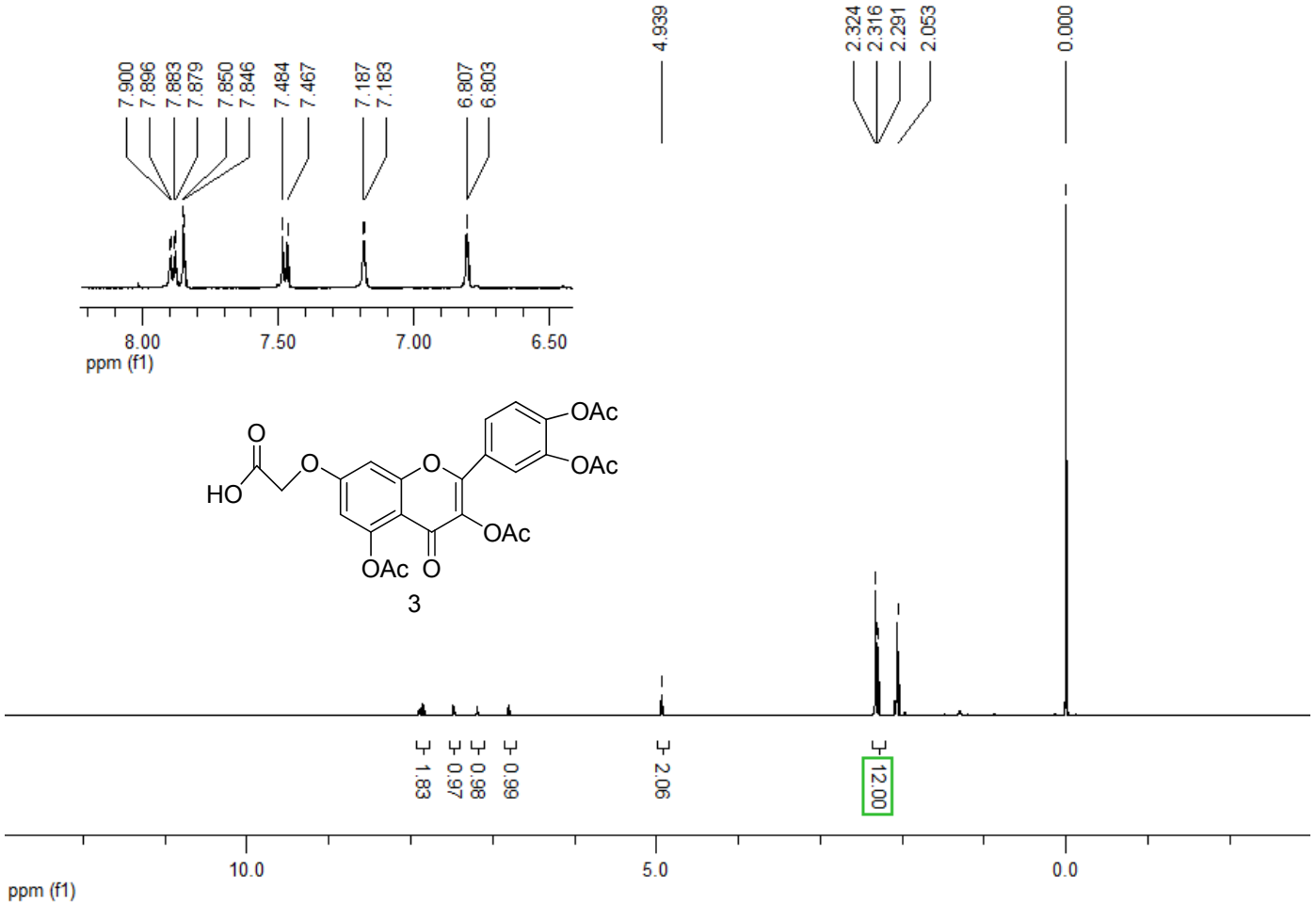

Figure 3.18 [1] HNMR (500MHz, [D_6] $(CD_3)_2CO$) spectrum of compound **3.**

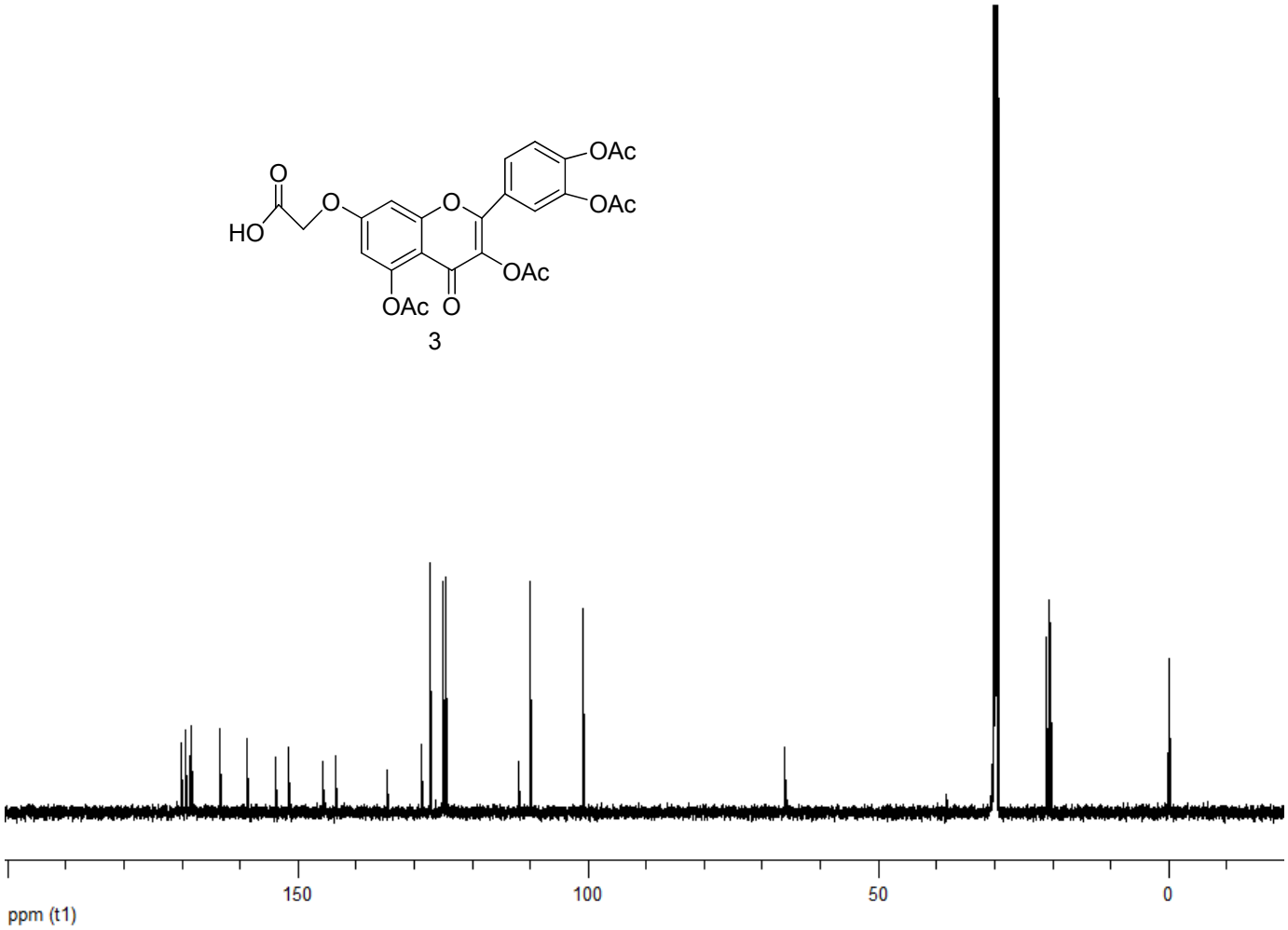

Figure 3.19 ^{13} CNMR (151MHz, [D_6] $(CD_3)_2CO$) spectrum of compound **3.**

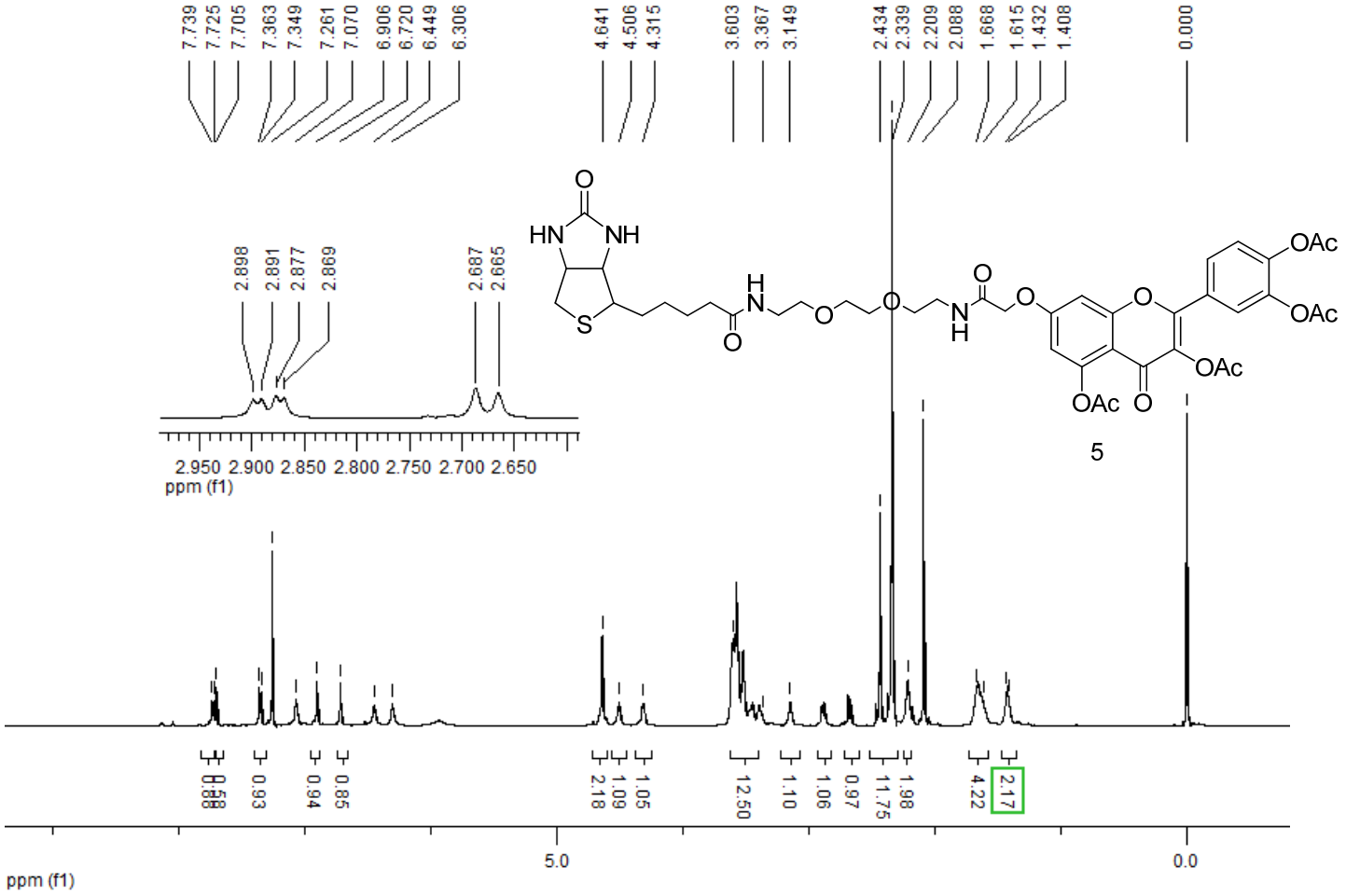

Figure 3.20 [1] HNMR (600MHz, $CDCl_3$) spectrum of compound **5.**

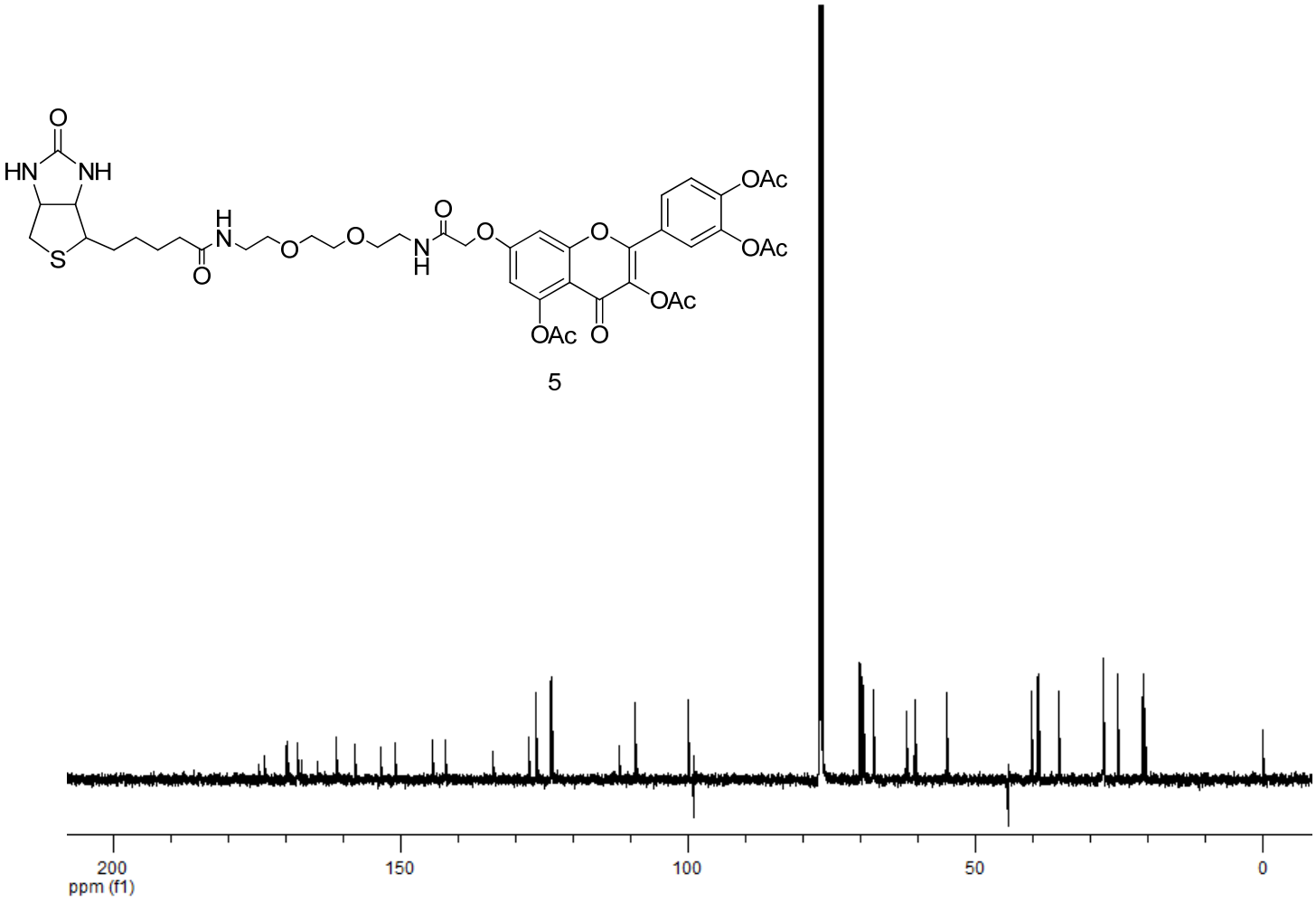

Figure 3.21 ^{13} CNMR (151MHz, [D_6]DMSO) spectrum of compound **5.**

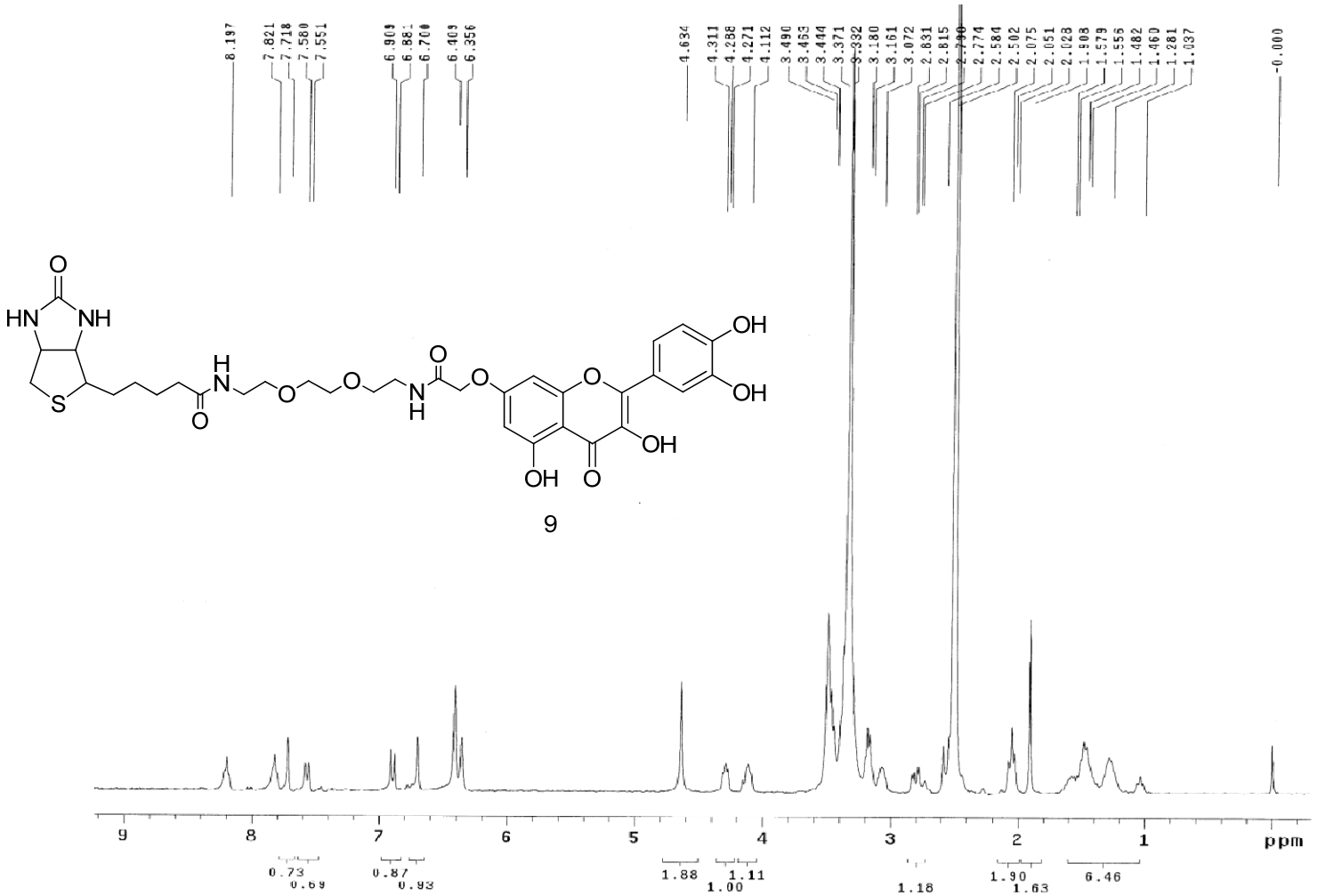

Figure 3. 22 [1] HNMR (300MHz, [D_6]DMSO) spectrum of compound **9.**

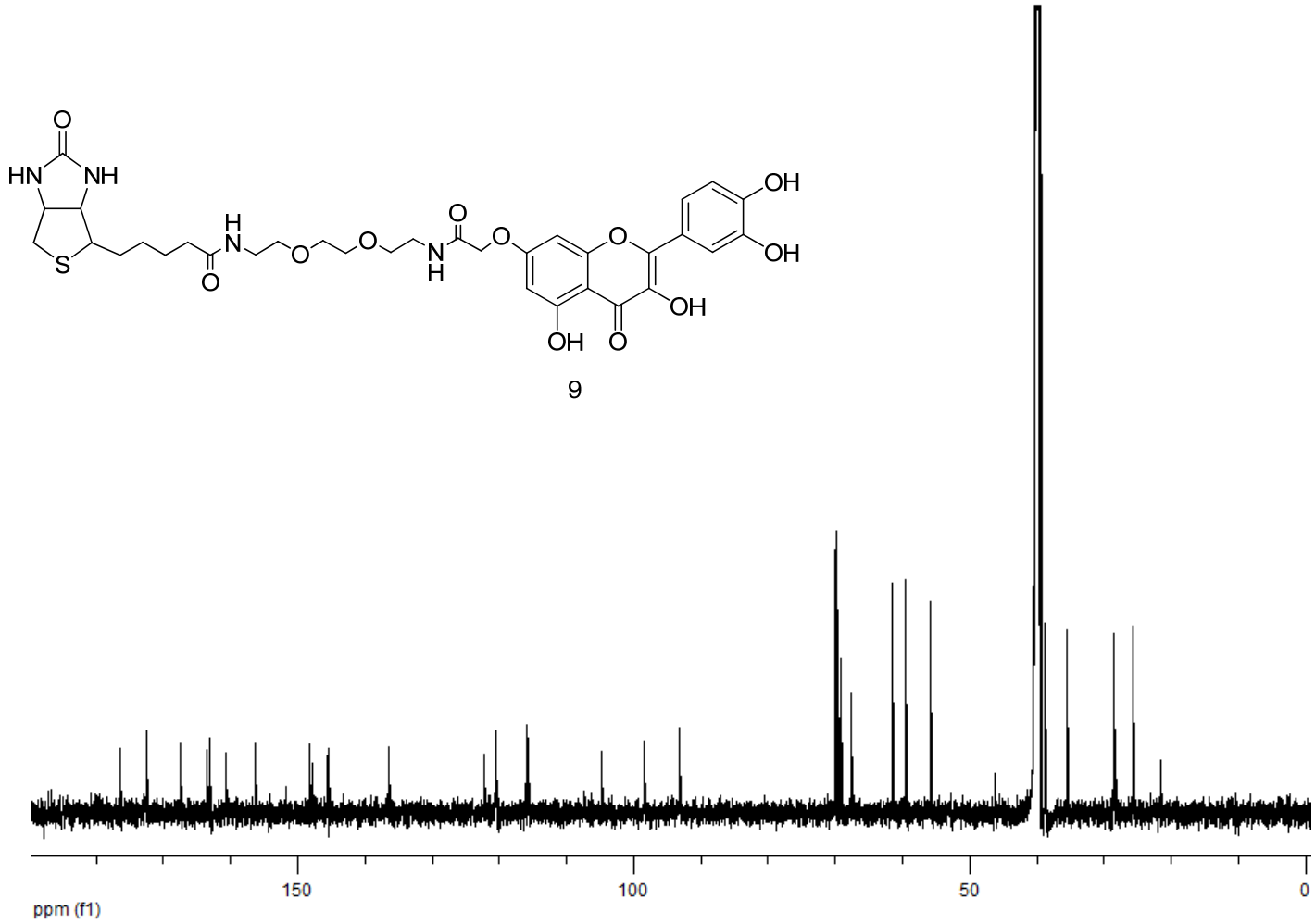

Figure 3. 23 ^{13}C NMR (151MHz, [D_6]DMSO) spectrum of compound **9.**

Chapter 4.

Inhibition of Heat Shock Transcription Factor Binding and Heat Shock Protein 70 Induction in vivo by a Linear Polyamide Binding in a 1:1 C→N Mode

The text of this chapter was taken in part from a manuscript coauthored with Raj K. Pandita, Jianfeng Cai, Clayton R. Hunt and John-Stephen Taylor (Washington University)

(Rongsheng E. Wang, Raj K. Pandita, Jianfeng Cai, Clayton R. Hunt & John-Stephen Taylor, 2010, Manuscript submitted)

Abstract

Heat shock proteins (HSPs) are known to protect cells from heat, oxidative stress, and the cytotoxic effects of drugs, and thus can enhance cancer cell survival. As a result, HSPs are a newly emerging class of protein targets for chemotherapy. Among the various HSPs, the HSP70 family is the most highly conserved and prevalent. Though a number of small molecule inhibitors of HSP70 induction are known, they have a number of drawbacks with regards to toxicity, potency, and specificity. Herein I am describing the development of a β-alanine rich linear polyamide that binds the GGA heat shock elements (HSEs) 3 and 4 in the HSP70 promoter in a 1:1 mode and inhibits heat shock transcription factor 1 (HSF1) binding in vitro and HSP70 induction in vivo.

Introduction

Although heat shock protein 70 (HSP70) is recognized as an emerging protein target for chemotherapy, few inhibitors have been developed so far that have potential to be administrated as drugs, due to the obstacle in druggability of HSP70, as explained in chapter 1. Of the known small molecule inhibitors of HSP70 induction, such as triptolide, KNK 437 and quercetin, quercetin requires high concentrations and, though it is known not to be toxic in humans, lacks specificity, inhibiting many off-target kinases and enzymes [1, 2]. However, quercetin appears to have an easy-modifiable structure and interfere with HSF1 activation by inhibiting HSF1phosphorylation to block the HSP70 induction [3] , making its derivative have advantage in potential specificity over other inhibitors which interfered with the down-stream pathways of HSP70 expression. We therefore introduced the optimization and study of quercetin derivatives and the identification of possible targets in previous chapters.

Besides the development of small molecules, a more general approach to developing HSP70 inhibitors as chemotherapeutic drugs would be to make use of highly programmable gene-specific agents, such as antisense, siRNA, and antigene agents, whose pharmaceutical properties might be more predictable and readily tailored [4]. Among these potential agents, nucleic acid-based agents such as antisense phosphorothioates, locked nucleic acids, siRNAs, and peptide nucleic acids can be made to predictably bind to their nucleic acid targets by simple Watson Crick base pairing [4, 5]. Unfortunately, all of these nucleic acid-based agents have poor membrane permeability, necessitating the use of liposomal, cell penetrating peptide, or nanoparticle delivery systems [4]. Anti-gene agents based on polyamides can also recognize a target

DNA sequence through predictable H-bonding interactions with the minor groove, but unlike antisense agents, have better membrane permeability properties [6, 7]. Minor groove binding polyamides have been shown to inhibit transcription factor binding in the minor groove through allosteric effects and by modifications that interfere with phosphate contacts [8-10]. Polyamides are also attractive for drug development, because they can be conveniently synthesized by standard Fmoc or Boc solid phase peptide synthesis methods.

Polyamides consist of oligomers of N-methyl-imidazole (Im) and N-methyl-pyrrole (Py) linked together through amide bonds [11]. Watson-Crick base pairs are recognized by hydrogen bonding in the minor groove with Im/Py recognizing G/C, Py/Im recognizing C/G, and Py/Py recognizing either A/T or T/A (Figure 4.1). N-methyl-3-hydroxypyrrole (Hp) can be used to discriminate between A/T from T/A base pairs by preferentially recognizing thymidine. Up to seven Im and Py units have been linked together to form linear polyamides with binding affinities in the nM concentration range [12]. The binding affinity drops after more than seven units because of divergent curvature of the polyamide and the minor groove. The binding size limit can be overcome by introduction of a flexible β-alanine linker, which makes it possible to create linear polyamides of 16 units in length, to target AT rich nucleic acid [13].

X-ray crystallography has revealed two binding modes, a 2:1 mode in which two polyamides bind in an antiparallel fashion to the DNA in either a fully overlapped or slipped form [12], and a 1:1 mode in which one polyamide binds in a single orientation [14]. While for most sequence contexts, polyamides bind in a 2:1 mode, polypurine sequences are bound in a 1:1 mode, which is proposed to result from a narrower minor

groove that prevents binding of second polyamide [15, 16]. It has also been observed that in polypurine rich sequences, linear polyamides tend to bind in the opposite direction (C→N, 5'→3') compared to most sequences (N→C, 5'→3') [14, 15].

Transcriptional induction of HSP70 involves trimerization and binding of the heat shock transcription factor (HSF1) to the major groove of the heat shock elements (HSEs) which consist of 3-4 tandem inverted repeats of a core NGAAN DNA element. Though polyamides bind to the minor groove, there are numerous examples in which hairpin polyamides can be made to inhibit major groove binding by incorporation of conjugated amino acids that block protein contacts with the major groove and/or DNA backbone [17], or by altering the geometry of the major groove [10, 18-20]. With regards to binding the heat shock element NGAAN motif, a linear polyamide has been previously designed to bind in a 1:1 mode to long GAA•TTC repeats in Friedreich's ataxia [16]. Herein, I report on the synthesis and binding properties of a series of linear polyamides targeted to the human heat shock elements, and demonstrate for the first time, inhibition of transcription factor binding by a polyamide binding in a 1:1 linear binding mode.

Results

There are three heat inducible HSP70 genes in humans, of which HSPA1A and HSPA1B are the most conserved and bear the same promoter structure [27]. Promoters of heat inducible HSP70 genes contain multiple adjacent and inverted NGGAN motifs, or heat shock elements (HSEs) that are recognized by the heat shock transcription factor, HSF-1.

Five adjacent HSEs are found in the HSPA1A/HSPA1B genes, two of which (site 3 and 4) (Figure 4.2a) are part of a sequence with dyad symmetry (GGAATATTCC). HSF-1 binds the heat shock promoter as a trimer and both footprinting and single nucleotide deletion analysis have shown that it preferentially binds to sites 3 and 4. The five HSEs manifest a distorted structure, especially after site 1 and 3, as evidenced by methidiumpropyl-EDTA footprinting [28]. It was proposed that purine tracts at site 1 and 3 have twisted DNA strands and narrowed minor grooves, which help the heat shock transcription factor contact the major groove.

Hairpin polyamide design and synthesis. The critical heat shock elements HSE3 and HSE4 within the HSP70 DNA promoter are quite challenging to target with polyamides because there is evidence from MPE footprinting that the DNA minor groove is distorted and much narrower than at polypurine tracts [28]. Recognizing that HSE3 and HSE4 were part of a pallindromic site, we initially decided to target the GGAAT sequence with a hairpin polyamide, as a hairpin polyamide has been previously successfully used to target the related sequence, GGAAA contained in the NF-kB binding site [9]. To this end I synthesized hairpin polyamides H0-H3 (Figure 4.2b). H1 was composed of only imidazole and pyrrole amino acids, whereas for H2 and H3 I replaced one pair of the pyrrole amino acids with β-alanine to relieve any potential strain induced by the site. β-alanine is preferred relative to pyrrole in structurally rigid DNA sites because of its flexibility [15]. H0 was used as a mismatch control for H1. The hairpins were synthesized by conventional solid phase Fmoc-synthesis on an oxime resin [22], in yields of 10%-20%.

Binding Sites and Affinity of the Hairpin Polyamides. Binding of the hairpin polyamides was determined by quantitative DNase I footprinting [26]. 5' Radiolabelled 152-mer DNA prepared by PCR containing the heat shock promoter was incubated with various concentrations of polyamide and subjected to DNase I cleavage. The extent of inhibition of DNase I cleavage at the observed binding sites as a function of polyamide concentration was then fit to a Hill-slope equation. DNase I footprinting showed that only H1bound specifically to the DNA at concentrations below 1 μM and at two distinct sites (Figure 4.3). One footprint not only encompassed the HSE3 and HSE4, but also HSE1 and 2, which contain a GGTTT site that could also be bound by H1. The site higher up on the gel (E) corresponds to a site that also contained a GGAA site. Quantitative footprinting over the range of 100 to 500 nM gave the best fit for a fixed Hillslope of 1 with a binding constant of only $3.0 \pm 0.4 \times 10^5$ M^{-1} for the HSE1-4 sites. The observed binding affinity is a much lower than that of $1.3 \pm 0.2 \times 10^9$ M^{-1} that was reported for the corresponding GGAA site in the NF-κB site [9]. Because this polyamide had such a low binding affinity and did not show any inhibition of HSF1 binding to the HSE (data not shown), we decided to investigate linear binding modes.

Linear Polyamide Design and Synthesis. It has also been shown that a GGAA sequence can be bound by linear polyamides in a 2:1 mode, N-C, 5'-3' orientaion at a quasi pallindromic site (AGGGAATCCCCT) [29]. A β-alanine was used to link two four-ring-polyamides to enable recognition of the longer site. We therefore designed a similar set of polyamides, in which additional pyrroles were also substituted with β-alanines in anticipation of stress induced by the HSE sequence. The number of β-alanines that can be used is limited, however, by the observation that too many β-alanines

decrease nuclear localization and cell permeability [16, 30]. We therefore designed a library of polyamides bearing a β-alanine opposite different A's and T's along with β-alanine at the carboxy terminus that originates from using a β-alanine solid phase support. This library consisted of four polyamides (P1, P2, P3, and P6) bearing two β-alanines, and one polyamide (P10) bearing a single β-alanine at the C-terminus to serve as a control (Figure 4.2c). Because we wanted to avoid having two β-alanines adjacent to each other at the C-terminal end, the polyamide in which the Py of P10 opposite T3 that would have been replaced with β-alanine was not synthesized. Polyamides containing an additional β-alanine were also synthesized (P5 and P9), in which no two β-alanines were adjacent to each other.

The first library of linear polyamides was designed to bind in the conventional N→C vs 5'→3' direction [7]. Due to the dyad symmetry of the DNA sequence being targeted, polyamides P1, P2, P3, P5, P6, P9 and P10 were expected to bind to either strand in a linear 1:1 mode, or simultaneously in a 2:1 mode. A second library consisting of P7, P4, and P8 was designed to bind in the C→N direction that has been observed to be preferred for polypurine sequences [14, 15]. The polyamide was also shifted to recognize the T to the 5'-side of the pallindromic sequence on the top strand (T-6) in an effort to enforce a unique orientation that might be detectable by footprinting. The bottom strand has a G at this position (Figure 4.2c). The sequences of the second library were based on the P5 sequence, after it was found to have the highest affinity in footprinting assay (Figure 4.4) among the members of the first library (vide infra). P11 and P12 were double mismatch controls for the first and second libraries, respectively. The polyamides were synthesized by solid phase Fmoc synthesis [21] and had yields

around 40% for P10, but lower yields when more β alanine building blocks were included. P1, P2, P3, P6 and P7 were obtained in yields between 20% and 30%, while P5, P9, P4, P8, P11 and P12 were obtained in yields between 10% and 20%.

Binding Sites and Affinity of the Linear Polyamides. The binding sites and affinity of the linear polyamides were also determined by quantitative DNase I footprinting as was carried out for the hairpin polyamides. Polyamides P1, P2, P3, P6 and P10 having one or no β-alanines in the body portion were the weakest binders as they did not show any readily discernable footprint at concentrations up to 500 nM (Figure 4.4a). Polyamides consisting of two β-alanines (P5 and P9) in the body portion showed a detectable footprint at the HSE3/4 site at 100 nM polyamide (Figure 4.4b). The mismatch polyamide P11, in which Im and β were switched, showed no distinct inhibition until 500 nM, at which point binding was fairly non specific (Figure 4.4c). Association constants determined by quantitative analysis of the footprinting gels (Table 4.3), show that within the limits of error, that the 8-mer polyamides binding in the N→C direction relative to the 5'→3' DNA direction (P5 and P9) have K_a's of approximately 1×10^7 M^{-1}. Whereas P9 appeared to bind in a 2:1 mode (Hillslope coefficient of 1.5), P5 appeared to bind in a 1:1 mode (Hillslope coefficient of 0.9).

Significantly higher binding affinity was observed for the second library of polyamides, P7, P4 and P8, which were designed to bind in the opposite direction (C→N) and asymmetrically to the two nucleotides to the 5'-side of HSE3 as shown in Figure 4.5. Whereas a footprint only began to emerge at about 100 nM for P7, much like for P5 and P9, a footprint began to emerge at 0.1 pM for the longer polyamides, P4 and P8. Quantitative analysis of the footprints in a lower concentration range (Figure 4.7) show

that polyamides P7, P4 and P8 have much higher affinity per amino acid than those binding in the normal direction, with K_a's of 1.15×10^7 M^{-1} for the 6-mer P7 to 3.44×10^8 M^{-1} for the 9-mer (Figure 4.8, Table 4.3). Within this group of polyamides, the binding affinity can also be seen to increase with increasing length, in the order P7 < P4 < P8. Binding to n+1 on-targeted sites was observed to occur at the 3'-end of the promoter sequence for P4 and P8, but only at 100 nM and higher concentrations. The mismatch control for P8, polyamide P12, only bound to DNA substrate non-specifically at concentrations of 400 nM and above (Figure 4.5). All of the C→N binding polyamides appeared to bind in a 1:1 mode based on the Hill Slope coefficient (Figure 4.8, Table 4.3).

Although DNase I footprinting is not able to determine the exact bases bound by a polyamide, or the orientation of the polyamide, close examination of the footprints for P7, P4 and P8 reveals an increase in the protected site with an increase in the size of the polyamide (Figure 4.6). Comparison of the blocked sites in the bracketed section of the gel indicates that the relative intensity of one cleavage band is greatly diminished in going from P7 to P4, and that then next band is lost in going from P7 to P8. Thus, increasing the polyamide chain length at the N-terminus increased its DNA binding and hindered DNase I accessibility to the bound DNA. The loss of DNase I bands on going from P7 to P4 to P8 is most consistent with the C→N orientation along the 5'→3' direction on the top strand, though we cannot rule out the same binding to the bottom strand in the reverse orientation.

In vitro inhibition of HSF-1 binding to heat shock element DNA by polyamides.

The ability of the polyamides to block binding of HSF-1 to its cognate heat shock element (HSE) DNA promoter sequence was determined by a gel mobility shift assay. Radiolabeled HSE oligodeoxynucleotide duplex (10 nM) was incubated with different polyamides at 100 nM before mixing with nuclear extracts prepared from heated Jurkat cells and the formation of HSE/HSF-1 complexes determined by gel electrophoresis (Figure 4.9). As expected, the HSE/HSF-1 complex readily forms with extracts prepared from heated control cell nuclei (lane C, position of arrow) in the absence of added polyamide. Addition of polyamides P1-P7, P9-P10 or P11-P12 to the HSE binding reactions did not significantly decrease complex formation. Polyamide P10 appeared to cause aggregation as a significant amount of material was trapped in the gel well. Polyamide P8, however, decreased the level of HSE/HSF-1 complex formed to 35% of control, indicating that polyamide binding either altered the DNA structure or was otherwise inhibiting HSF-1 access to the DNA structures required for complex formation. We then incubated the DNA with different concentrations of polyamides P8, P11 and P12, to determine the minimum inhibitory concentration (Figure 4.10). Whereas P11 had no effect on complex formation over a range of 10 to 100 nM, the P8 polyamide inhibited complex formation at 50 and 100 nM but not at lower concentrations (Figure 4.10a). Similar observations were made for P8 versus P12 (Figure 4.10b).

Polyamide inhibition of HSP70 expression in vivo. The ability of P8 and the P11 control polyamides to inhibit HSP70 expression in vivo was determined by measuring the level of HSP70 protein in Jurkat cells after heat shock. Jurkat cells were chosen because they have a very low basal level of HSP70 which is highly induced by heat [31]. Because no effect on HSP70 induction was observed on cells passively treated with the

polyamides, cells were electroporated with 5 μM P8 or P11 and then allowed to recover for 24 h in the presence of 5 μM polyamide before being heat shocked at 43 °C for 30 min to induce HSP70 gene transcription and protein synthesis. Western blot analysis of HSP70 protein levels (Figure 4.11), normalized to actin protein levels and corrected for cell viability, indicated that the P11 control polyamide had no effect on HSP70 expression (102 ± 6 % of control) while P8 decreased HSP70 levels to about 60% of normal (58 ± 9 %). This result is consistent with the gel shift analysis, which showed that polyamide P8 and not P11 inhibits HSF-1 binding to the heat shock promoter DNA elements required for transcriptional activation of HSP70 expression. The actual amount of HSP70 suppression may be greater than 40% if the HSP70 antibody is cross reacting with untargeted B' (also known as HSP70-6, HSPA6), which is also heat inducible, in addition to polyamide targeted HSPA1A/HSPA1B [32].

Discussion

There are several examples hairpin or cyclic polyamides that inhibit transcription factor binding to the DNA major groove, presumably by altering the minor groove conformation and as a consequence the major groove conformation [10, 18, 19, 33]. There are also some examples of linear polyamides that can alleviate inhibition of transcription in expanded GAA•TTC repeats that appear to work by stabilizing a B DNA conformation and interfering with intramolecular triplex formation and intermolecular interactions [16]. There have not to our knowledge been any reports of linear polyamides that can inhibit transcription factor binding.

The human HSP70 heat shock promoter is composed of five heat shock elements [28], three of which are GAA•TTC sequences, and two of which, HSE3 and HSE4, are involved in an inverted repeat separated by a TA sequence that would allow binding by both 1:1 and 2:1 modes. The heat shock elements are extremely twisted, suggesting that transcription factor binding might be inhibited by a polyamide that would stabilize a less twisted DNA conformation. Polyamides have usually been observed to bind from the N to C direction relative to the 5' to 3' direction of the DNA sequence, the only exception occurring with purine rich DNA sites, where an opposite orientation is observed [15]. Because the heat shock promoter contains both purine rich and mixed sequences, we designed hairpin and linear polyamides with both N to C and C to N orientations targeted to HSE3/4.

Our initial attempts with designing a hairpin polyamide to bind to the GGAA sequence along previously successful lines for a similar site in the NF-κB site [9], only yielded a weak binding polyamide that was not able to inhibit heat shock transcription factor binding in vitro. It may be that the conformation of the HSE3/HSE4 DNA does not support the hairpin motif. It was for this reason that we turned our attention to linear polyamides.

Because polyamide P10, which was composed of only internal pyrrole and imidazole building blocks, failed to bind to the HSE effectively, selected pyrroles were replaced with the more flexible β-alanine unit to improve polyamide curvature [15]. Different polyamide libraries incorporating an increasing number of internal β-alanines were prepared, of which only polyamides containing two internal β-alanines, P5 and P9, manifested binding to heat shock DNA elements at concentrations above 100 nM. The

region of protected DNA corresponded to the targeted 5'-GGAATTCCC-3' sequence of HSE3 and HSE4. Due to the pallindromic nature of this sequence P5 and P9 could be binding to either strand, or both, in an N→C orientation.

Because HSE3/4 contains polypurine tracts, it was also possible that the polyamides could bind in the C→N [14, 15]. In support of this idea, polyamide P8, which was designed to bind to the top strand with the C→N orientation by recognizing the T to the 5'-side of the pallindromic sequence, had significantly higher binding affinity than the sequences designed to bind in the N→C orientation. Also consistent with this analysis was the increase in the DNase I footprint size on going from P7 to P4 to P8 towards the 3'-side of the HSE3/4 sequence expected if the polyamides were binding to the top strand (Figure 4.6). In the case of the heat shock elements, the presence of two opposing polypurine tracts disrupted by a TA sequence may allow binding of polyamides in both N→C and C→N orientations. It is also noteworthy that linear polyamides generally adopt a 2:1 binding mode in the minor groove of mixed sequences, whereas all the polyamides investigated herein appear to bind in a 1:1 mode, with the possible exception of P9 (Table 4.3). It may be that pre-twisted nature of the sequence containing two HSE elements with dyad symmetry precludes binding of a second polyamide, whereas shorter sequences targeting only one HSE may be able to bind in a 2:1 cooperative mode.

Given the high association constant of P8, an *in vitro* gel shift assay was carried out to determine whether P8 specifically blocked heat shock factor binding to heat shock element (HSE) DNA. At a concentration of 100 nM, P8 effectively inhibited HSF binding while both P11 and P12, which had sequence mismatches, showed no activity (Figure 4.10). This result was consistent with a screen of all the linear polyamides at 100

nM that identified P8 as the most effective inhibitor (Fig. 4.9). Initial attempts to inhibit HSP70 induction *in vivo* by addition of P8 to the culture medium failed, suggesting that the polyamide might not be entering the cells efficiently as has been previously observed for longer polyamides [16]. When the P8 polyamide was electroporated into cells, an approximately 40% decrease in heat induced HSP70 protein synthesis was observed (Figure 4.11) indicating the ability of P8 to inhibit HSP70 induction in vivo. It may be that incorporation of the β-alanines hampers cell permeation by polyamides, [30, 34] and that future studies will need to focus on improving cell delivery [35, 36]. The 40% inhibition of HSP70 induction is promising, though effective suppression of the heat shock response may also require inhibiting HSP70B' (HSP70-6) which is induced from the HSPA6 gene. The HSE for HSPA6 gene is sufficiently different from that of HSPA1A/A1B, however, that a new polyamide would need to be developed. A cocktail of polyamides that target both the HSPA1A/A1B and HSPA6 promoters could be investigated in the future, as a way to more completely block induction of the heat shock response.

Conclusion

We have demonstrated for the first time the ability of a linear polyamide binding in a 1:1 mode to block transcription *in vivo*. More specifically, a linear polyamide with high affinity for the heat shock elements 3 and 4 of the HSPA1A/HSPA1B promoter was developed that interfered with binding of the heat shock transcription factor *in vitro* and inhibited heat shock protein 70 induction *in vivo*. We found that the polyamide design

that could best accommodate the structural constraints imposed by the G-rich polypurine tracts of the heat shock element consisted of a linear polyamide with a number of β-alanines that was designed to bind in the C→N orientation. Though this polyamide showed good inhibition of heat shock transcription factor binding in cell lysates, electroporation was required to observe an inhibitory effect in vivo. Unfortunately, the multiple β-alanines used to optimize binding affinity may have compromised the ability of the polyamide to penetrate the cell and/or nucleus. Future work will focus on improving polyamide cell permeation and further enhancing inhibition of heat shock transcription factor binding. Given that a considerable amount of heat shock protein may also be transcribed from the HSPA6 gene, polyamides targeting HSPA6 would also need to be used in conjunction with polyamides for HSPA1A/A1B to better suppress the heat shock response.

Experimental section

Abbreviations

HSP: heat shock protein; HSP 70: heat shock protein 70; NF-κB: nuclear factor kappa-light-chain-enhancer of activated B cells; HSF-1: heat shock transcription factor 1; CaMKII: Ca2+/calmodulin-dependent protein kinase II; CKII (CK2): casein kinase II; KNK437: 3-[(E)-1,3-Benzodioxol-5-ylmethylene]-2-oxopyrrolidine-1-carbaldehyde; SiRNA: small interference RNA; Im: N-methyl imidazole; Py: N-methyl pyrrole; Hp: N-methyl-3- hydroxypyrrole; HSE: heat shock element; EDTA: ethylenediaminetetraacetic acid; MPE: methidiumpropyl ethylenediaminetetraacetic acid; PCR: polymerase chain

reaction; DnaseI: deoxyribonuclease I; Ka: association constant; Fmoc: fluorenylmethyloxycarbonyl; DMF: dimethylformaldehyde; DCM: dichloromethane; UV: ultraviolet ; DIPEA: N,N-diisopropylethylamine; HATU: 2-(7-Aza-1H-benzotriazole-1-yl)-1,1,3,3-tetramethyluronium hexafluorophosphate; ; HPLC: high-performance liquid chromatography; MALDI: matrix-assisted laser desorption ionization; EC50: half maximal effective concentration; ODN: oligodeoxynucleotide; SDS: sodium dodecyl sulfate.

General procedures

Anhydrous dimethyl formamide was from EMD chemicals Inc. Anhydrous dichloromethane was freshly prepared by refluxing with calcium hydride followed by distillation. HATU was purchased from Genscript Corporation. All other reagents were directly purchased either from Omni Solvent or Sigma Aldrich unless otherwise specified. Amicon centrifugal filters were from Millipore. Analytical thin-layer chromatography was performed on Aldrich Silica gel 60 F_{254} plates (0.25 mm). Fmoc deprotection was qualitatively monitored by UVG-54 mineral light UV lamp at 254 nm.

Chemical synthesis of polyamides

Polyamide building blocks Fmoc-Im-COOH, Fmoc-Py-COOH, Fmoc-B-alanine and Im-COOH were synthesized according to published procedures as was the manual synthesis of polyamides with some modifications [21] . Synthesis of the hairpin polyamides was carried out on an oxime resin in plastic columns (Bio-Rad) that were shaken in an automatic shaker (Labnet International. Inc) [22], while the synthesis of the linear polyamides was carried on 200 mg of Fmoc-β-alanine-Wang's resin, (0.34 mmol/g). One

synthesis cycle was used for all couplings except when coupling to imidazole, when two synthesis cycles were used. One cycle of synthesis consisted of Fmoc deprotection followed by washing, coupling followed by washing, and finally a capping step followed by washing. Each washing step involved 3-5 mL of solvent. The deprotection step consisted of mixing the resin with 20% piperidine in DMF and shaking for 3 min. The deprotection solution was then drained and spotted on thin-layer chromatography plate to monitor the formation of the Fmoc deprotection product, which turns blue to purple under a UV 254 nM lamp. The column was then washed with DCM for 3 min followed by DMF for 3 min, and then 20% piperidine was added again and shaken for additional 20 min. The washing step involved shaking the resin with DCM for 3 min, followed by DMF for 3 min, repeating again with DCM and DMF for 3 min each and then a final 3 min wash with DMF. The coupling step involved 700 μL of DMF plus 300 μL DIPEA, containing Im/Py/β building block (0.136 mmol) and a molar equivalent of HATU (0.136 mmol). The building blocks were preincubated with HATU/DIPEA in DMF for 5 min before adding to the resin. The mixture was shaken for one hour in the case of pyrrole coupling and two hours in the case of imidazole coupling, while at least 8 h were required for coupling to imidazole. The capping reagent consisted of 5% pyridine and 20% acetic anhydride in DMF and was shaken with the support for 3 min, followed by draining and washing with DCM and DMF for three min each. Additional capping reagent was added and the suspension was shaken for 20 min before being drained. Before synthesis, resins were first immersed in a 1:1 DCM/DMF mixture for couple of hours to allow sufficient time for swelling. At the end of synthesis, polyamides were cleaved from resins (50 mg) at 55 °C by treatment with 2 mL of 1-dimethylaminopropylamine, for 24 h. The 1-

dimethylaminopropylamine solution was filtered and evaporated to afford a brownish residue that was triturated with diethyl ether. The yellow to white precipitates were purified by preparative reverse phase gradient HPLC on a Beckman System Gold HPLC system with a solvent pump module 125 and model 168 diode array UV detector, equipped with a reverse phase column XTerra Prep MS C18, (10 μm, 7.8 × 300 mm). Linear gradients of 0-5 % Solvent B in A over 0.05 min, followed by 5-100% solvent B in A over 50 min were used, where solvent A was water with 0.1% trifluoroacetic acid and solvent B was acetonitrile with 0.1% trifluoroacetic acid. The purified products were characterized by MALDI (Table 4.2) and their purity were also analyzed by HPLC reverse phase analytical column (Waters XTerra MS C18, 2.5 μm, 4.6×50 mm) using the same HPLC instrument and solvents as used for purification (Table 4.1). The elution method was linear gradients of 0-5% solvent B in A over 0.05 min, followed by 5-100% solvent B in A over 20 min.

Preparation of the DNase I footprinting substrate

The DNA substrate for the DNase I footprinting assays was prepared by polymerase chain reaction on a HSPA1A containing plasmid [23]. Two primers were chosen with melting temperatures around 55 °C (Left primer d(CACTCTGGCCTCTGATTGGT) and right primer d(CCCTGGGCTTTTATAAGTCGT)) to give the 152-mer product shown below.

d(CACTCTGGCCTCTGATTGGTCCAAGGAAGGCTGGGGGGCAGGACGGGAGG
CGAAACCCCTGGAATATTCCCGACCTGGCAGCCTCATCGAGCTCGGTGATTG
GCTCAGAAGGGAAAAGGCGGGTCTCCGTGACGACTTATAAAAGCCCAGGG)

The left primer was 5'-[^{32}P]-end labeled with kinase and [γ-^{32}P]-ATP by a standard procedure. After PCR, the products were cooled in cold block at 4 °C and mixed with Promega blue/orange loading dye (6×), which were then subjected to separation by non-denaturing polyacrylamide gel at a constant voltage of 800 V. The product band was excised with a razor, immersed in DNA extraction solution (25 mM Tris-HCl /250 mM NaCl, pH 8.0) and stirred overnight with a stirring bar. The crushed gel pieces were then filtered by centrifugation on an Ultrafree-CL centrifugal filter (Amicon, Millipore). The filtrate was equally distributed in 2.0 mL microfuge tubes, to which 1.5 volumes of isopropanol was added for precipitation at 14000 rpm in cold room, for at least 30 min. The DNA pellets were further washed with 75% ethanol and centrifuged for 2 min at 14000 rpm. DNA were redissolved in 500 μL water and stored at -80 °C for further use.

Sequence ladders

The Maxam-Gilbert A+G reaction was carried out according to standard procedures [24], while the A sequencing reaction was performed according to another procedure [25]. The A sequencing reaction was carried out by mixing 30 μL of a potassium tetrachloropalladate(II) solution (32.6 mg of K_2PdCl_4 in 10 mL of 100 mM HCl solution that was pre-adjusted to pH 2 with NaOH), with 50 μL 5'-end-labeled 152-mer, 1 μg sonicated calf thymus DNA carrier and 120 μL water to make a final concentration of 1.5 mM K_2PdCl_4. After 35 min incubation at room temperature, the reaction was quenched with 50 μL of 2 M sodium acetate, 0.8 M 2-mercaptoethanol and 15 μg of calf thymus DNA. The suspension was precipitated in ethanol and washed with 75% ethanol for desalting. The yellowish DNA pellet was then dissolved in 50 μL freshly made 10%

piperidine and heated at 90 °C for 30 min, before lyophilization in a SpeedVac. To ensure complete removal of the piperidine, 20 μL water was added and the DNA was redissolved by vigorous vortexing, before being dried again in the Speed Vac. The product was dissolved in 50 μL water and stored at -80^{0}C until use.

DNase I footprinting

Footprinting of the polyamides on the DNA was based on a standard procedure [26]. Generally, 300 pmol 5'-endlabelled DNA stock solution was dissolved in TKMC buffer (10 mM Tris-HCl, 10 mM KCl, 10 mM $MgCl_2$, 5 mM $CaCl_2$, pH 7.0). Polyamide stock solutions were prepared by serial dilution and 40 μL of each was mixed with 350 μL of the DNA solutions. The samples were incubated for 24 h at room temperature to allow for binding and then treated with 10 μL of the optimal amount of DNase I (Invitrogen) (approximately 1 mU/μL). After 5.5 min the reactions were quenched by treatment with 50 μL DNase I stop buffer (30 μL 20 mg/mL glycogen II, 0.1mg Calf thymus DNA, 788 μL 4 M NaCl, 425 μL of 0.5 M EDTA and 137 μL water, pH 8.0).

The quenched samples were then ethanol precipitated at 14000 rpm in a cold room for 30 min, washed with 75% ethanol and redissolved in 20 μL water by vigorous vortexing to ensure full recovery of all the DNA. Samples were immediately mixed with denaturing loading buffer (1× TBE, 80% formamide) and boiled in water bath for 10 min, before loading onto an 8% polyacrylamide denaturing gel (7 M urea). Gel electrophoresis was performed at 2000 V for roughly 2 h until the bromophenol blue marker completely migrated of the bottom of the gel. After detachment of the glass plates, the gel was covered with plastic wrap and imaged with phosphor screen for 12 h.

The screen image was detected with a Biorad Phosphor Imager and processed by Quantity One software.

Quantitative analysis of footprinting results

The intensity I of bands in the footprinting gels was quantified by Biorad Quantity One software. The fractional occupation θ by the polyamide was calculated as 1-$(I_{site}/I_{ref})/(I°_{site}/I°_{ref})$ where I_{site} is the intensity of a band within the binding site that is modulated by polyamide, I_{ref} is the intensity of a band outside the binding site that is not modulated by polyamide binding, and I^{o}_{site} I^{o}_{ref} are the intensities of the same sites in the absence of polyamide [26]. The observed fractional occupation as a function of polyamide concentration (L) was then fit to a variable Hill slope (n) equation with Graph PadPrism 5 using nonlinear regression analysis (equation 1) and equating EC_{50} with $1/K_a$ and averaged for three independent sets of measurements

$$(1) \quad \theta = \theta_{\min} + \frac{(\theta_{\max} - \theta_{\min})}{1 + 10^{n(\log EC_{50} - L)}}$$

In vitro gel-shift assay of heat shock factor 1 binding

Gel mobility shift assays were performed essentially as previously described [3] using nuclear extracts prepared from control and heated (43 °C for 30 min, 1 h recovery at 37 °C.) human HeLa cells. Two complementary ODNs, d(GTAGGCGAAACCCCTGGAATATTCCCGACCTG) and

d(CTGCCAGGTCGGGAATATTCCAGGGGTTTCG), derived from the human HSPA1A gene promoter that contained HSE 1-5 were synthesized and purified by polyacrylamide gel electrophoresis (Eurofins). After annealing, the 5'-overhanging ends of the duplex DNA were filled with α-^{32}P-dATP and cold nucleotides using Klenow polymerase to give a 36-mer radiolabelled duplex. Polyamides (10-500 nM) were bound to the labeled duplex ODNs (10 nM) by incubation together in annealing buffer (10 mM Tris pH 7.5, 10 mM NaCl, 1 mM EDTA) for 16 h at 25 °C. Mobility shift binding reactions containing 1.5 μg of nuclear proteins mixed with equivalent counts of labeled probe in a 25 μL final volume were incubated for 20 min at 25 °C before separation on 4.5% polyacrylamide gels. Labeled protein-DNA bands were detected and quantified on a Molecular Dynamics PhosphoImager.

Electroporation of polyamides

Approximately 2×10^6 human Jurkat cells were resuspended in 100 μL electroporation buffer (Amaxa, Inc.) with 5 μM polyamide and electroporated in an Amaxa Nucleofector using program I-010. Cells were re-plated in 5 mL RPMI media plus 5 μM polyamide and cell viability determined by trypan blue exclusion 24 h later. Cells were then heated at 43 °C. for 30 min and allowed to recover at 37 °C for 6-8 h before being harvested in Laemmli buffer for protein analysis.

Western blot assay

Proteins were separated on 7% SDS-polyacrylamide gels and transferred to Immobilon-P membranes and probed with mouse anti-HSP70 (SPA-810, Assay Designs) and mouse

anti-actin (C4, MP Inc) followed by AP-coupled goat anti-mouse. Band intensity was quantified by scanning on a BioRad ChemDoc XRS.

References:

1. Davies, S.P., et al., *Specificity and mechanism of action of some commonly used protein kinase inhibitors.* Biochem. J., 2000. **351**(Pt 1): p. 95-105.
2. Murakami, A., H. Ashida, and J. Terao, *Multitargeted cancer prevention by quercetin.* Cancer Lett, 2008. **269**(2): p. 315-25.
3. Wang, R.E., et al., *Inhibition of heat shock induction of heat shock protein 70 and enhancement of heat shock protein 27 phosphorylation by quercetin derivatives.* J Med Chem, 2009. **52**(7): p. 1912-21.
4. Mahato, R.I., K. Cheng, and R.V. Guntaka, *Modulation of gene expression by antisense and antigene oligodeoxynucleotides and small interfering RNA.* Expert Opin Drug Deliv, 2005. **2**(1): p. 3-28.
5. Alvarez-Salas, L.M., *Nucleic acids as therapeutic agents.* Curr. Top. Med. Chem., 2008. **8**(15): p. 1379-404.
6. Melander, C., R. Burnett, and J.M. Gottesfeld, *Regulation of gene expression with pyrrole-imidazole polyamides.* Journal of Biotechnology, 2004. **112**(1-2): p. 195-220.

7. Dervan, P.B., R.M. Doss, and M.A. Marques, *Programmable DNA binding oligomers for control of transcription.* Curr Med Chem Anticancer Agents, 2005. **5**(4): p. 373-87.

8. Bremer, R.E., E.E. Baird, and P.B. Dervan, *Inhibition of major-groove-binding proteins by pyrrole-imidazole polyamides with an Arg-Pro-Arg positive patch.* Chem Biol, 1998. **5**(3): p. 119-33.

9. Wurtz, N.R., et al., *Inhibition of DNA binding by NF-kappa B with pyrrole-imidazole polyamides.* Biochemistry, 2002. **41**(24): p. 7604-9.

10. Chenoweth, D.M. and P.B. Dervan, *Allosteric modulation of DNA by small molecules.* Proc Natl Acad Sci U S A, 2009. **106**(32): p. 13175-9.

11. Dervan, P.B. and B.S. Edelson, *Recognition of the DNA minor groove by pyrrole-imidazole polyamides.* Current Opinion in Structural Biology, 2003. **13**(3): p. 284-299.

12. Kelly, J.J., E.E. Baird, and P.B. Dervan, *Binding site size limit of the 2:1 pyrrole-imidazole polyamide-DNA motif.* Proc Natl Acad Sci U S A, 1996. **93**(14): p. 6981-5.

13. Youngquist, R.S. and P.B. Dervan, *A synthetic peptide binds 16 base pairs of A,T double helical DNA.* J. Am. Chem. Soc., 1987. **109**(24): p. 7564-7566.

14. Urbach, A.R. and P.B. Dervan, *Toward rules for 1:1 polyamide:DNA recognition.* Proc Natl Acad Sci U S A, 2001. **98**(8): p. 4343-8.

15. Urbach, A.R., et al., *Structure of a beta-alanine-linked polyamide bound to a full helical turn of purine tract DNA in the 1:1 motif.* J Mol Biol, 2002. **320**(1): p. 55-71.

16. Burnett, R., et al., *DNA sequence-specific polyamides alleviate transcription inhibition associated with long GAA.TTC repeats in Friedreich's ataxia.* Proc Natl Acad Sci U S A, 2006. **103**(31): p. 11497-502.

17. Bremer, R.E., et al., *Inhibition of major groove DNA binding bZIP proteins by positive patch polyamides.* Bioorg Med Chem, 2001. **9**(8): p. 2093-103.

18. Fechter, E.J. and P.B. Dervan, *Allosteric inhibition of protein--DNA complexes by polyamide--intercalator conjugates.* J Am Chem Soc, 2003. **125**(28): p. 8476-85.

19. Gearhart, M.D., et al., *Inhibition of DNA binding by human estrogen-related receptor 2 and estrogen receptor alpha with minor groove binding polyamides.* Biochemistry, 2005. **44**(11): p. 4196-203.

20. Schaal, T.D., et al., *Inhibition of human papilloma virus E2 DNA binding protein by covalently linked polyamides.* Nucleic Acids Res, 2003. **31**(4): p. 1282-91.

21. Wurtz, N.R., et al., *Fmoc solid phase synthesis of polyamides containing pyrrole and imidazole amino acids.* Org Lett, 2001. **3**(8): p. 1201-3.

22. Belitsky, J.M., et al., *Solid-phase synthesis of DNA binding polyamides on oxime resin.* Bioorg Med Chem, 2002. **10**(8): p. 2767-74.

23. Hunt, C. and R.I. Morimoto, *Conserved features of eukaryotic hsp70 genes revealed by comparison with the nucleotide sequence of human hsp70.* Proc Natl Acad Sci U S A, 1985. **82**(19): p. 6455-9.

24. Sambrook, J., E.F. Fritsch, and T. Maniatis, *Molecular Cloning.* 1989(18): p. 56.

25. Iverson, B.L. and P.B. Dervan, *Adenine specific DNA chemical sequencing reaction.* Nucleic Acids Res, 1987. **15**(19): p. 7823-30.

26. Trauger, J.W. and P.B. Dervan, *Footprinting methods for analysis of pyrrole-imidazole polyamide/DNA complexes.* Methods Enzymol, 2001. **340**: p. 450-66.

27. Rome, C., F. Couillaud, and C.T. Moonen, *Spatial and temporal control of expression of therapeutic genes using heat shock protein promoters.* Methods, 2005. **35**(2): p. 188-98.

28. Kroeger, P.E., K.D. Sarge, and R.I. Morimoto, *Mouse heat shock transcription factors 1 and 2 prefer a trimeric binding site but interact differently with the HSP70 heat shock element.* Mol Cell Biol, 1993. **13**(6): p. 3370-83.

29. Swalley, S.E., E.E. Baird, and P.B. Dervan, *A pyrrole-imidazole polyamide motif for recognition of eleven base pair sequences in the minor groove of DNA.* Chemistry--A European Journal, 1997. **3**(10): p. 1600-1607.

30. Nickols, N.G., et al., *Improved nuclear localization of DNA-binding polyamides.* Nucleic Acids Res, 2007. **35**(2): p. 363-70.

31. Beere, H.M., et al., *Heat-shock protein 70 inhibits apoptosis by preventing recruitment of procaspase-9 to the Apaf-1 apoptosome.* Nature Cell Biology, 2000. **2**(8): p. 469-475.

32. Leung, T.K.C., et al., *The Human Heat-Shock Genes Hspa6 and Hspa7 Are Both Expressed and Localize to Chromosome-1.* Genomics, 1992. **12**(1): p. 74-79.

33. Chenoweth, D.M. and P.B. Dervan, *Structural Basis for Cyclic Py-Im Polyamide Allosteric Inhibition of Nuclear Receptor Binding.* J Am Chem Soc, 2010.

34. Bao, X.Q. and G.T. Liu, *Induction of overexpression of the 27- and 70-kDa heat shock proteins by bicyclol attenuates concanavalin A-Induced liver injury through*

suppression of nuclear factor-kappaB in mice. Mol Pharmacol, 2009. **75**(5): p. 1180-8.

35. Liu, B. and T. Kodadek, *Investigation of the relative cellular permeability of DNA-binding pyrrole-imidazole polyamides.* J Med Chem, 2009. **52**(15): p. 4604-12.

36. Jacobs, C.S. and P.B. Dervan, *Modifications at the C-terminus to improve pyrrole-imidazole polyamide activity in cell culture.* J Med Chem, 2009. **52**(23): p. 7380-8.

37. Hertzberg, R.P. and P.B. Dervan, *Cleavage of DNA with methidiumpropyl-EDTA-iron(II): reaction conditions and product analyses.* Biochemistry, 1984. **23**(17): p. 3934-45.

38. Latham, K.A. and R.S. Lloyd, *Delta-elimination by T4 endonuclease V at a thymine dimer site requires a secondary binding event and amino acid Glu-23.* Biochemistry, 1995. **34**(27): p. 8796-803.

Table 4.1 HPLC analysis of polyamides.

	310 nM		280 nM		254 nM	
Polyamide	Retention time /min	Purity /%	Retention time /min	Purity /%	Retention time /min	Purity /%
P1	8.183	97.39	8.183	100	8.133	100
P2	8.167	99.14	8.167	98.46	8.083	97.50
P3	8.467	97.35	8.467	96.89	8.467	95.79
P4	7.633	99.56	7.633	99.31	7.633	98.57
P5	7.400	96.39	7.383	98.05	7.400	98.62
P6	8.317	98.15	8.317	99.16	8.317	99.74
P7	6.633	95.89	6.633	98.74	6.633	96.13
P8	8.000	96.22	8.000	97.23	7.983	100
P9	7.267	95.98	7.267	99.14	7.267	99.10
P10	8.950	99.87	8.967	99.80	8.983	99.80
P11	7.267	95.63	7.267	95.73	7.250	98.14
P12	8.000	97.93	8.000	97.49	7.900	100
H0	7.533	99.25	7.533	96.34	7.533	97.74
H1	7.600	97.77	7.600	99.19	7.600	100
H2	7.067	98.95	7.067	99.32	7.033	96.48
H3	7.617	98.66	7.617	98.20	7.617	97.29

Table 4.2 MALDI MS analysis of polyamides. Expected monoisotopic $(M+H)^+$ versus observed $(M+H)^+$.

	P1	P2	P3	P4
Formula	$C_{45}H_{58}N_{17}O_8$	$C_{45}H_{58}N_{17}O_8$	$C_{45}H_{58}N_{17}O_8$	$C_{44}H_{60}N_{17}O_9$
$(MW+H)^+$ (expected)	964.4654	964.4654	964.4654	970.4760
$(MW+H)^+$ (observed)	964.6	964.5	964.6	970.4
	P5	P6	P7	P8
Formula	$C_{42}H_{57}N_{16}O_8$	$C_{45}H_{58}N_{17}O_8$	$C_{35}H_{49}N_{14}O_7$	$C_{50}H_{66}N_{19}O_{10}$
$(MW+H)^+$ (expected)	913.4545	964.4654	777.3909	1092.5240
$(MW+H)^+$ (observed)	913.4	964.4	777.3	1092.5
	P9	P10	P11	P12
Formula	$C_{42}H_{57}N_{16}O_8$	$C_{48}H_{59}N_{18}O_8$	$C_{42}H_{57}N_{16}O_8$	$C_{50}H_{66}N_{19}O_{10}$
$(MW+H)^+$ (expected)	913.4545	1015.4760	913.4545	1092.524
$(MW+H)^+$ (observed)	913.5	1015.5	913.6	1092.6

	H0	H1	H2	H3
Formula	$C_{55}H_{68}N_{21}O_9$	$C_{55}H_{68}N_{21}O_9$	$C_{49}H_{66}N_{19}O_9$	$C_{49}H_{66}N_{19}O_9$
$(MW+H)^+$ (expected)	1166.5508	1166.5508	1064.5291	1064.5291
$(MW+H)^+$ (observed)	1166.2	1166.6	1064.5	1064.7

Table 4.3 Association constants and Hill slope coefficients for the linear polyamides

Polyamide	Length	K_a (M^{-1})	Hill Slope coefficient
P5	8	$1.39 \pm 0.46 \times 10^7$	0.89 ± 0.18
P9	8	$8.84 \pm 0.35 \times 10^6$	1.53 ± 0.18
P7	6	$1.15 \pm 0.24 \times 10^7$	0.95 ± 0.28
P4	8	$1.19 \pm 0.90 \times 10^8$	0.68 ± 0.41
P8	9	$3.44 \pm 1.4 \times 10^8$	0.86 ± 0.42

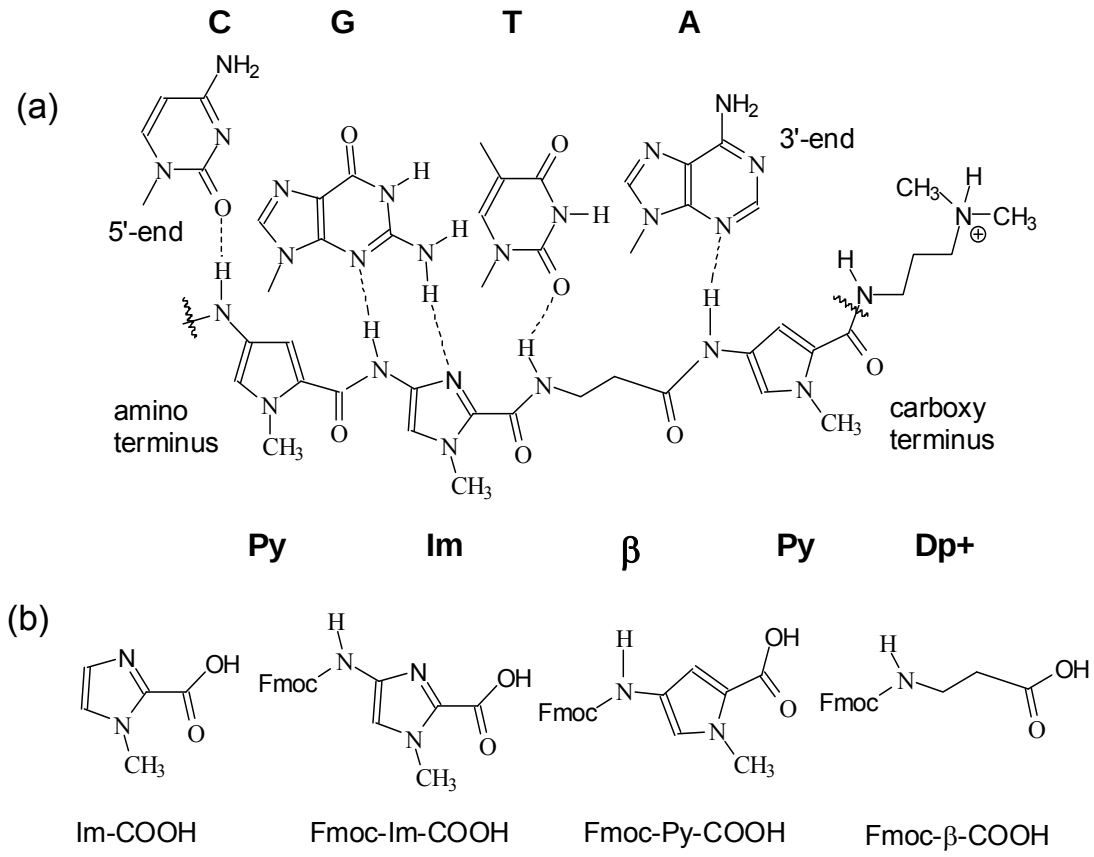

Figure 4.1 Polyamide structure, binding, and synthetic intermediates. a) Polyamides are composed of N-methyl-imidazole (Im), N-methyl-pyrrole (Py) and β-alanine (β) that recognize DNA sequences through hydrogen bonding to the minor groove of Watson-Crick base pairs by side pairing of Im/Py for G/C, Py/Im for C/G, and Py/Py for A/T or T/A, respectively. The more flexible β/β can also recognize A/T or T/A. b) The Fmoc aminoacids used to synthesize polyamides. Im-CO_2H is used when the N-terminal amino acid is N-methyl-imidazole.

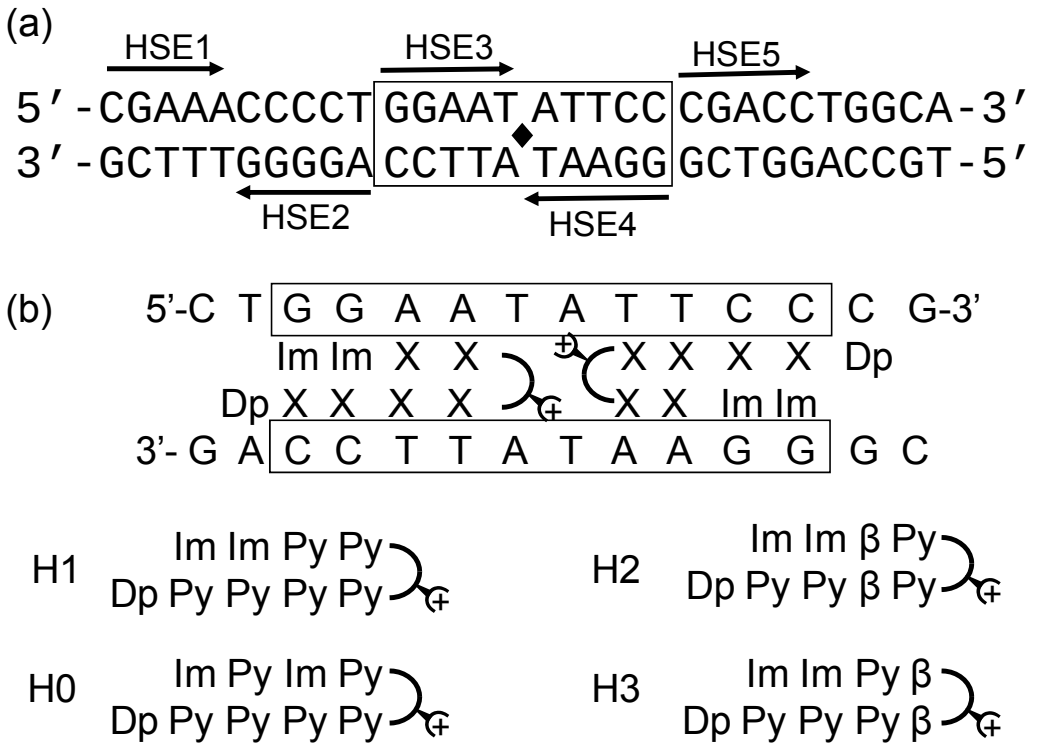

Figure 4.2 Design of polyamide libraries targeting the promoter region of DNA encoding for heat shock protein 70. a) The promoter region of the human heat shock protein A1A/A1B gene contains five adjacent heat shock elements (HSE), which binds to the trimerized form of heat shock transcription factor 1 (HSF1) in its major groove. HSE3 and HSE4 combine to form a pallindromic site (boxed) with the dyad axis indicated with a filled diamond. b) Hairpin polyamides targeted to the minor groove of the GGAA sequence.

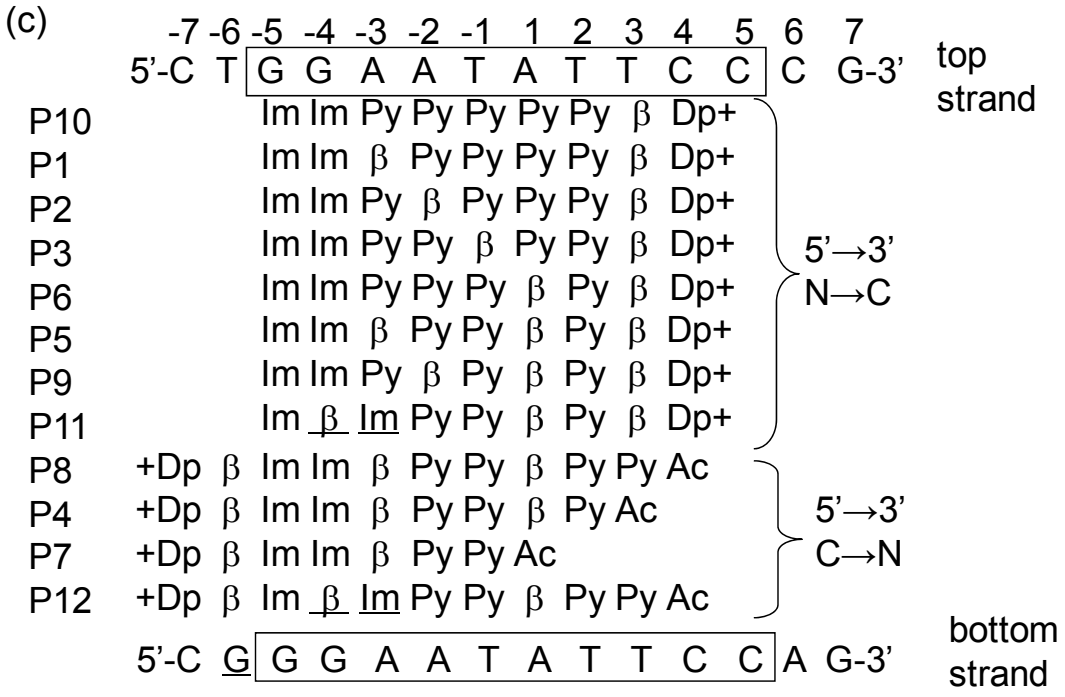

Figure 4.2 Design of polyamide libraries targeting the promoter region of DNA encoding for heat shock protein 70. c) Linear polyamide libraries designed to target the minor groove of heat shock elements HSE 3 and HSE 4. The orientation of the polyamide (N→C or C→N) with respect to the top strand (5'→3') is shown to the right, and mismatches in the polyamide are underlined. Polyamides 1-3, 5-6 and 9-10 can also bind to the bottom strand shown below in the reverse orientation with respect to the top strand

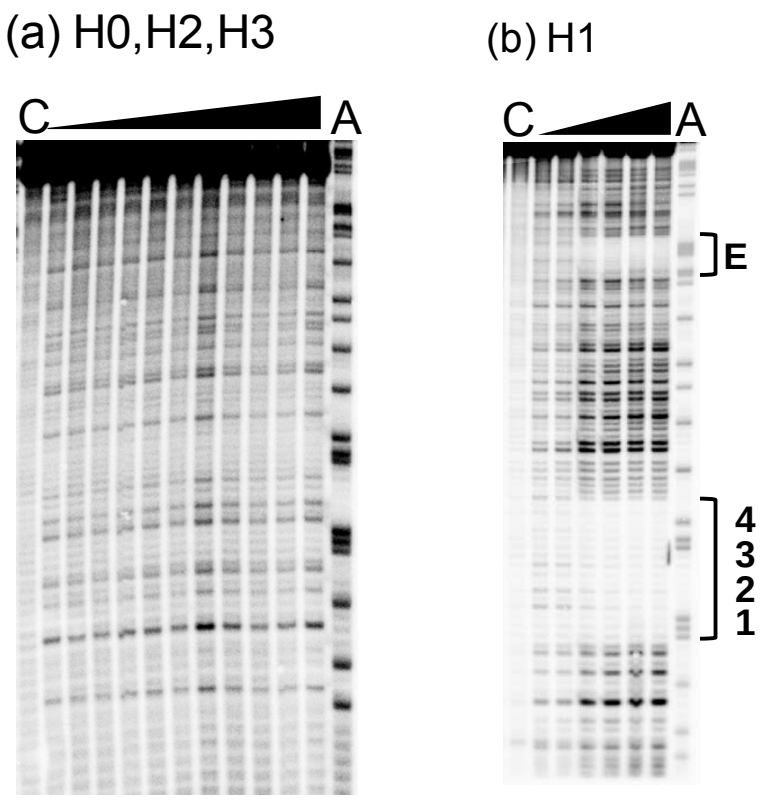

Figure 4.3 DNase I footprinting of the hairpin polyamide library. a) Representative denaturing polyacrylamide gel for H2, H3, and H0. The concentration of polyamide increased from left to right: 0, 10, 50, 100, 500 pM, 1, 5, 10, 50, 100, 500 nM, 1μM. b) The concentration of polyamide H1 increased from left to right: 0, 100, 200, 300, 400, 500 nM. C is a control with no polyamide or DNase I, A is the Maxam Gilbert A sequencing lane. Binding sites are labeled according to the scheme shown in panel c below.

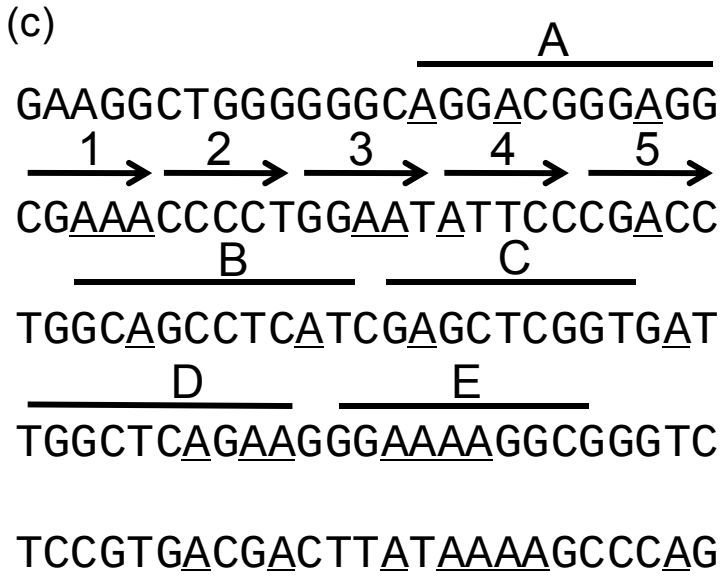

Figure 4.3 DNase I footprinting of the hairpin polyamide library. c) Sequence of the 152-mer (only 26150 shown) with HSE sites indicated as numbers 1-5, as well as other sites observed to be bound by the hairpin and linear polyamide, as letters A-E. The A's that appear in the sequencing lanes are underlined.

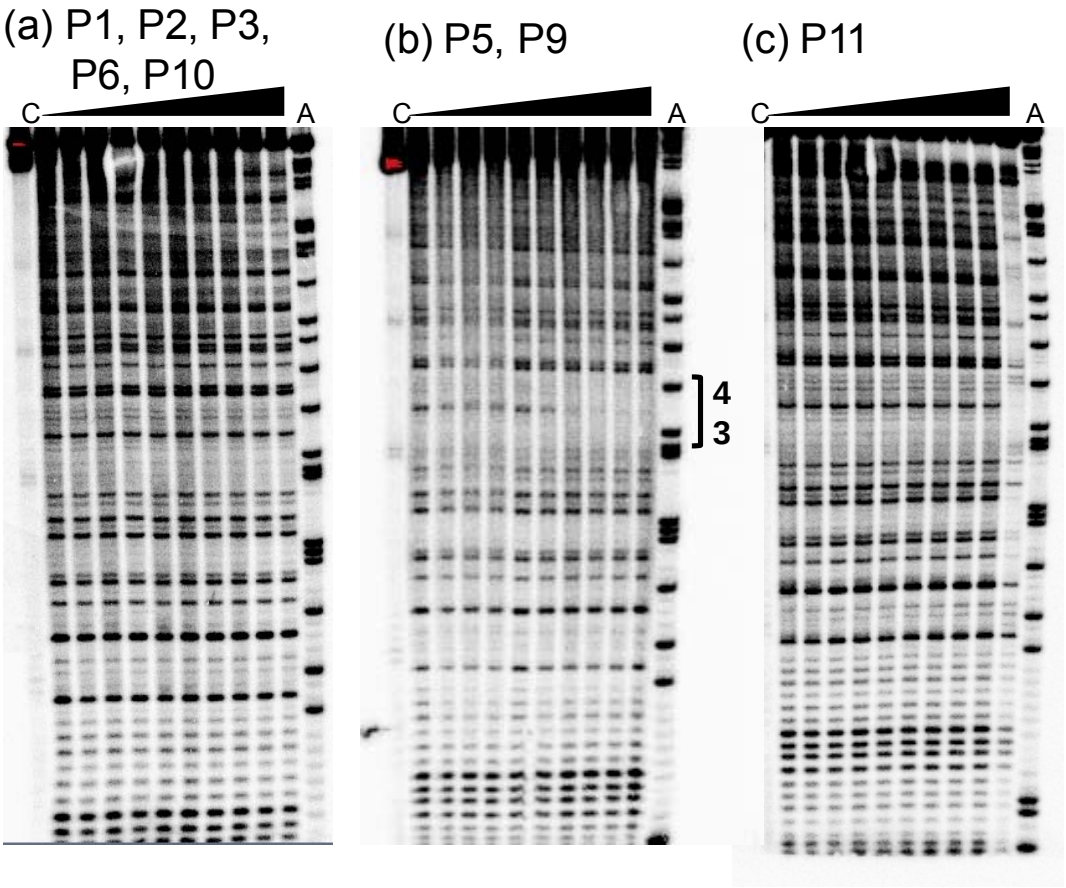

Figure 4.4 DNase I footprinting of the N→C linear polyamide library. Polyamide concentration increases from left to right at 0, 0.1, 1, 10, 50, 100, 200, 300, 400 and 500 nM. Lane C is a control lane containing only DNA and 500 nM polyamide and no DNase I. Lane A is the Maxam Gilbert A sequencing reaction lane. Gel a) shows the footprinting of P10 which is representative of P10, P1, P2, P3 and P6. Gel b) illustrates the footprinting of P9 which is representative of P5 and P9, and gel c) is the result of the mismatch control P11. Binding sites are labeled according to the scheme shown in Figure 4.3c.

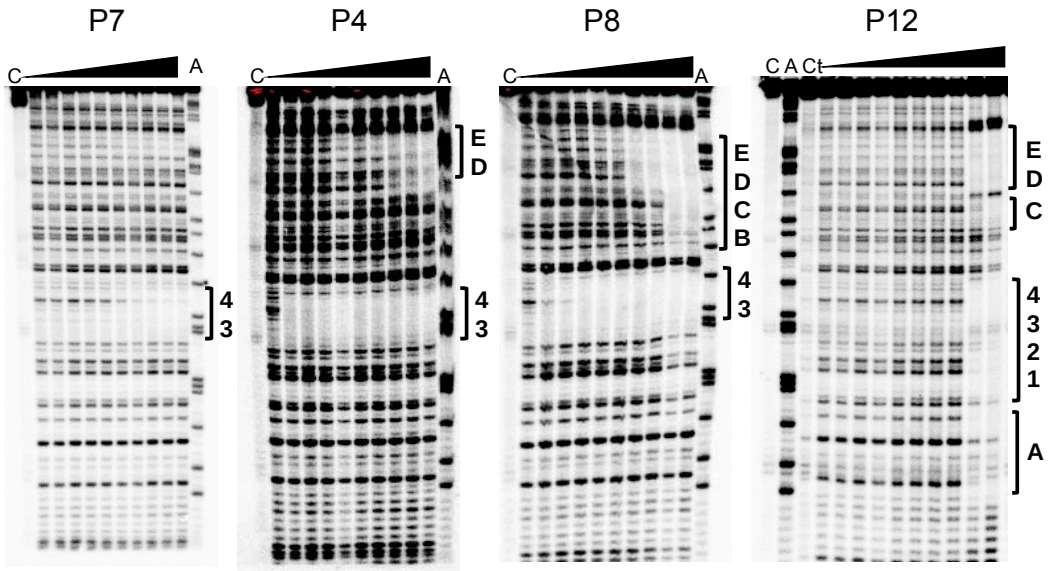

Figure 4.5 DNase I footprinting of the C→N linear polyamide library. Polyamide concentration increases from left to right at 0, 0.1, 1, 10, 50, 100, 200, 300, 400 and 500 nM. Lane C is a control lane with DNA and 500 nM polyamide and no DNase I. Lane A is the Maxam Gilbert A sequencing reaction. P12 is the mismatch control for P7, P4 and P8. Binding sites are labeled according to the scheme shown in Figure 4.3c.

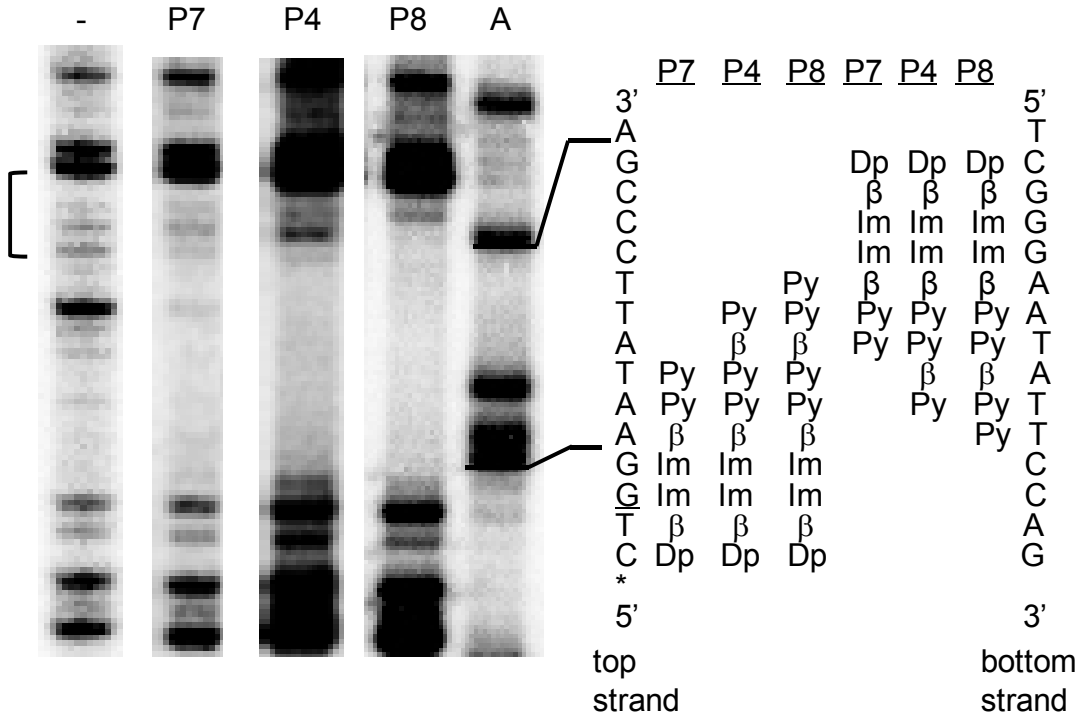

Figure 4.6 Analysis of the DNase I footprints of P4, P7 and P8 at HSE3 and HSE4. The bracket to the left indicates sites that become progressively blocked on going from P4 to P7 to P8. To align the DNase I bands with the A sequencing lane, one has to take into account that the DNA is 5'-end-labeled and that DNase I cleaves to the 3'-side of a nucleotide producing a 5'-end-labeled product with a 3'-OH. The Maxam Gilbert A reaction, on the other hand, cleaves to the 5'-side of the nucleotide and produces a 5'-end-labeled product with a 3'-phosphate. Because the a 3'-phosphate increases the mobility of a DNA fragment relative to a 3'-OH by about one nucleotide or more [37, 38], the band corresponding to cleavage to the 3'-side of an A by DNase I corresponds to a band about 2 nt higher up on the gel than produced by a Maxam Gilbert A reaction.

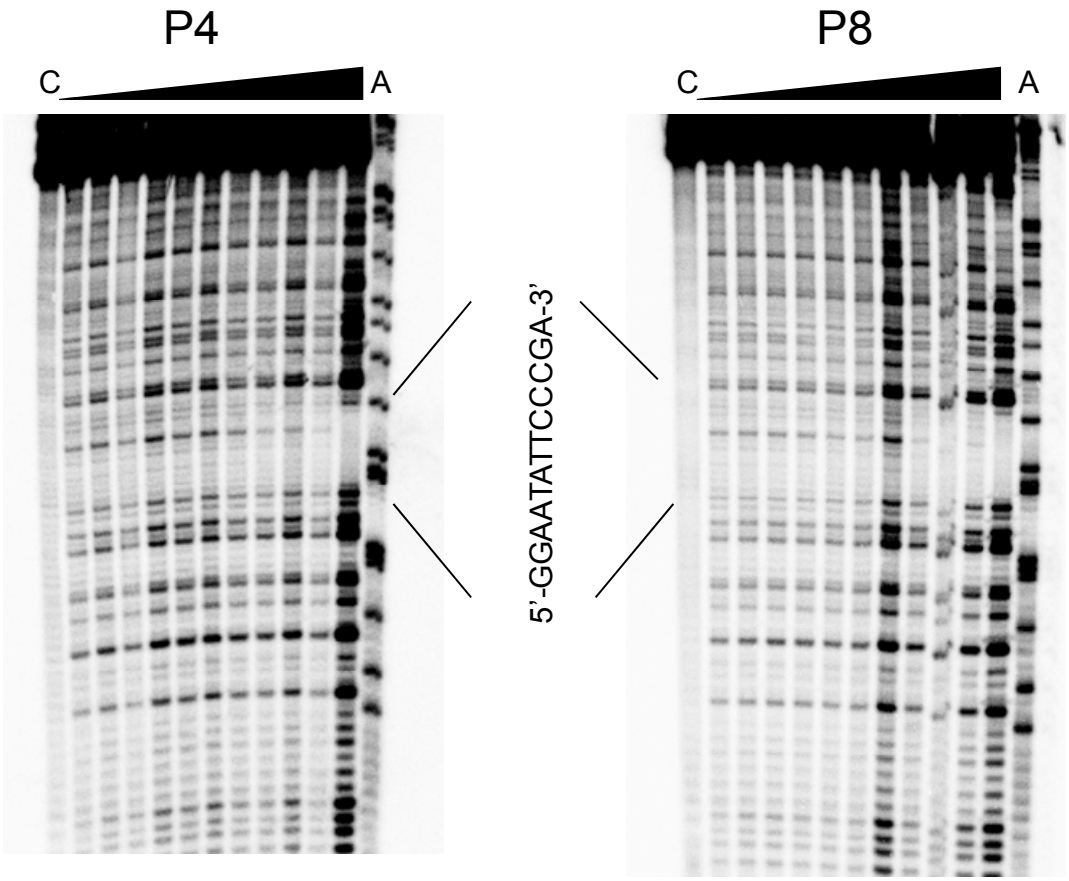

Figure 4.7 DNase I footprinting of polyamide P4 and P8 at lower concentrations for quantitative footprinting analysis. From Left to right, polyamide concentration increased as 0, 10, 50, 100, 500, and 800 pM, 1, 2, 5, 10, and 100 nM. "C", control DNA with 100 nM polyamide but no DNase I addition; "A" Adenosine sequencing of DNA substrate.

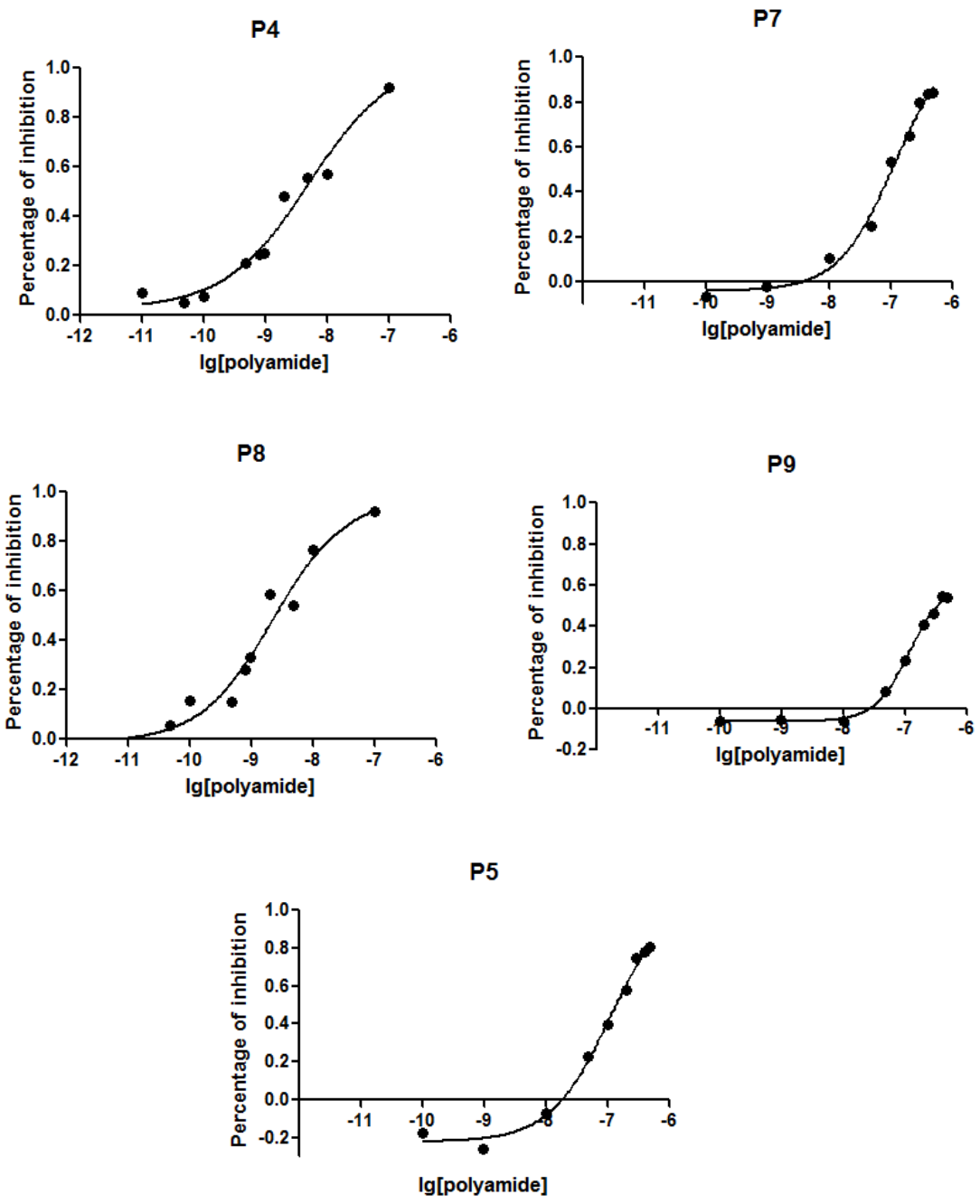

Figure 4.8 Curve fits of the percentage of "site occupation" or "DNaseI inhibition" versus polyamide concentration for P4, P7, P8, P5 and P9. Fits were generated by GraphPad Prism using a variable Hill slope equation with nonlinear regression analysis.

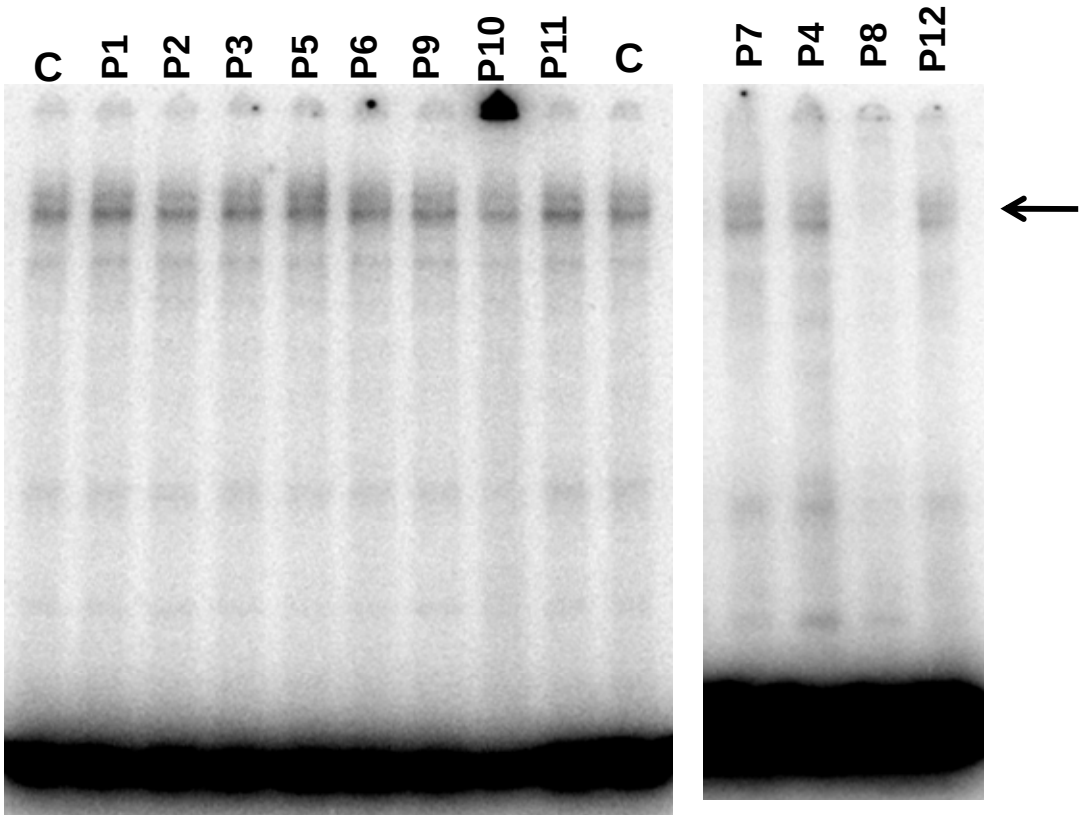

Figure 4.9 *In vitro* gel-shift assay of block of heat shock factor 1 binding by polyamides. Polyamides P1-P10 along with mismatch control P11 and P12 were tested each on their ability to block the binding of HSF-1 to its cognate HSE DNA promoter at a concentration of 100 nM. Radiolabeled HSE oligodeoxynucleotide (10 nM) was incubated with each polyamide at 100 nM for 16 h before mixing with nuclear extracts (1.5 μg protein) prepared from heated Jurkat cells (43 °C for 30 min with 30 min recovery at 37 °C.) and the formation of HSE/HSF-1 complexes determined by gel electrophoresis. Control lane C: radiolabeled oligodeoxynucleotide, in the absence of added polyamide, mixed with Jurkat extract from heated cells.

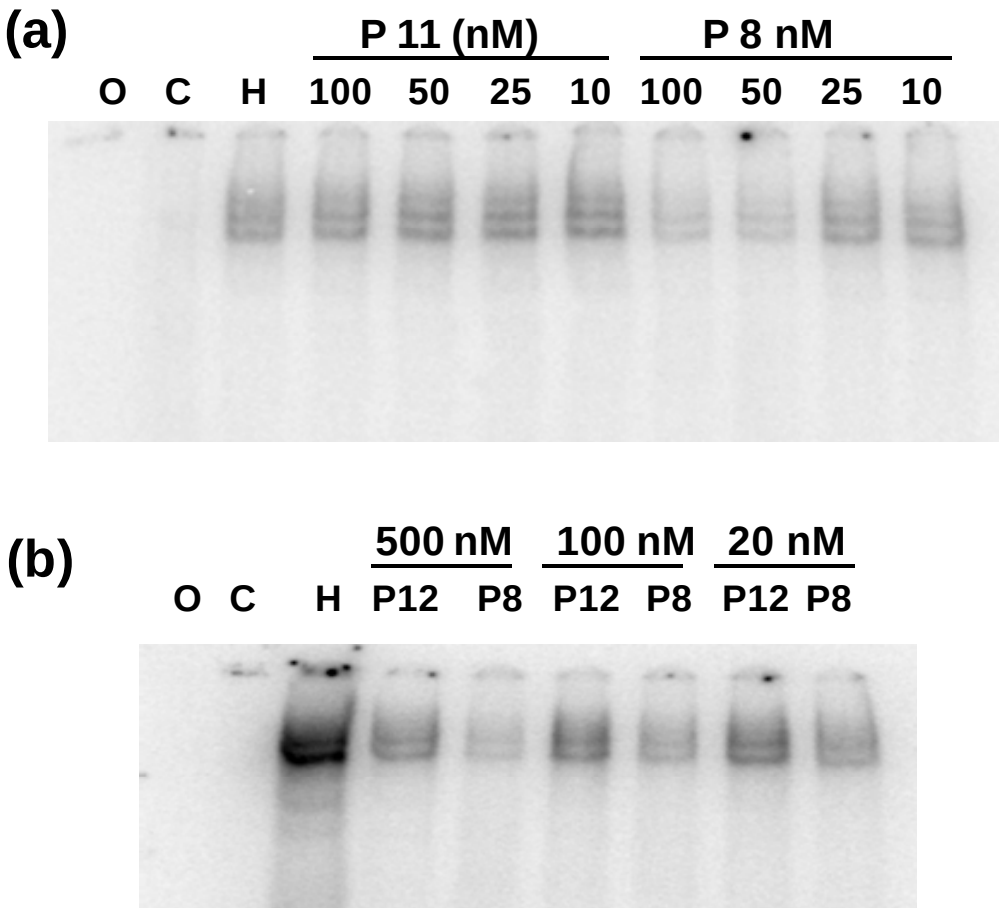

Figure 4.10 *In vitro* gel-shift assay of heat shock factor 1 binding in presence of P8, P11 and P12. Titration of the effective concentration of polyamide P8 against (a) mismatch control polyamide P11 and (b) mismatch control P12 for inhibition of heat shock factor/heat shock element complex formation was performed using nuclear extracts prepared from heated (43 °C for 30 min, 1 h recovery at 37 °C) human HeLa cells. Polyamides were incubated with a ^{32}P-radiolabeled 36-mer duplex DNA substrate containing the five heat shock elements in annealing buffer (10 mM Tris pH 7.5, 10 mM NaCl, 1 mM EDTA) for 16 h at 25 °C. Lane O is a DNA control without addition of nuclear extract. Lane C is a DNA control mixed with non-heated nuclear extract. Lane H is a DNA control with heat extract proteins but no added polyamide.

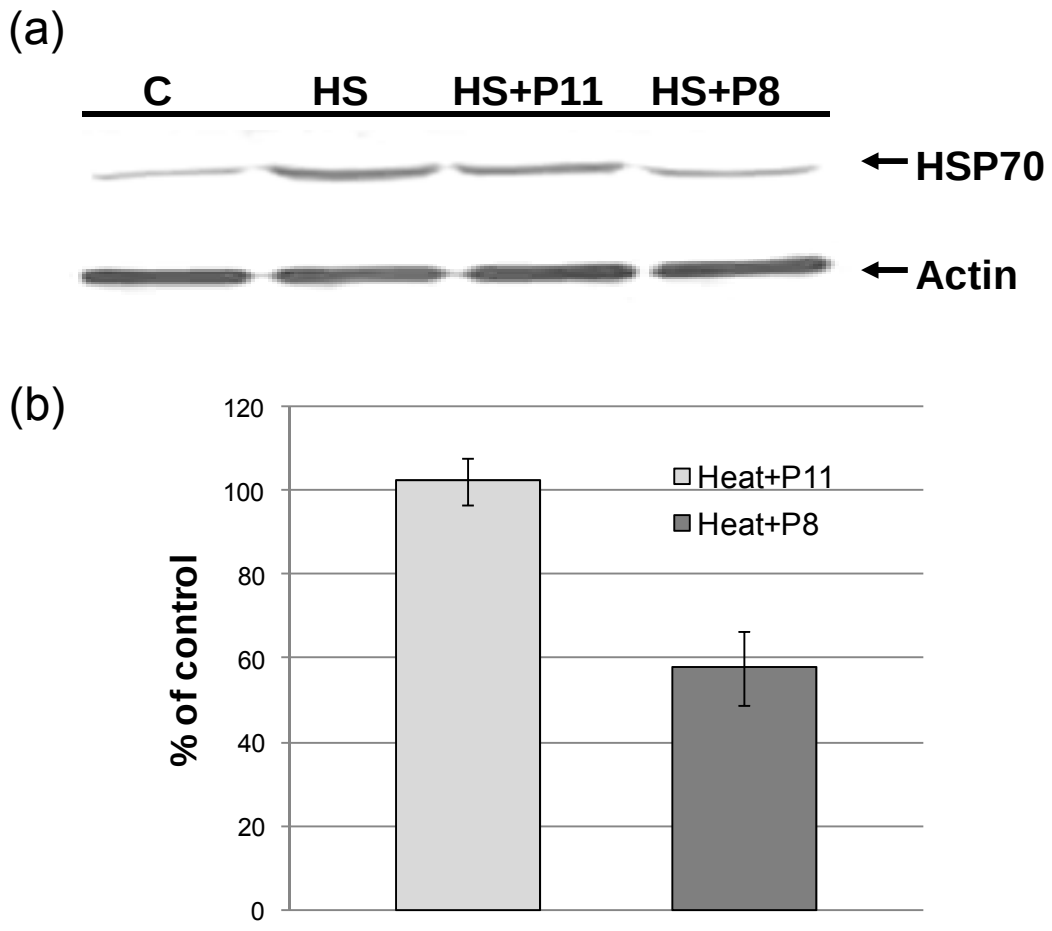

Figure 4.11 Polyamide inhibition of HSP70 expression *in vivo*. (a) Jurkat cells were electroporated with 5 μM P11 or P8 and then allowed to recover for 24 h in 5 μM polyamide before being heat shocked at 43 °C for 30 min to induce HSP70 gene transcription and protein synthesis. Western blot analysis was performed with mouse anti-HSP70 and mouse anti-actin followed by AP-coupled goat anti-mouse. Lane C is control cells without heat, lane HS is control cells with heat shock. (b) Band intensity on western blot was quantified by scanning on BioRad ChemDoc XRS. Percent of induced HSP70 was normalized to actin protein levels and corrected for cell viability. P8 treatment decreased HSP70 levels to 60% of normal.

Chapter 5.

Summary, Conclusions, and Future Studies

In this dissertation, we were interested in developing methods for inhibiting heat shock protein 70 (HSP70) which is considered an emerging drug target. In previous literature reports [1], its nucleotide binding domain is known to bind ATP with high affinity and thus make it difficult to replace it with drug-like molecules specific for HSP70 alone. This fact, together the fact that both its nucleotide binding domain and substrate binding domain are also highly hydrophilic, make the overall druggability of heat shock protein 70 (HSP70) poor [2]. Since heat shock protein 70 is only expressed at low levels in most cells except cancer cells, but is highly inducible when cells are under stress [3], our attention focused on inhibiting the induction of HSP70 by interfering with the activation or binding of the heat shock transcription factor. Inhibitors of HSP70 induction might therefore be better and more feasible drugs for cancer chemotherapy.

The goal of this dissertation was therefore to develop both small molecule inhibitors and gene inhibitors that specifically inhibit the induction of heat shock protein 70 by interfering with the activation of transcription. We also expected the inhibitors that we developed to better understand the underlying pathways of heat shock protein 70 induction, and identify other key proteins that might be involved that can serve as future targets for drug design.

Of all known natural products that can inhibit the induction of heat shock protein 70, quercetin has very low toxicity and has the advantage of being easily modified. Our first goal was therefore to carry out the structure and activity studies of quercetin derivatives to identify derivatives specific for HSP70 inhibition that could be potentially developed to chemotherapeutic drugs, and in the process to also map out the non-active sites on quercetin for attachment of biotin probes to pull down potential target proteins of

quercetin. As a result of my efforts, I successfully synthesized the mono-methyl, mono-carbomethoxy methylate and mono-carboxymethylate derivatives of quercetin. In collaboration with Dr. Clayton Hunt who tested their ability to inhibit HSP70 induction, we were able to identify two mono-derivatized classes of inhibitors having one of the hydroxyl groups modified (D1, D2 on 3'-OH; D7, D10 on 7-OH) that retained the ability to inhibit HSP70 induction. We also discovered that quercetin enhances the phosphorylation of HSP27 required for its anti-apoptotic action in cells to diminish the radiosensitizing or antitumor effects of inhibiting HSP70 induction. Two derivatives (D1 and D2), unlike quercetin, could also inhibit HSP70 induction without enhancing HSP27 phosphorylation. D1 and D2 could thus be candidates with more specificity for future drug development although the degree of their enhancement in different chemotherapy, anti-cancer therapy remains to be determined. In the course of evaluating these derivatives, I also discovered that their ability to inhibit HSP70 induction is related to their ability to inhibit both CK2 and CaMKII kinases that are known to phosphorylate heat shock transcription factor 1 [4]. This suggests that the ability of quercetin to inhibit HSP70 induction is due to its lack of specificity, rather than to high specificity which is commonly thought to be important for drug design, and may represent a new paradigm for drug design. This would also suggest that in the future, inhibitors for HSP70 induction could be found by screening for their ability to inhibit both CK2 and CaMKII kinases.

The second goal of this dissertation was to identify other possible targets of quercetin by attaching a biotin affinity label to the non-active sites of quercetin to enable us to pull down target proteins from cells. I demonstrated the feasibility of this approach by

conjugating biotin to the O7- position and showed that this probe (called BioQ) can be used as a photoaffinity agent to pull down CK2 *in vitro* and quercetin binding proteins *in vivo* through the use of steptavidin beads. I made use of quercetin's intrinsic photoreactivity to enable covalent binding of the quercetin moiety to target proteins to enable us to pull down low-affinity binding proteins as well as to make it possible to wash away non-specifically bound proteins. Using this probe, we discovered that many of the proteins that we pulled down have already been identified as potential therapeutic targets in cancer therapy suggesting that quercetin acts as an anticancer agent by interfering with many cancer pathways. The proposed targets CK2 and CaMKII were, however, not identified presumably because they were present at too low a level. Further studies of the photocrosslinking mechanism and amino acid specificity are also necessary. In the future, biotin probes will be constructed by linking to the other available hydroxyl sites on quercetin and additional photocrosslinking agents may be added to enhance the photocrosslinking efficiency. To confirm the identities of the protein candidates pulled down, western blot assays could be conducted. Finally a protein knock-out or knock-down studies could be carried out to verify the protein targets as viable targets for chemotherapy.

Another goal was to develop polyamide based anti-gene inhibitors of heat shock protein 70 induction. Towards this goal I designed and synthesized a library of polyamides aimed at blocking binding of the heat shock transcription factor 1to the heat shock promoter. After characterization of the binding specificity and affinity with DNase I footprinting and an *in vitro* transcription factor 1 binding study, I was able to identify one linear polyamide with high affinity for the heat shock elements 3 and 4 of the

HSPA1A/HSPA1B promoter. This polyamide binds to the twisted polypurine rich region in an unusual 1:1 mode and in the C→N orientation. Despite the *in vitro* performance, this linear polyamide was not able to efficiently penetrate cells and/or the nucleus, though we could show that it could inhibit HSP70 induction by about 40% by electroporation. Future work could focus on attaching some cell penetrating peptides to help cell permeation. To achieve complete knock down of HSP70 it may also be necessary to block binding to the HSPA6 promoter which has a different sequence from the HSPA1A/A1B promoter. Inhibition of HSP70 induction could then be carried out with a cocktail of these two polyamide inhibitors.

References:

1. Evans, C.G., L. Chang, and J.E. Gestwicki, *Heat shock protein 70 (hsp70) as an emerging drug target.* J Med Chem. **53**(12): p. 4585-602.
2. Massey, A.J., *ATPases as drug targets: insights from heat shock proteins 70 and 90.* J Med Chem. **53**(20): p. 7280-6.
3. Huang, L., N.F. Mivechi, and D. Moskophidis, *Insights into regulation and function of the major stress-induced hsp70 molecular chaperone in vivo: analysis of mice with targeted gene disruption of the hsp70.1 or hsp70.3 gene.* Mol Cell Biol, 2001. **21**(24): p. 8575-91.
4. Wang, R.E., et al., *Inhibition of heat shock induction of heat shock protein 70 and enhancement of heat shock protein 27 phosphorylation by quercetin derivatives.* J Med Chem, 2009. **52**(7): p. 1912-21.